



# UNIVERSITY OF TURIN

Department of Life Sciences and Systems Biology

## Ph.D. in Neuroscience



XXXII CYCLE

### **A study on the cellular and molecular mechanisms underlying adult hippocampal neurogenic niche response to neuroinflammation**

Thesis presented by: **Isabella Crisci**

Supervisor: Prof. **Silvia De Marchis**

Coordinator: Prof. **Marco Sassoé Pognetto**

Academic years: 2020 – 2021

Scientific disciplinary sector: BIO/06

# Table of contents

<b>Outline of the thesis.....</b>	<b>i</b>
<b>Summary .....</b>	<b>III</b>
<b>CHAPTER I.....</b>	<b>0</b>
<b>1 Introduction .....</b>	<b>1</b>
<b>1.1 The adult mouse hippocampus .....</b>	<b>1</b>
1.1.1 Fundamental neuroanatomical organization .....	1
1.1.2 Neural circuits and functional relevance.....	8
<b>1.2 The adult hippocampal neurogenesis .....</b>	<b>11</b>
1.2.1 The multistage process of adult hippocampal neurogenesis .....	13
1.2.2 The adult hippocampal neurogenic niche.....	20
1.2.3 The regulation and function of adult hippocampal neurogenesis.....	25
1.2.3.1 Intracellular and extracellular players.....	25
1.2.3.2 Environmental factors .....	32
1.2.4 Methods and mice models for studying adult hippocampal neurogenesis .....	37
<b>1.3 Neuroinflammation in the central nervous system.....</b>	<b>43</b>
1.3.1 Immune-to-brain communication pathways following peripheral inflammation .....	44
1.3.2 Neuro-immune crosstalk in the adult neurogenic niche.....	46
1.3.2.1 Microglial cells activation and polarization .....	51
1.3.2.2 Pro- and anti-inflammatory mediators .....	54
1.3.3 Inflammation and neuroprotection.....	57
1.3.3.1 Selective estrogen receptor modulators (SERMs).....	61
1.3.3.2 Tamoxifen activation of Cre-Lox system and its possible side effects.....	63
<b>Aim of the study.....</b>	<b>66</b>
<b>CHAPTER II.....</b>	<b>68</b>
<b>2 COUP-TFI is a key regulator in the neurogenesis/astrogliogenesis balance within the adult DG hippocampus with relevant implications upon neuroinflammation.....</b>	<b>69</b>
<b>2.1 Introduction.....</b>	<b>70</b>
<b>2.2 Materials and methods.....</b>	<b>73</b>
2.2.1 Animals and housing conditions .....	73
2.2.2 Genotyping.....	74
2.2.3 LPS treatments.....	74
2.2.4 Retro-Cre virus stereotaxic injection in the adult DG.....	74
2.2.5 Tissue collection, RNA extraction, and RT-qPCR.....	74
2.2.6 Tissue preparation .....	75
2.2.7 Immunofluorescence and immunohistochemistry .....	75
2.2.8 Microscope analysis and cellular quantification.....	76
2.2.9 Statistical analysis .....	76
<b>2.3 Results.....</b>	<b>78</b>

2.3.1	LPS-induced neuroinflammation leads to impaired neurogenesis coupled to COUP-TFI downregulation within the adult DG.....	78
2.3.2	Genetic inactivation of COUP-TFI in mitotic progenitors of adult DG impairs neurogenesis by promoting an astroglial fate .....	83
2.3.3	COUP-TFI overexpression rescues altered neuron-to-astrocyte generation upon neuroinflammation .....	89
<b>2.4</b>	<b>Discussion.....</b>	<b>92</b>
<b>CHAPTER III.....</b>		<b>95</b>
<b>3</b>	<b>Tamoxifen exerts direct and microglia-mediated regulation on the adult mouse hippocampal neurogenic niche preventing the detrimental effects of LPS-induced neuroinflammation.....</b>	<b>96</b>
<b>3.1</b>	<b>Abstract .....</b>	<b>96</b>
<b>3.2</b>	<b>Introduction .....</b>	<b>97</b>
<b>3.3</b>	<b>Materials and methods .....</b>	<b>100</b>
3.3.1	Animals .....	100
3.3.2	Drug treatments (i.e., administration of tamoxifen, LPS, PLX5622) .....	100
3.3.3	Tissue preparation and sectioning .....	101
3.3.4	Multiple immunofluorescence labeling .....	101
3.3.5	Confocal microscopy .....	102
3.3.6	Cell counting and morphometric analyses .....	102
3.3.7	Tissue collection, RNA extraction, and RT-qPCR .....	103
3.3.8	Statistics .....	103
<b>3.4</b>	<b>Results .....</b>	<b>105</b>
3.4.1	Tamoxifen modulates the expression of inflammatory cytokines within the adult mouse hippocampus .....	105
3.4.2	Tamoxifen alters the morphology of hippocampal DG microglial cells and prevents their increase upon LPS treatment.....	107
3.4.3	Tamoxifen counteracts the LPS-induced dysregulation on adult DG neurogenesis..	110
3.4.4	Newborn neurons and RGL cells respond to LPS-challenge and tamoxifen treatment in microglia-depleted mice.....	114
<b>3.5</b>	<b>Discussion.....</b>	<b>118</b>
<b>3.6</b>	<b>Supplementary figures.....</b>	<b>123</b>
<b>3.7</b>	<b>Supplementary tables .....</b>	<b>128</b>
<b>CHAPTER IV .....</b>		<b>134</b>
<b>Concluding remarks and future perspectives .....</b>		<b>135</b>
<b>CHAPTER V .....</b>		<b>139</b>
<b>References.....</b>		<b>140</b>
<b>CHAPTER VI .....</b>		<b>176</b>
<b>Acknowledgments.....</b>		<b>177</b>
<b>APPENDIX.....</b>		<b>178</b>





# Outline of the thesis

**Chapter I**, representing the introduction, consists of three different subchapters. The first part provides a general introduction to the neuroanatomy and connectivity of the hippocampal formation, with a particular focus on the dentate gyrus (DG). The second part deals with adult neurogenesis focusing on the DG hippocampal neurogenic niche. In particular, on the precise cellular composition and the multiple regulatory mechanisms underlying the function of the adult DG neurogenic niche. Finally, the last part describes the process of neuroinflammation and its known effects on the adult hippocampal neurogenic niche. Here, the main topics are the complex immune-to-brain communications, the description of neuroprotection mediated by estrogenic compounds like SERMs, and a report on the role of tamoxifen as a neuroprotectant and tool used for inducible and conditional mutagenesis.

**Chapter II** reports part of a paper published in Cell Reports in July 2018 concerning the role of the transcription factor COUP-TFI in the adult hippocampal neurogenesis (Bonzano, Crisci, et al., Cell Reports, 2018). In this study, I am the second author, and I contributed to the experimental design and procedures as well as to the analysis of data related to neuroinflammation that is the main subject of this chapter. Besides, an appendix reports the full published paper, including additional experiments.

**Chapter III** describes data on the neuroprotective effect exerted by tamoxifen in the adult DG neurogenic niche in a mouse model of LPS-induced neuroinflammation. For this work, I performed part of the experiments and collected part of the data in the laboratory “Brain development and Physiology”, directed by Dr. Wojciech Krezel, at the Institute of Genetics and Molecular and Cellular Biology (IGBMC) in Strasbourg, France. Here, I spent three months during the third year of my Ph.D. Like Chapter II, this part is organized in the manuscript format, ready for submission. In this study, I directly carried out all the experiments, analyzed the data, and wrote the manuscript with the supervision of Prof. S. De Marchis and Dr. W. Krezel and the contribution of Dr. Sara Bonzano.

**Chapter IV** provides a general discussion with an overview of the main findings of my studies and future perspectives.

**Chapter V** consists of references.

**Chapter VI** reports acknowledgments.

The appendix at the end of the thesis consists of the study published on Cell Reports , already mentioned in Chapter II.

# Summary

It is now fully accepted the existence of persisting pools of neural stem cells (NSCs) in restricted areas of the adult brain of many mammals, which originate newborn neurons throughout life, in a process known as “adult neurogenesis.” One of the main neurogenic sites in adult rodents is represented by the hippocampal dentate gyrus (DG), wherein a specialized microenvironment (i.e., neurogenic niche) harboring different cellular components contributes to the process of adult neurogenesis. There, adult NSCs localized in the subgranular zone (SGZ) undertake a multistage process characterized by proliferation, migration, and terminal differentiation into mature dentate granule neurons that functionally integrate into neuronal circuits of the hippocampus contributing to critical cognitive functions, such as learning and memory. Interestingly, adult hippocampal neurogenesis is very sensitive to biological changes determined by external and internal environment and individual behavior and experience. These changes may be beneficial or detrimental for adult neurogenesis and are strictly regulated by complex interactions between cell-intrinsic and -extrinsic factors. For example, neuroinflammation can alter the adult hippocampal neurogenic niche leading to dysfunctional neurogenesis and impaired cognitive functions. Neuroinflammation early activates the immune-to-brain communication pathways in an attempt for recovery, but sometimes may develop into chronic neuroinflammation with severe pathological consequences. At present, despite several neuroinflammatory conditions are acknowledged and treated by various anti-inflammatory and neuroprotective therapies, the effects and mechanisms of neuroinflammation on adult DG neurogenesis, and its consequences on cognitive functions are far from being fully elucidated, thus delaying the emergence of potentially new therapeutic strategies.

The main goal of my Ph.D. project has been to unravel cellular and molecular components involved in fine-tuning the DG neurogenic niche upon neuroinflammation, identifying the transcription factor COUP-TFI as a cell-autonomous driver of NSC fate choice, and defining the neuroprotective role of tamoxifen, challenging its suitability as a genetic tool under neuroinflammatory conditions.

At first, I designed and characterized an *in vivo* mouse model of neuroinflammation by exploiting peripheral injections of the endotoxin lipopolysaccharide (LPS) to assess the effects of a neuroinflammatory response in the DG neurogenic niche. Then, I observed an unbalance between neurogenesis and astrogliogenesis with concomitant downregulation of the transcriptional regulator COUP-TFI in adult hippocampal NSCs upon neuroinflammation. I thus investigated the possible role of COUP-TFI in the cell-fate decision of adult DG progenitors. To this purpose, by using an inducible retroviral-based CreERT2-LoxP system, coupled to genetic fate mapping, I achieved COUP-TFI loss- and gain-of-function approaches targeting mitotic progenitors in the SGZ/GCL of the adult hippocampal DG. Thanks to immunofluorescence analysis coupled to laser scanning confocal microscopy, I demonstrated that COUP-TFI deletion contributes to an unbalance of neuro/astrogliogenesis displaying a switch of mitotic progenitors toward a gliogenic fate. On the other side, I demonstrated that forced COUP-TFI expression is sufficient to repress astrogliogenesis and rescue neurogenesis during neuroinflammation.

The second part of my Ph.D. thesis investigates the effects of tamoxifen on the adult hippocampal neurogenic niche in naïve conditions and upon an LPS-induced inflammatory challenge. In particular, tamoxifen came to my attention during my previous research on COUP-TFI. I attempted to use tamoxifen as an activator of the Cre recombinase in CreERT2-LoxP inducible mouse lines to manipulate COUP-TFI under LPS treatment, but I failed to achieve the expected neuroinflammatory conditions in brain tissues (i.e., reactive microglia and astrogliosis). Following an in-depth analysis of the literature, I found out that tamoxifen exerts anti-inflammatory and neuroprotective functions; therefore, I planned to investigate the specific effects of tamoxifen on the DG neurogenic niche, performing the same protocol used to induce the recombination of CreERT2 mouse lines in a wild-type mouse model of LPS-induced neuroinflammation. Moreover, to specifically address the role of microglia in the DG response to LPS and tamoxifen treatments, I exploited a paradigm of oral food intake of Plexxikon (PLX5622) to ablate microglial cells from the adult mouse brain. I performed qPCR analyses to measure transcript levels of inflammatory cytokines and immunofluorescence staining coupled to confocal microscopy and image analysis for cell quantification and morphometric analyses. Interestingly, my data revealed that tamoxifen *per se* alters the expression of inflammatory molecules and microglial morphology in the adult DG and

counteracts LPS-induced changes acting on different components of the DG neurogenic niche, including NSCs, astrocytes, and newborn neurons. My results highlighted a major role of microglia in mediating the response of DG astroglia and NSCs to LPS and tamoxifen treatments, but also revealed the existence of direct effects of both LPS and tamoxifen on NSCs and newborn neurons, suggesting a possible direct interference between tamoxifen- and LPS- activated signaling pathways.

Altogether, the data obtained during my Ph.D. contributed to the characterization of the cellular and molecular mechanisms underlying the DG neuro-gliogenic response to neuroinflammation and identified a new role for the transcription factor COUP-TFI in adult hippocampal neurogenesis in physiological conditions. Finally, they add relevant information on the neuroprotective effect of tamoxifen in adult DG neurogenesis and its possible side effects in the context of inducible CreERT2-LoxP systems.

# **CHAPTER I**

# 1 Introduction

## 1.1 The adult mouse hippocampus

The hippocampus is one of the most studied brain structures in rodents as a powerful model for understanding its central role in learning, memory, spatial navigation, and behavioral processes as part of the limbic system (Ergorul and Eichenbaum, 2004; Moser et al., 2017; Zemla and Basu, 2017).

### 1.1.1 Fundamental neuroanatomical organization

The **hippocampus** or **hippocampal formation** (Figure 1) comprises three main subdivisions: the dentate gyrus (DG); the hippocampus proper, which is further subdivided into three *cornu ammonis* fields (CA1, CA2, and CA3); the subiculum (S).

All three hippocampal subregions share the characteristic three-layered structure, being part of the so-called allocortex. The hippocampal formation of the mouse appears as a bilateral C-shaped elongated structure from the septal nuclei of the basal forebrain rostr dorsally, over and behind the diencephalon, into the temporal portions of the brain caudoventrally (Witter and Amaral, 2004). The long axis of the hippocampal formation is the dorsoventral axis (with the dorsal pole located dorsally and rostrally), and the orthogonal axis defines the transverse axis (Witter, 2012). Based on “the dorsal-ventral dichotomy view,” the hippocampus may not act as a unitary structure because the dorsal and ventral hippocampal regions exhibit different patterns of gene expressions and cortical/subcortical connectivity (Witter and Amaral, 2004; Strange et al., 2014; Harland et al., 2018).

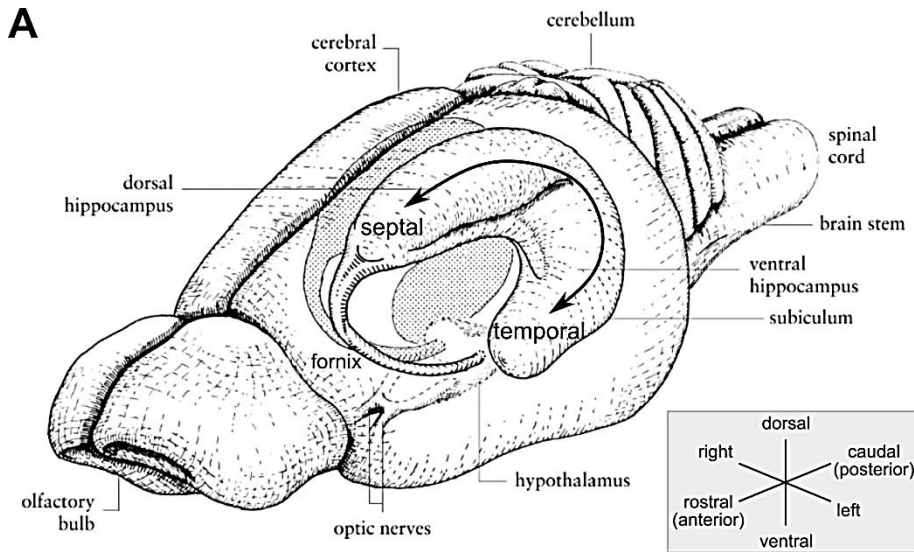


**Figure 1A. Drawings of the rodent brain.** The three-dimensional organization of the hippocampal formation is represented along the septo-temporal axis. [Modified from Witter and Amaral, 2004]

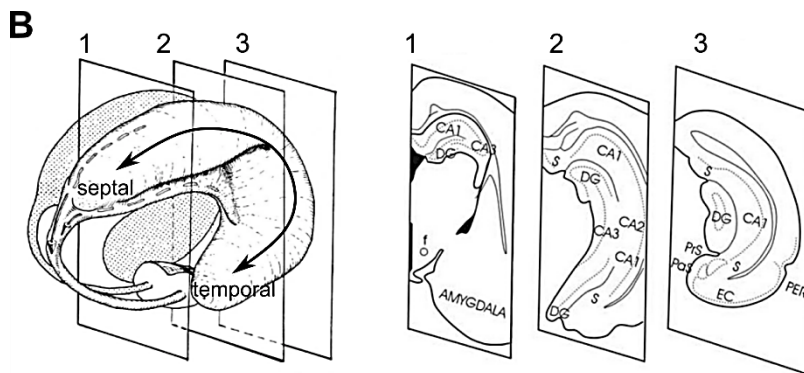


**Figure 1B. The C-shaped hippocampus following the septo-temporal axis.** Three coronal sections through the left hippocampus (1-3) are shown. CA1, CA2, CA3: cornu ammonis fields 1-3; DG: dentate gyrus; EC: entorhinal cortex; f: fornix; PER, perirhinal; POR, postrhinal; S, subiculum. [Modified from Witter and Amaral, 2004]



The **hippocampus proper** was initially divided by Ramón y Cajal into two distinct regions: the top portion, which consisted of small pyramidal neurons (*regio superior*), and the lower portion, which consisted of more giant pyramidal neurons (*regio inferior*). However, Lorente de Nó (1934) terminology has achieved more common usage dividing the hippocampus proper into three fields (CA3, CA2, and CA1). Each CA field shows peculiarity in its cellular structure, connectivity, and distinctive functions; moreover, its borders have been reliably established by protein and gene-expression data (Witter, 2012). Conversely, each CA field shows a similar laminar organization (Figure 2) which from the deepest (ventricular cavity) to the most superficial (vestigial hippocampus sulcus) consists of *alveus*, *stratum oriens*, *stratum pyramidale*, *stratum radiatum*, *stratum lacunosum-moleculare* (Amaral et al., 2007). In the CA3 field, a narrow acellular zone, called *stratum lucidum*, is located just above the pyramidal cell layer and is constituted by mossy fiber projection of DG granule cells, defining the CA3/CA2 border (Amaral et al., 2007). Several cell types distinguish the laminar organization of the hippocampus. For example, **pyramidal cells** of the *stratum pyramidale* are the primary neuronal cell type of the hippocampus characterized by a basal dendritic tree that extends into *stratum oriens* and an apical dendritic tree that extends to the hippocampal fissure. CA1 pyramidal neurons provide the principal output from the hippocampus, sending projections to many brain regions, including the neighboring subiculum, perirhinal cortex, prefrontal cortex, amygdala, as well as the retrosplenial cortex (Basu and Siegelbaum, 2015). Moreover, early Golgi studies identified various non-pyramidal cell types in *str. oriens*, *str. radiatum*, and *str. lacunosum-moleculare* of the hippocampus, primarily **GABAergic inhibitory interneurons** (Freund and Buzsáki, 1996; Witter, 2012). In mice, the overall numbers of GABAergic interneurons increase considerably from dorsal to ventral levels, and at least eight GABAergic subclasses have been differentiated by staining for specific markers, including parvalbumin, calretinin, calbindin, somatostatin, cholecystokinin, vasoactive intestinal polypeptide (VIP), and nitric oxide synthase (NOS) (Booker and Vida, 2019).

The **subiculum** has been early described by Rose (1929) as an area clearly distinguished from CA1 and the presubiculum. Although a three-layered structure, the subiculum lost *str. radiatum* and *oriens* in the laminar organization. As for CA fields, protein and gene expression contribute to delimit each region. The CA1/subiculum border is marked by an abrupt widening of the pyramidal cell layer, an abrupt loss of staining for calbindin, and increased staining

intensity of the neuropil for parvalbumin. Moreover, the staining for acetylcholinesterase (AChE) helps to establish the CA1/subiculum and subiculum/presubiculum borders (Witter, 2012). Medium-sized pyramidal neurons largely populate the *str. pyramidale*, and there are many smaller neurons, presumably representing the interneurons of the subiculum, which are intermingled among the pyramidal cells (Witter, 2012). The subiculum gives rise to longitudinal and local associational projections largely unidirectional involving its principal neurons. The subiculum receives its major intrahippocampal input from the CA1 field and entorhinal cortex (EC), while there are no direct interconnections with DG or CA2/CA3 fields. Moreover, there are numerous and robust subcortical projections to the subiculum that, in general, arise from the same sources that innervate the other hippocampal field, such as from the basal forebrain, the amygdaloid complex, the thalamus, and the supramammillary region. The subiculum is the central subcortical output structure of the hippocampal formation projecting to several cortical and subcortical regions, including the entorhinal, perirhinal, retrosplenial, medial prefrontal cortices, septal complex, and adjacent nucleus accumbens as well as to the mammillary nuclei and adjacent hypothalamic regions (Witter and Amaral, 2004).

The grey matter cortical regions that surround the hippocampus include the perirhinal cortex (PER), the postrhinal cortex (POR), the entorhinal cortex (EC), and the presubiculum and parasubiculum; these areas are collectively referred to as the **parahippocampal region**. In contrast to the hippocampus, the cortical regions forming the parahippocampal gyrus show five or six layers. The gyrus marks the transition from the hippocampus with its allocortex to the isocortical structure of the temporal lobe. The entorhinal cortex is considered the core of the parahippocampal region since it has massive reciprocal connections with the hippocampal formation and adjacent parahippocampal areas forming specific reciprocal relations with widespread cortical domains (Witter, 2012).

Moreover, fiber bundles cover the deep or ventricular surface of the subiculum and hippocampus in the so-called **alveus**. Alveus is composed of efferent fibers of the large pyramidal cells of the hippocampus, which course on the ventricular surface of the hippocampus and collect in an increasingly thicker fiber bundle called the **fimbria**. While, the **fornix**, which originates from these fibers (i.e., alveus and fimbria), leaves the hippocampus

and descends into the forebrain, connecting the hippocampus with the hypothalamus and other regions. The fornix splits around the anterior commissure to form a rostrally directed pre-commissural component and a caudally directed post-commissural component directed toward the diencephalon. Axons flow in both directions along with these fiber bundles, including the ventral hippocampal commissure (Witter and Amaral, 2004).

Among the structures of the hippocampal formation, the **dentate gyrus** (DG; Figure 2) plays a central role in many of the hippocampal-dependent cognitive functions and is among the few brain areas showing adult neurogenesis in mammalian species (Hainmueller and Bartos, 2020). The cytoarchitectonics of the DG is characterized by a transverse “V”- or “U”-shaped structure (depending on the dorsoventral position) where the upper and lower portions are called the suprapyramidal/upper blade (adjacent to CA1 field) and the infrapyramidal/lower blade, respectively, while the region joining the two blades (the apex of the V or U) is named the crest (Amaral et al., 2007).

The DG comprises three distinct layers (Figure 2) (Amaral et al., 2007; Witter, 2012):

I) the **molecular layer** (MCL) is the most superficial layer of the DG and closest to the hippocampal fissure. It is a relatively cell-free layer, mainly occupied by the dendrites of the granule, basket, and various polymorphic cells and terminal axons arbors from multiple sources, including the EC. Nevertheless, three neuronal cell-types are present: i) the basket-like cells, immunoreactive for the neuro-vasoactive intestinal peptide (VIP), with aspiny dendrites confined in the MCL; ii) the axo-axonic or “chandelier” cells, whose axons extend into the GCL to contact the axons of granule cells exclusively; and, iii) the molecular layer perforant path-associated cells (MOPP) with the cell bodies located in the deep MCL, while their axons extend outer two-thirds of MCL. These cells are GABAergic interneurons providing further inhibitory control of granule cell outputs. Besides these interneurons, many astrocytes also reside in the MCL and microglial cells (Jinno et al., 2007).

II) the **granule cell layer** (GCL) is the principal cell layer, made up primarily of densely packed small glutamatergic neurons named **mature granule cells** (GCs). GCs have an elliptical cell body with 10-12 $\mu$ m of diameter and are closely connected, forming packed columnar stacks. Also, few other cells (e.g., glial cells) interposed between them (Jinno et al.,

2007). The dendritic tree of GCs has a cone-shape with spiny branches directed apically toward the MCL, and their most distal tips end just at the hippocampal fissure or at the ventricular surface. GCs give rise to unmyelinated axons called **mossy fibers** that form synapses with the mossy cells of the hilus and with the CA3 pyramidal cells of the hippocampus proper. Mossy fiber collaterals occasionally enter the GCL, but they rarely enter the MCL under normal conditions. Moreover, many **GABAergic inhibitory interneurons** are also present in GCL characterized using various chemical markers (Freund and Buzsáki, 1996). For example, the best investigated are **parvalbumin-expressing interneurons (PVs)**, comprising fast-spiking axo-axonic cells and basket cells. PVs have extensive axonal arbors forming strong perisomatic synapses comprised of many release sites. They evoke GABA postsynaptic currents (GPSCs) characterized by two different profiles of PV-mediated neurotransmission. GPSCs with fast rise and decay phases in mature GCs control spike timing precision, while GPSCs with slow kinetics in adult-born GCs mediate activity-dependent regulation of early events in adult neurogenesis (Vaden et al., 2020). Finally, the GCL harbors **adult neural stem/progenitor cells** in the subgranular zone (SGZ), a narrow area between the deep GCL and the hilus, while their **neural committed-progenies** within two-thirds of GCL. Notably, adult NSCs located in the SGZ give rise to adult-born GCs in the process of adult hippocampal neurogenesis (Denoth-Lippuner and Jessberger, 2021).

III) the **polymorphic layer** or hilus, is the third and deepest layer of DG, which harbors many interneurons: the glutamatergic mossy cells; the fusiform-type cells; the triangular or multipolar/HICAP cells (hilar commissural-associational pathway-related cells); and the long-spined multipolar/HIPP cells (hilar perforant path-associated cell). In the hilus, the most abundant and important are the **mossy cells**. They are glutamatergic and mostly immunopositive for calretinin, whose expression levels increase along the dorsoventral axis. Interestingly, all of the proximal dendrites are covered by large and complex spines called “thorny excrescences,” which are the sites of termination of the mossy fiber axons and become smaller and simpler excrescences along the dorsoventral axis (Amaral et al., 2007). Like in MCL, astrocytes and microglia are also disseminated throughout the hilus (Jinno et al., 2007).

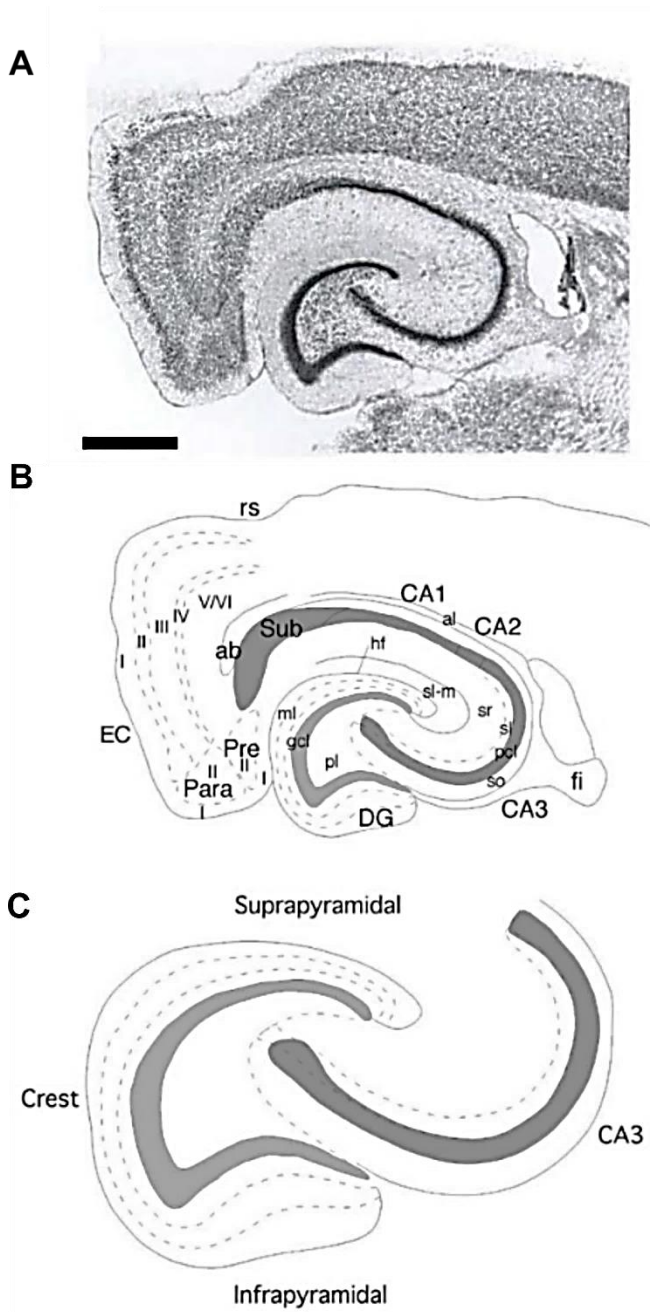


**Figure 2. Horizontal section through the rodent hippocampal formation.** (A) Nissl-stained section. (B) Line drawing shows the various regions, layers, and fiber pathways. Abbreviations: ab, angular bundle; al., alveus; CA, cornu ammonis; DG, dentate gyrus; EC, entorhinal cortex; fi, fimbria; gcl, granule cell layer; hf, hippocampal fissure; ml, molecular layer; Para, parasubiculum; pcl, pyramidal cell layer; pl, polymorphic layer; Pre, presubiculum; sl, stratum lucidum; sr, stratum radiatum; sl-m, stratum lacunosum moleculare. Roman numerals: cortical layers. (C) Schematic illustration indicates the position of the suprapyramidal blade, infrapyramidal blade, and crest of the DG. Scale bar= 500 $\mu$ m. [from Amaral and Lavenex, 2006]

### 1.1.2 Neural circuits and functional relevance

The “dorsal-ventral dichotomy view” states that the dorsal parts of the hippocampus mediate cognitive functions — particularly spatial memory — whereas ventral portions of the hippocampus are involved in emotional responses. However, differences in connectivity with cortical and subcortical structures along the dorsoventral axis of the hippocampus are gradual rather than absolute. Thus, anatomical and genetic patterns may result in more complex hippocampal long-axis functional organization, particularly in spatial processing, emotional responses, action, and episodic memory (Strange et al., 2014; Hainmueller and Bartos, 2020). At a single cell level, the integration and association of inputs build neuronal connectivities that map the temporal and spatial dimension constituting the neuronal output; these circuits result in the information flow within the brain.

In the **classical cortico-hippocampal glutamatergic circuit** (Figure 3), the primary source of cortical input to the hippocampus comes from the entorhinal cortex (EC). This polymodal sensory association area transmits both non-spatial sensory information (from the lateral entorhinal cortex [LEC]) and spatial information (from the medial entorhinal cortex [MEC]). MEC contains two largely distinct populations of principal cells: stellate cells and pyramidal cells; moreover, both types could be putative grid cells (Rowland et al., 2018). Grid cells are peculiar MEC cell types responsible for a metric organization to the neuronal representation of space (‘where’) and non-spatial variables, such as sound or time intervals; on the other hand, neurons placed in LEC represent non-spatial information, such as objects (‘what’), and object-related spatial organizations, such as egocentric behavior towards an object or previous object locations. The most well-characterized information path is the “trisynaptic loop,” where stellate cells from the superficial EC layers (LII and LIII) send excitatory projections through the perforant path (PP) to DG-GCs. Mossy fiber projections of GCs excite CA3 pyramidal neurons, which in turn excite CA1 pyramidal cells through the Schaffer collateral (SC) pathway. Finally, hippocampal CA1 back projections to the deep layers of EC and complete the loop (EC LII → DG → CA3 → CA1 → EC). In addition, all of these areas receive PP input from the EC, creating multiple parallel loops by which information can flow through the hippocampus (PP, EC → CA1 loop; PP, EC → CA3 → CA1 loop) (Basu and Siegelbaum, 2015; Hainmueller and Bartos, 2020).

In the **neoclassical cortico-hippocampal circuit** (Figure 3), CA1 neurons also receive solid excitatory input from the CA2 region of the hippocampus (CA2 → CA1). Similar to CA1 neurons, CA2 pyramidal neurons receive both direct input from LII EC neurons (EC LII → CA2) onto their distal dendrites and indirect input from the CA3 SC pathway (EC LII → DG → CA3 → CA2) onto their proximal dendrites. Also, CA2 receives weaker mossy fiber excitatory input directly from GCs (EC LII → DG → CA2). Notably, CA2 is a “transitional” zone for transmitting information to integrate a memory episode. Thus, such a direct projection from EC to CA2 indicates a much stronger excitatory stimulation to CA2 pyramidal neurons, perhaps reducing the loss of sensory information during transmission (Hainmueller and Bartos, 2020). The DG also receives neuronal inputs from **subcortical structures** that influence how DG processes the information depending on ‘global’ behavioral states, such as locomotion, awakening, or sleep. For example, cholinergic inputs from the medial septum that terminate principally on GCs are high during spatial learning but low during awake inactivity and sleep. This high cholinergic tone may increase GC firing via hilar astrocytes that release glutamate and activate GABAergic interneurons (Hainmueller and Bartos, 2020). Moreover, the DG receives a particularly prominent noradrenergic input from the locus coeruleus, which preferentially terminate in the zones occupied by mossy fibers and dopaminergic inputs from the ventral tegmental area and locus coeruleus, which facilitate memory acquisition and consolidation. Finally, from the median and dorsal divisions of the raphe nuclei, serotonergic projections depart towards the hilar region (Amaral et al., 2007). The neuroanatomical organization of the hippocampus is unique, arranged as a set of parallel loops fundamental in hippocampal information processing and mnemonic operations (Amaral et al., 2007; Hainmueller and Bartos, 2020).

In animals and humans, the activity of hippocampal neurons denotes distinct memory elements, such as individuals, places, and the associations between them. Pattern separation, pattern completion, novelty detection, contextual discrimination learning, and working memory are primary mnemonic functions related to DG. By performing conventional hippocampal lesions, animals showed severe learning and memory deficits, particularly in episodic and spatial domains. Today, advanced electrophysiological and genetic techniques (i.e., optogenetic or genetic knockout studies) are helpful tools to record the activity of identified DG neurons and their synaptic connections in rodents during memory-dependent

behaviors. (Hainmueller and Bartos, 2020). For example, optogenetic experiments have shown that temporally specific and transient inactivation of dorsal CA1 pyramidal neurons in rodents markedly impairs memory recall, i.e., the retrieval of information from the past, thus previously encoded and stored in the brain (Goshen et al., 2011). The inactivation of CA2 causes a pronounced deficit in social memory, i.e., the animal's ability to recognize and remember individual members of its species (Hitti and Siegelbaum, 2014). Specific genetic lesions or optogenetic silencing of glutamatergic MEC inputs to the CA1 impaired trace fear conditioning, a form of temporal association memory, as well as spatial working memory (Suh et al., 2011). Lesions in the DG result in an impaired ability to distinguish between closely related environments, a process termed pattern separation (Sahay et al., 2011). Interestingly, the DG is a site of adult neurogenesis, and the newborn neurons appear to be preferentially involved in pattern separation (Nakashiba et al., 2012). Although several studies demonstrated the critical role of the DG in memory encoding, the exact DG neuronal processes underlying mnemonic functions remain unresolved.

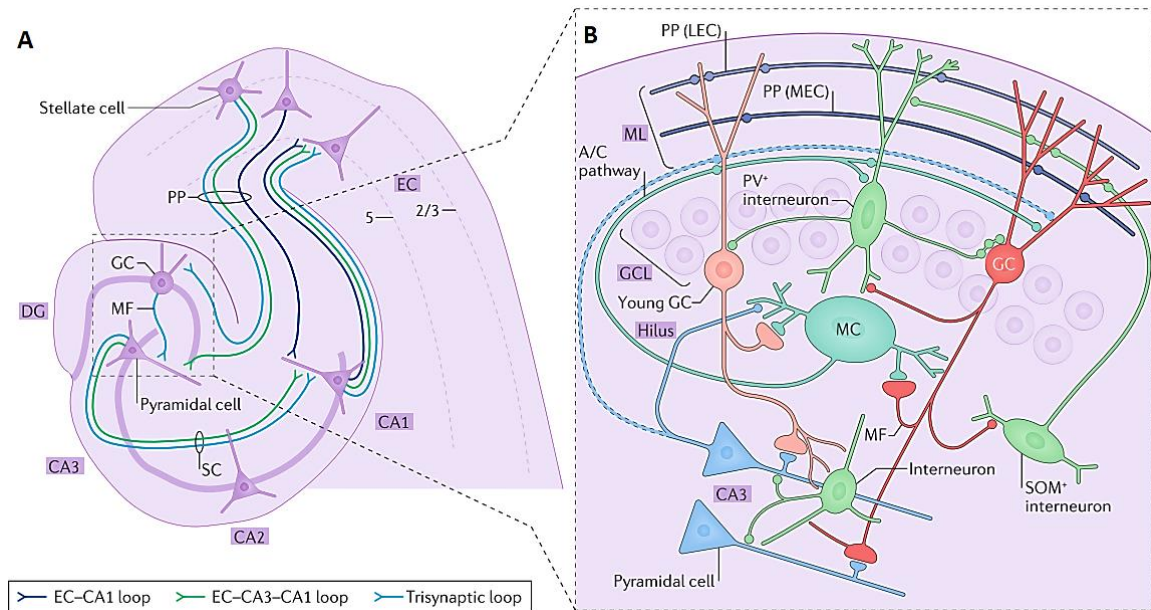


**Figure 3. The cortico-hippocampal circuit.** (A) Representation of mouse hippocampal formation and its primary synaptic connections. (B) DG microcircuitry, its intrinsic connections, and outputs to the CA3. Abbreviations: A/C, associational–commissural; CA1-3, the hippocampal fields of the Ammon’s hom; DG, dentate gyrus; GCs, granule cells; GCL, GC layer; LEC, lateral entorhinal cortex; MEC, medial entorhinal cortex; MF, mossy- fiber; ML, molecular layer; PP, perforant- path; SC, Schaffer- collateral. [from Hainmueller and Bartos, 2020]



## 1.2 The adult hippocampal neurogenesis

Adult neurogenesis generates functional mature neurons from neural stem cells (NSCs) in the adult brain. In mammals, it occurs in restricted brain regions wherein new neurons are generated throughout life and integrated into established neuronal circuits.

In the last decades, the existence of adult neurogenesis has become undisputed by several opinion articles and reviews (Gross, 2000; Specter, 2001; Kempermann, 2011b; Kempermann et al., 2018), establishing the death of the illustrious “central dogma” which denied the presence of newborn neurons into the adult mammalian brain. This dogma came from the doctrine of Ramòn y Cajal, who claimed, *“Once development has ended, the fonts of growth and regeneration of the axons and dendrites have dried up irrevocably. In adult centers, the nerve paths are fixed and immutable, everything may die, nothing may be regenerated. It is for the science of the future to change, if possible, this harsh reality”* (Cajal, 1914).

In the 1960s, the introduction of the [<sup>3</sup>H]-thymidine autoradiography technique challenged this central dogma, allowing the incorporation of the tritiated thymidine into the DNA of dividing cells that label their progeny, and, thus, their time and place of birth. The pioneering work of Altman (Altman and Das, 1965) and Kaplan (Kaplan and Hinds, 1977), using tritiated thymidine autoradiography, provided clear evidence for adult neurogenesis in rats and monkeys: in particular, they observed [<sup>3</sup>H]-thymidine-labeled cells both in the olfactory bulb and the granule cell layer of the hippocampal DG. Furthermore, using electron microscopy, Kaplan and Hinds were able to show that the labeled cells were indeed neurons with distinguishable dendrites, axons, and synapses: *“... the labeled granule cells observed in dentate gyrus and olfactory bulb of the adult rat represent newly formed neurons. A corollary of this conclusion is that the synapses found on labeled granule cells in the olfactory bulb must also have been newly formed in an adult animal. These results indicate that the old concept that the adult mammalian brain is largely static is no longer tenable ...we have confirmed that growth and plasticity, including neurogenesis and synaptogenesis, can also occur in the mature, unoperated, mammalian brain.”*(Kaplan and Hinds, 1977).

Next, in the 1980s, a trustworthy challenge to the central dogma occurred when a series of pioneering studies by Fernando Nottebohm and his colleagues showed that adult neurogenesis

occurs seasonally in the song control system of songbirds (Goldman and Nottebohm, 1983). In the 1990s, Reynolds and Weiss (1992) reported one of the first observations about the presence of neuronal progenitor cells in the adult mammalian brain. They could isolate adult brain cells *in vitro*, induce them to proliferate, and differentiate into cells with either a neuronal or astroglial phenotype (Reynolds and Weiss, 1992). Then, in the same decade, the first *in vivo* evidence for mammalian adult neurogenesis was favored by the introduction of bromodeoxyuridine (BrdU), a nucleotide analog that, unlike [<sup>3</sup>H]-thymidine, was more easily compatible with immunocytochemical staining for neuronal and glial markers in double-/triple-labeled sections, obtaining the phenotypic characterization of the dividing cells *in vivo* as neurons and/or glia (Cameron and Gould, 1994; Kuhn et al., 1996). Based on this progress, further crucial studies emerged and persuaded the scientific community that adult neurogenesis existed; from that moment, an explosion of interest in this field continues to these days. Moreover, numerous brain regions of various species such as sparrows (LaDage et al., 2011), reptiles (Font et al., 2001), and fish (Zupanc, 2006), attested adult neurogenesis, making it necessary to theorize this process within an evolutionary, comparative perspective.

Nevertheless, it is fair to note that a controversial and actual discussion still debates the existence of adult neurogenesis in humans. Ensuing the publication of two recent papers with opposite conclusions (Boldrini et al., 2018; Sorrells et al., 2018), a noted review tried to reconcile the differences concluding, with the author's words, "*...that there is currently no reason to abandon the idea that adult-generated neurons make important contributions to neural cognition and plasticity across the human lifespan*" (Kempermann et al., 2018).

Constitutive adult neurogenesis undoubtedly occurred in two "neurogenic" brain regions: the subgranular zone (SGZ) in the dentate gyrus (DG) of the hippocampus where new granule cells originate (Gonçalves et al., 2016); and the subventricular zone (SVZ) of the lateral ventricles whereby the newly generated neurons travel through the rostral migratory stream into the olfactory bulb differentiating into GABAergic interneurons (Lim and Alvarez-Buylla, 2016). Furthermore, the hypothesis exists that the subependymal zone of the third ventricle wall in the hypothalamus (hypothalamic ventricular zone, HVZ) could be another neurogenic brain region. In this latter, four types of radial glia-like tanycytes (i.e.,  $\alpha 1$ ,  $\alpha 2$ ,  $\beta 1$ , and  $\beta 2$ ) can self-renew and give rise to newborn hypothalamic neurons, astrocytes, and more rarely

oligodendrocytes, potentially involved in the regulation of energy balance (Cheng, 2013; Rojczyk-Gołębiewska et al., 2014; Feliciano et al., 2015; Yoo and Blackshaw, 2018). The adult neurogenic niches in mentioned brain areas (i.e., SGZ, SVZ, and HVZ) share features like cellular cytoarchitecture, vascularization pattern, or extracellular matrix properties but differ in the profile of NSC/progenitor cell markers and cell-type-specific molecular signatures of neuronal and glial progeny. Complex intrinsic and extrinsic cues influence each process of adult neurogenesis indiscriminately. However, an overview of these interesting canonical sites of adult neurogenesis in the mammalian brain is beyond the scope of this thesis.

In particular, the objective of my study deals with adult hippocampal neurogenesis, which is attracting considerable attention because of its relevance for cognition in health and disease (Toda et al., 2019).

### **1.2.1 The multistage process of adult hippocampal neurogenesis**

The transition from neonatal to adult DG neurogenesis occurs around the second week of life in mice. At postnatal day 14 (P14), the upper and lower blades of the DG are already present, and the source of new neurons (i.e., NSCs) becomes restricted to the neurogenic region called the subgranular zone (SGZ), a thin area between the granule cell layer (GCL) and the hilus, which starts forming around P7 to its whole from P14 onwards (Nicola et al., 2015). The SGZ neurogenic niche provides a unique permissive microenvironment for developing adult NSCs throughout a complex multistage process involving proliferation, specification, and differentiation in glutamatergic mature granule cells (GCs). Precisely, this multistage process consists of i) a precursor cell phase; ii) an early survival phase; iii) a postmitotic maturation phase; and iv) a late survival phase that culminates in the functional integration of new GCs (Kempermann et al., 2015) (Figure 4).

In the **precursor cell phase**, precursor type-1 cells (i.e., NSCs) and type-2 cells (i.e., progenitors) are two main populations, morphologically detectable, located in the SGZ. **Type-1 cells** mainly display a **radial glia-like (RGL)** morphology; however, a type-1 cell with horizontal morphology has also been identified (Lugert et al., 2010). RGL cells reside with their cell body in the SGZ and show a long radial process together with a little arbor of secondary processes extending beyond the GCL into the first third of the MCL. Moreover,

they express glial and stem cell markers such as glial fibrillary acidic protein (GFAP), nestin, brain lipid-binding protein (BLBP), and sex-determining region Y-box 2 (Sox2) (Seri et al., 2004; Gebara et al., 2016; Berg et al., 2018). On the other hand, non-radial adult NSCs show shorter horizontal processes located in the SGZ. Although abundant, radial and non-radial type-1 cells are largely quiescent (i.e., in a resting state, mostly in the G0 phase of the cell cycle) and divide slowly (Seri et al., 2001; Kempermann et al., 2004). Once activated (i.e., abandoning quiescence and entering the cell cycle), adult RGL cells can go through symmetric and asymmetric cell divisions, self-renewal, and bi-lineage differentiation. In the last years, two main models of hippocampal NSC behavior emerged. Encinas and colleagues (2011) proposed a “disposable stem cell model” in which NSC activation leads to a series of asymmetric divisions depleting the NSC pool through astrocytic (Encinas et al., 2011) or neuronal (Pilz et al., 2018) differentiation. Thus, NSC potential is intrinsically controlled, and the precursor cell population becomes exhausted with time. Bonaguidi and colleagues (2011) proposed an alternative “long-term self-renewal model” whereby hippocampal NSCs can return to quiescence after division so that the NSC pool drops slightly with age (Bonaguidi et al., 2011). Both studies might be right but show different pieces of the same matter. Recently, Guillemot’s group (2021) helps to join these conflicting models and put forward that early changes in NSC properties enable a transition from high levels of proliferation coupled with exhaustion beyond the juvenile period in mice (i.e., since P30) towards lower but sustainable levels of proliferation throughout adulthood (Harris et al., 2021). Moreover, Jessberger’s group (2021) added new information to outline a unifying hypothesis of adult NSC behavior *in vivo*, demonstrating that adult DG NSCs are heterogeneous. Indeed, they revealed at least two distinct subsets of adult DG NSCs expressing either *Gli1* (glioma-associated oncogene 1) or *Ascl1* (achaete-scute complex homolog 1), showing different properties in terms of self-renewal capabilities and depletion. In particular, *Gli1*-expressing NSCs show long-term self-renewal in the adult hippocampus, while *Ascl1*-expressing NSCs undergo limited proliferative activity once activated before they become completely exhausted (Bottes et al., 2021). Considering all these models, I illustrated a unified NSC model, depicted in figure 6. Although signs of progress, future studies are fundamental to discriminate the molecular mechanisms underlying the phenotypic heterogeneity of adult hippocampal NSCs. The RGL and horizontal type-1 cells subsequently generate **intermediate progenitor cells** (IPCs), also called **type-2**

**cells** or transit-amplifying progenitors (TAPs), representing the important stage of clonal expansion, a further step of lineage choice. IPCs rapidly divide and quickly re-enter the cell cycle a couple of times (Kronenberg et al., 2003; Encinas et al., 2011; Farioli-Vecchioli et al., 2014; Pilz et al., 2018) and comprise two subpopulations characterized by the transition from a glial/stem-like phenotype (i.e., called type 2a cells or early IPCs) to neuronal phenotype (i.e., called type-2b cells or late IPCs). Phenotypically, all type-2 cells showed an irregularly shaped cell body with relatively small and short horizontal processes (Filippov et al., 2003; Bonaguidi et al., 2011; Encinas et al., 2011). Whereas **type-2a cells** still express some glial markers such as BLBP and Sox2, as well as stem cell markers such as nestin, **type 2b cells** show the first signs of neuronal commitment, including the expression of the proneural basic helix-loop-helix factor NeuroD1, the homeobox factor Prox1, and the microtubule-associated neuronal protein doublecortin (DCX) (Brandt et al., 2003; Steiner et al., 2006; Kempermann et al., 2015). In general, IPCs guarantee the expansion of the precursors' pool required to generate a surplus of cells that might survive and mature into functionally integrated GCs (Lugert et al., 2012). Then, type-2b cells begin to undergo further differentiation to become **neuroblasts** or **type-3 cells**. Neuroblasts initially display medium/long horizontally oriented processes (early type-3 cells) and subsequently assume a more polarised morphology with dendrites projecting into MCL and axons directed to the hilus (late type-3 cells). Even if slowly proliferating, type-3 cells represent the last proliferative precursor stage in the adult DG neurogenic lineage. Indeed, after considerable tangential migration along blood vessels followed by restricted radial migration in GCL (Sun et al., 2015), neuroblasts exit the cell cycle to become early postmitotic immature neurons, transiently expressing the calcium-binding protein calretinin (Brandt et al., 2003; Ming and Song, 2011). During the **early survival phase** that defines the exit from the cell cycle and lasts approximately 2 weeks in rodents, a massive negative selection of newborn neurons occurs. This strong elimination of newborn neurons happens through apoptosis within 2 to 15 days after their generation (Biebl et al., 2000; Kempermann et al., 2003; Steiner et al., 2004; Kuhn et al., 2005; Encinas et al., 2011). This negative selection phase occurs before neuroblasts establish functional connections (i.e., axonal targeting to CA3 and dendritic spine development to receive afferent input) (Bergami and Berninger, 2012; Kempermann et al., 2015). Apparently, after this time point, only minimal changes in neuronal cell numbers occur. The subsequent **postmitotic maturation phase**

relates to establishing functional connections, growing axons and dendrites, together with the synaptogenesis of **immature granule cells** (GCs). Indeed, within few days after cell cycle exit, axons of the newborn GCs, called mossy fibers, gradually increase in length and extend into the CA3 to establish functional synapses. In parallel, the dendritic tree increases in complexity until dendritic spines arose in 17-days old cells (Zhao et al., 2006), and around at 3 weeks of age, excitatory synapses appear on the newly formed dendritic spines, which continue to develop in number and complexity over the next weeks to months (van Praag, 2002). Moreover, a late critical period is associated with the N-methyl-D-aspartate-type glutamate receptor (NMDAR)-dependent survival/death, meaning that NMDAR-dependent integration of the newborn neurons into the hippocampal circuitry determines the newborn cell survival in the third week of a cell life (Tashiro et al., 2006). Upon establishing functional glutamatergic connections, electrophysiological features characterize young GCs. Indeed, at this age, adult-born GCs are more excitable than preexisting mature ones resulting in enhanced synaptic plasticity: adult-born immature neurons have lower threshold levels than mature GCs to induce long-term potentiation (LTP) and increased LTP amplitude (Ge et al., 2007). These unique features of excitability and plasticity hallmark the late critical period where adult-born immature neurons respond to many stimuli and quickly strengthen active connections (Gonçalves et al., 2016). As newborn neurons developed further around 4 to 8 weeks of age, newborn GCs undergo refinement and a **late maturation phase** (Ge et al., 2007), where newborn neurons become morphologically and electrophysiologically indistinguishable from the older preexisting mature GCs (van Praag, 2002; Gonçalves et al., 2016).

In parallel to the neurogenic lineage, adult precursor type-1 cells may also generate astrocytes with the adult DG in mice (Steiner et al., 2004; Bonaguidi et al., 2011; Encinas et al., 2011; Kempermann, 2011b; Urbach and Witte, 2019) (Figure 5). The precise mechanisms underlying astrogliogenesis are still under debate, and two main hypotheses exist. On one side, Encinas and colleagues (2011), in their “disposable stem cell model” (already discussed above), proposed a precise scheme of the neurogenic and astrogliogenic route where adult NSCs after up to three rounds of neurogenic divisions may terminally differentiate into postmitotic astrocytes without any additional proliferative event (i.e., without production of intermediate astroglial progenitors) (Encinas et al., 2011). This mechanism of division-coupled astrocytic differentiation supports the continuous age-related decrease of the adult

NSC pool observed by Encinas' group. On the other side, Bonaguidi and colleagues (2011), through clonal analysis, support the heterogeneity of NSCs able to symmetric and asymmetric multilineage differentiation: indeed, by long-term lineage tracing, many clones consist of RGLs, neurons, and astrocytes (Bonaguidi et al., 2011). Presumably, the truth is in the middle, and these two models might coexist, meaning that postmitotic astrocytes may derive both through direct differentiation (Encinas et al., 2011; Sierra et al., 2015) and through proliferative events (also involving putative astroglial progenitors) from adult NSCs (Bonaguidi et al., 2011; Dranovsky et al., 2011; Gebara et al., 2016; Rolando et al., 2016) (Figure 5).

In conclusion, adult hippocampal neurogenesis is a complex process characterized by a continuum of cell stages within sequential developmental phases whose directionality is almost wholly defined under healthy conditions (Figures 4 and 5).

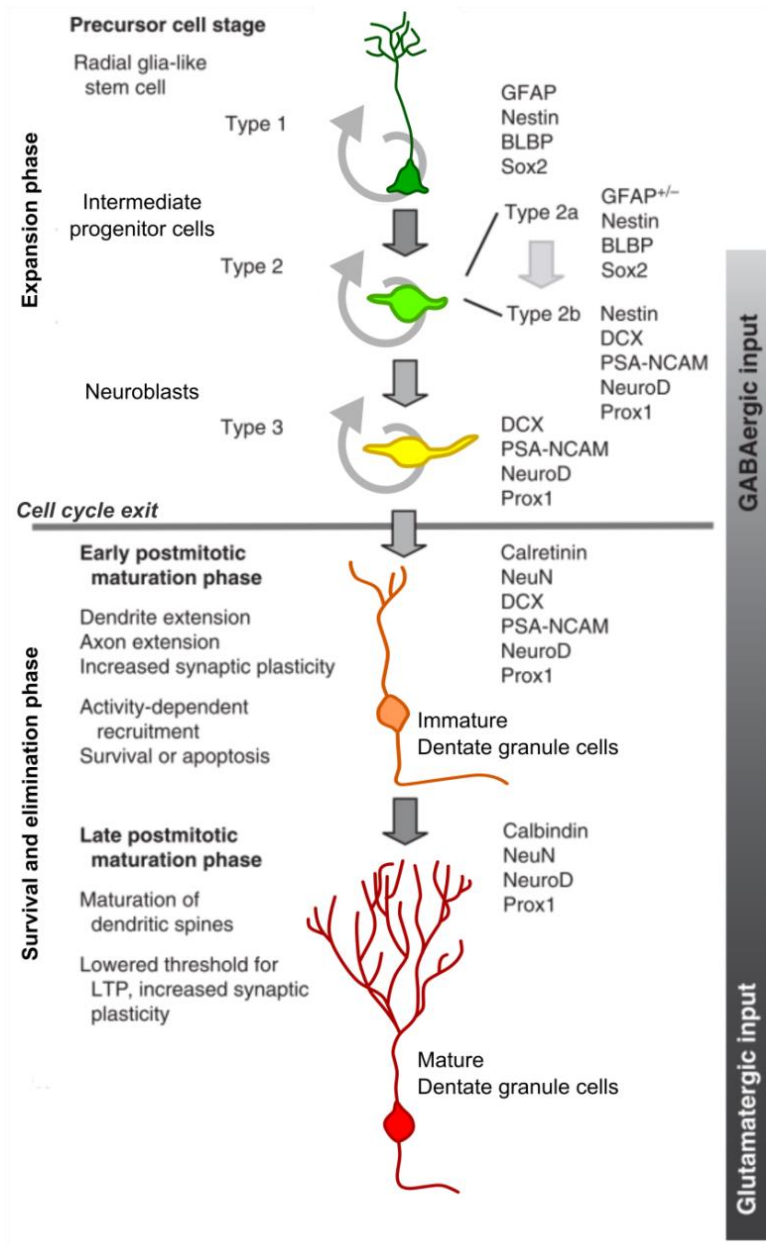


**Figure 4. The multistage process of adult hippocampal neurogenesis.** GFAP, Glial fibrillary acidic protein; BLBP, brain lipid-binding protein; DCX, doublecortin; PSA-NCAM, polysialylated-neural cell adhesion molecule; LTP, long-term potentiation. [Modified from Kempermann et al., 2015]



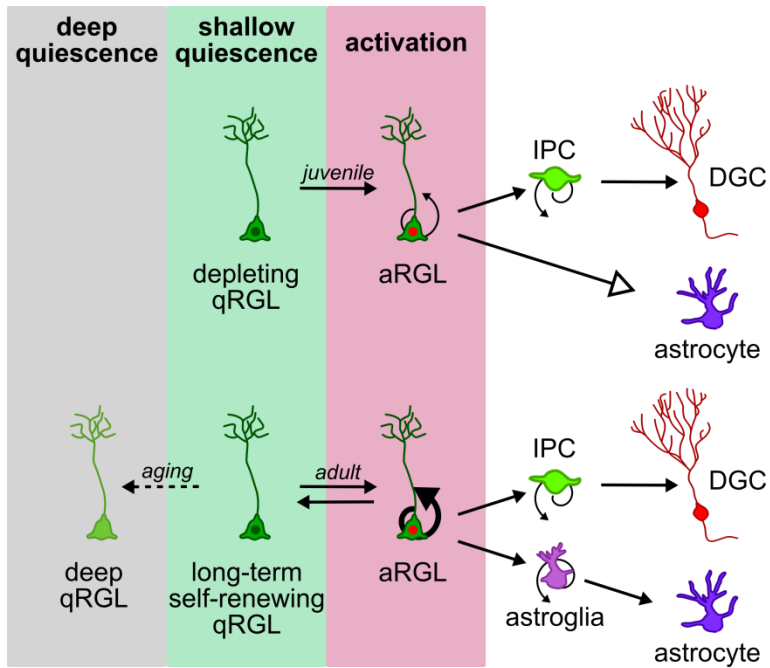


**Figure 5. A unified hypothesis of adult hippocampal neuro-gliogenesis dynamics.** qRGL, quiescent radial glia-like cell; aRGL, active radial glia-like cell; GC, dentate granule cell; IPC, intermediate progenitor cell [Adapted from Kempermann, 2011; Bonaguidi et al., 2012; Harris et al., 2021; Bottes et al., 2021]

### 1.2.2 The adult hippocampal neurogenic niche

The multistage process of adult DG NSCs represents the main critical event of adult hippocampal neurogenesis; however, further fundamental DG players determine adult neurogenesis organizing the **adult hippocampal neurogenic niche** (Figure 6), a specialized and dynamic microenvironment, which involves both cellular and molecular components of the DG. Indeed, the DG neurogenic niche is not only the *in vivo* physical location for adult NSCs; rather, precursor cells and their niche form a functional unit involved in the homeostasis of the adult DG neurogenic system. Therefore, a better understanding of the heterogeneity and complexity in the adult DG neurogenic niche has become fundamental for comprehending adult DG neurogenesis (Fuentelba et al., 2012; Bonafina et al., 2020; Vicidomini et al., 2020).

Some critical features of the DG neurogenic niche distinguish the stem cell maintenance:

1. Intercellular cross-talk, dependent on molecular signalings and direct cell-cell contact. For example, vascular endothelial cells and astrocytes regulate NSC proliferation and differentiation by physical cell-cell contact (Palmer et al., 2000; Liu et al., 2020); the ligand/receptor interactions (e.g., Notch/JAG1/DLL1 and Eph/ephrins) between NSCs and adjacent cells (Lavado and Oliver, 2014); soluble diffusible factors released by niche cells like growth and trophic factors (e.g., BMPs, WNT, IGF-1, and VEGF) (Lie et al., 2005; Seib et al., 2013); the exosomes, small membrane extracellular vesicles containing an array of proteins, lipids, and mRNAs, released by several DG niche cells (Bátiz et al., 2016).

2. Long-range and local inputs, where signaling via neurotransmitters controls NSC quiescence and activation as well as cell fate decisions. For instance, neurotransmitter gamma-aminobutyric acid (GABA) through its receptors plays a critical role in modulating DG neuronal networks since it is inhibitory in mature neurons but excitatory in immature neurons and neuroblasts and stem/progenitor cells (NSCs/NPCs) (Bao et al., 2017).

3. The extracellular matrix and associated molecules are essential components of the NSC niche, building a favorable microenvironment and architecture to sustain NSCs and neurogenesis (Cope and Gould, 2019).

4. The microglial immune cells shape neurogenesis by clearance of cell corpses, provide trophic supports for NSCs, and dynamically regulate the niche and NSCs in response to inflammation and brain damage (Sierra et al., 2014).

5. Physical parameters such as stiffness and blood flow direct NSC maintenance, proliferation, and differentiation (Keung et al., 2011).

Astrocytes, microglia, endothelial cells, and neuronal components are part of the adult DG neurogenic niche. In the following section, I describe the contribution of distinct niche cell types to adult neurogenesis. In addition, I also mention the importance of the components of the extracellular matrix (ECM) in the function of the adult neurogenic niche (Figure 6).

**Mature astrocytes** are glial cell types abundantly present in the DG neurogenic niche that provide functional and structural support for NSCs and adult-born GCs representing one of the central modulators of the DG neurogenic niche (Song et al., 2002; Araki et al., 2020). Song et al. (2002) showed that hippocampal mature astrocytes promote neurogenesis through fibroblast growth factor-2 (FGF-2) molecule by using dissociated and purified cells. Morphologically, an astrocyte has multiple processes arising from its cell body that can contact other cells as well as blood vessels (Haydon and Carmignoto, 2006). Hippocampal mature astrocytes drive the synaptic integration and connectivity of adult-born GCs within the hippocampal network by remodeling their processes to provide appropriate ensheathing glia function and allowing glutamate buffering to guide the trajectory of the nascent dendritic spines and axon terminals of new GCs (Krzisch et al., 2015). Astrocyte-derived factors such as glutamate, ATP, and D-serine regulate adult DG neurogenesis (Araki et al., 2020). For example, D-serine acts as an agonist of the N-methyl-D-aspartate receptor (NMDAR), and its concentration modulates the maturation, synaptic integration, and survival of adult-born hippocampal neurons (Sultan et al., 2015). Astrocyte-derived WNT (Wingless) ligands promote neuronal differentiation of adult DG NSCs and play a key role in hippocampal spatial memory (Lie et al., 2005; Jessberger et al., 2009). In adult animals, astrocytes store brain glycogen, which is the energy source of cells degraded on-demand to produce glucose and lactate (Brown and Ransom, 2007); interestingly, astrocytes-derived L-lactate promotes adult hippocampal neurogenesis showing energetic and signaling properties (Lev-Vachnisch et al., 2019; Pöttsch et al., 2021). Finally, like microglia, astrocytes act as mediators of inflammation

and release inflammatory cytokines (e.g., IL-6, TNF- $\alpha$ , and IFN- $\gamma$ ), underlining the role of glial cells on neurogenesis in pathological conditions (Cassé et al., 2018; Araki et al., 2020).

**Microglia** are the resident macrophages and primary immune cells of the brain responsible for many functions ranging from phagocytosis to neuroprotection (Sierra et al., 2010; Ekdahl, 2012; Rodríguez-Iglesias et al., 2019). In the adult DG, microglia appear homogeneously arranged in the hilus and MCL parenchyma, while in the GCL, microglial cell bodies are mainly located along inferior and superior borders extending their processes inside the densely populated GCL (Wirenfeldt et al., 2003; Jinno et al., 2007). A recent study emphasized the functional role of phagocytic microglia as a sensor of local cell death, necessary to modulate the balance between cell proliferation and cell survival in the DG neurogenic niche (Diaz-Aparicio et al., 2020). In the brain parenchyma, microglia exclusively express the fractalkine receptor, CX3CR1, which binds the chemokine, CX3CL1, also known as neurotactin or fractalkine, mainly expressed by neurons. The fractalkine-CX3CR1 signaling represents a pathway for direct communication between neural cells and microglia, fundamental for normal brain development (Paolicelli et al., 2011). In the adult DG, mice lacking CX3CR1 exhibit dysfunctional microglia, reduced cell proliferation, and decreased synaptic integration of adult-born GCs (Vukovic et al., 2012; Bolós et al., 2018). Moreover, brain-wide ablation of microglia becomes a practical approach to clarify the roles of these cells in biological processes. The principal methods of microglial depletion include toxin-based, genetic, and pharmacological approaches to inhibit colony-stimulating factor 1 receptor (CSF1R), which is essential for microglial cell survival (Green et al., 2020). In hippocampal DG, diphtheria toxin-aided MG ablation showed a reduction in the survival of newly formed neuroblasts without affecting their origin and maturation, revealing unique properties of DG microglia in the hippocampal neurogenic niche (Kreisel et al., 2019). Finally, the contribution of microglia to the adult DG neurogenic niche depends on cytokine and chemokine release whose pro- and anti-inflammatory profile derives from the type of stimulus (Monje et al., 2003; Cacci et al., 2005; Ekdahl et al., 2009) and from the temporal component that determines whether activated microglia induce or inhibit neurogenesis (Cacci et al., 2008). A better description of microglia activation occurs in a later paragraph of this chapter.

**Endothelial cells** exert their influence over adult DG neurogenesis throughout the so-called “hippocampal vascular niche” described by Palmer and Gage (2000), which first proposed the unique and robust link between neurogenesis and angiogenesis by showing clusters of proliferating neuronal, glial, and endothelial precursors associated with the vasculature in the SGZ (Palmer et al., 2000). Later, other studies described RGL stem cells also in contact with blood vessels (Gebara et al., 2016; Moss et al., 2016). Endothelial cells are a direct source of neurogenic factors such as brain-derived neurotrophic factor (BDNF), vascular endothelial growth factor (VEGF), and chemokines including CCL11, which in turn affect adult NSCs proliferation and neuronal maturation (Cao et al., 2004; Licht and Keshet, 2015). Moreover, endothelial cells represent the primary transporter within tissues providing signaling molecules secreted by local or distal sources within the adult DG niche, including trophic factors, hormones, lipids, and exosomes (Licht and Keshet, 2015; Bátiz et al., 2016). The functional relationships between the vasculature and adult DG neurogenesis emerged by experiments on running to study the effects of aerobic exercises on adult DG neurogenesis. Indeed, besides discovering the pro-proliferative effect of exercise on neurogenesis (Van Praag et al., 1999; van Praag, 2009), specific comparisons between running and sedentary mice demonstrated that exercise increased the surface area and perimeter of DG blood vessels in young animals (Van Praag et al., 2005). Another group showed that running increased the density of blood vessels in the GCL of DG in adult mice in concomitance with increased neurogenesis (Clark et al., 2009), supporting the positive correlation between exercise, adult neurogenesis, and cerebral blood volume in the adult DG (Pereira et al., 2007). Since hippocampal vasculature changes occur during aging and many pathologies are coupled to decreased metabolic supply and neurogenesis, further research is necessary to broaden our understanding of the neuro-glia-vascular network in adult hippocampal neurogenesis.

**Extracellular matrix (ECM)** is a complex and dynamic network of macromolecules with different physical and biochemical properties such as glycoproteins (e.g., tenascin C), proteoglycans (bearing heparan sulfate, chondroitin sulfate, or dermatan sulfate side chains), and cell adhesion molecules that surrounds cells to provide a functional scaffold for maintaining signaling gradients and stiffness. The mechanical properties of the ECM, such as stiffness, have been shown to modulate adult NSC behavior and fate *in vitro* by using a synthetic, interfacial hydrogel culture system (Saha et al., 2008; Keung et al., 2011). For

example, the Rho family of GTPases that regulate the assembly and activity of cytoskeletal processes transduce mechanical ECM-derived signals such as cellular stiffness as biophysical regulators of NSC lineage commitment (Keung et al., 2011). The modulation of adult DG neurogenesis by ECM is complex, as ECM molecules can act by interacting directly with cellular receptors or indirectly as modulators of soluble factors (Mosher and Schaffer, 2018; Bonafina et al., 2020; Vicidomini et al., 2020). Among ECM molecules, the extracellular glycoprotein reelin and the laminin receptor  $\beta$ 1-integrin are crucial regulators of adult DG neurogenesis (Teixeira et al., 2012; Porcheri et al., 2014).

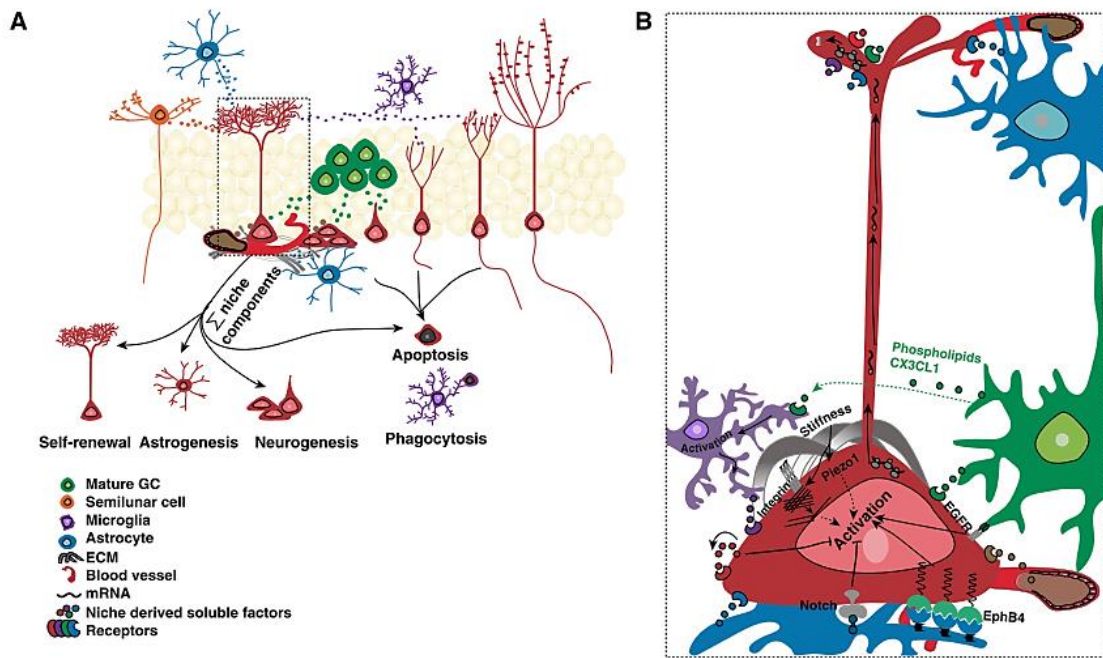


**Figure 6. Cellular and molecular components of adult DG neurogenic niche.** (A) Different niche components may release ligands and/or physically interact with discrete domains of NSCs and their progeny. (B) Magnification of RGL in dashed line box in (A) conveying niche-derived secreted ligands (astrocyte-derived factors [blue]; vasculature-derived factors [brown]; mature GC-derived factors [green]; and microglia-derived factors [purple]) signal in paracrine or juxtacrine modes. NSCs and progenitors may regulate their fate choices by autocrine signaling (red). ECM regulates NSC behavior through ligands, such as laminin, reelin, and stiffness-dependent modulation of Piezo signaling in NSCs. [from Vicidomini et al., 2020]

### 1.2.3 The regulation and function of adult hippocampal neurogenesis

Adult hippocampal neurogenesis is a complex process, and many different factors are involved in its “regulation,” meaning that these regulators act on the basic mechanisms that “control” neurogenesis. Therefore, these two terms, “control” and “regulation” of adult DG neurogenesis, are not equal: “control” refers to the genetic and molecular programs of adult neurogenesis; while “regulation” refers to the intrinsic or extrinsic factors that could promote or suppress neurogenesis (Kempermann, 2011a; Aimone et al., 2014). Indeed, adult NSC activation and commitment of their progeny to specific cellular identities are controlled by extrinsic regulatory factors such as experiential, environmental, pathophysiological, and pharmacological signals, integrated into a defined gene expression pattern (Zhao et al., 2008; Sun et al., 2011; Encinas and Fitzsimons, 2017). The integration of these extrinsic signals occurs through the mediation and functional interface of transcription factors (TFs), representing the primary controllers of gene transcription. In the following sections, I overview some of the most important players within adult hippocampal neurogenesis.

#### 1.2.3.1 Intracellular and extracellular players

Cell-intrinsic and cell-extrinsic mechanisms regulate different aspects of adult neurogenesis (Figure 7). Cell-cycle regulators, transcription factors, and epigenetic factors are major **intracellular players** of adult DG neurogenesis (Zhao et al., 2008). In addition, microRNAs (miRNAs), which represent a class of post-transcriptional gene expression regulators, are a crucial part of the gene regulatory networks governing adult neurogenesis (Sun et al., 2011; Stappert et al., 2018). Concerning the **extracellular players**, several morphogens serve as niche signals to regulate maintenance, activation, and fate choice of adult neural precursors, including Notch, Shh, Wnts, and bone morphogenetic proteins (BMPs). Moreover, growth factors, neurotrophins, cytokines, and hormones are also significant regulators of adult neurogenesis (Zhao et al., 2008). Although many of these factors also play a role during embryonic neurogenesis and hippocampal development, the same players do not perform the same functions over time, and significant differences emerged in the adult brain modulating the activity and the plasticity of adult neurogenesis (Espósito et al., 2005; Duan et al., 2008; Ming and Song, 2011; Gonçalves et al., 2016; Abbott and Nigussie, 2020).

The **maintenance of type-1 cells** is crucial to guarantee hippocampal neurogenesis throughout life. Key determinants for the function of NSCs are their proliferative capacity and their potential for multi-lineage differentiation (“multipotency”). Cell-specific signaling molecules influence type-1 cells, including BMPs, Notch, GABA, transcription factors (e.g., Sox2, FoxO), and the repressor element 1-silencing transcription (REST) (Gonçalves et al., 2016; Abbott and Nigussie, 2020). **BMPs** are ligands that constitute the largest subgroup of the transforming growth factor-beta (TGF-beta) superfamily of cytokines (Bond et al., 2014). BMPs provide essential signals for regulating the balance between quiescence and proliferation; indeed, the high expression of BMPR-Ia receptor in type 1 cells decreased in IPCs (Mira et al., 2010). Conditional inactivation of BMPR-Ia or ablation of BMP-activated Smad4 from adult NSCs results in a transient increase in mitotic NSCs, leading to a reduction in neurogenesis, presumably because the stem cell pool becomes exhausted (Mira et al., 2010). Neural precursor cells endogenously produce BMPs, which promote a physiological neural precursor exit from the cell cycle and loss of precursor characteristics. Indeed, virally mediated overexpression of BMP4 highly increased NSC cell cycle exit and slowed down the normal maturation of neural progenitors, resulting in a long-term reduction in neurogenesis. Conversely, the BMP inhibitor Noggin is essential for the NSC maintenance in the adult DG. Thus, overexpression of Noggin promotes NSC cell cycle entry and accelerates the maturation of IPCs (Bond et al., 2014). Another important pathway maintaining the balance between quiescence and activation in adult NSCs is the canonical **Notch signaling**. It is a highly conserved and pleiotropic cell signaling system expressed during development in both invertebrates and vertebrates. In adult DG neurogenesis, acting through the RBPJ $\kappa$ -signaling pathway (Ehm et al., 2010), Notch signaling positively influences NSC proliferation leading to self-renewal and expansion of type-1 cells. Indeed, RBPj inactivation initially increased hippocampal neurogenesis by causing premature differentiation of Sox2-positive progenitors, resulting in depletion of the progenitor cell pool and suppression of adult DG neurogenesis (Ehm et al., 2010). The predominant source for Notch signaling within the adult DG is hippocampal mature astrocytes (Wilhelmsson et al., 2012). **Sonic hedgehog (Shh)** ligand initiates Hedgehog signaling and is fundamental in forming adult germinal niches in the brain. Therefore, adult NSCs in the DG likely originate from Shh-responsive progenitors in the ventral hippocampus (Ahn and Joyner, 2005; Li et al., 2013). Shh signaling is active in type-1



cells (Ahn and Joyner, 2005) and promotes cell proliferation in the adult hippocampal neurogenic niche (Lai et al., 2003). Indeed, both adult type-1 and type-2 DG progenitor cells express Shh-receptor Patched and Shh-transmembrane protein Smoothed and show a decreased proliferation upon pharmacological inhibition of Shh signaling (Lai et al., 2003). Canonical **Wnt signaling** regulates various developmental processes in the embryonic brain and controls progenitor proliferation and neuronal differentiation in adult tissues, including the adult DG. By *in vivo* lentiviral-based loss- and gain-of-function studies, it has been demonstrated that overexpression of Wnt3 is sufficient to increase adult DG neurogenesis, while by contrast blocking Wnt signaling abolishes neurogenesis almost completely (Lie et al., 2005). Moreover, lentiviral-mediated knockdown of inhibitory sFRP3 (secreted frizzled-related protein 3) induces activation of the Wnt pathway in the DG, resulting in increased activation of quiescent RGLs (Jang et al., 2013). The SRY-related HMG-box family member **Sox2** is among the most extensively studied transcription factors in NSC behavior and function. Sox2 is highly expressed in type-1 and type-2a precursor cells (Steiner et al., 2006; Lugert et al., 2010; Beckervordersandforth et al., 2015). The transcriptional regulation of Sox2 occurs via Notch/RBPJk signaling, acting on adult NSC maintenance (Ehm et al., 2010). Loss-of-function studies demonstrated that the inducible deletion of Sox2 in adult NSCs results in a strong reduction in type-1 RGLs and cell proliferation, subsequently followed by decreased numbers of newborn GCs (Favaro et al., 2009). On the other hand, Sox2 regulates the expression of several target genes to control the proliferative capability and multipotency of precursor stem cells. Indeed, Sox2 positively regulates the expression of the orphan nuclear receptor **tailless (Tlx)**, promoting proliferation and self-renewal of hippocampal NSCs through the canonical Wnt pathway (Niu et al., 2011; Shimozaki et al., 2012). Moreover, Tlx may also control NSC proliferation by suppressing pathways that promote quiescence, including cell-cycle inhibitors p53 and p21 (Niu et al., 2011). In addition, Sox2 controls the expression of sonic hedgehog (Shh) that itself drives cell proliferation and maintenance (Favaro et al., 2009). Finally, Sox2 inhibits the transcriptional activation of proneuronal genes (such as NeuroD1), which are dependent on the Wnt pathway, thereby maintaining multipotency and preventing neuronal differentiation (Kuwabara et al., 2009). Nevertheless, Sox2 can arrange the chromatin state for the proper neurogenic gene activation upon exposure to a neurogenic stimulus (Amador-Arjona et al., 2015). Other transcription factors active in

NSCs are those of the Forkhead O-box (FoxO) family, initially identified as longevity factors operating downstream from the insulin/IGF-1 signaling pathway (Kenyon et al., 1993). In particular, **FoxO3** inactivation in adult NSCs blocks the return to quiescence after proliferative events leading to long-term depletion of the NSC pool (Renault et al., 2009). Adult hippocampal NSCs express repressor element 1–silencing transcription factor (**REST**, also known as neuron-restrictive silencer factor, NRSF) (Gao et al., 2011). Loss of REST from type-1 cells promotes an early neuronal differentiation and premature exit from NSC quiescence, which triggers a depletion in NSCs at later time points and, consequently, a drop in neurogenesis (Gao et al., 2011). Multiple signaling molecules, including Notch, Wnt, and Shh, could crosstalk with REST, suggesting that it may integrate diverse signaling pathways to control neurogenesis. For example, BMP signaling induces REST/NRSF expression to maintain astrocyte identity (Beckervordersandforth et al., 2015). Also, REST is required to recruit its corepressor (CoREST) to repress target genes in adult NSCs and control stage-specific neuronal gene expression (Gao et al., 2011). The phosphatase and tensin homolog **PTEN** is a tumor suppressor and a regulator of stem cell behavior in multiple adult somatic tissues (Hill and Wu, 2009). In adult DG, PTEN deletion in quiescent RGLs reduced the overall RGL pool due to increased symmetric divisions at the expense of asymmetric ones (Bonaguidi et al., 2011). Epigenetic mechanisms, including DNA methylation, histone modifications, and non-coding RNAs, are important for maintaining cell-type-specific gene expression profiles, coordinating cell-extrinsic environmental signals and cell-intrinsic genetic programs during adult neurogenesis (Sun et al., 2011; Encinas and Fitzsimons, 2017). Moreover, the role of spatial chromatin organization in adult NSC is another critical factor. For example, the chromatin remodeling factor chromodomain helicase-DNA-binding protein 7 (CHD7) cooperates with other signals to maintain NSC into a quiescent state (Jones et al., 2015). In addition, recent works have highlighted a crucial role of post-transcriptional control of gene expression in neural progenitors of the developing and adult brain (Pilaz and Silver, 2015; Rolando et al., 2016). In the adult DG, the RNaseIII Droscha, a component of the miRNA biogenesis pathway, directly controls adult NSC maintenance and cell fate acquisition through a miRNA-independent mechanism (Rolando et al., 2016).

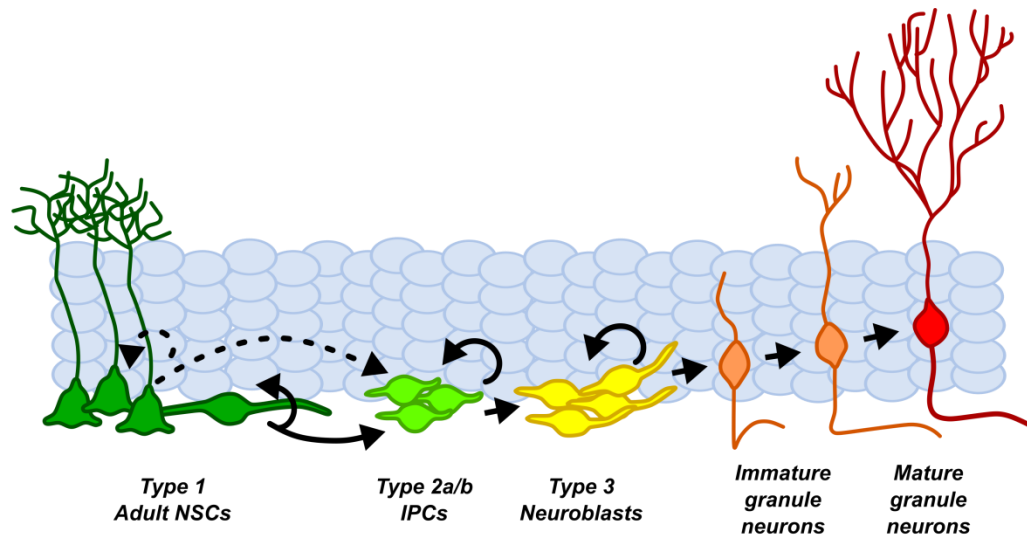
In the precursor phase, after multiple symmetric and asymmetric divisions, adult type-1 and type-2 progenitors start the decision-making process of their cell fate towards a **neuronal**

**fate commitment.** The cell-fate commitment to the neuronal lineage in adult NSCs happens from type-2a/early IPCs to type-2b/late IPCs transition. Many factors are critical during this cell-stage transition, such as *Ascl1*, *Sox21*, *Tbr2*, *Neurod1*, and *Prox1*. The proneural transcription factor achaete-scute homolog 1 (**Ascl1**, also known as *Mash1*) is predominantly expressed by the dividing type-2a precursors (Lugert et al., 2012), but also by a small subset of cycling type-1 cells (Kim et al., 2011), promoting proliferation, specification, and differentiation into neurons (Castro et al., 2011). Interestingly, NSCs react to activating signals, first by inducing expression of *Ascl1* and subsequently by leaving quiescence (Andersen et al., 2014). Indeed, the inactivation of *Ascl1* blocks the exit from quiescence and leaves NSCs unresponsive to activating stimuli (Andersen et al., 2014). Moreover, **Sox21** and **Tbr2** expression peaks in type-2a cells, and both factors display a similarly crucial role in neuronal lineage progression (Hodge et al., 2012). Blocking *Tbr2*, **NeuroD1**, or **Prox1** resulted in decreased neuronal differentiation in the adult DG niche. Thus, the expression of *Prox1* and *NeuroD1* appears to be critical to signal type-2b cells to differentiate into GCs (Hodge et al., 2012). Moreover, *NeuroD1* and *Prox1* also play a crucial role in the early survival phase. *Prox1* ablation results in cell death of *Tbr2*+ precursors and *DCX*+ immature positive neurons (Lavado et al., 2010), whereas *NeuroD1* deficiency decreased the survival of newborn neurons (Gao et al., 2009). Interestingly, some genes mentioned above still play a functional role in type-3 cells (e.g., *Wnt*, *Notch*, *NeuroD1*, and *Prox1*) (Gonçalves et al., 2016; Abbott and Niggussie, 2020). *Notch* has pleiotropic functions from proliferation to apoptosis, while *Wnt* signaling is involved in neuronal cell fate, including activation of *NeuroD1* in neuronal progenitor cells (Gonçalves et al., 2016). Additional genes are newly expressed at this stage of maturation, including brain-derived neurotrophic factor (*BDNF*), *Reelin*, cAMP response element-binding protein (*CREB*), and activation protein transcription factor (*AP-1*) (Gonçalves et al., 2016). The expression of some of these “regulatory” factors continues in immature and mature GCs during the postmitotic and late maturation phases. **Reelin**, an extracellular glycoprotein, influences neuronal fate and migration, the formation of dendritic spines, and the final integration of granule neurons into the hippocampal circuitry (Ampuero et al., 2017). The active form of transcription factor cAMP response element-binding protein (phosphorylated *CREB*, **pCREB**) is also required for the late maturation and survival of new

GCs. Loss of CREB function impairs dendritic development, decreases the expression of NeuroD and DCX, and compromises the survival of newborn neurons (Jagasia et al., 2009).

A wide range of hormones has significant regulatory effects on adult hippocampal neurogenesis and dendritic morphology (Triviño-Paredes et al., 2016). **Estradiol** is the dominant estrogen form in many species, enhances cell proliferation, and prevents cell death in the SGZ through estrogen receptors (ERs) (Galea, 2008; Mahmoud et al., 2016). Androgens, instead, comprise **testosterone** and its metabolite dihydrotestosterone which upregulates hippocampal neurogenesis (via cell survival), but not cell proliferation, through an androgen-dependent pathway in adult rodents (Galea, 2008; Spritzer and Roy, 2020). Both estradiol and testosterone display neurotrophic and neuroprotective effects with potential influence on adult hippocampal neurogenesis (Lee and McEwen, 2001; Galea, 2008). **Stress hormones**, including cortisol or corticosterone, appear to have a general inhibitory influence on hippocampal neurogenesis (Lucassen et al., 2015; Mahmoud et al., 2016). Stress increases glucocorticoids, which decreases adult neurogenesis; moreover, stress relies on morphogen signaling pathways, such as Shh and Wnt, involved in the maintenance, activation, and fate choice of adult neural precursors (Egeland et al., 2015; Lucassen et al., 2015). Instead, **thyroid hormones** promote the survival of postmitotic newborn neurons, possibly through modulation of BDNF expression (Sánchez-Huerta et al., 2016).

In parallel to neurogenesis, adult NSCs also generate astrocytes, but little is known about the regulatory factors involved in the astroglial fate commitment (i.e., astrogliogenesis) within the adult hippocampus. Many signaling pathways that occur during embryonic development are also present in adulthood, playing similar roles. In this line, because Notch signaling pathways are implicated in the balance between astrogliogenesis and neurogenesis in the developing DG (Hu et al., 2013), it could be involved in the adult DG. Another regulator of the cell fate choice (neurogenic-to-gliogenic) within embryonic NSC/progenitors is the transcription factor COUP-TFI (Naka-Kaneda et al., 2014). We recently investigated the role of COUP-TFI in the adult DG neurogenic niche and found it play a critical role in regulating the neuro-astrogliogenesis balance in the adult SGZ (Bonzano, Crisci, *et al.*, 2018). Part of the results are detailed in Chapter II, and the paper is presented as an appendix.



	Quiescence	Proliferation/ Activation	Fate specification	Morphogenesis and differentiation	Maturation
<b>Signals</b>	BMP, Notch, GABA	Canonical Wnt, IGF, Shh, FGF-2, EGF, Dopamine	Canonical Wnt, NT-3	Wnt/PCP, Notch, BDNF, Reelin, GABA	Glutamate, NRG2, Neuronal activity
<b>Transcription factors</b>	Hes5, FoxO, REST	Sox2, TLX	Tbr2, Ascl1/Mash1, NeuroD1, Prox1	NeuroD1, Prox1, CREB, AP-1	CREB
<b>Epigenetic regulation</b>	CHD7, Drosha	Gadd45b, LSD1	Fmrp, Mbd1, Drosha	Gadd45b, MeCP2	MeCP2, HDAC2

**Figure 7. Signals, Transcription Factors, and Epigenetic Regulators during Adult Hippocampal Neurogenesis.** Stage- and cell-specific effects of different signaling pathways, transcription factors, and epigenetic regulators during lineage progression. [modified from Gonçalves et al. 2016]

### 1.2.3.2 Environmental factors

Intriguing features of adult hippocampal neurogenesis are its sensitivity to different external stimuli at almost every stage (Figure 8) (Ming and Song, 2011; Toda et al., 2019). Environmental factors, such as physical activity and seizures, are nonspecific, pro-proliferative stimuli that lead to expansion and a transient increase in the potential for new neurons. However, additional survival-promoting stimuli, presumably more specific to hippocampal function such as learning and enriched environment, define the final net result of adult neurogenesis (Fabel et al., 2009; Kempermann, 2015).

**Physical activity (PA)** can be considered a nonspecific, physiological component of the enriched environment and is usually modeled in rodents by providing voluntary access to running wheels/discs. Within the DG, PA leads to a robust increase in the number of proliferating precursor cells (Van Praag et al., 1999; Kronenberg et al., 2006; Lugert et al., 2010; Farioli-Vecchioli et al., 2014; Gebara et al., 2016; Overall et al., 2016). The dynamics of precursor cell proliferation in response to running are not linear. Indeed, PA causes a transient increase in proliferation of adult type-2b cells that returns to basal levels after approximately two weeks, followed by a sustained effect on new neuron production attributed primarily to enhanced survival (Kronenberg et al., 2006). The cellular mechanism to explain PA-induced proliferation has still not been established. To date, it is clear that there is a quickening of the cell cycle after prolonged exercise (Farioli-Vecchioli et al., 2014)(Farioli-Vecchioli et al., 2014); but signals mediating the running-induced neurogenesis only recently start to be delineated, such as miR-135a and the regulator of G protein signaling 6 (RGS6) (Pons-Espinal et al., 2019; Gao et al., 2020).

**Environmental enrichment (EE)** is defined as housing conditions that provide enhanced social, physical, and sensory stimulation and is considered a specific promoting stimuli for adult DG neurogenesis. The term “enriched environment” is often used to describe an environmental manipulation administered to rodents such as larger cage areas, novel objects, and running wheels but also some social and dietary enrichment (van Praag et al., 2000; Kempermann, 2015; Zocher et al., 2020). EE modulates hippocampal neurogenesis and hippocampal-dependent cognitive capabilities, resulting in increased newborn neurons and enhanced hippocampus-dependent cognition (van Praag et al., 2000). Notably, early-life EE

determines persistent behavioral individuality (i.e., interindividual differences in behavior, brain plasticity, and epigenetic) in mice, even upon the removal of EE (Zocher et al., 2020). Exposure to EE or hippocampus-dependent learning stimuli increases the survival at the postmitotic stage in a critical time window between 2 and 3 weeks after the birth of the neuron (Steiner et al., 2008; Kempermann, 2015)(Döbrössy et al. 2003; Kempermann, 2015). Indeed, acute exposure (24 hours) to either EE-only or running wheel showed that exercise increases proliferation in early type-2a progenitor cells, whereas EE-only may exert a more specific influence on postmitotic type-3 cells (Steiner et al. 2008). Functionally, animals exposed to EE-only showed improvements in various memory functions (i.e., spatial, working, recognition, and contextual fear memory) (Birch et al., 2013; Clemenson et al., 2015). Many of these cognitive improvements may be attributed to the exploration and learning of complex environments. Many studies have revealed the underlying molecular mechanism of regulating neurogenesis by exercise and enrichment. Both EE exposure and voluntary exercise can induce the expression of BDNF, a neurotrophin that supports survival, differentiation, and neurite growth in existing neurons (Vaynman et al., 2004; Rossi et al., 2006), and VEGF, a growth factor associated with vasculogenesis and angiogenesis (Cao et al., 2004; Fabel et al., 2009; Van Der Borght et al., 2009). The effects of **learning** on the proliferation and survival of new neurons are quite complex, and it is fundamental to choose the correct investigation tasks. Indeed, not all learning paradigms and tasks are equivalent. The early and late phases of learning in the water-maze (a hippocampal-dependent spatial task) have distinct effects on adult DG neurogenesis (Döbrössy et al., 2003). An increase in cell survival occurs during the early phase of learning and involves cells that have been produced in a previous stage. An increase in cell proliferation occurs during the late learning phase and seems to involve cells generated during this phase. While it is hypothesized that cell death seems to occur during the consolidation of the memory trace suppressing neurons that have not established learning-related synaptic connections (Döbrössy et al., 2003). In general, the concept that newly formed DG neurons are the primary recipient of learning sustains the functional role for adult DG neurogenesis in pattern separation, in encoding temporal context (i.e., discrimination between the novel and familiar information), and in memory resolution (i.e., integration of spatial and nonspatial information - “where, what, and when”- into memories) (Aimone et al., 2014; Toda and Gage, 2018). Interestingly, the “**pattern separation**” theory states that two different

contexts composed of many of the same objects can be discriminated, and spatial features should be stored as distinct memories (Aimone et al., 2014; Toda and Gage, 2018). By coupling behavioral discrimination tasks to different neurogenesis knockdown approaches, strong evidence emerged to support a link between adult DG neurogenesis and pattern separation (Clelland et al., 2009; McTighe et al., 2009; Sahay et al., 2011). Lifestyle choices such as **diet** can have an impact on cognitive functions such as learning and memory. In the last years, the neurogenic roles of nutrient-sensing signaling pathways emerged, providing a connection between adult neurogenesis, nutritional imbalances, metabolic disorders, accelerated brain aging, and cognitive impairment (Aimone et al., 2014; Cavallucci et al., 2016). For example, the metabolism of fatty acids participates in NSC fate determination during adult neurogenesis (Knobloch et al., 2017); thus, a diet enriched in omega-3 fatty acids influence the fate and behavior of adult NSCs, enhancing neuroprotection by anti-apoptotic, anti-oxidative, and anti-inflammatory effects during brain impairments (Van et al., 2019). Diet effects on adult hippocampal neurogenesis may depend on calorie intake, meal frequency, meal texture, and meal content. It was shown that a reduction in calorie intake of 30–40% increases the numbers of newly generated neurons in adult DG of rodents and that this effect is partly mediated by BDNF (Lee et al., 2000; Cavallucci et al., 2016). On the other side, chronic overnutrition or metabolic imbalances deregulate nutrient signaling in the brain and potentially lead to NSC exhaustion and accelerated brain aging (Cavallucci et al., 2016). Polyphenolic-rich fruits such as blueberries enhanced DG proliferation, extracellular receptor kinase (ERK) activation, and IGF-1/IGF-1R levels in correlation with improvements in spatial memory in aged rats (Casadesus et al., 2004). Therefore, it becomes of particular interest to identify individual compounds that effectively enhance neurogenesis and cognitive function to developing dietary interventions, particularly with the elderly population. Other external factors are consistent with a decline in hippocampal neurogenesis levels, such as aging and stress. **Aging** is responsible for reductions in cell proliferation, survival, and neuronal differentiation following significant changes in the adult neurogenic niche such as increasing levels of inhibitory molecules or decreasing levels of neurogenesis-promoting factors (Kuhn et al., 2018; Mosher and Schaffer, 2018; Smith et al., 2018). In murine hippocampus, a progressive age-related decline of precursor cell proliferation occurs between 6 and 12 months of age (up to >80%), stabilizing at a low level thereafter (Kuhn et al., 1996;



Kempermann, 2015). This alteration in the cell-intrinsic response of precursor cells also occurs due to age-related epigenetic changes. For example, the age-related decline of DCX cells is associated to a significant decrease of H3K4me3, a positive epigenetic marker of chromatin accessibility, and increase of H3K27me3, a repressive epigenetic marker of compacting chromatin, at the DCX promoter resulting in its gene silencing and in the impairment of neurogenesis (Kuzumaki et al., 2010). Recently, the term “inflammaging” is born to underlie the chronic, low-grade inflammation which naturally develops in the elderly (Franceschi et al., 2018) and is linked to age-related epigenetic remodeling (Nardini et al., 2018). Interestingly, physically and mentally stimulating environments that improve adult neurogenesis and/or neuroinflammation in young animals counteract the age-related biological decline (Kuhn et al., 2018). For example, physical activity ameliorates some of the deleterious consequences of aging in mice restoring spatial learning and inducing adult neurogenesis (Van Praag et al., 2005; Kronenberg et al., 2006; Gebara et al., 2016). In addition, during aging, a dysregulation of the hypothalamic-pituitary-adrenal (HPA) system occurs even in the absence of stressful experience resulting in increased corticosteroid levels and decreased adult neurogenesis (Kempermann, 2015). Finally, **stress** is one of the best-known environmental suppressors of adult neurogenesis. Various types of stressors are used in animal studies, including physical restraint, social defeat, inescapable foot shock, and sleep deprivation (Mirescu and Gould, 2006; Schoenfeld and Gould, 2012; Lucassen et al., 2015). The main common pathway underlying stress effects on adult neurogenesis is accompanied by HPA activity, in particular the adrenal glucocorticoid hormones. Indeed, stress elevates glucocorticoid levels and stimulates glutamate release in the hippocampus resulting in an NMDA-dependent down-regulation of precursor cell proliferation in the adult DG. By contrast, removal of the adrenal glands by adrenalectomy induces cell proliferation and adult DG neurogenesis (Cameron and Gould, 1994). In a recent study, oscillations of glucocorticoid hormones preserve a dormant NSC/progenitor pool in aged mice through glucocorticoid receptors. Age-related stressful events disrupt these glucocorticoids oscillations affecting neurogenesis, and knockdown of glucocorticoid receptors reactivate NSC/progenitor proliferation in aged mice (Schouten et al., 2020). Finally, stress further influences adult DG neurogenesis by inhibiting the expression of neurotrophins and survival-promoting factors like BDNF, reducing microglia and their DG-related functional activities (Lucassen et al., 2015).

In conclusion, the effects of environmental factors (Figure 8) are complex and additive, although involving different mechanisms (Fabel et al., 2009; Aimone et al., 2014; Kempermann, 2015; Lucassen et al., 2015; Kuhn et al., 2018). Nevertheless, extrinsic factors with a positive influence on adult neurogenesis represent fundamental targets to improve neurogenic decline in several neuropathologies, such as Alzheimer’s disease, Parkinson’s disease, mood disorders, and epilepsy.

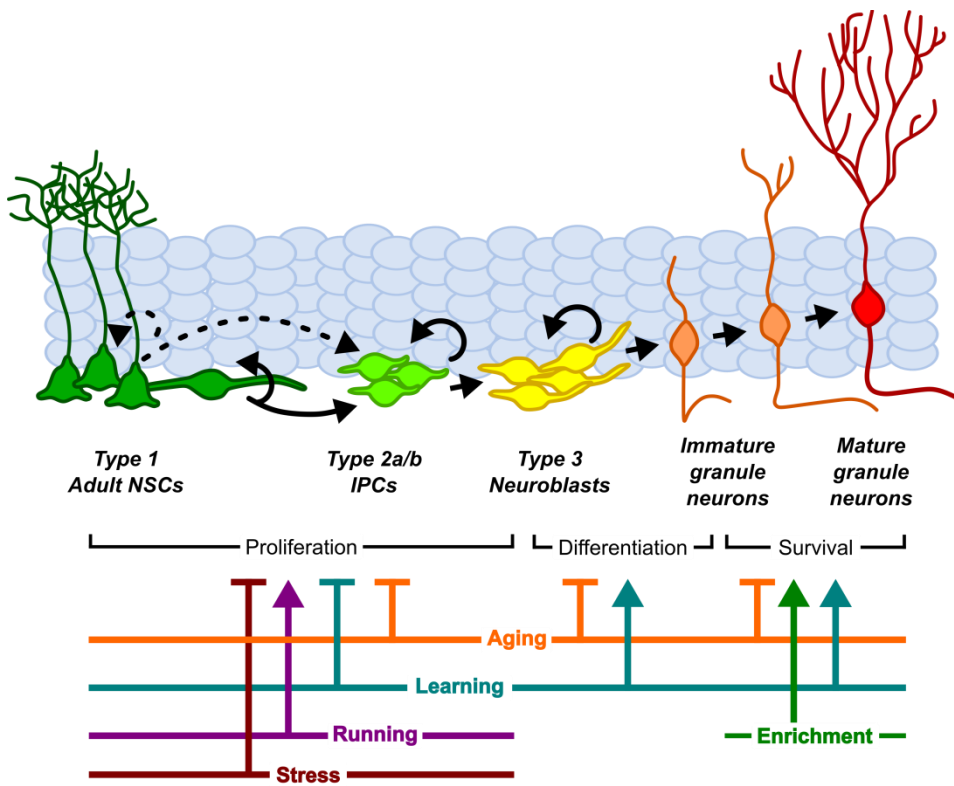


**Figure 8. Regulation of adult hippocampal neurogenesis by environmental factors.** Many behavioral factors regulate neurogenesis. Running or physical activity is one of the most potent inducers of precursor cell proliferation, and environmental enrichment exerts a complementary survival-promoting effect on newborn neurons at a critical stage of their maturation. Stress is a severe negative regulator of new neuron birth, suppressing proliferation. Learning is a more complex factor suppressing the neurogenesis process at some stages while increasing it at other stages. Aging is a detrimental factor at every stage of the neurogenic process. [modified from Aimone et al., 2014]

#### 1.2.4 Methods and mice models for studying adult hippocampal neurogenesis

*In vivo* methodological approaches capable of identifying adult NSCs and follow the fate of newly formed neurons are central for the study of adult neurogenesis.

The “expansion phase” represents an important event of adult neurogenesis and involves the cell-cycle progression of adult NSCs and IPCs. Thus, the ability to label a cohort of dividing cells *in vivo* is useful to verify the whole process of adult neurogenesis (i.e., from the proliferative events to the late maturation of newborn neurons) and to monitor changes in neurogenesis under different conditions (Kuhn et al., 2016). To this aim, the incorporation of **thymidine analogs** (such as BrdU, CldU, EdU, IdU) represents the most common and efficient method for scientists to mark the S-phase of the cell cycle in proliferating live cells and using immunohistochemical methods for their visualization (Leuner et al., 2009; Cavanagh et al., 2011). Among thymidine analogs, bromodeoxyuridine (**BrdU**) is the most used one. Depending on the protocols, these compounds are a tool for detect different cell stages and types. For example, the “pulse-chase labeling” protocol consists of single or multiple close BrdU injections to label all proliferating cells. Then, during the chase period, fast cycling cells dilute BrdU labeling by half with each cell division until the label is undetectable (in practice, 3–4 divisions for BrdU). Slow-cycling cells proliferate only rarely during the chase, retaining their BrdU labeling, thus referred to as label-retaining cells at the end of the chase. This protocol is useful to study the cell cycle properties of a mixed population of cells like heterogeneous cells harboring the adult DG neurogenic niche. Notably, pulse-chase BrdU labeling coupled to genetic lineage tracing demonstrated that BrdU+Ascl1+ type 2a IPCs divide but rapidly declines in BrdU labeling, indicating that they do not amplify the neuronal lineage (Lugert et al., 2012). Moreover, through “temporal separation” of multiple thymidine analogs, given at different time-points (e.g., double IdU/CldU labeling protocol), can be used to study total cell cycle length and estimation of the G2/M, G1, and S-phase duration (Brandt et al., 2012; Farioli-Vecchioli et al., 2014; Fischer et al., 2014). Then, a combination of thymidine analogs and endogenous cell-cycle markers, including Ki67, PCNA (proliferating cell nuclear antigen), Cdk1 (cyclin-dependent kinase 1), pHH3 (phosphohistone H3), and MCM2 (mini-chromosome maintenance 2), is also advantageous to calculate cell-cycle kinetics (Kuhn et al., 2016). Ethynyl-2'-deoxyuridine (**EdU**) represents an alternative

thymidine analog that allows detection using so-called “click chemistry” (Zeng et al., 2010), avoiding the DNA denaturation step for detecting BrdU, thereby preserving other epitopes and increasing reproducibility. BrdU labeling highlighted some limitations from dose-dependent cytotoxicity to possible artifacts in DNA-repair incorporation (Taupin, 2007; Llorens-Martín and Trejo, 2011). Besides birth-dating, immunofluorescence and fluorescence-based imaging technology are common strategies to visualize, identify, and quantify adult NSCs and their progeny in the adult brain (Figure 9). Various molecular biomarkers expressed at different cell stages during the progressions of adult hippocampal neurogenesis are used. For example, detection of neural stem/progenitor cells is usually achieved by GFAP, Sox2, Nestin, and BLBP, and their multiple labeling helps to identify different subtypes (Gebara et al., 2016; Berg et al., 2018). However, these immunohistological approaches have the disadvantage of not mark cells in live tissue. The advent of genetically encoded fluorescent proteins and improved transgenic mouse models make it possible to label live cells (Dhaliwal and Lagace, 2011). In the **constitutive gene-expression reporter mice** (Figure 9), transgenic mouse lines are generated with a transgene construct in which fluorescent-protein reporters (e.g., green fluorescent protein, GFP; or red fluorescent protein, *Discosoma sp.* derived, DsRed) are combined to the regulatory elements of a cell-type-specific gene (e.g., GFAP). With this design, reporter protein expression depends on the endogenous activity of the cell type-specific promoter (Dhaliwal and Lagace, 2011). The power of genetically encoded fluorescent reporters in adult neurogenesis studies can be observed in Couillard-Despres’ report (2006), which investigated the fundamental properties of newborn neuronal precursors in aged and young mice taking advantage of the DCX-specific expression pattern. By performing electrophysiological analysis on DCX-DsRed brains, it was found that newborn GCs are continuously generated in aged mice, although at a lower rate. However, these newborn neuronal precursors share the same physiological properties, such as the high excitability of those found in younger animals, with important implications in contrasting age-related neuronal loss and cognitive declines by stimulating neurogenesis (Couillard-Despres et al., 2006). At present, it has become more common to use **conditional and inducible transgenic mice** (Figure 9) in which the genetic manipulation and the expression of the reporter gene are usually permanent and occur in all progeny of the recombined cell (Dhaliwal and Lagace, 2011). The first created Cre/loxP system (Orban et al., 1992) is only conditional, meaning that

Cre enzyme (i.e., cyclization recombination, a member of the integrase family of recombinases) is expressed under the control of a cell- or tissue-specific promoter (e.g., Nestin-Cre mouse line). By crossing Cre-mice with mice carrying a conditional allele of a gene flanked by two loxP sites (“floxed” allele), double-transgenic conditional offspring originate with target cells expressing both Cre and loxP recombination sequences. Then, site-specific DNA recombination of target floxed gene occurs, allowing fate-mapping analysis, loss- or gain-of-function studies to inactivate or activate a target floxed gene (Dhaliwal and Lagace, 2011). However, in the conditional Cre/loxP system, many promoter genes expressing Cre are already existent in embryonic or perinatal brains, making it difficult to examine the process of adult neurogenesis independently from development (Dhaliwal and Lagace, 2011). To overcome the Cre recombination in the embryo and early postnatal mice, **CreER inducible transgenic mice** have been developed in which Cre is linked to estrogen receptor (ER) gene, allowing the temporal control of recombination through treatment with an estrogen ligand, such as tamoxifen (Dhaliwal and Lagace, 2011). To further limit the background of Cre activity and enhance the sensitivity to tamoxifen, mutant ligand-binding domains of the ER, ERT2, were developed (Indra et al., 1999; Casanova et al., 2002). Different publications described the power of the inducible CreERT2-LoxP transgenic system to study adult neurogenesis in the same period. For example, Carlén and coworkers (2006) enabled the visualization of adult NSC/progenitors and their progeny by crossing Nestin-CreERT2 mice with Z/EG recombination reporter mice, which express  $\beta$ -gal before, and GFP after Cre-mediated recombination upon five daily tamoxifen injections in adult mice (Carlén et al., 2006). Similarly, another report showed high recombination efficiency in both the SVZ and SGZ in the Nestin-CreERT2 /R26R-YFP mice (Lagace et al., 2007). Then, Mori and colleagues (2006) designed a GLAST-CreERT2 mouse line that highlighted the great potential of this inducible system for both fate mapping and functional analysis of astroglial cells in adult brains. They first characterized Cre expression's specificity under the locus of GLAST (astrocyte-specific L-glutamate/L-aspartate transporter) in astrocytes and radial glia by using classic GLAST-Cre/GFP mice. Then, upon tamoxifen administration, they investigate the cell-type specificity of inducible Cre-mediated recombination in different adult brain regions. This new mouse line, GLAST-CreERT2xR26R, targeted many of the astrocytes and adult NSCs in the dentate gyrus (Mori et al., 2006). Another report demonstrated that Cdk5 (cyclin-

dependent kinase 5) is critical for adult hippocampal neurogenesis by using inducible and conditional deletion of Cdk5 gene from either adult NSC and immature neurons in adult DG (Lagace et al., 2008). To this aim, inducible and conditional Nestin-CreERT2, R26R-YFP, and floxed Cdk5 transgenic mice were cross-breed to create Cdk5 knockout mice (nKO Cdk5). Upon the administration of the estrogen ligand tamoxifen, CreERT2 recombines DNA loxP sites progenitors, allowing YFP expression and Cdk5 deletion only in DG nestin-expressing progenitors of adult mice (Lagace et al., 2008). Moreover, they investigated the loss-of-function of Cdk5 in adult hippocampal neurogenesis, finding that Cdk5 has an essential role in the survival, but not proliferation, of adult-born hippocampal (Lagace et al., 2008). These examples showed the power and usefulness of the conditional and inducible CreERT2-LoxP system to study the dynamic and complex aspects of adult hippocampal neurogenesis, allowing the *in vivo* manipulation of endogenous genes in specific cells subtypes at a precise developmental stage.

In addition to transgenesis-based approaches, **viral vectors** represent another tool to study adult neurogenesis. The viral approach has the main advantage of localizing genetic manipulation in a precise and small brain area using stereotaxic injection, resulting in local cell transduction (Enikolopov et al., 2015). An intrahippocampal stereotaxic injection of viral vectors is necessary to manipulate adult DG neurogenesis and target only DG niche cells. However, stereotaxic injection and virus delivery are quite invasive, increasing the risk of unwanted trauma and neuroinflammation (Enikolopov et al., 2015). Several viral vectors exist regarding infection efficiency, expression levels, duration of expression, time to start the expression, host cell toxicity, and host cell preference. **Adeno-associated virus** (AAV) is a non-pathogenic and non-enveloped virus that is a member of the parvovirus family. It is naturally replication-deficient, impeding the integration into the host genome. Recombinant AAV vectors can transduce both dividing and non-dividing cells, and stable transgene expression is possible for years in postmitotic cells, while viral vector dilution occurs in dividing cells (Kotterman et al., 2015). Some AAV variants, such as wild-type AAV2/AAV6 serotype or AAVr3.45, characterize the transduction in adult DG NSCs *in vivo* (Kotterman et al., 2015). Another type of viral vector used to transduce neural cells is the **lentivirus** (LV) of the Retroviridae family, having an RNA genome, resulting in reverse transcription of cDNA that migrates to the nucleus integrating into the genome of host cells, irrespectively of their

mitotic or postmitotic state. Injection of lentiviral vectors expressing fluorescent reporters (i.e., LV PGK-GFP) in the DG of the adult hippocampus allows an efficient, strong, and long-term labeling of self-renewing adult NSCs and their progeny (Suh et al., 2018).

Moreover, to target only adult progenitors in a proliferative state, **retroviral vectors** (RV) have been engineered to integrate into the host genome only during mitosis (M-phase) when the nuclear membrane breakdown occurs (Enikolopov et al., 2015). After integration, the infected host cells and their progeny carry the reporter transgene. The high precision of RV targeting allows birth-dating and clonal analysis and a high potential for the physiological analysis of the progeny in adult neurogenesis (Enikolopov et al., 2015). Retroviral labeling through RV expressing GFP enables the functional study of GFP+ newborn DG neurons, investigating their morphological and electrophysiological properties (van Praag, 2002; Gao et al., 2007). Moreover, a retrovirus-driven Cre strategy is a broad and valuable tool to manipulate dividing cells in adult DG (Rolando et al., 2016; Sun et al., 2018). Developing an RV-mediated single-cell knockout technique in adult new neurons *in vivo* further shows the power of RV-mediated strategy in adult hippocampal neurogenesis (Tashiro et al., 2007).

Notably, the two studies described in Chapters II and III of this thesis took advantage of most of the methods described above, including immunofluorescence labeling coupled to confocal microscopy analysis, inducible and conditional CreERT2-LoxP system, and RV-Cre genetic approach to answer specific questions on adult hippocampal neurogenesis.

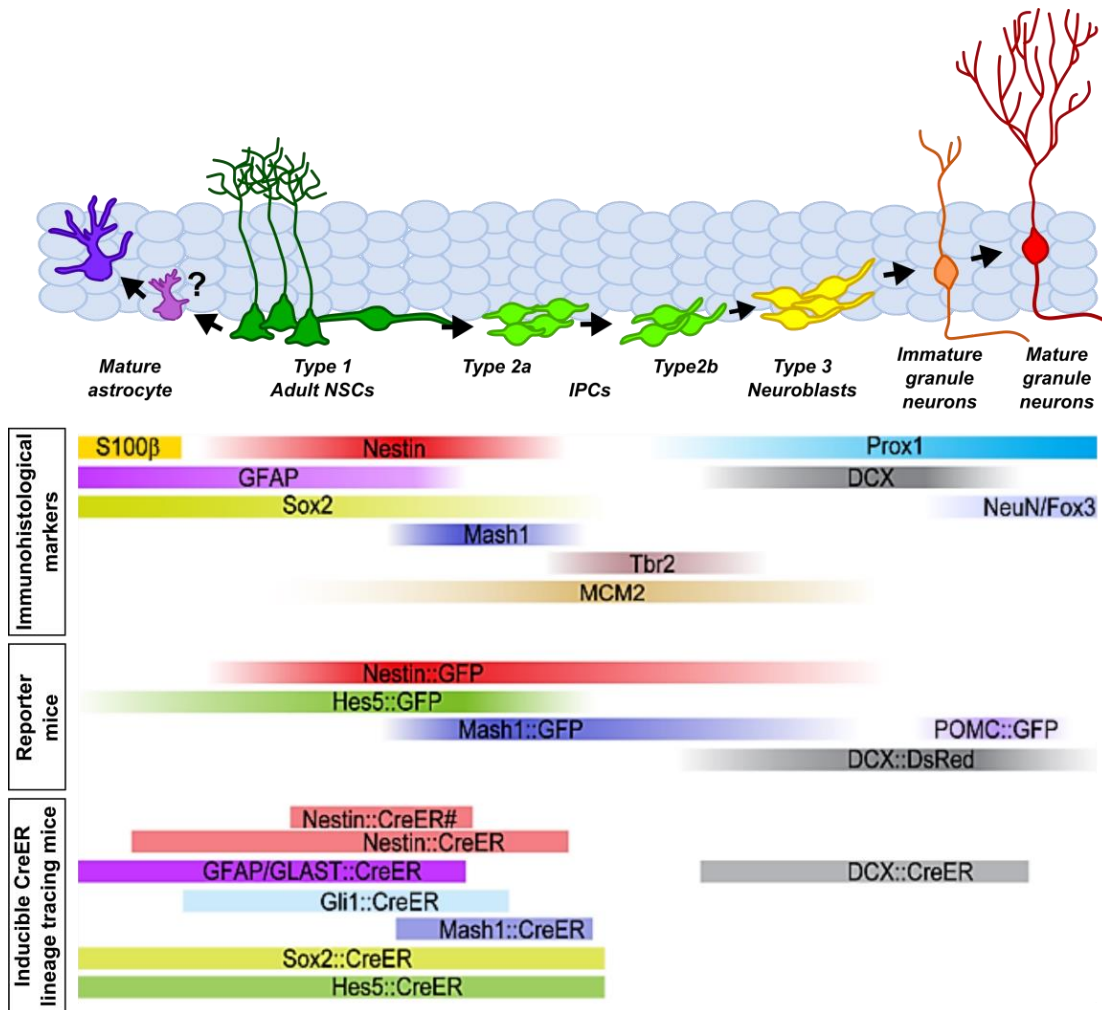


**Figure 9. Animal models used to visualize and manipulate gene expression during adult hippocampal neurogenesis.** Stage-specific markers are shown for each cell type. Mice references: Nestin-GFP (Mignone et al., 2004); Hes5-GFP (Basak and Taylor, 2007); Sox2-GFP (Couillard-Despres et al., 2006); POMC-GFP (Overstreet et al., 2004); Ascl1/Mash1-GFP (Leung et al., 2007); DCX-dsRed (Wang et al., 2007); Nestin-CreER (Balordi and Fishell, 2007; Dranovsky et al., 2011); GFAP-CreER (Favaro et al., 2009); GLAST-CreER (Mori et al., 2006); Gli1-CreER (Ahn et al., 2004); Ascl1-CreER (Kim et al., 2011); Dcx-CreER (Cheng et al., 2011); Sox2-CreER (Favaro et al., 2009); Hes5-CreER (Lugert et al., 2012); NeuroD1-CreER (Aprea et al., 2014). [modified from Bonaguidi et al., 2012]



### 1.3 Neuroinflammation in the central nervous system

For many years the concept of “immune privilege” in the central nervous system (CNS) persisted as indispensable for damage limitation during inflammation in a sensitive organ with inadequate regenerative capacity. This notion came to light in the mid-20<sup>th</sup> century based on Medawar's seminal experiments (1948) describing the brain's relative tolerance to graft (Medawar, 1948). Immune privilege has been attributed to various tissue properties of the CNS, including the presence of physical barriers (e.g., the blood-brain barrier and the blood-cerebrospinal fluid), the absence of conventional lymphatic vessels, and the lack of major histocompatibility complex (MHC) class II-expressing antigen-presenting cells (APCs) such as dendritic cells (Perry, 1998). Actually, the immune system is abundantly widespread in the CNS, as evidenced by the presence of macrophages and dendritic cells in meninges, choroid plexus, and blood-brain-barrier, as well as microglia within the brain parenchyma. Moreover, the complex neuro-immune crosstalk critically emerged under physiological but mainly pathological conditions (Galea et al., 2007; Ransohoff and Brown, 2012; Forrester et al., 2018). The peripheral inflammatory response of the innate immune system occurring under various hazardous stimuli usually leads to a mirrored immune response within the CNS, referred to as **neuroinflammation**. Different degree of neuroinflammation exists depending on the context, duration, and persistence of primary stimulus or insult. If the inflammatory response enables the resolution of inflammation in time to avoid significant and permanent cell death within the brain, then brain homeostasis is restored. If neuroinflammation is extremely strong or prolonged, then cell death within the CNS results in irreversible loss of function (McCusker and Kelley, 2013).

It came to light that neuroinflammation and its inflammatory mediators act as extrinsic cues altering the adult hippocampal neurogenic niche, ending with impaired neurogenesis (Ekdahl et al., 2003; Monje et al., 2003; Fujioka and Akema, 2010; Kohman and Rhodes, 2013). Interestingly, most of the neurodegenerative disorders in the CNS are associated with ongoing inflammation and dysfunctions of adult hippocampal neurogenesis (Taupin, 2010). In the following paragraphs, I give an overview of the process of neuroinflammation in the CNS and its cellular and molecular mediators, focusing on its effect on adult hippocampal neurogenesis.

### 1.3.1 Immune-to-brain communication pathways following peripheral inflammation

The activation of immune cells in response to pathogens and tissue injury commonly elicits inflammation, and this immune response follows a stereotypical sequence of events. Once a local innate immune signaling occurs in the periphery, outside the brain, the activated proinflammatory cascade delivers inflammatory information to the brain using humoral and neuronal communication pathways (Dantzer et al., 2008). Several murine models of neuroinflammation arose to investigate changes occurring in the inflamed CNS. The **lipopolysaccharide (LPS)-induced neuroinflammation model** is one of the most used in rodents (Catorce and Gevorkian, 2016; Batista et al., 2019). LPS is an immunogenic cell wall component of Gram-negative bacteria (e.g., *Escherichia coli*, *Salmonella enterica*, *Helicobacter pylori*) and a potent inducer of proinflammatory cytokines such as TNF $\alpha$ , IL-1 $\beta$ , and IL-6 (Moreillon and Majcherczyk, 2003). Systemic administration of LPS often occurs by intraperitoneal injection (i.p.) to achieve an inflammatory response in mice. However, LPS-induced inflammatory symptoms depend on dose and time, ranging from sickness behaviors (i.e., fatigue, social withdrawal, cognitive dysfunction, and loss of motivation) and depressed mood to chronic neuroinflammation and progressive neurodegeneration (Qin et al., 2007; Dantzer et al., 2008; Batista et al., 2019). Immune sentinel cells located throughout the body (e.g., peritoneal macrophages within the peritoneal cavity; Kupffer cells within the liver; giant cells and histiocytes within connective tissue; dust cells and alveolar macrophages within lungs; and osteoclasts within bone) (Douglas and Musson, 1986), first respond to the infectious agents by pattern-recognition receptors (PRRs). PRRs distinguish two classes of molecules: pathogen-associated molecular patterns (PAMPs) as non-self-molecules and damage-associated molecular patterns (DAMPs) as self-molecules associated with cell components or released proteins during cell damage or death (Newton and Dixit, 2012; McCusker and Kelley, 2013). The **Toll-like receptor (TLR)** family is a primary form of PRRs with specific members expressed in neuronal cells in the CNS (Konat et al., 2006; Lehnardt, 2010). In addition, several kinds of stem and progenitor cells (e.g., mesenchymal, hematopoietic, placental, and neural stem cells) express TLRs, which can determine stem cell behavior depending on the conditions, including basal motility, self-renewal, differentiation potential, and immunomodulation (Sallustio et al., 2019). So far, 13 different TLRs have been identified in mice and 10 in humans with distinct specificities to recognize general classes of

PAMPs or DAMPs (Roach et al., 2005). Their activation mostly results in the recruitment of the adapter protein Myd88 (myeloid differentiation primary response gene 88), which calls for intracellular enzymes that initiate a cascade to activate the NF- $\kappa$ B (nuclear factor kappa-light-chain-enhancer of activated B cells) pathway (Newton and Dixit, 2012). Interestingly, NF- $\kappa$ B is a "rapid-acting" primary transcription factor involved in the first response to harmful cellular stimuli. NF- $\kappa$ B nuclear translocation directly regulates the transcription of genes involved in immune responses, including pro-inflammatory cytokines such as TNF $\alpha$ , IL-1 $\beta$ , and type II interferon (IFN $\gamma$ ). In addition, alternative adaptor molecules resulted in transducing signals via a MyD88-independent pathway to express interferon (IFN)-inducible genes following TLR4 activation (Takeda and Akira, 2004; Kielian, 2006). After TLRs activation and transduction of inflammatory signals, the neural and humoral pathways provide direct input to the brain (Dantzer et al., 2008; McCusker and Kelley, 2013). In the **neural pathway** (also referred to as BBB-independent pathway), peripherally produced PAMPs and cytokines activate primary afferent nerves, such as the vagal nerves, during abdominal and visceral infections (Bluthe et al., 1994) and the trigeminal nerves during oro-lingual infections (Romeo et al., 2001). Indeed, pioneer studies found that LPS i.p. injection caused a rapid increase in *c-fos* immunoreactivity, a marker of neuronal activation, within the primary and secondary areas of projection of the vagus nerve (Wan et al., 1993). Similarly, the trigeminal nerve activated neurons within the hypothalamus known to control feeding behavior (Malick et al., 2001). Vagotomy experiments (i.e., surgically removing the vagus nerve) greatly reduced the sickness response to LPS indicating the vagal nerve as direct neural input of the infection to the brain.; however, the persistence of few signs of sickness suggested an additional pathway (Bluthé et al., 1996; Quan, 2008). Indeed, even after vagotomy, LPS i.p. injection increased IL-1 $\beta$  levels within the brain (Van Dam et al., 2000), likely related to the ability of the LPS to increase cytokine levels in circulating plasma (Gaykema et al., 2000; Hansen et al., 2000). In the **humoral pathway** (also referred to as BBB-dependent pathway), circulating PAMPs reach the brain at the level of the choroid plexus and the circumventricular organs where macrophage-like cells reside and express the TLRs (Quan, 2008). PAMPs bind to the TLRs, producing and releasing pro-inflammatory cytokines by macrophage-like cells (Newton and Dixit, 2012; Yang and Zhou, 2019). Since the circumventricular organs place outside the BBB, these cytokines reach the brain in different ways like volume diffusion in the

extracellular space (Vitkovic et al., 2000), cytokines transporters at the BBB (Banks, 2005), and IL-1 receptors located on perivascular macrophages and endothelial cells lining the brain vessels (Konsman et al., 2004). Although the prevalent concept that BBB disruption is essential to reach CNS, the non-disruptive BBB changes are evident underlying the BBB role as a signaling modulator within the neuro-immune crosstalk (Quan, 2008; Varatharaj and Galea, 2017; Banks, 2019). Finally, once peripheral factors and signals get into the brain, inflammatory signals are propagated by cytokine production from the immune brain resident microglia, principal players in neuroinflammation (McCusker and Kelley, 2013; Yang and Zhou, 2019). In this context, it is noteworthy that the hippocampus is a highly vascularized area in the brain, particularly in the SGZ, where neuronal, glial, and endothelial precursors divide into tight clusters associated with the vasculature (Palmer et al., 2000). In the so-called hippocampal vascular niche, microglia reside and act as a sensor of extrinsic cues under physiological and pathological conditions (Palmer et al., 2000; Leiter et al., 2016).

### **1.3.2 Neuro-immune crosstalk in the adult neurogenic niche**

Glial cells constitute a significant fraction of the mammalian brain (Herculano-Houzel, 2014) and, through their processes, interact with neurons, immune cells, and vasculature, mediating the neuro-immune crosstalk in the CNS (Figure 10). Glial cells include astrocytes, microglia, and oligodendrocyte lineage cells as their major components and play distinct roles under neuroinflammatory conditions (Yang and Zhou, 2019). In the adult hippocampal neurogenic niche, the largest niche-resident populations with immune properties are microglia and astrocytes (Barres, 2008; Russo et al., 2011; Lana et al., 2017; Yang and Zhou, 2019; Araki et al., 2020).

**Microglia** are distinct from other brain cells because they embryonically derive from the mesoderm; specifically, immature macrophages located in the yolk sac enter the CNS during hematopoiesis, proliferate, and afterward, differentiate in microglia (Ajami et al., 2007; Ginhoux et al., 2010; Gomez Perdiguero et al., 2015). Microglial cells are always active in “surveying” the adult neurogenic niche with their long and thin cellular processes continuously scanning the tissue microenvironment (Nimmerjahn et al., 2005). In the last years, a considerable interest increased in characterizing the molecular signature of microglia at the single-cell levels under healthy and disease conditions (Li et al., 2019a; Stratoulis et

al., 2019). Notably, DG microglia exhibit unique properties and heterogeneity compared with microglia in other brain areas (Jinno et al., 2007; Lana et al., 2017; Kreisel et al., 2019; Diaz-Aparicio et al., 2020; Tan et al., 2020). For example, DG microglia express unique transcriptome and exceptional responsiveness to VEGF, a well-known angiogenic and neurogenic factor in the DG (Kreisel et al., 2019). The transcriptome of VEGF-induced DG microglia showed upregulation of both anti-inflammatory/M2 (e.g., *Axl*, *Clec7a*, *SPP1*) and pro-inflammatory/M1 (e.g., *IL1 $\beta$* , MHC class II, *TNF*, *CD68*) genes underlying a unique MG behavior to provide a suitable “neurogenic niche” for the development of newborn DG cells (Kreisel et al., 2019). Notably, Sierra and colleagues revealed a unique phagocytic process of DG microglia, showing that the removal of apoptotic cells triggers neurogenic modulatory factors to maintain the homeostasis of the adult hippocampal neurogenic niche (Diaz-Aparicio et al., 2020). Indeed, knockout mice deficient for two phagocytic receptors, the purinergic receptor P2Y<sub>12</sub> and the tyrosine kinases of the TAM family Mer (MerTK)/Axl (i.e., P2Y<sub>12</sub> KO and MerTK/Axl KO mice models), exhibited disrupted adult hippocampal neurogenesis. Moreover, the secretome of DG phagocytic microglia reduces the production of newborn neurons (Diaz-Aparicio et al., 2020). The intriguing results of Sierra’s group strengthen microglia as a sensor of DG parenchyma and local cell death to balance proliferation and survival in the adult DG neurogenic niche.

Microglia are more sensitive to hazardous challenges; thus, they quickly and early activate in the timeline of inflammation, secreting inflammatory molecules to trigger astrocyte reactions. Activated microglia shows phenotypical characteristics like enlarged cell bodies, shorter, thicker, and more cellular processes, higher motility, and increased Iba-1 immunoreactivity (Stence et al., 2001; Davalos et al., 2005; Nimmerjahn et al., 2005; Norden et al., 2016). Under pathologic conditions, **astrocytes** contribute to innate and adaptive immune responses, and, similar to microglia, astrocytes undergo a significant transformation becoming reactive and displaying enlarged cytoskeleton, extended processes, increased GFAP expression, and glial scar formation (Ransohoff and Brown, 2012; Yang and Zhou, 2019; Zhou et al., 2019). Interaction, communication, and cooperation between microglia and astrocytes amplify the inflammatory signals to improve immune performance (Norden et al., 2016; Lana et al., 2017; Liu et al., 2020). Notably, the neuroinflammatory response is a complex cascade of molecular and cellular changes that also involve neurons. Interestingly

studies of Lana and coworkers focused on the cross-talk between microglia-astrocyte-neuron in the hippocampus under health and disease (Lana et al., 2021). In particular, they demonstrated that these triads are mainly present in the hilus of DG relating to the phagocytic process and that astrocytes and microglia differentially respond to the same insult in the three hippocampal areas (i.e., CA1, CA3, and DG) (Lana et al., 2017). Considering the neuro-glia-immune crosstalk, also **adult NSCs and neuronal lineage cells** express receptors and ligands related to the innate and adaptive immune responses, including TLRs, cytokine and chemokine receptors, major histocompatibility complex I (MHC I), cell adhesion molecules like cadherin and integrin (Rolls et al., 2007; Tran et al., 2007; Carpentier and Palmer, 2009; Covacu et al., 2009). For example, the characterization of chemokine receptors CXCR4 and CCR2 in the DG revealed coexpression with several neural progenitors markers (i.e., nestin, TLX, and the Ki67) (Tran et al., 2007). Under pathological conditions, neural progenitor cells upregulate chemokine receptors to sense chemokines and differentiate properly for repair purposes (Tran et al., 2007). Moreover, adult hippocampal NSCs and progenitors also express TLR4 and TLR2 both in vitro and in vivo, giving them the ability to respond to LPS directly and other inflammatory ligands (Rolls et al., 2007; Covacu et al., 2009). For instance, TLR2-deficient mice have impaired adult hippocampal neurogenesis, whereas the absence of TLR4 resulted in enhanced NSC/progenitor proliferation and neuronal differentiation (Rolls et al., 2007). Both activation of TLR2 and TLR4 in NSCs and progenitor cells induced the NF- $\kappa$ B-mediated gene transcription via MyD-88-dependent and independent pathways. Therefore, adult neural stem and progenitor cells seem to adapt their proliferative and differentiation capabilities upon sensing inflammatory molecules through TLRs and via a cross-talk with immune-competent cells (Rolls et al., 2007).

The detrimental effect of neuroinflammation on adult neurogenesis is well documented, although data on the cellular processes involved are still largely obscure. Ekdahl and coworkers (2003) demonstrated that activated microglia proliferate by intracortical infusion of LPS while BrdU-positive newborn neurons double-labeled for the neuron-specific marker NeuN decrease in the SGZ/GCL of adult rat hippocampus (Ekdahl et al., 2003). Remarkably, Monje and colleagues (2003) showed that even a single i.p. injection of LPS in adult rats induced an immune signaling cascade resulting in microglial activation and neurogenesis reduction by quantification of BrdU-positive cells that co-express the early neuronal marker

DCX in the SGZ/GCL (Monje et al., 2003). Interestingly, both studies found a significant negative correlation between the number of activated microglia expressing ED1 marker (also referred to as CD68, a lysosome protein indicator for phagocytic activity) in the neurogenic zone and the number of BrdU-positive newborn neurons (Ekdahl et al., 2003; Monje et al., 2003). These and other studies showed that LPS-derived inflammatory cascade inhibits neuronal maturation and survival rather than directly influencing the NSC proliferative activity (Monje et al., 2003; Bastos et al., 2008; Ekdahl et al., 2009). Nevertheless, Fujioka and Akema (2010) found that peripheral LPS administration quickly reduced the number of cells labeled with BrdU one day before sacrifice without affecting the number of BrdU proliferating cells labeled 7 or 28 days before and TUNEL positive apoptotic cells. These results suggested that LPS acutely suppresses neurogenesis in the adult DG by inhibiting neural precursors proliferation without enhancing cell death (Fujioka and Akema, 2010). In another study, Sierra and colleagues (2010) showed no significant NSC/progenitor proliferation changes either at 8 or 22 hours after LPS treatment. However, a decreased survival of 2-day-old IdU-positive cells (thymidine/BrdU analog) increased apoptosis and a concomitantly increased phagocytic activity by microglia (Sierra et al., 2010). Finally, LPS-induced detrimental effect on hippocampal neurogenesis persists long-term upon a single i.p. LPS injection, including a decrease in the number of DCX-positive newborn neurons, their volume, and their dendritic spines, followed by spatial memory deficits (Valero et al., 2014). Altogether, these conflicting data may result from many variables in the specific LPS-derived neuroinflammatory model used in the different studies: in particular, the route through which LPS reaches the brain tissue (systemic administration vs. intracerebral infusion), LPS bacterial serotype (from *Escherichia coli* to *Salmonella typhimurium*), protocols (single vs. multiple administration; different LPS doses), animal model (rat vs. mouse), murine strain and genetic background, as well as age and gender (Catorce and Gevorkian, 2016; Lopes, 2016; Erickson et al., 2018; Meneses et al., 2018).

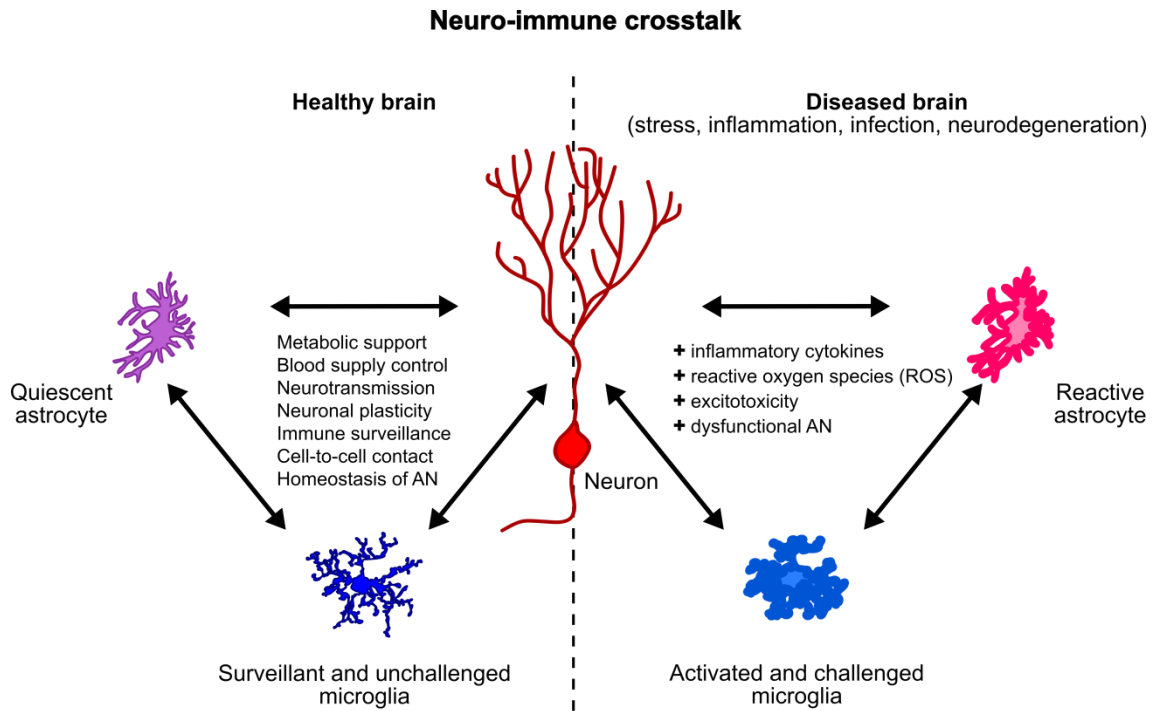


**Figure 10. A simplified schematic illustration of the neuro-immune crosstalk between neurons, astrocytes, and microglia in the CNS under physiological and pathological conditions.** Healthy neurons can communicate and regulate the activation of their neighboring glial cells. Meanwhile, both astrocytes and microglia help maintain the neuronal activity and the homeostasis of adult neurogenesis (AN). Under various diseased conditions, this homeostasis is broken so that neurons lose their controlling ability and deliver damage signals to glial cells, which may exacerbate neuronal damage through inflammation. [modified from Tian L. et al., 2012]



### 1.3.2.1 Microglial cells activation and polarization

The classical characterization of microglia by Pío del Río Hortega (1919) described microglia in two states: resting in the healthy CNS and activated in the diseased CNS (Sierra et al., 2016). Today, microglia are always active in a surveillance state, never in a quiescent or resting state, to play its central role of immune sentinel cell of the CNS. Therefore, the term “activation” simplifies the complex transformation of microglia featured by a range of many intermediate activated stages (Ransohoff, 2016; Prinz et al., 2019). Nevertheless, two different categories of activated microglia still widely exist, referred to as M1/M2 microglial polarization. The M1 classical activation involves pro-inflammatory mediators (e.g., TNF $\alpha$ , IL-6, IL-1 $\beta$ , and IFN $\gamma$  cytokines; iNOS enzyme; ROS molecules; MHC II, CD86 markers), whereas M2 alternative activation consists of anti-inflammatory ones (e.g., IL-4, IL-13, IL-10, TGF- $\beta$  cytokines; Arg1 enzyme; YM1, FIZZ1 markers)(Orihuela et al., 2016; Ransohoff, 2016). Taking advantage of single-cell advanced technologies (e.g., single-cell RNA-sequencing [scRNA-seq], single-cell mass spectrometry [cytometry by time of flight, CyTOF], and two-photon microscopy), a high degree of microglial heterogeneity recently emerged throughout different brain regions, pre- and postnatal development, adult homeostasis, and distinct pathologies (Li et al., 2019a; Masuda et al., 2019; Priller and Prinz, 2019; Prinz et al., 2019; Tan et al., 2020).

Single intraperitoneal injection of moderate LPS (dose: 0.5 - 1 mg/kg) represents a broad and suitable model for understanding the basic timeline of neuroinflammation following microglial activation (Norden et al., 2016). Microglia, firstly activated via TLR4 by LPS challenge, during the **acute activation phase** (at 2–4 h after LPS challenge), release proinflammatory mediators including IL-1 $\beta$ , TNF- $\alpha$ , and CCL2 (Norden et al., 2016). Notably, in this phase, microglia also trigger an early and weak expression of the anti-inflammatory IL-10 cytokine ready for the subsequent resolution phase. This early activated microglia still display a ramified and unchallenged morphology (Norden et al., 2016). Meanwhile, the activation of astrocytes to LPS via TLRs is almost dependent on the presence of microglia (Holm et al., 2012; Liddel et al., 2017). Indeed, in the absence of functional microglia, astrocytes are quite incapable of responding to inflammatory mediators both *in vitro* and *in vivo* (Holm et al., 2012; Liddel et al., 2017). Following activation of reactive astrocytes to








microglia-released factors, astrocytes induce a cytokine expression without any apparent morphological alterations. Finally, this acute activation phase achieves individual sickness behavior during infection, displaying depressed locomotor activity, decreased exploratory, social, and sexual behavior, reduced food and water intake, and impaired learning and memory (Dantzer, 2001; Dantzer et al., 2008; Norden et al., 2016; Batista et al., 2019).

Then, in the **transition phase** (Figure 11), by 12 h after LPS, the expression of anti-inflammatory regulatory genes such as IL-4Ra, IL-10, YM-1 reaches a peak in microglia. At the same time, astrocytes display the highest level in the expression of pro-inflammatory cytokines and chemokines (e.g., IL-1 $\beta$ , CCL2, and TNF- $\alpha$ ), but still without changes in their morphology. The acute activation and transition phases may correspond more generally to the classical activation/M1 state, where microglia potentiate phagocytic activity, increase the expression of many immune receptors. Moreover, in this phase, microglia increase phagocytic oxidase (PHOX), inducible nitric oxide synthase (iNOS), as well as the increased generation of nitric oxide (NO), the primary cytotoxic mediator in acute and chronic inflammatory responses (Norden et al., 2016; Orihuela et al., 2016).

Then, upon the inflammatory stimuli is over, a distinct molecular and cellular response attempts to restore tissue homeostasis. At this point, during the alternative activation/M2 state, microglia change their phenotype and promote the blockade of the immune response and the initiation of specific programs aimed at repairing the damaged tissue (Martinez et al., 2009). In this **resolution phase** (Figure 11), by 24–48 h after LPS, microglial pro-inflammatory cytokines and chemokines return to baseline levels, while the expression of some regulatory genes such as IL-10 and YM-1 remain at high levels. Interestingly, microglia-derived IL-10 stimulates astrocytic TGF- $\beta$  providing negative feedback on microglia, attenuating inflammation (Norden et al., 2016). Thus, in the resolution of the inflammatory response, reactive astrocytes modulate microglial activation. For example, GABAergic astrocytes secrete GABA sensed by GABAergic microglia, suppressing the reactive inflammatory response of astrocytes and microglia (Lee et al., 2011). Moreover, many astrocytic-derived soluble factors regulate microglial levels of ROS preventing excessive inflammatory microglial responses (Min et al., 2006). Notably, inflammatory mediators account for trophic effects and tissue-remodeling functions, including remodeling of the extracellular matrix

(Dzyubenko et al., 2018), angiogenesis (Muramatsu et al., 2012), and in neural stem cell niches, adult neurogenesis (Battista et al., 2006; Mathieu et al., 2010; Araki et al., 2020).

In conclusion, the response of glial cells to inflammatory stimuli is finely regulated by a well-timed synthesis of pro-inflammatory and anti-inflammatory molecules for an early response in the presence of insults before returning to a surveying stage as the immune emergency is over (Figure 11). Failure of such homeostatic mechanisms usually results in **chronic neuroinflammation** in which an excessive, prolonged, or asynchronous immune activation leads to severe pathological consequences, ranging from chronic pain and epilepsy to neurodegeneration and psychiatric disorders (Perry et al., 2007; Jha et al., 2012; Liaury et al., 2012; Perry and Holmes, 2014; Batista et al., 2019; Araki et al., 2020).

Sequential glial activation after LPS i.p. challenge				
Timing	2-4 h post LPS	8-12 h post LPS	24-48 h post LPS 1x	24-48 h post LPS 4x
Behavior	Active Sickness Behavior	Resolving Sickness Behavior	Recovered Sickness Behavior	
Microglia profile	"Active Phase" Microglia	"Transition" Microglia	"Resolution" Microglia	
Microglia morphology	 "Ramified/unchallenged"		 "Reactive/challenged"	
Microglia markers	+++IL-1 $\beta$ , TNF $\alpha$ , IL-6, CCL2 +++ IL-4R $\alpha$ , IL-10 ++Acute phase	+IL-1 $\beta$ , TNF $\alpha$ , IL-6, CCL2 +IL-4R $\alpha$ , IL-10, YM-1 ++Acute phase	+IL-10, YM-1 +Acute phase +Iba-1	++YM-1 ++Acute phase +Iba-1
Astrocyte morphology				
Astrocyte markers	-TGF $\beta$	++TNF $\alpha$ , CCL2 +IL-1 $\beta$	+TGF $\beta$ +GFAP	+TGF $\beta$ +GFAP

**Figure 11. Time course of microglial and astrocyte activation upon LPS-induced sickness behavior.** The table summarizes the molecular and morphological alterations of microglia and astrocytes after the peripheral LPS challenge. Activation, transition, and resolution are the three phases illustrated. [modified from Norden et al., 2016]

### 1.3.2.2 Pro- and anti-inflammatory mediators

Inflammatory mediators are pleiotropic and multifunctional; indeed, a dynamic and continuously shifting balance between pro-inflammatory cytokines and anti-inflammatory components exist (Mathieu et al., 2010; Yang and Zhou, 2019; Araki et al., 2020).

**Tumor necrosis factors (TNFs)** are a family of cytokines known to cause apoptosis. Although TNF- $\alpha$  is overexpressed under inflammation and mainly acts like pro-inflammatory and neurotoxic cytokines, it is also present in the brain under healthy conditions. In the context of adult hippocampal neurogenesis, the effect of TNF- $\alpha$  in healthy and diseased conditions depends on the type of TNF receptors (TNF-Rs) involved (Pickering and O'Connor, 2007). For example, TNF- $\alpha$  produced by astrocytes enhances synaptic efficacy by increasing surface expression of AMPA receptors in both cultured hippocampal neurons and hippocampal slices, while a soluble form of TNF-R1 functions as a TNF- $\alpha$  antagonist (Beattie et al., 2002). Other reports demonstrated that the signaling through TNF-R1 abolishes neuronal progenitor proliferation and neurogenesis, whereas binding of TNF- $\alpha$  to TNF-R2 improves the proliferation and survival of newly formed hippocampal neurons (Cacci et al., 2005; Iosif et al., 2006). Moreover, blocking TNF- $\alpha$  by an antagonist antibody reduces the number of striatal and hippocampal neuroblasts generated after stroke, suggesting a possible neuroprotective action of TNF- $\alpha$ -mediated via TNF-R2 (Heldmann et al., 2005). Exposure of hippocampal neural progenitor cells to TNF- $\alpha$  during differentiation but not proliferation leads to a detrimental neurogenic effect mediated through increased expression of Hes1, a transcription factor that negatively regulates neurogenesis by antagonizing pro-neuronal genes (Keohane et al., 2010).

**Interleukin-1 (IL-1) and its single receptor (IL-1R)** are constitutively expressed in the hippocampus (Ban et al., 1991; Pickering and O'Connor, 2007). Similar to TNF- $\alpha$ , endogenous IL-1 $\beta$  shows physiological neuromodulator roles in the adult brain, positively modulating hippocampal LTP, learning, and memory processing (Schneider et al., 1998; Depino et al., 2004). However, in pathological conditions, DG progenitor cells highly express IL-1R that mediate the decrease of cell proliferation via the NF $\kappa$ B signaling pathway showing a critical role as an anti-neurogenic mediator (Ja and Duman, 2008). *In vivo* conditional loss-of-function of MyD88 in nestin-positive hippocampal cells promotes astrogliogenesis through

the inhibition of TLR2 signaling only in the presence of sustained IL-1 $\beta$  expression. In contrast, MyD88 deficiency does not alter the cell fate in the absence of inflammation. These results show a MyD88-independent and indirect negative effect of sustained IL-1 $\beta$  on adult hippocampal neurogenesis (Wu et al., 2013). Finally, elevated levels of IL-1 $\beta$  in the brains of patients affected by neurodegenerative diseases alert the immune system. Indeed, in early amyloid pathogenesis, IL-1 $\beta$  overexpression reprograms the molecular and cellular profile of microglia in such a way to enhance amyloid plaque clearance (Rivera-Escalera et al., 2019).

**Interleukin-6 (IL-6)** is a small multifunctional protein and is the ligand of membrane-bound IL-6 receptor (mIL-6R) in the “classical signaling” or the soluble form IL-6 receptor (sIL-6R) in the “trans-signaling” (Gadient and Otten, 1997), and of the membrane-bound  $\beta$ -subunit glycoprotein 130 (gp130), ubiquitously expressed (Wolf et al., 2014). In the classical signaling, IL-6 binds to IL-6R and gp130 receptors leading to IL-6-signal transduction, which includes activation of JAK/STAT, ERK, and PI3K signal transduction pathways (Wolf et al., 2014). sIL-6R is formed physiologically either by proteolysis of the extracellular domain of mIL-6R or by alternative splicing of the IL-6R mRNA (Wolf et al., 2014). In contrast to classical signaling with anti-inflammatory features, sIL-6R trans-signaling is responsible for the pro-inflammatory effects of IL-6 (Scheller et al., 2011). This pleiotropic cytokine plays either detrimental and beneficial roles in various neurological conditions (Campbell et al., 2014; Codeluppi et al., 2014; Rothaug et al., 2016). In the GFAP-IL6 transgenic mouse model, astrocytes drive the production of IL-6, and GFAP-IL6 mice exhibit a localized neuroinflammatory and neurodegenerative disorder associated with a decreased adult hippocampal neurogenesis (Vallières et al., 2002; Campbell et al., 2014). Blocking trans-signaling via a soluble form of gp130 (sgp130) rescues neurogenesis (Campbell et al., 2014). In spinal cord injury, IL-6 is beneficial for recovery after injury (Codeluppi et al., 2014). It seems that IL-6 plays different roles depending on the timeline of inflammation, localization, and production levels. Indeed, even though there is no serum circulating IL-6 after spinal cord injury, a high level of IL-6 mRNA was detected in astrocytes, neurons, and microglia, suggesting that these cells locally secrete IL-6 in the recovery phase (Codeluppi et al., 2014). Moreover, IL-6 trans-signaling participates in a neuroprotective and pro-regenerative phenotype of repopulating microglia in hippocampal DG neurons (Willis et al., 2020). Finally, IL-6, as a neuro-immunoregulatory cytokine, modulates inflammatory mediators by inhibiting

the effect of IFN- $\gamma$ , IL-1 $\beta$ , and TNF $\alpha$  in glial cells (Shrikant et al., 1994; Van Wagoner et al., 1999) and regulates hippocampal adenosine A1 receptors under excitotoxicity with a beneficial impact on neuronal survival (Biber et al., 2008).

**Interleukin-4 (IL-4) and its functional IL-4 receptor (IL-4R)** are present on hippocampal DG GCs, and their activated signaling cascade exerts an anti-inflammatory effect by down-regulating both IL-1R and IL-1 $\beta$  expression (Nolan et al., 2005). Interestingly, decreased hippocampal IL-4 concentration occurs in age-related and LPS-induced impairment of LTP, and the rescue of IL-4 levels results in the maintenance of LTP with beneficial cognitive functions (Nolan et al., 2005). Another study showed that vasoactive intestinal peptide (VIP), a neuropeptide released by DG interneuron, induces microglia-derived IL-4, promoting the proliferation of neuronal progenitors (Nunan et al., 2014). In Alzheimer's disease APP1/PS1 mouse model, external and force expression of IL-4 into the hippocampus results in reduced glial activation, amyloid- $\beta$  peptide oligomerization and deposition, and enhanced neurogenesis (Kiyota et al., 2010). By *in vitro* analysis on neural progenitor cells, IL-4 administration promotes a neuroprotective microglia phenotype that correlates with the down-regulation of TNF- $\alpha$  and the up-regulation of insulin-like growth factor 1 (IGF-1) signaling pathway (Butovsky et al., 2006). Interestingly, IL-4-stimulated microglia induce oligodendrogenesis, whereas IFN- $\gamma$ -activated microglia promotes DG neurogenesis from adult NSCs/progenitor cells (Butovsky et al., 2006). Finally, the hippocampal-BDNF-signaling pathway acts through IL-4R for successful learning and reference memory (Brombacher et al., 2020).

**Transforming growth factor- $\beta$  (TGF- $\beta$ )** is constitutively expressed at low levels in the adult CNS and up-regulated in glial cells under inflammatory conditions (Finch et al., 1993). TGF- $\beta$  acts as an anti-inflammatory cytokine that inhibits the synthesis of pro-inflammatory mediators such as TNF- $\alpha$ , prostaglandins, and NO, thus promoting the resolution of inflammation (Mathieu et al., 2010). TGF- $\beta$  is also an endogenous neurotrophic factor exerting neuroprotective roles (Boche et al., 2003; Battista et al., 2006). TGF- $\beta$ 1 mRNA expression was reported to increase in response to signals from dying cells within the SGZ/GCL of hippocampal DG during aging, thus protecting neurons from the progression of the apoptotic cascade (Bye et al., 2001). Other studies demonstrated that TGF- $\beta$ 1 expression

levels are context-dependent, determining differential roles in adult hippocampal neurogenic niche from maintaining stem cell quiescence to neuronal differentiation, maturation, and survival of newborn neurons (Daynac et al., 2014; Kandasamy et al., 2014). Indeed, in the healthy DG, a persistent expression of TGF- $\beta$ 1 is required for homeostasis, while in the diseased or aged DG, elevated TGF- $\beta$ 1 levels induce cell cycle arrest, blocking proliferation and driving the disease/age-related declines in neurogenesis (Daynac et al., 2014; Kandasamy et al., 2014). Moreover, in animals deprived of their adrenal gland as a model to identify factors modulating neurogenesis, microglia activation occurs following a positive correlation between increased neurogenesis, activated microglia, and elevated TGF- $\beta$  expression in the GCL of DG (Battista et al., 2006). Finally, in Alzheimer's disease, the hyperphosphorylation of tau protein impairs the TGF- $\beta$  signaling pathway, compromising its neuroprotective action and contributing to neurodegeneration (Baig et al., 2009).

In conclusion, pro-and anti-inflammatory cytokines play differential roles in healthy and diseased brains. Their regulation is rigorously controlled, and their final positive or negative contribution to the neurogenic niche depends on their concentration, balance, the secreting-cell type, and the parallel action of other secreted factors in the microenvironment.

### **1.3.3 Inflammation and neuroprotection**

Neuroprotection can be defined as the challenge to preserve cellular and molecular homeostasis in the brain, resulting in the overall maintenance of cognitive function (Ehrenreich et al., 2001). Neuroprotection implies protecting neural functions, preventing cell death, restoring functional activities in damaged neurons, and maintaining neuronal numbers (Ehrenreich et al., 2001). Two categories of neuroprotection mainly exist prophylactic and therapeutic. Prophylactic neuroprotection means the prevention of functional loss before it occurs. Therefore, this prevention depends on the knowledge and identification of predictors/risk factors (e.g., genetic or environmental) about the pathogenesis of brain dysfunction to modulate the disease-related signaling pathways. On the contrary, therapeutic neuroprotection acts when the damage is ongoing and promotes safeguard and recovery of remained functions as much as possible (Ehrenreich et al., 2001). An example of endogenous neuroprotection happens in the “preconditioning or tolerance” phenomenon, which was introduced firstly in 1964 by Janoff (Janoff, 1964). This term indicates a weak stimulus

resulting in protection against more deleterious secondary insults. Indeed, the first insult below the threshold primes the system and reprograms an adaptive response involving multiple genes of cellular defense/survival strategies (Stenzel-Poore et al., 2007). In the endotoxin (e.g., LPS) preconditioning, repeated low-dose exposures to endotoxins lead to neuroprotective function characterized through a unique microglia phenotype leading to enhanced anti-inflammatory function or repair allowing protection from the hyper-inflammatory conditions associated with CNS injury (Rosenzweig et al., 2007; Chen et al., 2012; Schaafsma et al., 2015; Norden et al., 2016).

Endogenous neuroprotection naturally occurs in the local synthesis of steroids by the brain. Indeed, the brain is a steroidogenic organ as it expresses all the molecules and enzymes necessary for converting cholesterol into steroids, such as progesterone, testosterone, and estradiol (Arevalo et al., 2015). These neurosteroids regulate different neurobiological processes and physiological parameters, such as cognition, stress and anxiety, body temperature, blood pressure, feeding, and sexual behaviors. Moreover, neurosteroids provide endogenous neuroprotective cues in different animal models of neuroinflammation, neurodegeneration, cognitive decline, and mood disorders (Garcia-Segura and Balthazart, 2009; Arevalo et al., 2015). Among steroidal hormones, estrogens play a pivotal role in CNS as neuroactive, neurotrophic, and neuroprotective hormones (Behl, 2002; Bustamante-Barrientos et al., 2021). Endogenous estrogens are cholesterol-derived sex hormones consisting of one benzene ring, a phenolic hydroxyl group, and a ketone group (estrone, E1), or one (17 $\beta$ -estradiol, E2), two (estriol, E3), or three (estretrol, E4) hydroxyl groups; 17 $\beta$ -estradiol/E2 is the most prevalent and potent form of circulating estrogen, also in human (Behl, 2002). Extra-gonadal sites of estrogen biosynthesis exist, and in the CNS, astrocytes, neurons, and ependymal cells can synthesize estradiol (Acaz-Fonseca et al., 2014; Larson, 2018). Notably, ER ligands consist of five main categories: endoestrogens, phytoestrogens (non-steroidal compounds produced by plants like isoflavones), xenoestrogens (non-natural synthetic chemical compounds with estrogenic effects like bisphenol-A), selective estrogen receptor modulators (SERMs, like tamoxifen), and metalloestrogens (inorganic compounds in the form of heavy metal ions like aluminum, Al<sup>3+</sup>) (Fuentes and Silveyra, 2019). Binding to estrogen receptors (ERs), ER $\alpha$  and ER $\beta$ , and G-protein coupled ER1 (GPER1), inducing a direct or indirect genomic signaling to change the expression pattern of several genes (Figure



12) (Fuentes and Silveyra, 2019). In the direct genomic signaling, once activated, classical ERs dissociate from heat shock protein, dimerize, translocate to the nucleus, inducing transcriptional changes in estrogen-responsive genes to induce/repress transcription. In the indirect genomic signaling, the membrane-bound receptor GPER1 induces cytoplasmic events such as modulation of membrane-based ion channels, second-messenger cascades (such as CREB, MAPK, and PI3K), and transcription factors. Moreover, ligand-independent ER signaling also exists (Figure 12), mainly activated by phosphorylation on specific residues (e.g., serine and tyrosine) in the receptors themselves or their association with coregulators, integrators of signals controlling gene expression and transcriptional activity. The ER-independent mechanism needs many regulatory molecules, including kinases (e.g., PKA, PKC, MAPK), inflammatory cytokines (e.g., interleukin-2), cell adhesion molecules (e.g., heregulin), cell cycle regulators (e.g., RAS p21 protein activator) (Fuentes and Silveyra, 2019).

Several reports demonstrated that estrogenic compounds play critical roles in brain homeostasis, particularly in neurogenesis, gliogenesis, and regulation of the neuroprotection/neurodegeneration balance (Tanapat et al., 2005; Hajszan et al., 2007; Barha et al., 2009; Mahmoud et al., 2016; Larson, 2018; Bustamante-Barrientos et al., 2021). Finally, evidence of the distribution of ER $\alpha$ , ER $\beta$ , and GPER1 in the adult DG highlighted the estrogenic effects on adult DG neurogenesis. Indeed, by *in situ* hybridization, detection of ER $\alpha$  and ER $\beta$  mRNA occurs on proliferating (i.e., Ki-67+) and differentiating cells of neuronal phenotype (i.e., DCX+) in the SGZ/GCL of adult DG in rats (Isgor and Watson, 2005). Moreover, BrdU-labelled cells showed protein expression of ER $\alpha$  and ER $\beta$  in the SGZ/GCL of rats treated with estradiol (Perez-Martin et al., 2003). Finally, NSC from the embryonic and adult brains are immunoreactive for both ER $\alpha$  and ER $\beta$ , and western blot and RT-PCR analyses confirmed the presence of ERs in adult NSCs in rat hippocampus (Brännvall et al., 2002). GPER-expressing cells are also localized in the SGZ/GCL of adult DG (Brailoiu et al., 2007; Duarte-Guterman et al., 2015; Waters et al., 2015).

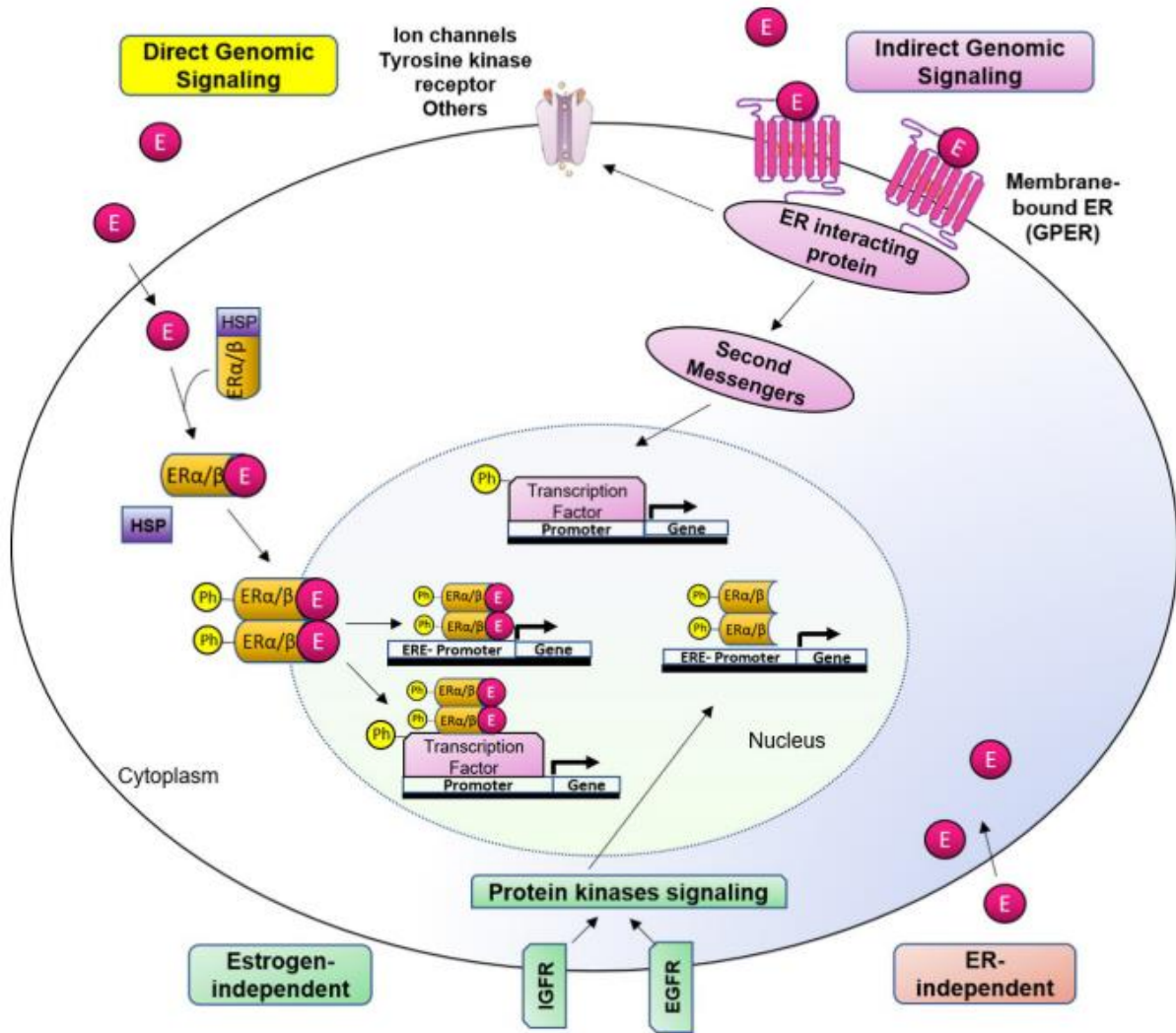


**Figure 12. Genomic and non-genomic estrogen signaling pathways.** There are different estrogen-mediated signaling mechanisms. (1) Direct genomic signaling: estrogen binds to ERs. (2) Indirect genomic signaling. (3) ER-independent: estrogen exerts antioxidant effects in an ER-independent manner. (4) Estrogen independent: ligand-independent genomic events. [modified from Fuentes & Silveyra, 2019]

### 1.3.3.1 Selective estrogen receptor modulators (SERMs)

The selective estrogen receptor modulators (SERMs) represent one of the five categories of ER ligands (Fuentes and Silveyra, 2019). SERMs are born for clinical use since mimicking estrogenic properties but avoiding the endoestrogen-derived actions within reproductive organs, such as the estrogen-like stimulation of the uterus and its relation with endometrial and breast cancer risk (Bryant, 2002; Martinkovich et al., 2014). SERMs show functional duality acting as estrogen agonists or estrogen antagonists in a tissue-specific manner (Bryant, 2002; Martinkovich et al., 2014). Moreover, their distinct profiles depend on the tissue-specific expression of ER subtypes (i.e., ER $\alpha$ , ER $\beta$ , and GPER), differential ERs conformational changes induced by ligand binding, and diversified tissue-specific recruitment to ER of co-activators and co-repressors (Martinkovich et al., 2014). **Tamoxifen** is one of the most important SERMs. It is a first-generation, approved by the Food and Drug Administration (FDA) in 1977 as a pioneering drug for treating and preventing women with ER-positive breast cancer (Jordan, 2003). Indeed, tamoxifen acts as an antagonist in breast tissue representing the selected treatment for ER-positive breast, reducing cancer cell proliferation through NCoR and SMRT co-repressor proteins (Jordan, 2003; Martinkovich et al., 2014). On the other hand, tamoxifen acts as an estrogen agonist on the reproductive, skeletal, cardiovascular, and CNS systems (Riggs and Hartmann, 2003). Notably, in the CNS, tamoxifen exerts neuroprotective actions in different animal models of neural dysfunction such as traumatic spinal cord injury, cranial irradiation, stroke, experimental autoimmune encephalomyelitis (EAE) model for multiple sclerosis, Parkinson's and Alzheimer's disease model, cognitive and mood disorders like anxiety and depression (DonCarlos et al., 2009; Arevalo et al., 2011, 2012, 2015; Acaz-Fonseca et al., 2014; Baez-Jurado et al., 2019). Tamoxifen can cross the BBB and distribute into brain tissues binding to ERs with high affinity (Lien et al., 1991; Pareto et al., 2004). Tamoxifen-dependent brain protection ensues by reducing the neuroinflammatory responses (Tian et al., 2009; Franco Rodríguez et al., 2013; Wang et al., 2017); by repairing demyelinated lesions through the induction of oligodendrocyte progenitors differentiation (Gonzalez et al., 2016); by reducing lipid peroxidation, ROS production and ROS-mediated mitochondrial dysfunctions (Moreira et al., 2005; Zhang et al., 2007); by directly inhibiting microgliosis and astrogliosis (Barreto et al., 2009; Arevalo et al., 2012; Colón and Miranda, 2016); and, by decreasing the infiltration of

leukocytes into injury zone (Wei and Ma, 2014). Tamoxifen acts as a “therapeutic” neuroprotective action with various beneficial effects on learning and memory. For example, in the experimental subarachnoid hemorrhage (SAH) model produced by needle insertion into the brain to generate an aneurysm, tamoxifen showed anti-inflammatory effects promoting neurological function and behavioral recovery after SAH (Sun et al., 2013). In particular, by western-blot analysis, tamoxifen inhibits protein levels of TLR4, NF- $\kappa$ B, and intercellular adhesion molecule-1 (ICAM-1); and, by ELISA assay, tamoxifen decreases the concentration of downstream molecules such as IL-1 $\beta$ , TNF- $\alpha$ , IL-6 in the rat brain after SAH (Sun et al., 2013). Notably, tamoxifen develops a better performance in morris water maze (MWM) trials, indicating that downregulation of TLR4/NF- $\kappa$ B signaling improves the SAH-induced spatial working memory dysfunction (Sun et al., 2013). Similarly, microglia and astrocytes express TLR4 on their plasma membrane, and upon LPS-derived neuroinflammation, tamoxifen inhibits the LPS/TLR4/NF- $\kappa$ B- induced transcription of pro-inflammatory chemokines and cytokines, and thus the reactive phenotypes of glial cells (Ghisletti et al., 2005; Suuronen et al., 2005; Tapia-Gonzalez et al., 2008; Barreto et al., 2009; Cerciat et al., 2010; Arevalo et al., 2011, 2012).

Finally, tamoxifen is a classic “pro-drug” and thus requires metabolic activation to elicit pharmacological activity. By the action of the cytochrome P450 enzyme in the liver, active metabolites derived, including N-desmethyl-tamoxifen (NDM), 4-hydroxy-tamoxifen (4-OH-Tam), tamoxifen-N-oxide, a-hydroxy-tamoxifen, and N-didesmethyl-tamoxifen (Goetz et al., 2008; Valny et al., 2016; Jahn et al., 2018). Moreover, tamoxifen and its active metabolites bind to ERs with different affinities; for example, 4-OH-Tam possesses a much higher affinity for ERs and is 30- to 100-fold more potent than tamoxifen (Goetz et al., 2008; Valny et al., 2016; Jahn et al., 2018). They also show different pharmacokinetic profiles depending on the single or multiple tamoxifen administration and its concentration (Goetz et al., 2008; Valny et al., 2016; Jahn et al., 2018). In conclusion, tamoxifen pharmacology in the brain depends on many factors ranging from cell-type-specific ERs expression, CNS pathology to hepatic cytochrome enzyme activity.

### 1.3.3.2 Tamoxifen activation of Cre-Lox system and its possible side effects

Several reports investigated the pharmacokinetics and metabolism profile of tamoxifen in adult mouse brains in the last years. Indeed, the knowledge of tamoxifen metabolism is of great importance for genetic fate-mapping studies using the tamoxifen-inducible Cre-loxP system, a molecular technique that controls site-specific DNA recombination in different regions of the brain (Valny et al., 2016; Jahn et al., 2018). Different protocols of tamoxifen administration for inducible DNA recombination showed that after a single intraperitoneal (i.p.) injection, the bioactivity of tamoxifen and its metabolites are between 4 and 24 hours post-injection. In contrast, after repeated injections over three consecutive days, the peak concentration in the brain happens from 4 hours up to 5 days later. In general, minor and irrelevant levels of all metabolites were measured after one week (Valny et al., 2016; Jahn et al., 2018). Considering the prominent role of tamoxifen as an activator of the Cre-LoxP system and as an ER-agonist in the brain resulting in therapeutic neuroprotection, some reports investigated the basal effects of tamoxifen under physiological conditions in animal studies. Chen and colleagues (2002) investigated the effect of tamoxifen (Tam) on spatial information in mice by morris water maze (MWM) testing after a single i.p. injection of tamoxifen at the doses of 1–10 mg/kg in female SWISS mice (age not indicated). This study demonstrated that Tam-treated mice (i.p., 30 min before test) have no apparent effects on learning but induces a significant impairment in memory retrieval, in which adult hippocampal neurogenesis is critically involved (Chen et al., 2002). Afterward, Vogt and colleagues (2008) investigated the consequences of tamoxifen-dependent inducible Cre-LoxP protocol on mouse behaviors; specifically, C57BL/6 male mice (8 weeks-age-old) were i.p. injected twice a day with 100  $\mu$ l (i.e., 1 mg/day) for 5 consecutive days. After a latency period of 4 weeks, mice performed MWM, T-maze, and Fear conditioning tests displaying regular locomotion, exploration, anxiety-related behavior, learning, and memory. However, the Forced swim test data showed a significant increase in depression-like despair behavior even 4 weeks after tamoxifen treatment (Vogt et al., 2008). These results do not exclude earlier but transient effects during or immediately after the treatment period of tamoxifen, as observed after 30 min by Chen (Chen et al., 2002). More recently, another group investigated the sub-acute impact of short-term tamoxifen administration on adult hippocampal neurogenesis and behavior, testing the open field, the elevated plus-maze, and the MWM tasks (Rotheneichner et al., 2017). This

study exploited 5 month-old nestin-CreERT2/R26R-YFP transgenic mice in which tamoxifen (100mg/kg bodyweight; 10mg/ml stock solution) was daily i.p. injected daily for 5 days in parallel to BrdU injections (50mg/kg bodyweight; 10mg/ml stock solution). Saline and corn-oil vehicle were used as controls. Behavioral tests were performed from day 8 to 12, and cellular analysis occurred after a latency time of 10 days from the last injection of tamoxifen (Rotheneichner et al., 2017). Behavioral analyses showed no significant differences between groups. No differences occurred by the quantification of cell proliferation (PCNA+ cells), cell survival (BrdU+ cells), and dendritic arborization (DCX+ cells), as well as by cellular analysis on fate and maturation rate of the newborn neurons (%DCX+/BrdU+, DCX+NeuN+/BrdU+, and NeuN+/BrdU+ cells) within the SGZ/GCL of adult DG. Thus, from this study, the use of tamoxifen to induce the Cre/loxP system shows no persisting effects on adult hippocampal neurogenesis and behaviors (Rotheneichner et al., 2017). However, it is noteworthy that adult hippocampal neurogenesis changes rapidly during aging with a substantial decline in 5-6 month-old mice (Kuhn et al., 1996, 2018; Ben Abdallah et al., 2010; Seib and Martin-Villalba, 2015). This timeline of neurogenesis results in widely used 2-3 month-old mice, named young-adult mice, in adult hippocampal neurogenesis studies. Therefore, considering the early age-related decline of neurogenesis, the study of Rotheneichner (2017) showed a critical aspect in using 5-month middle-aged mice.

Adverse effects of tamoxifen on adult neurogenesis and behaviors have been recently reported using inducible Cre/loxP protocol in adult mice. For example, Li X. and colleagues (2019) investigated tamoxifen acute and chronic effects on three different depression mouse models (i.e., social defeat/learned helplessness/isolation models). C57BL/6 male mice received a single Tam i.p. injection (75 mg/kg/day) once a day for 7 days starting at 8 weeks-age-old (Li et al., 2019b). Behavioral tests followed 3 days after the last injection and showed that tamoxifen could alter locomotor activity in the open field test (i.e., decrease in the velocity, vertical movement number, and vertical movement time). Moreover, data from the elevated plus-maze test (i.e., lower total distance traveled, less open arm time, and fewer open arm entries) and the forced swimming test (i.e., less immobility time) revealed increased anxiety and anti-depressive behavior (Li et al., 2019b). To analyze the chronic effects of tamoxifen, mice underwent behavioral tests after 4 weeks from the last injection. They showed a more depressive behavior spending more immobility time in the forced swimming test, while

tamoxifen slightly influenced locomotor activity, social interaction, and anxiety (Li et al., 2019b). Another study revealed the long-lasting adverse effects of tamoxifen in pre and postnatal neurogenesis (Lee et al., 2020). Interestingly, a single prenatal exposure to tamoxifen dramatically changes the genomic profile of cells in the cerebral hemisphere and has a long-lasting impact on cortical neurogenesis, patterning, and neural circuit formation in perinatal and postnatal offspring (Lee et al., 2020). Moreover, considering the adult mouse brain, 3- to 4-week-old C57BL/6 male mice were i.p. injected with tamoxifen (2 mg/animal/day) once a day for 5 consecutive days. After a latency period of 5 days from the last injection, tamoxifen significantly reduced the number of BrdU- and Ki67-labeled proliferating cells both in the SVZ and in the DG (Lee et al., 2020).

In conclusion, although these reports above employed different protocol designs, side effects of tamoxifen treatment emerged in healthy mice underlying that care must be taken when using the Tam-induced CreER/LoxP system for neural lineage tracing and genetic manipulation studies. Notably, the study reported in Chapter III of this thesis adds another piece of the puzzle, investigating the anti-inflammatory and neuroprotective effects of tamoxifen pretreatment on adult hippocampal neurogenesis in LPS-induced neuroinflammation mouse models.

## **Aim of the study**

In the last years, the research on neuroinflammation and neuroprotection is driving the efforts of many scientists to figure out the complex molecular and cellular mechanisms underlying the immune-to-brain communication and the neuro-to-gliogenesis balance within the adult hippocampal neurogenic niche. Until now, significant evidence emerged to give a better and broader framework of the process of adult hippocampal neurogenesis under physiological and pathological conditions. However, the mechanisms which regulate the crosstalk among cell-intrinsic/-extrinsic cues, neuroinflammation/neuroprotection, adult neurogenesis/gliogenesis are still largely unknown.

To address this issue, I developed and characterized a mouse model of neuroinflammation by peripherally injecting the endotoxin lipopolysaccharide (LPS) to study the outcomes at the molecular and cellular level, focusing on the adult neurogenic niche of the hippocampal dentate gyrus.

To the best of my knowledge, few data exist on cell-intrinsic factors that drive the early cell-fate decision of adult hippocampal NSCs under neuroinflammation; here, I chose to focus on the transcription factor COUP-TFI that was found to be involved in the development of the hippocampal formation and is highly expressed in the adult dentate gyrus, including in the neural progenitor cells. Thereby, a key question of my thesis was to investigate COUP-TFI as a potential cell-intrinsic regulator of adult neurogenesis to understand its function in the healthy tissue and upon neuroinflammation. A second main focus of my thesis was on the effects exerted by tamoxifen, a molecule widely used in association with inducible CreERT2-LoxP mouse technology, to study the dynamics/potential of adult neural stem cells and whose anti-inflammatory/neuroprotective function could impact on the regulation of adult neurogenesis.

Specific aims of this thesis were:

- 1) Understand if the transcription factor COUP-TFI is involved in the regulation of adult DG neurogenesis and unravel its implication in inflammatory conditions



2) Define if and how tamoxifen treatments interfere with the process of adult hippocampal neurogenesis in healthy conditions and upon LPS-induced neuroinflammation

3) Unravel the role of microglia in the DG neurogenic niche response to LPS and tamoxifen treatments

## **CHAPTER II**

## **2 COUP-TFI is a key regulator in the neurogenesis/astrogliogenesis balance within the adult DG hippocampus with relevant implications upon neuroinflammation**

In this chapter of my thesis, I describe the results obtained from the investigation of the expression and function of COUP-TFI in the adult DG neurogenic niche upon neuroinflammation. To this aim, I exploited a mouse model of neuroinflammation by intraperitoneally injecting the *E. Coli*-derived lipopolysaccharide (LPS) to induce an acute neuroinflammatory status in the adult mouse brain, involving the microglia reaction and affecting the neuro/astrogliogenesis balance in the adult DG. First, I showed the efficacy of the LPS-induced neuroinflammation model by the occurrence of an inflammatory response at the molecular and cellular level in the adult hippocampus. Next, I demonstrated that COUP-TFI levels were downregulated upon induced neuroinflammation, followed by increased astrogliogenesis. To understand whether COUP-TFI was directly involved in the cellular response to neuroinflammation, I manipulated its expression by targeting mitotic progenitors through loss- and gain-of-function experiments *in vivo*. Using a retroviral-based approach, coupled to genetic fate mapping, I found that COUP-TFI deletion in adult DG neural progenitors impairs neurogenesis and increases astrogliogenesis, indicating a switch of neural progenitors toward an astrocyte cell lineage. Finally, by complementary gain-of-function experiments, I showed that COUP-TFI overexpression in mitotic progenitors was sufficient to repress astrogliogenesis and, importantly, to rescue neurogenesis during neuroinflammation. Altogether, these data unravel COUP-TFI as a critical transcriptional regulator in the choice between neuro/astrogliogenesis within the healthy and inflamed adult hippocampus. The results described in this chapter are part of a publication, inserted as an appendix of this thesis (Bonzano, Crisci, *et al.*, 2018).

## 2.1 Introduction

Neurons and glial cells originate from neural stem cells (NSCs) found throughout the developing brain but persist only into restricted neurogenic niches of the mature brain during adulthood, where adult neurogenesis occurs. The subgranular zone (SGZ) of the hippocampal dentate gyrus (DG) is one of such neurogenic niches (Ming and Song, 2011; Kempermann et al., 2015). In the mouse DG, adult NSCs in the SGZ are composed of radial glia-like (RGL) and horizontal Type-1 cells, which are early precursor cells largely quiescent. When activated, NSCs can divide to self-renew and/or give rise to intermediate progenitors (IPCs or Type-2 cells) (Song et al., 2012), which exhibit limited rounds of proliferation before generating neuroblasts (Type 3 cells) (Berg et al., 2015). Only a small subset of these neuroblasts survive, exit the cell cycle, and eventually mature to become granule neurons in the DG (Kempermann et al., 2003; Lugert et al., 2012; Bond et al., 2015). Functional studies showed that adult DG neurogenesis is critical for multiple hippocampus-dependent cognitive skills, including learning and memory (Deng et al., 2010; Sahay et al., 2011; Christian et al., 2014). Alongside neurogenesis, adult NSCs also generate a small but significant astrocyte amount (Steiner et al., 2004; Suh et al., 2007; Bonaguidi et al., 2011; Dranovsky et al., 2011; Encinas et al., 2011). Genetic and molecular programs tightly control adult neurogenesis and astrogliogenesis in the adult DG neurogenic niche. However, additional regulatory cell-extrinsic factors influence these processes either by promoting or suppressing the activity of NSCs and by affecting the generation of new neurons and/or astrocytes (Aimone et al., 2014). Interestingly, running enhances DG neurogenesis and astrogliogenesis (Steiner et al., 2004), whereas pathological conditions, such as inflammation, lead to NSC dysfunction, altering the neuron/astrocyte production rate in favor of astrocytes (Wu et al., 2012; Woodbury et al., 2015). Despite the identification of many endogenous and exogenous regulators, the cell-intrinsic fate-determining factor(s) guiding the choice between neuronal versus astrocytic fate in adult hippocampal neural stem/progenitor cells remains to be fully identified. Thus, the first intent of my Ph.D. project aims to investigate the possible involvement of the transcription factor COUP-TFI in the regulation of DG NSCs/progenitors fate-choice.

COUP-TFI belongs to the chicken ovalbumin upstream promoter transcription factors (COUP-TFs), originally found to regulate the expression of the chicken ovalbumin gene by

specifically binding to its promoter (Pastorcic et al., 1986; Sagami et al., 1986). COUP-TFs are also named “NR2F” for subfamily 2 group F members of the steroid thyroid hormone superfamily of nuclear receptors (Auwerx et al., 1999) and defined as “orphan” receptors since no specific physiological ligand has been characterized so far. In vertebrates, two COUP-TF homologs have been identified, COUP-TFI (EAR3) (Miyajima et al., 1988) and COUP-TFII (ARP-1) (Ldias and Karathanasis, 1991), also known as nuclear receptor 2 family 1 and 2 (NR2F1 and 2) (Tsai and Tsai, 1997). Among COUP-TFs, COUP-TFI shows the highest expression in the nervous system, acting as a transcriptional regulator both inducing and repressing target gene transcription (Pereira et al., 2000). During brain development, COUP-TFI is involved in several processes, including (i) the regulation of neuroblast migration (Adam et al., 2000; Alfano et al., 2011; Touzot et al., 2016; Parisot et al., 2017), (ii) directing axonal elongation and arborization (Qiu et al., 1997; Adam et al., 2000; Armentano et al., 2006), (iii) controlling identity and temporal competency of neuronal progenitor cells (Faedo et al., 2008; Naka et al., 2008; Okano and Temple, 2009; Naka-Kaneda et al., 2014), and (iv) establishing area-specific identity in progenitors and neurons (Armentano et al., 2007; Tomassy et al., 2010; Alfano et al., 2014; Harb et al., 2016). Moreover, COUP-TFI is involved in developing hippocampal formation, controlling its anatomical and functional properties (Flore et al., 2017; Parisot et al., 2017). Indeed, COUP-TFI loss-of-function during early developmental stages results in dysmorphic hippocampus along its dorsal-to-ventral axis (Flore et al., 2017) and the abnormal formation/morphogenesis of the postnatal DG (Parisot et al., 2017), ultimately leading to spatial memory deficits (Flore et al., 2017). Importantly, in humans, the haploinsufficiency of COUP-TFI leads to the Bosch-Boonstra-Schaaf optic atrophy-intellectual syndrome (BBSOAS), a rare autosomal-dominant disorder characterized by multiple clinical features that include global developmental delay, mild-to-severe intellectual disability, optic nerve atrophy, seizures, and autism spectrum disorder (ASD) (Al-Kateb et al., 2013; Bosch et al., 2014; Bertacchi et al., 2019).

Notably, COUP-TFI continues to be highly expressed in the adult brain, including the neurogenic niches (Dye et al., 2011; Bovetti et al., 2013; Llorens-Bobadilla et al., 2015). In the SGZ/GCL of young adult mice (i.e., 2 to 3 month-old mice), COUP-TFI-immunopositive nuclei are observed among NSCs and throughout the neurogenic lineage, although at different levels (RGLs 60/70%; Type 1 cells <80%; Type 2 cells <90%; Type 3 cells, and

immature/mature granule neurons =100%), implying a tight regulation for this transcription factor in different cellular components of the adult DG niche (Figure 1). These observations placed the starting point of my research project on the functional role of COUP-TFI in the adult hippocampal NSCs.

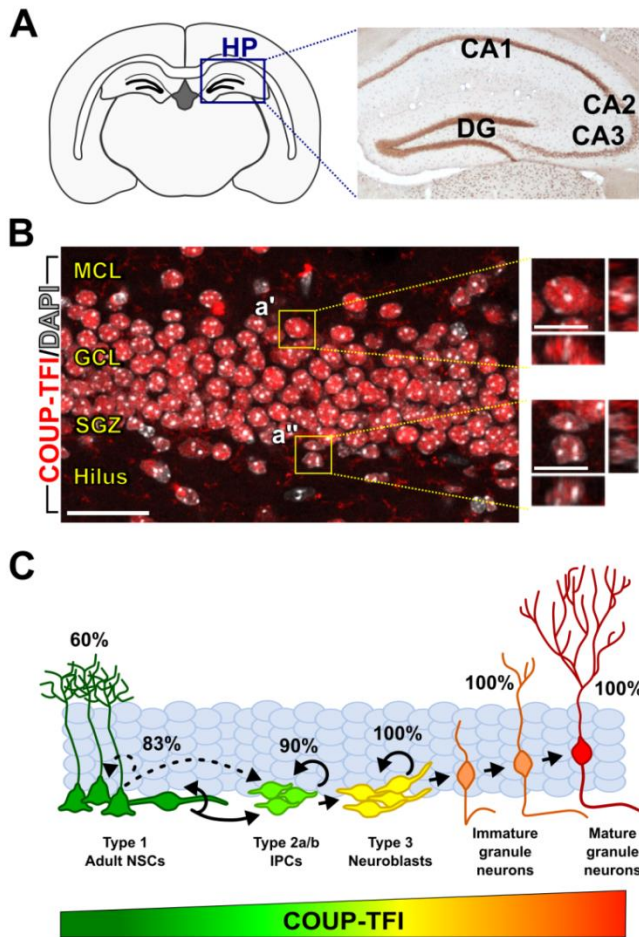


**Figure 1. COUP-TFI is expressed in NSC/progenitor cells and in the neurogenic lineage of the adult hippocampus.** (A) Schematic drawing of a coronal section of an adult mouse brain. The box indicates the hippocampus (HP), where COUP-TFI immunostaining is shown. (B) Confocal images of COUP-TFI+ cells (red) in an adult DG section counterstained with DAPI (white). Scale bar, 50  $\mu$ m. (C) Schema illustrating COUP-TFI protein expression (in percentage) in different cell types of the adult DG.

## 2.2 Materials and methods

### 2.2.1 Animals and housing conditions

Adult C57BL/6J wildtype mice (2-month-old male mice; Charles River) were used for the analysis of COUP-TFI mRNA expression and immunofluorescence in the adult hippocampal neurogenic niche once evaluated the efficacy of the LPS-induced neuroinflammatory model in the same animals. To study the specific role of COUP-TFI in progenitors and their descendants in adult hippocampal neurogenic niches *in vivo*, *COUP-TFI*<sup>wt/wt</sup>;*R26-YFP*<sup>+/+</sup> (Ctrl<sup>RV-Cre</sup>), *COUP-TFI*<sup>fl/fl</sup>;*R26-YFP*<sup>+/+</sup> (COUP-TFI-cKO<sup>RV-Cre</sup>), and *hCOUP-TFI*<sup>+/wt</sup>;*R26-YFP*<sup>+/+</sup> (COUP-TFI-O/E<sup>RV-Cre</sup>) mice were used for loss- and gain-of-function experiments obtained by RV-Cre stereotaxic injections within the adult DG. For inactivation of COUP-TFI, *COUP-TFI*<sup>fl/fl</sup> animals, in which exon 3 of COUP-TFI gene is flanked by loxP sites (Armentano et al., 2007), were bred with Rosa26-floxed stop-YFP reporter mice (Srinivas et al., 2001) to generate *COUP-TFI*<sup>fl/fl</sup>;*R26-YFP* mice, which were homozygous for *COUP-TFI*<sup>fl/fl</sup> and *R26-YFP*. For overexpression of COUP-TFI, *hCOUP-TFI*<sup>+/wt</sup> animals, where in CAG-S-*hCOUP-TFI* allele is silent due to a floxed STOP cassette inserted between the promoter and the transgene (Wu et al., 2010), were bred with *Rosa26-floxed stop-YFP* reporter mice to obtain *hCOUP-TFI*<sup>+/wt</sup>;*R26-YFP*<sup>+/+</sup> mice. Control mice were obtained by breeding Rosa26-floxed stop-YFP reporter mice with *COUP-TFI*<sup>wt/wt</sup> mice, in which both alleles for COUP-TFI were wildtype to obtain *COUP-TFI*<sup>wt/wt</sup>;*R26-YFP*<sup>+/+</sup> mice. All mouse lines were maintained in a C57BL/6J genetic background and were 8-12 weeks old at the onset of the experiments. Both male and female transgenic mice were included in the analysis of COUP-TFI deletion/overexpression.

All mice were housed in standard cages (n=2-4 mice/cage) under a 12 h light/dark cycle with access to food and water *ad libitum*. All procedures were conducted in accordance with the Guide for the Care and Use of Laboratory Animals of the European Community Council Directives (2010/63/EU and 86/609/EEC) and approved by local bioethics committees, the Italian Ministry of Health, and the French Ministry for Higher Education and Research.

### 2.2.2 Genotyping

The PCR primers used for genotyping are the following: R1 (5'-AAAGTCGCTCTGAGTTGTTAT-3'), R2 (5'-GCGAAGAGTTTGTCTCAACC-3'), and R3 (5'-GGAGCGGGAGAAATGGATATG-3') for Rosa26-floxed stop-YFP; ARM-5-3' (5'-CTGCTGTAGGAATCCTGTCTC-3'), and EX-3-5' (5'-AATCCTCCTCGGTGAGAGTGG-3') for COUP-TFI; Tg forward (5'-GCTTTCTGGCGTGTGACC-3'), and Tg reverse (5'-ATTAAGGGCCAGCTCATTCC-3') for CAG-S-hCOUP-TFI.

### 2.2.3 LPS treatments

To induce a cellular/molecular cascade able to initiate an inflammatory response, the *E.coli*-derived lipopolysaccharide (LPS, SIGMA, L2880) was dissolved in a sterile physiological solution and injected intraperitoneally into adult mice for either 1 or 4 consecutive days at the dose of 0.5 mg/kg/day. Saline solution (0.9%) was injected as a control.

### 2.2.4 Retro-Cre virus stereotaxic injection in the adult DG

Adult mice *R26-YFP<sup>+/+</sup>;COUP-TFI<sup>fl/fl</sup>* (*COUP-TFI-cKO<sup>RV-Cre</sup>*), *R26-YFP<sup>+/+</sup>;COUP-TFI<sup>wt/wt</sup>* (*Ctrl<sup>RV-Cre</sup>*), *R26-YFP<sup>+/+</sup>;hCOUP-TFI<sup>+/wt</sup>* (*COUP-TFI-O/E<sup>RV-Cre</sup>*) were anesthetized in a constant flow of Isoflurane (3%) in oxygen, positioned in a stereotaxic apparatus (Stoelting) and injected with a pneumatic pressure injection apparatus (PicospritzerII, General Valve Corporation). The skull was exposed by an incision in the scalp and a small hole (about 1 mm) drilled through the skull. 1  $\mu$ l of retrovirus-Cre (RV-pMIG::Cre; titer  $2.7 \times 10^7$ , Rolando et al., 2016) was injected in the DG using a sharpened glass capillary at the following stereotaxic coordinates: -2 mm (antero-posterior), 1.5 mm (lateral) to Bregma, and -2.0 mm below the surface of the skull. Mice (n=4/5 genotype/experiments) were killed 2, 14, or 18 days after virus infection. Brain tissue was processed and analyzed by immunohistochemistry as described below.

### 2.2.5 Tissue collection, RNA extraction, and RT-qPCR

Adult mice were perfused with ice-cold PBS. Hippocampi were microdissected and lysed, and RNA isolation was performed using the RNeasy Micro Kit (Qiagen, France). Reverse



transcription was carried out using QuantiTect kit (Qiagen, France). The qPCR reactions were performed in duplicates in a LightCycler480 (Roche) using QuantiTect SYBR Green PCR kit (Qiagen, France) and gene-specific primers (**Table 1**). The amount of transcripts was evaluated relative to the expression level of the housekeeping gene acidic ribosomal phosphoprotein P0 (Rplp0 or 36B4). Fold change was calculated with respect to the control saline-injected group.

### **2.2.6 Tissue preparation**

For immunostaining experiments, adult mice were deeply anesthetized with an intraperitoneal injection of a mixture of ketamine (75 mg/kg; Ketavet; Gellini) and xylazine (30 mg/kg; Rompun; Bayer) and perfused transcardially with ice-cold 0.9% saline solution, followed by ice-cold 4% paraformaldehyde (PFA) in 0.1 M phosphate buffer (PB), pH 7.4. Brains were removed from the skull, postfixed for 4 hours in the same PFA solution, cryoprotected in a 30% sucrose solution (in 0.1 M PB, pH 7.4), OCT-embedded, frozen at -80°C, and finally sectioned using a cryostat (Leica Microsystems). Free-floating coronal serial sections (40µm for retroviruses experiments, and 30µm for all other experiments) were collected in multi-well dishes. Sections were stored at -20°C in antifreeze solution until use.

### **2.2.7 Immunofluorescence and immunohistochemistry**

Immunofluorescence (IFL) reactions for selected markers were performed on free-floating coronal serial sections as detailed below: sections have been incubated either overnight (o/n) or for 48 hours at 4°C with primary antibodies (**Table 2**) diluted in 0.01M PBS (pH 7.4), 0.5% Triton X-100, and 1% normal serum of the same species of the secondary antibody (normal donkey serum, NDS). Sections were washed in PBS and incubated for 1 hour at room temperature with secondary antibodies (**Table 3**) in 0.01 M PBS (pH 7.4), 0.5% Triton X-100, and NDS (1%). Sections were washed in 0.01M PBS (pH 7.4) and incubated for 15 minutes at room temperature with 4,6-diamidino-2-phenylindole (DAPI, 1 µg/ml) to label nuclei. Sections were washed in 0.01M PBS (pH 7.4) then mounted on gelatine coated slides, air dried, and coverslipped with antifade mounting medium Mowiol (4-88 reagent, Calbiochem 475904).

### **2.2.8 Microscope analysis and cellular quantification**

Images of multiple labeled sections employing immunofluorescence were acquired with a TCS SP5 confocal microscope (Leica). Confocal image z-stacks were captured through the thickness of the slice (30/40  $\mu\text{m}$ ) at 1- $\mu\text{m}$  optical steps with an objective 40X/1.25-0.75 (oil immersion lens), zoom (1.2) and resolution of 1024/1024 pixels and 100Hz (1 pixel = 0.38  $\mu\text{m}$ ) comprising both upper and lower blades of the DG. Images were then analyzed with NIH ImageJ (<http://rsb.info.nih.gov/ij>) using the cell counter and channel tools plug-ins.

For COUP-TFI ablation and overexpression experiments, marker+YFP+ cells were quantified through multi-stack images (50-150 YFP+ cells/slice; n=3-5 animals/genotype) acquired at the confocal microscope. DAPI staining was used to trace the granule cell layer (GCL) in DG of the hippocampus and to counterstain clustered cells and be able to discriminate single YFP+ cells among packaged YFP+ cells. At least three different levels among the rostro-caudal extension of the DG (bregma: from -1.30 to -3.80) per animal were analyzed, taking into account both upper and lower blades of the DG (as above). For analysis of GFAP+YFP+ RGL, cells were deemed to be radial if the cell body, clearly associated with a DAPI+ nucleus, was located in the SGZ and had a single thin radial process extending throughout GCL and branching into the MCL. The cell density (D) was calculated by dividing the total number of counted cells over the area of interest (SGZ, SGZ+GCL, or MCL) and expressed as the mean number of cells per squared millimeters ( $\text{cells}/\text{mm}^2$ ; n=3-5 animals/genotype).

### **2.2.9 Statistical analysis**

Statistical comparisons were conducted using two-tailed unpaired Student's t-test or one-way ANOVA and the Bonferroni post-hoc test when appropriate (in Microsoft Excel and GraphPad Prism8). For unpaired Student's t-test, Levene's test was conducted to compare variances, and Welch's correction was applied in case of unequal variance distribution. Significance was established at  $p < 0.05$ . Cell counts are presented as mean  $\pm$  SD and are derived from at least three different animals/groups or genotypes.

**Table 1. List of primers**

<b>Gene</b>	<b>Forward</b>	<b>Reverse</b>
<b>IL1A</b>	TGCAGTCCATAACCCATGATC	ACAAACTTCTGCCTGACGAG
<b>IL1<math>\beta</math></b>	ACGGACCCCAAAAGATGAAG	TTCTCCACAGCCACAATGAG
<b>TNF<math>\alpha</math></b>	CTTCTGTCTACTGAACTTCGGG	CAGGCTTGTCACTCGAATTTTG
<b>IL6</b>	CAAAGCCAGAGTCCTTCAGAG	GTCCTTAGCCACTCCTTCTG
<b>DCX</b>	CAGTCAGCTCTCAACACCTAAG	CATCTTTCACATGGAATCGCC
<b>COUP-TFI (NR2F1)</b>	AACTGGCCTTACATGTCCATC	ATCATAACCAGCATCCCCAAAG
<b>GFAP</b>	GAAAACCGCATCACCATTCC	CTTAATGACCTCACCATCCCG
<b>Rplp0 (36B4)</b>	ACCCTGAAGTGCTCGACATC	AGGAAGGCCTTGACCTTTTC

**Table 2. List of primary antibodies**

<b>Primary Antibodies</b>				
<b>Antigen name</b>	<b>Host</b>	<b>Dilution</b>	<b>Source</b>	<b>Catalogue n°</b>
<b>COUP-TFI</b>	Mouse	1:500	R&D System	PP-H8132-10
<b>COUP-TFI</b>	Rabbit	1:700	M. Studer's Lab	-
<b>DCX</b>	Goat	1:1500	Santa Cruz Biotechnology	Sc-8066
<b>GFAP</b>	Goat	1:200	Abcam	ab53554
<b>GFAP</b>	Rabbit	1:2000	Dako	Z 0334
<b>GFP</b>	Chicken	1:1000	AvesLab	GFP-1020

**Table 3. List of secondary antibodies**

<b>Secondary Antibodies</b>				
<b>Antigen name</b>	<b>Host</b>	<b>Dilution</b>	<b>Source</b>	<b>Catalogue n°</b>
<b>AlexaFluor488 Anti-Chicken</b>	Donkey	1:400	Jackson ImmunoResearch	703-545-155
<b>AlexaFluor488 Anti-Rabbit</b>	Donkey	1:400	Jackson ImmunoResearch	711-545-152
<b>AlexaFluor647 Anti-Mouse</b>	Donkey	1:600	Jackson ImmunoResearch	715-605-151
<b>AlexaFluor647 Anti-Rabbit</b>	Donkey	1:600	Jackson ImmunoResearch	711-605-152
<b>Cy3 Anti-Goat</b>	Donkey	1:800	Jackson ImmunoResearch	705-165-147

## 2.3 Results

### 2.3.1 LPS-induced neuroinflammation leads to impaired neurogenesis coupled to COUP-TFI downregulation within the adult DG

Neuroinflammation severely affects adult neurogenesis and increases astrocyte production in the adult hippocampal DG (Monje et al., 2003; Wu et al., 2012; Kohman and Rhodes, 2013). However, little is known about the mechanisms underlying these processes and the modifications occurring in the NSC/progenitor pool.

With the final aim to identify novel cell-intrinsic regulators involved in controlling neurogenesis and astrogliogenesis within the adult hippocampus upon neuroinflammation, I acutely administered the *E. coli*-derived lipopolysaccharide (LPS) by intraperitoneal (i.p.) injection to initiate an inflammatory response in adult wild type mice that were sacrificed the day after the injection (Figure 2A).

The occurrence of inflammatory response was demonstrated by RT-qPCR analysis on hippocampal tissue extracts, which showed a strong transcript increase of the pro-inflammatory cytokines interleukin-1b (IL-1b), interleukin-1A (IL-1A), and tumor necrosis factor- $\alpha$  (TNF $\alpha$ ) in the hippocampi of LPS-treated mice compared with control saline-injected mice at 1-day post-injection (1dpi). In contrast, interleukin-6 (IL-6) showed no differences (Figure 2B). In parallel, I also evaluated the expression profile of genes expressed by neuronal and astroglial cell types, and I found that LPS treatment downregulated the expression of the immature neuronal markers doublecortin (DCX) and upregulated the glial fibrillary acid protein (GFAP) (Figure 2C). No statistically significant differences were observed in the expression of the bHLH transcription factor NeuroD expressed by immature hippocampal neurons (Figure 2C). Next, to integrate the molecular analysis obtained from the whole hippocampus following acute treatment, I switched to a prolonged treatment to evaluate the cellular responses to neuroinflammation occurring in the DG. To this aim, I treated adult mice once a day for 4 consecutive days with LPS (d1–d4) and performed the analyses at 1dpi (Figure 3A). I found a reduced number of DCX<sup>+</sup> immature newborn neurons (Figures 3B-C) and an increase in GFAP<sup>+</sup> astrocytes within the GCL of LPS-treated mice compared to saline controls (Figures 3D-E). These results are in line with previously reported data concerning an alteration in newborn neuron/mature astrocyte ratio during neuroinflammation (Wu et al.,

2012) and thus validated the efficacy of our LPS-induced neuroinflammation at one (LPS 24h) and four days (LPS 4d) protocols.

The next step was to analyze whether and how COUP-TFI expression was affected by neuroinflammation (Figure 4). Interestingly, I found that COUP-TFI was downregulated in LPS 24h treated mice (Figures 4A-B), indicating a direct response of this transcriptional regulator to inflammation in the adult hippocampus. To identify changes in COUP-TFI expression at the cellular level in mice treated for 4 days with LPS, I analyzed COUP-TFI immunostaining focusing on the adult DG RGL cell pool on day 5, thus discriminating adult NSC cells by their radial glia-like morphology (Figures 4C). I found a decrease of GFAP+ RGL cells expressing COUP-TFI in the DG of LPS-treated mice (Sal,  $75.56 \pm 3.966\%$  vs. LPS,  $58.19 \pm 1.977\%$ ) (Figures 4D-E). Moreover, I observed that DCX+ immature newborn neurons (100% COUP-TFI+ in a healthy condition; Figure 1) were never be found negative for COUP-TFI either in saline or LPS-treated mice (qualitative data).

Thus, based on the selective COUP-TFI downregulation in RGL cells upon LPS-derived inflammatory insult, we hypothesized that COUP-TFI could be directly involved in changes in the RGL cell behavior that could contribute to the altered neurogenesis and astroglialogenesis observed within the DG upon neuroinflammation.

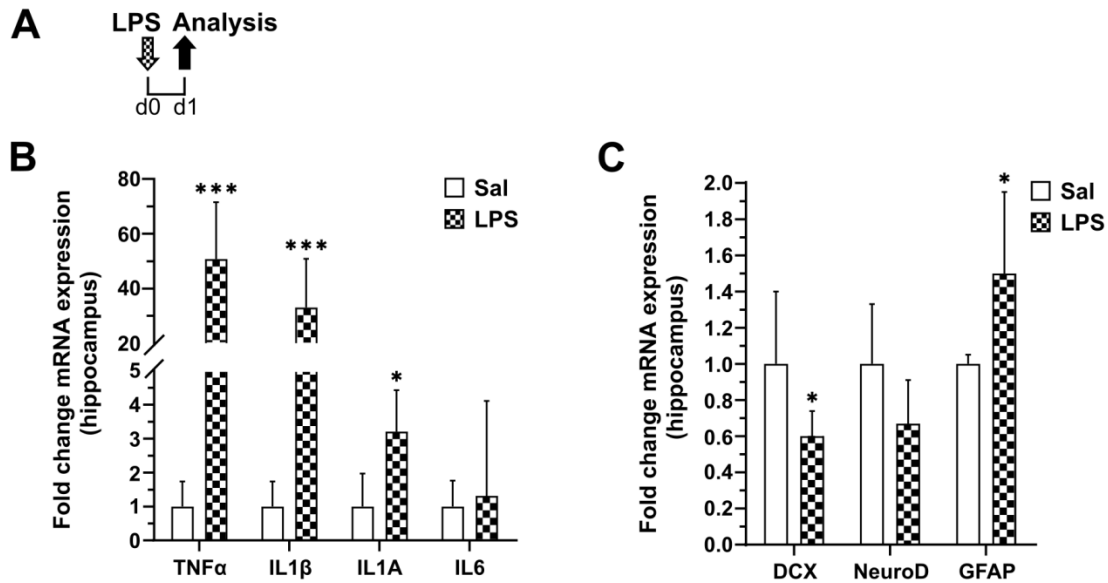


**Figure 2. A single LPS administration results in an altered hippocampal transcripts profile.** (A) Experimental design for transcript expression analysis on hippocampal tissue extracts. (B and C) Changes in pro-inflammatory cytokines (B), neuronal (DCX, NeuroD), and glial (GFAP) gene transcripts (C) in the hippocampi of LPS-treated mice, revealed by RT-qPCR. n = 5 mice/treatment; technical replicates = 2. Data are presented as fold change  $\pm$  SD. Student's t-test \*p<0.05, \*\*\*p<0.001.

**Table F2**

Unpaired Student's t-test, two-tailed ( $\alpha < 0.05$ )				
Figure	Parameter	Groups	Statistics	P
2B	TNF $\alpha$	Sal vs LPS	$t_{(8)} = 10.35$	P < 0.0001
2B	IL-1 $\beta$	Sal vs LPS	$t_{(8)} = 8.296$	P < 0.0001
2B	IL-1A	Sal vs LPS	$t_{(7)} = 2.855$	P = 0.0245
2B	IL-6	Sal vs LPS	$t_{(8)} = 0.4022$	P = 0.6981
2C	DCX	Sal vs LPS	$t_{(8)} = 2.424$	P = 0.0416
2C	NeuroD	Sal vs LPS	$t_{(8)} = 1.634$	P = 0.1409
2C	GFAP	Sal vs LPS	$t_{(7)} = 2.582$	P = 0.0364

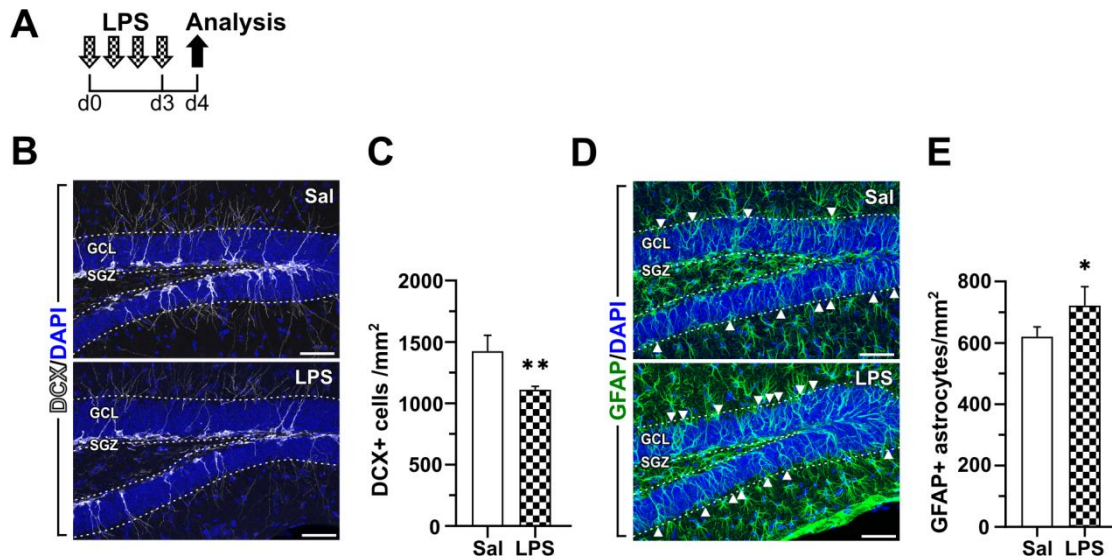


**Figure 3. LPS-induced neuroinflammation reduces newborn neurons, and increases astrocytes within the adult inflamed DG.** (A) Experimental design for immunofluorescence analysis on the DG. (B) Confocal images of DCX+ (white) cells in the DG of saline (control) and LPS-treated mice. (C) DCX+ cell density in the DG of LPS-treated mice versus saline. (D) Confocal images of GFAP+ (green) cells in the DG of saline and LPS-treated mice. Arrowheads show mature-shaped astrocytes. (E) GFAP+ astrocyte density in the DG of LPS-treated mice versus saline. n=5 mice/treatment. Cell nuclei are counterstained with DAPI (blue). GCL, granule cell layer; SGZ, subgranular zone. Data are presented as mean  $\pm$  SD. Scale bars: B, D, 50 $\mu$ m. Student's t-test \*p<0.05, \*\*p<0.01.

**Table F3**

Unpaired Student's t-test, two-tailed ( $\alpha < 0.05$ )				
Figure	Parameter	Groups	Statistics	P
3C	Cell density of DCX+ cells	Sal vs LPS	$t_{(5)} = 4.045$	P = 0.0099
3E	Cell density of GFAP+ astrocytes	Sal vs LPS	$t_{(8)} = 3.269$	P = 0.0114

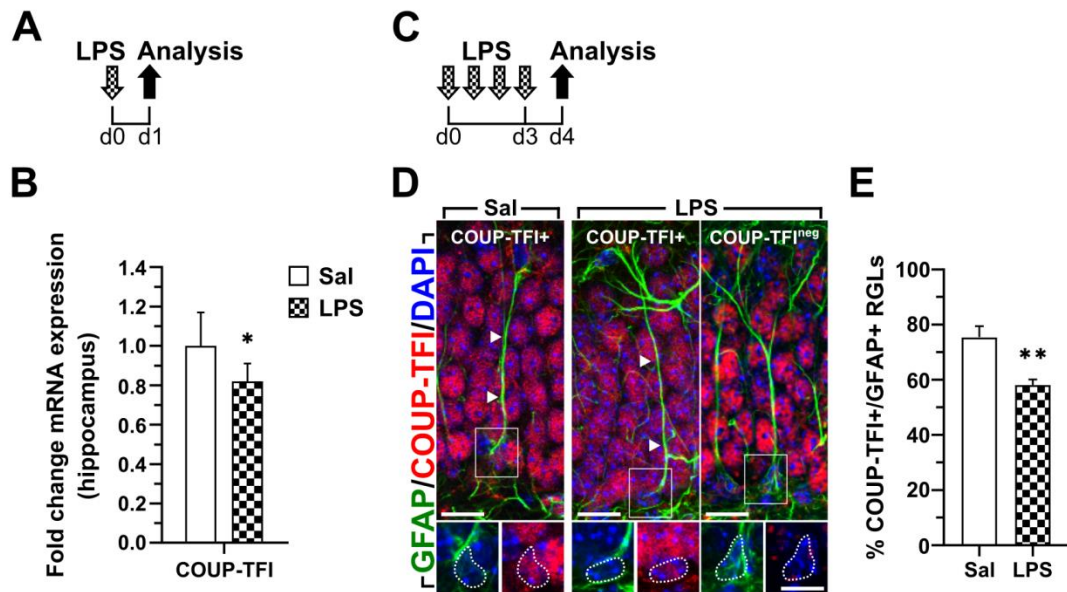


**Figure 4. Acute neuroinflammation leads to COUP-TFI downregulation within the adult DG.** (A) Experimental design for transcript expression analysis on hippocampal tissue extracts. (B) Changes in COUP-TFI gene transcripts in the hippocampi of LPS-treated mice revealed by RT-qPCR.  $n = 5$  mice/treatment; technical replicates = 2. (C) Experimental design for immunofluorescence analysis on the DG. (D) Confocal images of GFAP+ (green) RGLs either positive (+) or negative (neg) for COUP-TFI (red) in DG sections of saline- and LPS-treated mice. Cell nuclei are counterstained with DAPI (blue). Arrowheads indicate radial cell processes. Scale bar, 10  $\mu$ m. (E) Quantification of COUP-TFI+ nuclei among GFAP+ RGL cells (RGLs) in saline ( $75.56 \pm 3.966\%$ ,  $n=257/353$  double+ cells out of 3 mice) and LPS-treated mice ( $58.19 \pm 1.977\%$ ,  $n=220/379$  double+ cells out of 3 mice). Data are presented as fold-change  $\pm$  SD (B) and mean  $\pm$  SD (E). Student's t-test: \* $p < 0.05$  and \*\* $p < 0.01$ .

**Table F4**

		Unpaired Student's t-test, two-tailed ( $\alpha < 0.05$ )		
Figure	Parameter	Groups	Statistics	P
4B	COUP-TFI mRNA expression	Sal vs LPS	$t_{(8)} = 2.256$	$P = 0.0540$
4E	% COUP-TFI+/GFAP+ RGLs	Sal vs LPS	$t_{(4)} = 6.790$	$P = 0.0025$



### 2.3.2 Genetic inactivation of COUP-TFI in mitotic progenitors of adult DG impairs neurogenesis by promoting an astroglial fate

To investigate COUP-TFI function in adult neurogenic progenitors, we adopted a loss-of-function approach coupled with fate mapping under healthy conditions. In particular, to target mitotically active cells, I injected a retrovirus expressing Cre-recombinase (RV-Cre) (Rolando et al., 2016) in the DG of two transgenic mouse lines. The *Rosa26-YFP;COUP-TFI<sup>fl/fl</sup>* mice, derived from the interbreeding of *COUP-TFI<sup>fl/fl</sup>* mouse line (Armentano et al., 2007) with *Rosa26-YFP* reporter line (Srinivas et al., 2001) and injected with RV-Cre at postnatal day 60 (P60), were named COUP-TFI-cKO<sup>RV-Cre</sup> (i.e., cKO<sup>RV-Cre</sup>); they allowed the fate mapping of dividing progenitor cells that had undergone selective COUP-TFI deletion by retroviral transduction. In parallel, COUP-TFI wild-type mice carrying the *Rosa26-YFP* reporter transgene and injected with RV-Cre were used as controls (Ctrl<sup>RV-Cre</sup>) (Figure 5A).

Two days after retroviral injection (i.e., 2dpi, Figure 5B), I quantified the densities of YFP+ cells in the DG of the two experimental groups and found no significant difference (Figure 5C) demonstrating comparable levels of recombination in Ctrl and COUP-TFI-cKO mice. Then, the genetic inactivation of COUP-TFI was evaluated by analyzing the YFP+ cells that were immunopositive for COUP-TFI. As shown in Figure 5D, the percentage of double COUP-TFI+YFP+ cells dramatically dropped in cKO<sup>RV-Cre</sup> mice (from 92.23% to 6.64%). An in-depth analysis taking into account the different phenotypes among YFP+ cells (i.e., GFAP+ RGL and horizontal stem cells, GFAP-DCX- progenitors, DCX+ progenitors/neuroblasts, and GFAP+ astrocytes) revealed that at this time, the large majority of YFP+ cells were DCX+ progenitors/neuroblasts, and there were no differences between cKO<sup>RV-Cre</sup> and Ctrl<sup>RV-Cre</sup> mice (Figure 5E). These data, obtained at 2dpi, showed that RV-Cre targeted and recombined the population of interest (i.e., neuronal committed progenitors) correctly, representing a good model to investigate the effect of COUP-TFI deletion.

To explore possible changes in the fate of the cellular progeny derived from the mitotically active progenitor population, a longer survival time after RV-Cre injection was chosen (i.e., 18 dpi; Figure 6A). In line with the previous short-term survival time experiment, no significant changes were observed in the total YFP+ cells within the SGZ/GCL area between cKO<sup>RV-Cre</sup> and Ctrl<sup>RV-Cre</sup> mice (Figures 6B). However, differently from the 2dpi protocol, in the DG of

mice belonging to the 18dpi protocol, I observed that the YFP+ population was almost equally composed of DCX+ immature newborn neurons and GFAP+ astrocytes in Ctrl<sup>RV-Cre</sup> mice, while, on the contrary, COUP-TFI deletion impaired neurogenesis by promoting astrogliogenesis in cKO<sup>RV-Cre</sup> (Figures 6C). Moreover, a fold change analysis showed an increase in double GFAP+YFP+ astrocytes (red) and an equivalent reduction in double DCX+YFP+ newborn neurons (pink) in cKO<sup>RV-Cre</sup> compared with Ctrl<sup>RV-Cre</sup> mice (Figures 6E).

These findings indicate that COUP-TFI is needed for neurogenesis and strongly suggest its direct involvement in repressing an astroglial fate in dividing neurogenic progenitors of the adult DG.

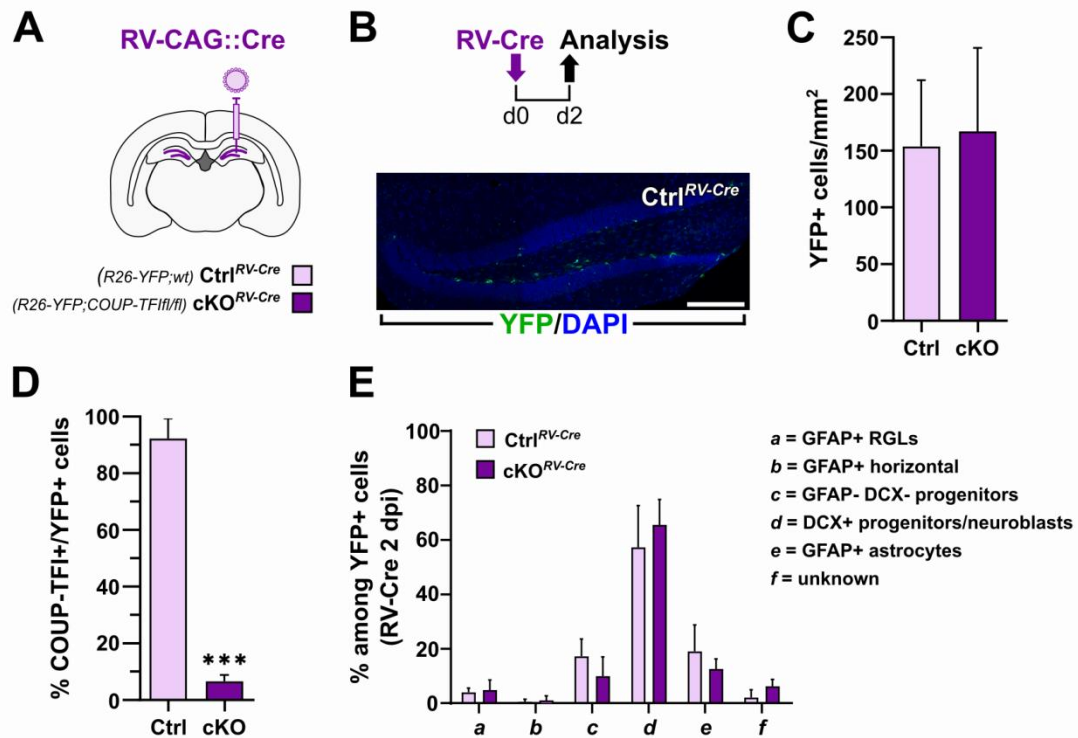


**Figure 5. In vivo targetting of COUP-TFI LOF in adult DG neurogenic progenitors by retroviral vector.** (A) Experimental strategy used for COUP-TFI loss-of-function in dividing DG neural progenitors by Cre-expressing retrovirus (RV-Cre) stereotaxic injection. (B) Short RV-Cre injection protocol. Confocal image showing YFP + (green) cells recombined following *RV-Cre* injection in a DG section counterstained with DAPI (blue). Scale bar, 100 $\mu$ m. (C) Quantification of YFP+ cells in COUP-TFI-cKO<sup>RV-Cre</sup> and Ctrl<sup>RV-Cre</sup> DG (2dpi). (D) Quantification of COUP-TFI+ nuclei among YFP+ cells in COUP-TFI-cKO<sup>RV-Cre</sup> and Ctrl<sup>RV-Cre</sup> DG at 2dpi (92.23  $\pm$  7.178%, n=125/136 in Ctrl<sup>RV-Cre</sup> and 6.646  $\pm$  2.186%, n=8/130 in COUP-TFI-cKO<sup>RV-Cre</sup>). (E) Histograms reporting quantification of different cell phenotypes among YFP+ cells in both Ctrl<sup>RV-Cre</sup> and COUP-TFI-cKO<sup>RV-Cre</sup> DG at 2 dpi. a, Ctrl<sup>RV-Cre</sup> 4.0  $\pm$  1.5% vs. cKO<sup>RV-Cre</sup> 4.8  $\pm$  3.7%; b, Ctrl<sup>RV-Cre</sup> 0.46  $\pm$  0.93% vs cKO<sup>RV-Cre</sup> 0.99  $\pm$  1.7%; c, Ctrl<sup>RV-Cre</sup> 17.2  $\pm$  6.3% vs cKO<sup>RV-Cre</sup> 9.9  $\pm$  7.0%; d, Ctrl<sup>RV-Cre</sup> 54.5  $\pm$  11.3 vs cKO<sup>RV-Cre</sup> 65.5  $\pm$  9.3%; e, Ctrl<sup>RV-Cre</sup> 19.0  $\pm$  9.7% vs cKO<sup>RV-Cre</sup> 12.6  $\pm$  3.7%; f, Ctrl<sup>RV-Cre</sup> 2.0  $\pm$  2.9% vs cKO<sup>RV-Cre</sup> 6.1  $\pm$  2.5%. n=3/4 animals per genotype. Data are presented as mean  $\pm$  SD.; Student's t-test \*\*\*p<0.001.

**Table F5**

<b>Unpaired Student's t-test, two-tailed (<math>\alpha &lt; 0.05</math>)</b>				
<b>Figure</b>	<b>Parameter</b>	<b>Groups</b>	<b>Statistics</b>	<b>P</b>
<b>5C</b>	Cell density of YFP+ population	Ctrl <sup>RV-Cre</sup> vs COUP-TFI-cKO <sup>RV-Cre</sup>	t <sub>(5)</sub> = 0.2635	P = 0.8027
<b>5D</b>	% COUP-TFI+/YFP+ population	Ctrl <sup>RV-Cre</sup> vs COUP-TFI-cKO <sup>RV-Cre</sup>	t <sub>(5)</sub> = 19.56	P < 0.0001
<b>5E</b>	% GFAP+RGLs/YFP+ population	Ctrl <sup>RV-Cre</sup> vs COUP-TFI-cKO <sup>RV-Cre</sup>	t <sub>(5)</sub> = 0.4165	P = 0.6943
<b>5E</b>	% GFAP+horizontal/YFP+ population	Ctrl <sup>RV-Cre</sup> vs COUP-TFI-cKO <sup>RV-Cre</sup>	t <sub>(5)</sub> = 0.5339	P = 0.6163
<b>5E</b>	% GFAP-DCX-progenitors/YFP+ population	Ctrl <sup>RV-Cre</sup> vs COUP-TFI-cKO <sup>RV-Cre</sup>	t <sub>(5)</sub> = 1.445	P = 0.2081
<b>5E</b>	% DCX+progenitors and neuroblasts/YFP+ population	Ctrl <sup>RV-Cre</sup> vs COUP-TFI-cKO <sup>RV-Cre</sup>	t <sub>(5)</sub> = 1.372	P = 0.2283
<b>5E</b>	% GFAP+ astrocytes/YFP+ population	Ctrl <sup>RV-Cre</sup> vs COUP-TFI-cKO <sup>RV-Cre</sup>	t <sub>(5)</sub> = 1.065	P = 0.3356
<b>5E</b>	% unknown/YFP+ population	Ctrl <sup>RV-Cre</sup> vs COUP-TFI-cKO <sup>RV-Cre</sup>	t <sub>(5)</sub> = 1.929	P = 0.1116

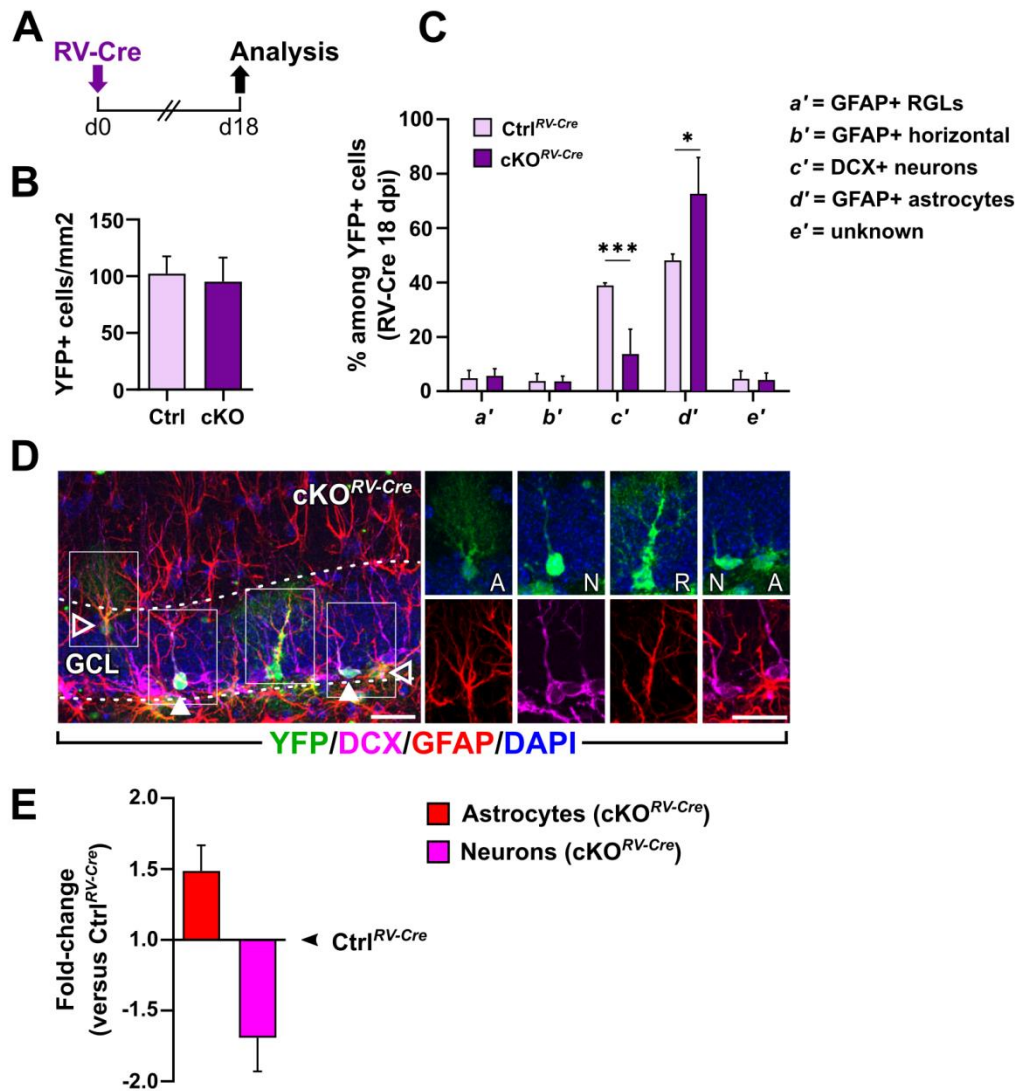


**Figure 6. COUP-TFI deletion in adult DG neurogenic progenitors impairs neurogenesis and increases astrogliogenesis.** (A) Experimental design for RV-Cre injection and analysis of newborn cell phenotype at 18dpi. (B) Quantification of total YFP+ cells within the SGZ/GCL of Ctrl<sup>RV-Cre</sup> and COUP-TFI-cKO<sup>RV-Cre</sup> DG. (C) Histograms reporting quantification of different cell phenotypes among YFP+ cells in both Ctrl<sup>RV-Cre</sup> and COUP-TFI-cKO<sup>RV-Cre</sup> DG at 18 dpi. a, Ctrl<sup>RV-Cre</sup>  $4.8 \pm 2.8\%$  vs. cKO<sup>RV-Cre</sup>  $5.7 \pm 2.6\%$ ; b, Ctrl<sup>RV-Cre</sup>  $3.8 \pm 2.6\%$  vs cKO<sup>RV-Cre</sup>  $3.6 \pm 2.0\%$ ; c, Ctrl<sup>RV-Cre</sup>  $38.9 \pm 0.9\%$  vs cKO<sup>RV-Cre</sup>  $13.7 \pm 9.0\%$ ; d, Ctrl<sup>RV-Cre</sup>  $48.1 \pm 2.3$  vs cKO<sup>RV-Cre</sup>  $72.6 \pm 13.3\%$ ; e, Ctrl<sup>RV-Cre</sup>  $4.6 \pm 2.8\%$  vs cKO<sup>RV-Cre</sup>  $4.1 \pm 2.6\%$ . (D) Confocal images of multiple staining for YFP (green), DCX (magenta), GFAP (red), and DAPI counterstaining (blue) in sections from COUP-TFI-cKO<sup>RV-Cre</sup> and Ctrl<sup>RV-Cre</sup> DG. A, newborn astrocyte; N, newborn neuron; R, RGL cell. Empty arrowheads indicate astrocyte cell bodies, and full arrowheads indicate neurons. GCL, granule cell layer. Scale bars, 20  $\mu$ m. (E) The histogram shows the fold change in the densities of newborn GFAP+YFP+ astrocytes (red) and DCX+YFP+ newborn neurons (pink) within the SGZ/GCL of COUP-TFI-cKO<sup>RV-Cre</sup> mice compared with Ctrl<sup>RV-Cre</sup> mice. n = 3/4 animals per genotype. GCL, granule cell layer. Data are presented as mean  $\pm$  SD (B, C) and fold-change  $\pm$  SD (E). Student's t-test: \*p < 0.05, \*\*\*p < 0.001.

**Table F6**

<b>Unpaired Student's t-test, two-tailed (<math>\alpha &lt; 0.05</math>)</b>				
<b>Figure</b>	<b>Parameter</b>	<b>Groups</b>	<b>Statistics</b>	<b>P</b>
<b>6B</b>	Cell density of YFP+ population	Ctrl <sup>RV-Cre</sup> vs COUP-TFI-cKO <sup>RV-Cre</sup>	$t_{(4)} = 0.4697$	P = 0.6630
<b>6C</b>	% GFAP+RGLs/ YFP+ population	Ctrl <sup>RV-Cre</sup> vs COUP-TFI-cKO <sup>RV-Cre</sup>	$t_{(4)} = 0.3901$	P = 0.7164
<b>6C</b>	% GFAP+horizontal/ YFP+ population	Ctrl <sup>RV-Cre</sup> vs COUP-TFI-cKO <sup>RV-Cre</sup>	$t_{(4)} = 0.1053$	P = 0.9212
<b>6C</b>	% DCX+ neurons/ YFP+ population	Ctrl <sup>RV-Cre</sup> vs COUP-TFI-cKO <sup>RV-Cre</sup>	$t_{(5)} = 7.157$	P = 0.0008
<b>6C</b>	% GFAP+ astrocytes/ YFP+ population	Ctrl <sup>RV-Cre</sup> vs COUP-TFI-cKO <sup>RV-Cre</sup>	$t_{(4)} = 3.159$	P = 0.0342
<b>6C</b>	% unknown/ YFP+ population	Ctrl <sup>RV-Cre</sup> vs COUP-TFI-cKO <sup>RV-Cre</sup>	$t_{(4)} = 0.2235$	P = 0.8341

### 2.3.3 COUP-TFI overexpression rescues altered neuron-to-astrocyte generation upon neuroinflammation

Results obtained from COUP-TFI loss-of-function experiments recalled our previously described findings of COUP-TFI downregulation within the adult DG upon acute LPS-induced neuroinflammation (Figure 4). Therefore, because COUP-TFI seemed necessary to suppress astrogliogenesis favoring neurogenesis in adult neurogenic progenitors, we wondered whether forcing COUP-TFI expression under a neuroinflammatory condition could prevent enhanced astrogliogenesis and rescue neurogenesis. To this aim, I performed a complementary COUP-TFI gain-of-function experiment by injecting the retrovirus RV-Cre in the DG of adult COUP-TFI-O/E<sup>RV-Cre</sup> mice, a *Rosa26-YFP;lox-stop-lox-hCOUP-TFI* transgenic line overexpressing a third COUP-TFI allele in mitotically active neurogenic progenitors and their lineage upon Cre-mediated inducible recombination (Wu et al., 2010). In parallel, *Rosa26-YFP* reporter mouse line, wildtype for COUP-TFI, was also injected with RV-Cre as controls (Ctrl<sup>RV-Cre</sup>) (Figure 7A). Then, one day later, I treated mice with saline (only for controls) or LPS (both controls and COUP-TFI overexpressing mice) for four days (i.e., Ctrl<sup>RV-Cre</sup>+Sal, Ctrl<sup>RV-Cre</sup>+LPS, and O/E<sup>RV-Cre</sup>+LPS; Figures 7B). Two weeks after the RV-Cre injection, I found comparable densities of YFP+ recombined cells within the SGZ/GCL compartment of saline- or LPS-treated Ctrl<sup>RV-Cre</sup> and LPS-treated COUP-TFI-O/E<sup>RV-Cre</sup> mice (Figure 7C). By quantifying the percentage of newborn immature neurons and astrocytes, the LPS-induced phenotype was confirmed by data showing decreased neurogenesis and increased astrogliogenesis within LPS-treated Ctrl<sup>RV-Cre</sup> mice compared to the saline ones (Figure 7D-E). Notably, in LPS-treated COUP-TFI-O/E<sup>RV-Cre</sup> mice, newborn neurons were found more abundant while astrocytes were reduced than LPS- and saline-treated Ctrl<sup>RV-Cre</sup> (Figures 7D and 7E). Indeed, LPS-treated Ctrl<sup>RV-Cre</sup> mice showed a 2-fold increase in GFAP+YFP+ astrocytes (red) and a reduction in DCX+YFP+ newborn neurons (pink) versus saline-treated Ctrl<sup>RV-Cre</sup> animals (Figures 7G). Thus, in the overexpressing mice, LPS-induced effects were completely reverted by COUP-TFI gain-of-function (Figures 7G) within the adult inflamed DG.

These data demonstrate that forced COUP-TFI expression in adult neurogenic progenitors is sufficient to rescue the imbalance in newborn neuron-to-astrocyte ratio during neuroinflammation.

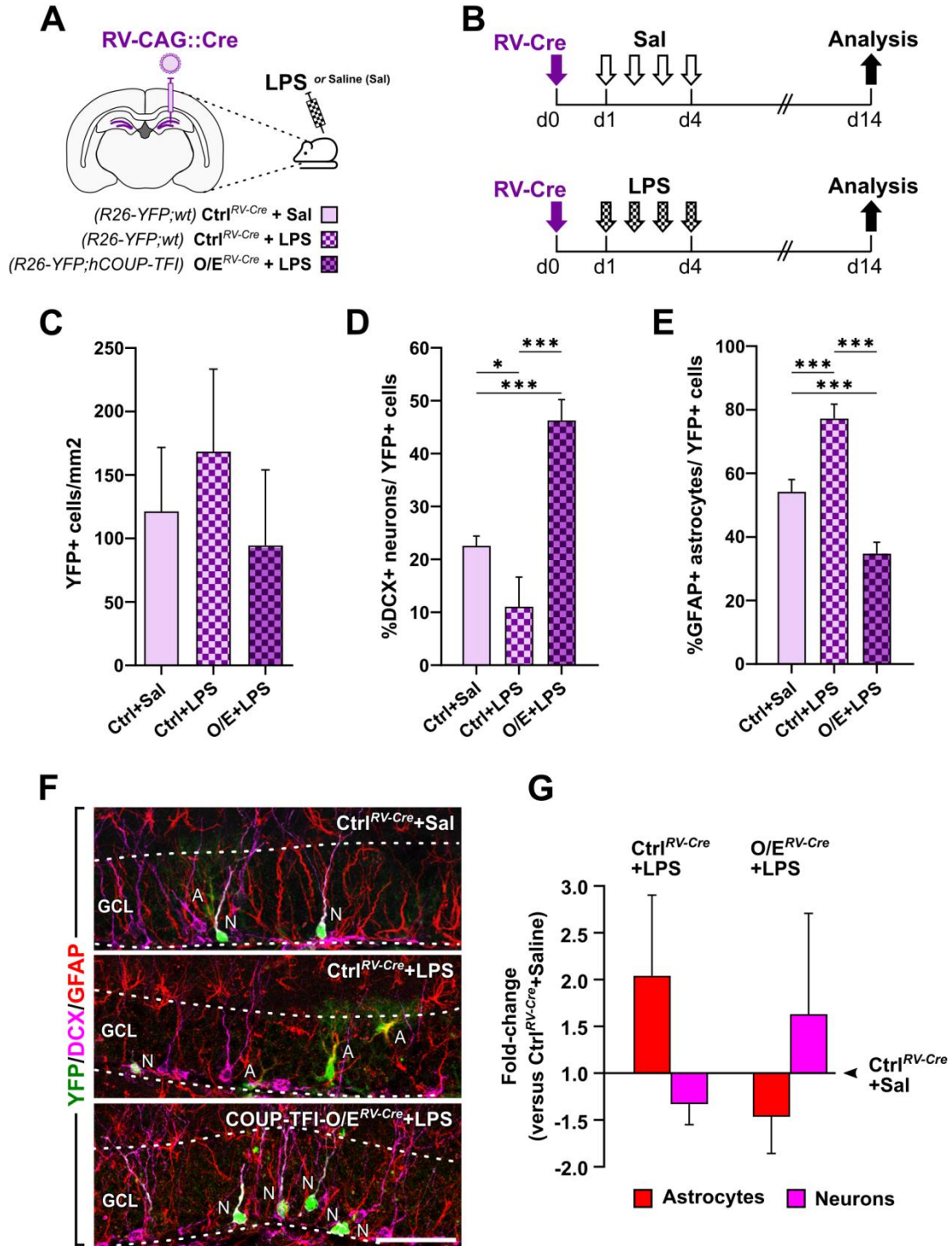


**Figure 7. Forced COUP-TFI expression rescues altered neuron-to-astrocyte generation upon neuroinflammation.** (A) Experimental strategy to induce COUP-TFI gain of function in diving neural progenitors by Cre-expressing retrovirus (RV-Cre) stereotaxic injection in LPS treated mice. (B) Experimental design for analyzing newborn cell phenotype on inflamed RV-Cre injected COUP-TFI-O/E DG. (C) Quantification of YFP+ cells within the SGZ/GCL of Ctrl<sup>RV-Cre</sup>+Saline, Ctrl<sup>RV-Cre</sup>+LPS, and COUP-TFI-O/E<sup>RV-Cre</sup>.



<sup>Cre</sup>+LPS mice. One-way ANOVA:  $F(2,8) = 1.4546$ ,  $p = 0.2892$ , with Bonferroni post-hoc-test: Ctrl<sup>RV-Cre</sup>+Saline versus Ctrl<sup>RV-Cre</sup>+LPS versus COUP-TFI-O/E<sup>RV-Cre</sup>+LPS,  $p > 0.05$ . (D) Quantification of GFAP+ newborn astrocytes on the YFP cell pool within the SGZ/GCL in Ctrl<sup>RV-Cre</sup>+Saline, Ctrl<sup>RV-Cre</sup>+LPS, and COUP-TFI-O/E<sup>RV-Cre</sup>+LPS DG at 14dpi (one-way ANOVA  $F(2;8)= 96.83$ ,  $p<0.0001$  followed by Bonferroni post hoc test). (E) Quantification of DCX+ newborn neurons on the YFP cell pool within the SGZ/GCL in Ctrl<sup>RV-Cre</sup>+Saline, Ctrl<sup>RV-Cre</sup>+LPS, and COUP-TFI-O/E<sup>RV-Cre</sup>+LPS DG at 14dpi (one-way ANOVA  $F(2;8)= 63.51$ ,  $p<0.01$ , followed by Bonferroni post hoc test). (F) Confocal images of DG sections immunostained for YFP (green), DCX (magenta), and GFAP (red) in Ctrl<sup>RV-Cre</sup>+Saline, Ctrl<sup>RV-Cre</sup>+LPS, and COUP-TFI-O/E<sup>RV-Cre</sup>+LPS mice. A, newborn astrocyte; N, newborn neuron. Scale bar, 50  $\mu$ m. (G) Histogram showing the fold change in densities of newborn GFAP+YFP+ astrocytes (striped pattern) and DCX+YFP+ newborn neurons (checkerboard pattern) within the SGZ/GCL of Ctrl<sup>RV-Cre</sup>+LPS and COUP-TFI-O/E<sup>RV-Cre</sup>+LPS mice normalized to Ctrl<sup>RV-Cre</sup>+Saline.  $n = 3/4$  animals per genotype. Data are presented as mean  $\pm$  SD (C, D, and E) and fold-change  $\pm$  SD (G). One-way ANOVA followed by Bonferroni post hoc test. \* $p < 0.05$ , \*\*\* $p < 0.001$ .

**Table F7**

One-way ANOVA ( $\alpha < 0.05$ )				Bonferroni <i>post hoc</i> test		
Fig.	Parameter	Statistics	P	Ctrl+Sal vs Ctrl+LPS	Ctrl+Sal vs O/E+LPS	Ctrl+LPS Vs O/E+LPS
7C	Cell density of YFP+ population	$F_{(2,8)} = 1.455$	$P = 0.2892$	$P = 0.8658$	$P > 0.9999$	$P = 0.4105$
7D	%DCX+neurons /YFP+ population	$F_{(2,8)} = 63.51$	$P < 0.0001$	$P = 0.0127$	$P = 0.0002$	$P < 0.0001$
7E	%GFAP+astrocytes /YFP+ population	$F_{(2,8)} = 96.83$	$P < 0.0001$	$P = 0.0001$	$P = 0.0007$	$P < 0.0001$

## 2.4 Discussion

The continuous addition of newly formed and functional DG granule neurons into the existing circuitry over a lifetime implies that adult hippocampal neurogenesis represents an extreme form of plasticity in the adult brain strongly associated with learning and memory (Gonçalves et al., 2016; Toda and Gage, 2018). In addition to new granule neurons, adult DG NSCs/progenitors give rise to new astrocytes which migrate into the granule cell layer, the hilus, and the molecular layer, and whose functional significance and underlying mechanisms of generation are not as well characterized (Bonaguidi et al., 2011; Encinas et al., 2011; Bond et al., 2015). Interestingly, the decision-making process of adult NSCs/progenitors to become a neuron or an astrocyte is subject to dynamic modulation dependent on the animal's behavior, experience, and emotional/biological status (Aimone et al., 2014). Among the different stimuli, neuroinflammation contributes to impaired hippocampal neurogenesis, which is paralleled by increased generation of astrocytes, observed in mouse models (Kohman and Rhodes, 2013); this imbalance could contribute to the inflammation-associated cognitive decline, possibly by remodeling neural circuits and acting on memory consolidation (Valero et al., 2014). Thus, understanding NSC/progenitor cell-intrinsic responses to inflammation might be crucial not only to elucidate the mechanisms of how NSCs/progenitors react to tissue damage, but also to shed light on the regulatory functions occurring in physiological conditions. Although significant progress has been made in understanding extrinsic and intrinsic cues regulating adult NSC/progenitor cell activity in vertebrates, little was known on the transcriptional program controlling astroglial versus neuronal fate choice of adult hippocampal NSCs/progenitors.

The data reported in this chapter, together with complementary data obtained in the laboratory, contributed to unraveling an unexpected role for the transcriptional regulator COUP-TFI in balancing neuro- and astroglialogenesis within the adult DG in physiologic and pathologic conditions (Bonzano, Crisci, *et al.*, 2018).

First, based on the observation that COUP-TFI was downregulated in RGL cells upon neuroinflammation, we hypothesized that it could be related to the increase in astroglia at the expense of newborn neurons observed in the adult DG upon inflammation, implying a possible function of COUP-TFI in NSCs/progenitors in the control of cell-fate choice. Indeed, by using

*in vivo* retroviral-based COUP-TFI loss-of-function experiments, I found that COUP-TFI inactivation in DG neurogenic progenitors prompted these cells to acquire an astroglial fate. These data support complementary findings obtained in the laboratory (by S. Bonzano) on the loss of COUP-TFI function by using the tamoxifen (Tam)-inducible form of Cre-recombinase (CreERT2) under *Glast* transcriptional control (i.e., *Glast-CreERT2* mouse line) to delete COUP-TFI in adult RGL cells and their progeny. Indeed, the loss of COUP-TFI in the RGL cell pool severely impaired neurogenesis (without altering NSC/progenitor proliferation and/or newborn cell survival) and promoted astroglial fate within the adult DG (Bonzano, Crisci, *et al.*, 2018).

Altogether, by using two different loss-of-function approaches, and genetic fate mapping, we demonstrated that COUP-TFI is necessary to inhibit an astroglial fate and drive adult NSCs/progenitors toward a neuronal lineage into the hippocampal neurogenic niche. The persistence of neurogenesis within the adult brain has been suggested to result from the action of several neurogenic factors counteracting a pro-gliogenic environment (Götz *et al.*, 2016). In this perspective, COUP-TFI might exert its neurogenic function by cell-intrinsically repressing a “default” astroglial fate within the adult neurogenic niche. Interestingly, the retroviral-based approach targeted the mitotically active population of the SGZ, which is mainly composed of IPCs or Type-2 cells, indicating they might still be multipotent, as also recently suggested (Harris *et al.*, 2018) and need COUP-TFI to restrict their potential to a neuronal fate.

Notably, through the retroviral-based gain-of-function approach, I also demonstrated that forced COUP-TFI expression in mitotically active progenitors is sufficient to prevent LPS-induced astroglial fate, further supporting the implication of COUP-TFI in the fate-choice of neural progenitors and suggesting that modulating COUP-TFI expression protects NSCs/progenitors from inflammatory insults. Thus, COUP-TFI may act as a molecular “sensor” in the adult DG neurogenic niche by responding to external cues and allowing multipotent NSCs/progenitors to take either an astroglial or a neuronal lineage. Understanding how NSCs/progenitors can integrate environmental signals via COUP-TFI and/or other factors and identify the molecular pathways downstream of their activity deserve further investigation.

The published paper (Bonzano, Crisci, *et al*, 2018) includes all the data reported in this chapter, and it is presented as an appendix of the Ph.D. thesis.

As a final note, it is noteworthy that in the gain-of-function experiments, the retroviral-based approach was the only method reliable to manipulate *in vivo* transgenic mouse lines under LPS-induced inflammatory conditions. Indeed, the use of tamoxifen to induce the COUP-TFI overexpression on the Glast-CreERT2 mouse line interfered with the inflammatory response (not shown) and thus was not used here. However, this observation inspired me to investigate further the effects of tamoxifen on the DG neurogenic niche; the data obtained are described in the following Chapter III.

## **CHAPTER III**

# **3 Tamoxifen exerts direct and microglia-mediated regulation on the adult mouse hippocampal neurogenic niche preventing the detrimental effects of LPS-induced neuroinflammation**

## **3.1 Abstract**

Tamoxifen is a selective estrogen receptor modulator used in experimental animal research to activate the CreERT2-LoxP system, an essential tool for genetic manipulation *in vivo* that is widely exploited to investigate the dynamics and potential of neural stem cells (NSCs) within the mouse brain. In the adult hippocampal dentate gyrus (DG), NSCs generate neurons and astrocytes in a tightly regulated process that is affected by neuroinflammation and could be influenced by tamoxifen. Here we report that lipopolysaccharide (LPS)-induced neuroinflammation beside unbalancing neuron/astrocyte generation in the adult DG, also alters adult NSCs. Moreover, we show that a two-day tamoxifen treatment moderately enhanced the expression of inflammatory mediators within the hippocampus both in basal condition and upon LPS-induced neuroinflammation. Such treatment was sufficient to prevent the microglia activation and the alterations in the DG neurogenic niche observed in LPS-treated mice. We provide evidence that the consequences of LPS and tamoxifen treatments imply both direct effect on NSCs and newborn neurons and indirect microglia-mediated actions on NSCs and astrocytes, as demonstrated upon depletion of microglia through PLX5622 treatment. While tamoxifen alone did not alter DG NSCs and neuron/astroglia-genesis, our study points to a strong protective role of tamoxifen against neuroinflammation-induced gliosis and reduced neurogenesis. These effects need to be considered when using tamoxifen-inducible CreER systems.

## 3.2 Introduction

The hippocampal dentate gyrus (DG) is one of few sites where neurogenesis (i.e., the generation and functional integration of new neurons) occurs in adulthood within the mammalian brain due to the occurrence of adult neural stem cells (NSCs) (Bonaguidi et al., 2012; Bond et al., 2015; Kempermann et al., 2015). In adult mice, radial glial-like (RGL) NSCs, located in the subgranular zone (SGZ) of the DG, give rise to both neurons and astrocytes (Bonaguidi et al., 2011; Encinas et al., 2011; Song et al., 2012; Kempermann et al., 2015; Berg et al., 2018). The balanced generation of neurons and astrocytes in the adult healthy DG is regulated by cell-intrinsic factors in RGL/progenitors (Bonaguidi et al., 2011; Encinas et al., 2011; Bonzano et al., 2018) and is influenced by multiple environmental or physio-pathological factors that can increase (e.g., enriched environment or voluntary exercise) or decrease (e.g., aging, stress, and neurodegenerative diseases) the production and integration of adult-born neurons (Steiner et al., 2004, 2008; Dranovsky et al., 2011; Aimone et al., 2014; Sierra et al., 2015; Gebara et al., 2016; Beccari et al., 2017). Such factors often display opposite effects on astrogliogenesis, as in the case of aging and neuroinflammation, which leads to enhanced production of astrocytes (Wu et al., 2012; Zonis et al., 2013; Woodbury et al., 2015; Pérez-Domínguez et al., 2017; White et al., 2020). Adult DG neurogenesis plays a key role in cognitive processes such as memory, learning, and mood control (Deng et al., 2010; Gonçalves et al., 2016). Several studies on animal models and human patients suggest that impairments in cognitive functions observed in multiple neurological diseases and disorders, like depression, epilepsy, and Alzheimer's disease (AD), are associated with dysregulated adult DG neurogenesis (Sahay et al., 2011; Snyder et al., 2011; Baptista and Andrade, 2018; Toda et al., 2019). Moreover, neuroinflammation, a common feature of many neurodegenerative disorders associated with astrogliosis (Perry et al., 2010), is sufficient to affect adult DG neurogenesis (Ekdahl et al., 2003; Monje et al., 2003; Fujioka and Akema, 2010; Kohman and Rhodes, 2013). Beside astrocytes, one of the key cell types involved in the neuroinflammatory response and thereby contributing to the pathophysiology of neurodegenerative diseases are microglia. In the healthy adult DG, microglial cells act by "surveying" the neurogenic niche to maintain homeostasis and fine-tune adult neurogenesis, being responsible for multiple functions, including phagocytosis of cellular debris and synaptic pruning (Ekdahl, 2012; Sierra et al., 2014; Diaz-Aparicio et al.,

2020); however, their specific role in mediating dysfunctional neurogenesis upon neuroinflammation remains largely unknown.

Transgenic animals bearing the tamoxifen-inducible CreERT2-LoxP system are a useful tool for manipulating gene expression in specific cell types in a temporally controlled manner (Hirrlinger et al., 2006; Mori et al., 2006; Valny et al., 2016; Jahn et al., 2018). These models have been widely exploited in studies of adult neurogenesis and astroglialogenesis to label and analyze the dynamics of adult RGLs and their progeny within the adult DG (Zhang et al., 2010; Bonaguidi et al., 2011; Dranovsky et al., 2011; Encinas et al., 2011; Kim et al., 2011; Yang et al., 2015; Moura et al., 2020; Bottes et al., 2021; Harris et al., 2021). In these models, Cre-recombination is induced by the administration of tamoxifen which belongs to the first generation of selective estrogen receptor modulators (SERMs), initially produced in the '60s as an anti-cancer drug (Jordan, 2003). Tamoxifen is a mixed agonist/antagonist of the estrogen receptor that crosses the blood-brain barrier (Lien et al., 1991; Pareto et al., 2004), reaching the nervous system. Although no persisting effects on adult DG neurogenesis have been reported upon tamoxifen activation of Cre-recombinase (Rotheneichner et al., 2017), a recent study showed long-lasting adverse effects of tamoxifen on neurogenesis in embryonic and adult brains (Lee et al., 2020). On the other hand, tamoxifen has been reported to exert anti-inflammatory and neuroprotective therapeutic activity in different pathologies, including spinal cord injury (Tian et al., 2009; Colón and Miranda, 2016), retinal diseases (Wang et al., 2017), and aneurysmal subarachnoid hemorrhage (Sun et al., 2013) where its neuroprotective effect was correlated with a decreased microglial activation and reduced production of inflammatory mediators (Tian et al., 2009; Sun et al., 2013; Wang et al., 2017). Thus, tamoxifen treatments used to activate the Cre recombinase could interfere with adult DG neurogenesis in animal models of neuroinflammation.

Here, we investigated the effects of a two-day tamoxifen administration on the adult DG neurogenic niche in healthy mice and in a lipopolysaccharide (LPS)-induced model of neuroinflammation (Cardona et al., 2006; Norden et al., 2016). Focusing on the granule and subgranular zone of the adult DG, we investigated how these treatments impacted on microglia, astroglia, RGL/progenitor cells, and newborn neurons, identified by specific immunofluorescent stainings. Finally, to specifically address the role of microglia in



mediating LPS and/or tamoxifen effects on the adult DG neurogenic niche, we extended such analysis in mice depleted of microglia following chronic treatment with PLX5622, an inhibitor of the colony-stimulating factor 1 receptor (CSF1R).

### 3.3 Materials and methods

#### 3.3.1 Animals

Experiments were performed on adult C57BL/6J and C57BL/6N mice aged P60 to P90 at the onset of each experiment. Mice were housed under a 12-hour light/dark cycle as groups of three to five animals per cage in an environmentally controlled room with access to food and water *ad libitum*. Experiments were designed to minimize the number of animals used (N=65 total animals used for the study, both sexes). Mice were randomized from each group. All experimental procedures were conducted in accordance with the Guide for the Care and Use of Laboratory Animals of the European Community Council Directives (2010/63/EU and 86/609/EEC) and approved by local bioethics committees, the Italian Ministry of Health, and the French Ministry for Higher Education and Research (authorization number 864/2018-PR to SDM and 2019042614306844 to WK)

#### 3.3.2 Drug treatments (i.e., administration of tamoxifen, LPS, PLX5622)

The following groups were used for molecular and cellular analyses of various hippocampal cell populations at shorter (forty-eight hours post injections; 48 hpi) and longer (seven days post injections, 7dpi) chase periods between two treatments. For all short-chase experiments (Figures 1-3), tamoxifen (Tam; T-5648, Sigma-Aldrich) was dissolved in corn oil (C8267, Sigma-Aldrich) and used as a pretreatment by daily intraperitoneal (i.p.) injections of 2.5 mg/mouse/day, for two consecutive days. Tamoxifen administration was then followed, after 48 hours, by daily i.p. injections of either *E. coli*-derived lipopolysaccharide (LPS; 0.5 mg/kg/day) for four consecutive days (L2880, Sigma-Aldrich) in the *Tam+LPS* group or saline physiological solution as a control (Sal; 0.9%) in the *Tam+Sal* group. The other two groups, named Sal or LPS solely, were injected with Tam vehicle (i.e., corn oil) followed by either saline or LPS, respectively. For the analysis of the effect of tamoxifen pretreatment on neuroinflammation elicited at a longer chase period (Figure 4), mice named *L-Tam+LPS* were injected with LPS (0.5 mg/kg/day) seven days after tamoxifen injections (7dpi), once a day for four consecutive days, and compared to the mice that received only LPS (i.e., *LPS* group). All experimental groups were then sacrificed one day after the last LPS or Sal injection for

analyses. A sample size of at least three mice was randomly assigned to each experimental group, and the number of animals used for each experiment is specified in figure legends.

Pharmacologic ablation of brain microglia was obtained by administration of the CSF1R inhibitor PLX5622 (Plexxikon, Inc.; Berkley, CA) formulated at 1200 parts per million (ppm) into standard rodent diet AIN-76A (12% fat, caloric density 3.86kcal/g; Research Diets, Inc. (New Brunswick, NJ). Animals were fed *ad libitum* with either the PLX5622 formulated diet or a standard chow diet (AIN-76A) starting from five days before receiving the first Tam/corn oil injection and for the entire duration of the experiment.

### **3.3.3 Tissue preparation and sectioning**

For immunofluorescence analysis, mice were deeply anesthetized with a mixture of tiletamine/zolazepam (80 mg/kg, Zoletil 100, Virbac Corporation, France) by i.p. injection, and perfused transcardially with ice-cold 0.9% saline solution, followed by ice-cold 4% paraformaldehyde (PFA) in 0.1 M phosphate buffer (PB), pH 7.4. Brains were removed from the skull and postfixed for 4 hours in the same PFA solution at 4°C. Post-fixation was followed by a cryopreservation step with a 30% sucrose solution in 0.1 M PB pH 7.4 at 4 °C for 48 hours. Then, the two hemispheres were separated and embedded in optimal cutting temperature compound (OCT, Killik, Bio-Optica), frozen, and stored at -80 °C until sectioning. One hemisphere was then cut with a cryostat (Leica Microsystems), and serial free-floating 30µm-thick coronal sections were collected in multi-well dishes and stored at -20°C in antifreeze solution (30% ethylene glycol, 30% glycerol, 10% PB: 189 mM NaH<sub>2</sub>PO<sub>4</sub>, 192.5 mM NaOH; pH 7.4) until use.

### **3.3.4 Multiple immunofluorescence labeling**

Brain sections were rinsed in phosphate buffer solution (PBS, 0.01M, pH 7.4) and pre-incubated at room temperature (RT) for 1 h in PBS containing 10% of the normal sera that matched the host species of the secondary antibodies (i.e., normal donkey serum, NDS; Jackson ImmunoResearch, 017-000-121) and 0.5% Triton X-100 (Sigma- Aldrich T8787) for blocking unspecific bindings. Then slices were incubated with primary antibodies (**Table A**) diluted in PBS containing 0.5% Triton X-100 and 1% NDS at 4°C for 48 hours. After three rinses in PBS, slices were incubated with fluorochrome-conjugated secondary antibodies

(**Table A**) in PBS for 1,5 h at RT. Sections were finally counterstained with the nuclear dye 4',6-diamidino-2-phenylindole (DAPI; 1:1000; Sigma-Aldrich, D9542) for 15 minutes at RT and coverslipped with the anti-fade mounting medium Mowiol (4-88 reagent, Calbiochem 475904).

### **3.3.5 Confocal microscopy**

Confocal images were acquired with a TCS SP5 confocal microscope (Leica Microsystems). Images were captured as z-stacked focal planes through the thickness of the slice (30  $\mu\text{m}$ ) at 1- $\mu\text{m}$  optical steps with an oil-immersed Plan-Apochromat 40X/1.25 objective, zoom 1.0, and resolution of 1024/1024 pixels and 100Hz (1 pixel = 0.38  $\mu\text{m}$ ) comprising both upper and lower blades of the hippocampal DG.

### **3.3.6 Cell counting and morphometric analyses**

For cell quantification, images were analyzed with NIH ImageJ (<https://imagej.nih.gov/ij/>) using the cell counter and channel tool plugins. At least three different levels along the rostrocaudal DG axis were analyzed, and the cell density was calculated by dividing the total number of counted cells over the area of interest (MCL, SGZ+GCL, or Hilus) and expressed as the mean number of cells per squared millimeters ( $\text{cells}/\text{mm}^2$ ). Microglia cells were visualized by Iba1 expression and counted separately in each DG region (MCL, SGZ/GCL, and Hilus). For DCX and NeuroD1 analysis, immunopositive cells were counted in the SGZ and deep GCL area, where DAPI staining was used to trace the granule cell layer in DG and counterstain clustered cells discriminating single marker+ cells among packaged marker+ cells. For analysis of GFAP+ RGL, cells were deemed radial if the cell body, clearly associated with a DAPI+ nucleus, was located in the SGZ and had a single thin radial process extending throughout GCL and branching into the MCL (Gebara et al., 2016).

For microglia morphological analyses, tridimensional reconstruction of Iba1+ cells was performed in z-multi-stack with NIH ImageJ using Simple Neurite Tracer (SNT) plugin upon manual image editing (i.e., subtract background and grayscale attribute filtering). Then, manual 3D reconstruction was finalized with the filling tool to measure morphological parameters: the territory area as the convex hull area, where the convex hull is the smallest convex polygon (that with all interior angles smaller than 180°) containing the whole-cell

shape (Fernández-Arjona et al., 2017), and the total number of branches including their different levels [i.e., the degree of ramification quantified by counting the number of segments at each level up to level 5 (Figure S1F); (Raj et al., 2014)].

### **3.3.7 Tissue collection, RNA extraction, and RT-qPCR**

For whole-hippocampus RT-PCR, mice were sacrificed by cervical dislocation, and hippocampi were microdissected and quickly frozen in liquid nitrogen and stored at  $-80^{\circ}\text{C}$  until further processing. Total RNA was extracted from brain homogenate using RNeasy Micro Kit (Qiagen, France) following the manufacturer's protocol. Reverse transcription was carried out using the QuantiTect kit (Qiagen, France). The qPCR reactions were performed in duplicates in a LightCycler480 (Roche) using QuantiTect SYBR Green PCR kit (Qiagen, France) and gene-specific primers (**Table B**). The number of transcripts was evaluated relative to the expression level of the housekeeping gene acidic ribosomal phosphoprotein P0 (Rplp0 or 36B4). Fold change was calculated with respect to the control saline-injected group.

### **3.3.8 Statistics**

Results were presented as mean  $\pm$  s.d. and derived from at least three different animals/group. A two-tailed independent t-test was performed to compare the differences between two groups; moreover, an F-test of equality of variances was conducted to compare variances, and Welch's correction was applied in case of unequal variance distribution. Two-way analysis of variance (ANOVA) with Dunnett's multiple comparisons test was used for qPCR analyses to compare each means with the saline-control mean. Then, for cellular analyses, Student-Newman-Keuls' post hoc test was used for multiple comparisons of unequal sample sizes regardless of rows and columns. Data distribution was assumed to be normal with the Shapiro-Wilk test ( $\alpha=0.05$ ). The confidence interval was expressed with 95% confidence. The statistical significance was defined as follows: \* $p<0.05$ , \*\* $p<0.01$ , and \*\*\* $p<0.001$ . All statistical analyses were performed using Microsoft Excel and Graphpad Prism 8 software. For cell countings, outliers were identified with Tukey's method following 1.5xIQR (Interquartile range) rule.

**Table A. List of primary and secondary antibodies**

Antigen name	Host	Dilution	Source	Catalog number
<b>Primary Antibodies</b>				
<b>Iba1</b>	Rabbit	1:1000	Wako	019-19741
<b>DCX</b>	Goat	1:1500	Santa Cruz Biotechnology	Sc-8066
<b>NeuroD1</b>	Goat	1:400	Santa Cruz Biotechnology	Sc-1804
<b>GFAP</b>	Goat	1:200	Abcam	ab53554
<b>GFAP</b>	Mouse	1:700	Immunological Science	MAB12029
<b>S100<math>\beta</math></b>	Rabbit	1:10000	SWANT	37A
<b>Ki67</b>	Rabbit	1:1000	Abcam	ab15580
<b>Secondary Antibodies</b>				
<b>AlexaFluor488 Anti-Ms</b>	Donkey	1:400	Jackson ImmunoResearch	715-545-151
<b>AlexaFluor488 Anti-Rb</b>	Donkey	1:400	Jackson ImmunoResearch	711-545-152
<b>AlexaFluor647 Anti-Rb</b>	Donkey	1:600	Jackson ImmunoResearch	711-605-152
<b>Cy3 Anti-Gt</b>	Donkey	1:800	Jackson ImmunoResearch	705-165-147

**Table B. List of primers**

Gene	Forward (5'-3')	Reverse (5'-3')
<b>TNF<math>\alpha</math></b>	CTTCTGTCTACTGAACTTCGGG	CAGGCTTGTCACTCGAATTTTG
<b>IL1<math>\beta</math></b>	ACGGACCCCAAAGATGAAG	TTCTCCACAGCCACAATGAG
<b>IL6</b>	CAAAGCCAGAGTCCTTCAGAG	GTCCTTAGCCACTCCTTCTG
<b>IL4R</b>	ATTGTCTACTCAGCCCTTAC	CAGCAGCCACAGCAAGGACT
<b>TGF<math>\beta</math></b>	TGATACGCCTGAGTGGCTGTCT	CACAAGAGCAGTGAGCGCTGAA
<b>Rplp0 (36B4)</b>	ACCCTGAAGTGCTCGACATC	AGGAAGGCCTTGACCTTTTC

## 3.4 Results

### 3.4.1 Tamoxifen modulates the expression of inflammatory cytokines within the adult mouse hippocampus

Tamoxifen has been reported to exert neuroprotective actions on CNS in various experimental or clinical conditions, including anti-inflammatory activity (Baez-Jurado et al., 2019). Here, we investigated whether a short tamoxifen treatment, as used for inducible DNA recombination based on the CreERT2-LoxP system (Rolando et al., 2012; Yang et al., 2015; Bonzano et al., 2018), can modulate inflammatory signaling in the adult mouse hippocampus. To this end, we treated young adult mice with tamoxifen or its vehicle (i.e., corn-oil) once a day over two consecutive days, followed by an intraperitoneal (i.p.) injection of *E. coli*-derived lipopolysaccharide (LPS, as pro-inflammatory stimulus) or saline solution (as control), 48 hours later and repeated for four days (Figure 1A).

The expression level of selected pro-inflammatory (i.e., IL-1 $\beta$ , IL-6, TNF $\alpha$ ) and anti-inflammatory (IL-4R, TGF $\beta$ ) genes was quantified by RT-qPCR six days after the tamoxifen treatment in the presence or absence of LPS treatment. Results showed a general up-regulation for all inflammatory genes in the hippocampi of treated mice, compared to control groups (Sal; Figure 1B-F). In particular, the increase in the expression level of IL-1 $\beta$  was statistically significant following LPS treatment (i.e., LPS and Tam+LPS groups) compared with control saline-injected mice (Sal; Figure 1B). Unexpectedly, IL-1 $\beta$  expression increased in Tam+Sal treated mice (Figure 1B) which also showed augmented levels of IL-6 (Figure 1D), and a tendency to increase in TNF $\alpha$  (P=0.059; Figure 1C), suggesting tamoxifen *per se* can positively modulate pro-inflammatory molecules. In parallel, we also found a positive effect of tamoxifen on the expression of the anti-inflammatory genes IL-4R (Figure 1E) and TGF $\beta$  (Figure 1F), both in the absence and presence of LPS treatment. These observations indicate that tamoxifen confers a unique inflammatory signature to the adult hippocampus, likely involving glial cell activation.

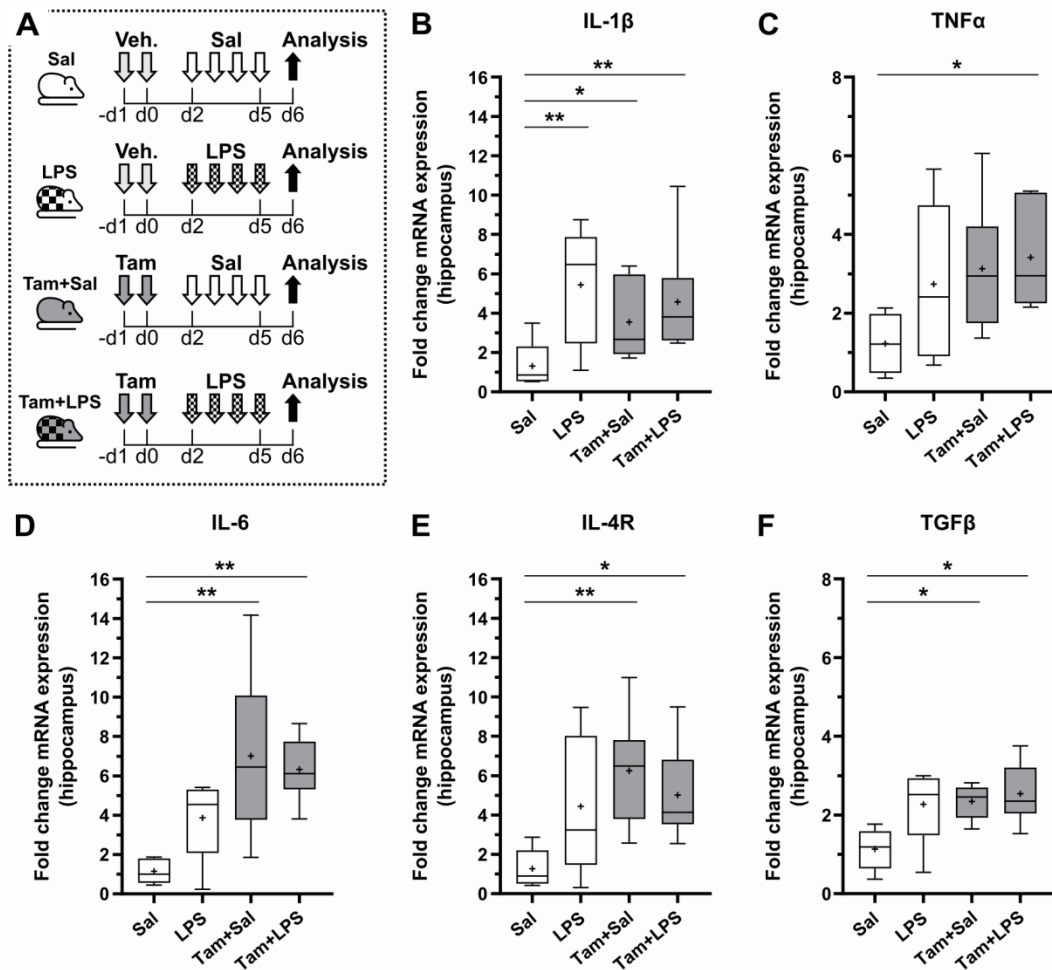


**Figure 1. Tamoxifen induces changes in the expression of pro- and anti-inflammatory mediators within the adult mouse hippocampus.** (A) Experimental design. Veh. (Vehicle, i.e., corn oil), Tam (Tamoxifen, 2.5 mg/mouse/day), Sal (saline solution 0.9%), and LPS (E. coli-derived lipopolysaccharide, 0.5 mg/kg). Treatments were administered by intraperitoneal injections. (B-F) Histograms showing fold changes in IL1 $\beta$  (B), TNF $\alpha$  (C), IL6 (D), IL4R (E), and TGF $\beta$  (F) gene transcripts in the hippocampi of mice injected with LPS alone (LPS) or treated with tamoxifen before Sal (Tam+Sal) or LPS (Tam+LPS) injections normalized to control hippocampi of mice injected with Saline (Sal). TNF $\alpha$ , tumor necrosis factor alpha; IL1 $\beta$ , interleukin 1 beta; IL6, interleukin 6; IL4R, interleukin 4 receptor; TGF $\beta$ , transforming growth factor-beta. n=5-6 mice/group; technical replicates = 2. Data are presented as box plots with whiskers indicating minimum-maximum range; median and media values are shown as a horizontal line and a cross symbol. Two-way ANOVA followed by Dunnett's multiple comparison test: \*p<0.05, \*\*p<0.01. See statistical table S1.



### 3.4.2 Tamoxifen alters the morphology of hippocampal DG microglial cells and prevents their increase upon LPS treatment

Microglial cells play an active role in the brain neuroinflammatory response by the early release of cytokines associated with changes in their morphology (Chen et al., 2012; Walker et al., 2014; Morganti et al., 2016; Norden et al., 2016). In the adult hippocampus, microglia contribute to the microenvironment of the DG neurogenic niche, modulating adult neurogenesis (Sierra et al., 2010; Ekdahl, 2012; Gebara et al., 2013; Diaz-Aparicio et al., 2020; Zhang et al., 2020). To understand the possible impact of tamoxifen on microglia, we performed a detailed analysis of this cell population *in situ*, focusing on the DG. The timing and protocol of tamoxifen pretreatment combined with LPS or saline i.p. injections were the same as in the previous experiment (Figure 1A). The day after the last LPS treatment, animals were perfused, and the brain tissue was processed for immunofluorescence staining for the cytoplasmic microglia marker Iba1 (Ito et al., 1998), followed by confocal laser scanning microscopy coupled to morphometric analyses (Figure 2).

We first assessed the cell density of Iba1+ microglia within the DG and found an increase in LPS-injected mice compared to controls that was prevented by tamoxifen in Tam+LPS mice, while tamoxifen alone (i.e., Tam+Sal) did not alter microglial cell density (Figure 2A, B). Similar results emerged confining the analysis to the DG granule cell layer (GCL) (Figure S1B), and a similar trend was observed as well for the molecular cell layer (MCL) and the hilus (Figure S1A, C). We next analyzed the percentage of area covered by the Iba1+ signal (i.e., microglia fractional area) in the DG of the different groups (Figure S1D). No statistically significant difference was observed in the microglia fractional area comparing LPS to Sal group (Figure 2C). In contrast, a net reduction was found in both Tam+Sal and Tam+LPS groups compared to Sal and LPS groups, respectively (Figure 2C). However, no differences were found in the soma size of microglial cells among the four groups (Figure S1E).

To disclose possible morphological alterations at a single cellular resolution, we exploited the three-dimensional reconstruction of individual Iba1+ cells (Figure 2D) (Davis et al., 2017). Analysis of the territory area, calculated as the smallest convex polygon containing the whole microglia cell shape (Fernández-Arjona et al., 2017), revealed a net reduction in LPS compared to Sal group (Figure 2E). However, no differences were observed by comparing Sal

and LPS groups with Tam+Sal and Tam+LPS groups, respectively (Figure 2E). In contrast, a statistically significant reduction was found in the total number of branches per cell in tamoxifen-treated groups (Figure 2F), mainly due to decreased secondary and tertiary branches in Tam+Sal and Tam+LPS versus Sal and LPS groups, respectively (Figure S1F). The total number of branches per cell was similar in LPS and Sal groups (Figure 2F), with a slight increase in the secondary branches in LPS treated mice (Figure S1F).

Overall, these data indicate that a two-day-long tamoxifen treatment is sufficient to alter microglial cells in the DG by preventing their increase upon LPS-induction and reducing the morphological complexity of their processes both in unchallenged and reactive microglia.

According to pharmacokinetic studies in mice, tamoxifen and its active metabolites are completely degraded to negligible levels in the brain within 7 days (Valny et al., 2016; Jahn et al., 2018). We run a new experiment comparing LPS-injected mice with mice that received tamoxifen (single i.p. injection for two consecutive days) one week before LPS injections (i.e., Long-chase; L-Tam+LPS) (Figure S2A). Interestingly enough, quantification of Iba1+ microglia on L-Tam+LPS treated mice revealed a reduction in microglia numbers and fractional area compared to LPS group (Figure S2B-D), indicating that the consequences of tamoxifen treatment extend behind its bioavailability.

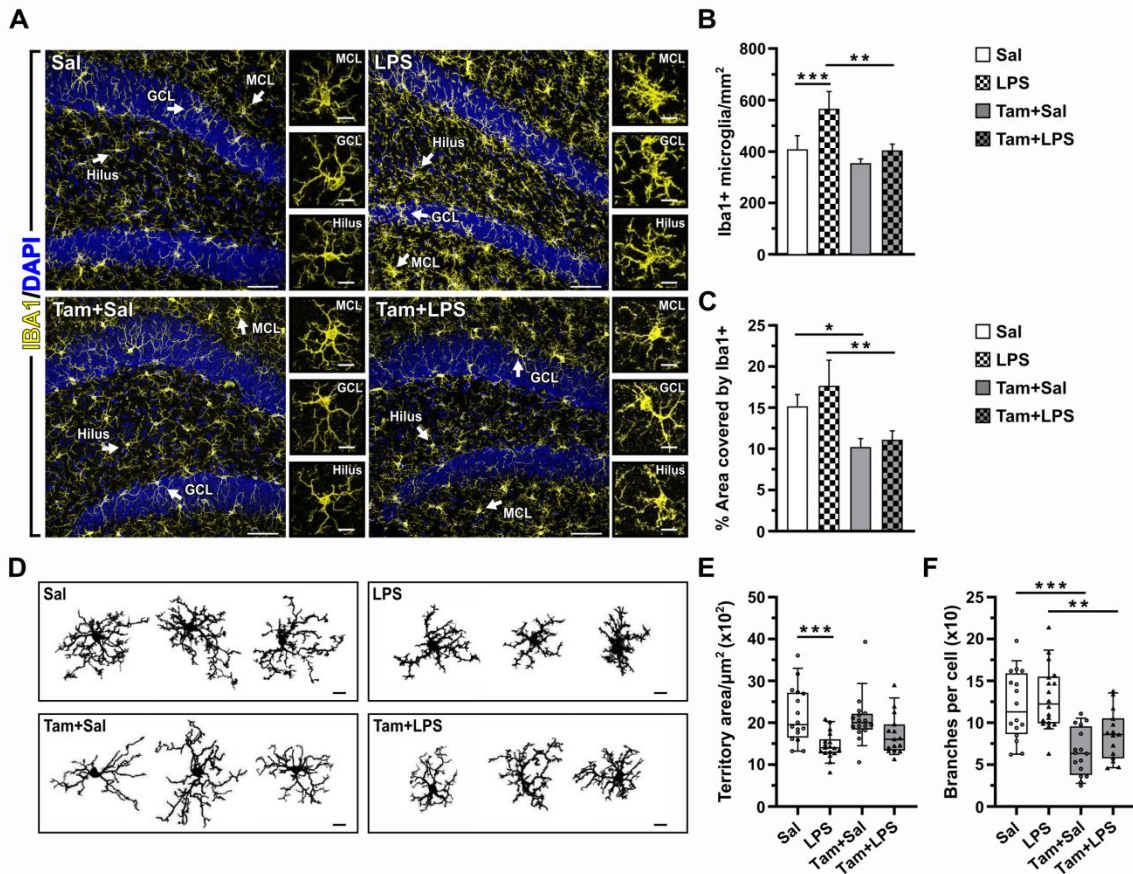


**Figure 2. Tamoxifen alters hippocampal DG microglia activation upon LPS treatment.** (A-F) Refers to the experimental design shown in Figure 1A. (A) Representative confocal images depict microglia immunopositive for Iba1 (yellow) in the DG of the four experimental groups. Cell nuclei are counterstained with DAPI (blue). Insets show high-magnification images of Iba1+ microglial cells (arrows) for each DG subregion (ML, molecular layer; GCL, granule cell layer; Hilus). (B) Quantification of Iba1+ microglial cell density within the DG of the four experimental groups. (C) Percentage of the area covered by Iba1+ microglial cells within the DG of the four experimental groups. (D) Representative binarized max projections of 3D-reconstructed Iba1+ microglial cells within the DG of the four experimental groups. Scale bar, 10  $\mu\text{m}$ . (E, F) Quantification of the territory area occupied by a single microglial cell (E) and the total number of branches per cell (F) of 3D-reconstructed microglial cells within the DG of the four experimental groups.  $n=3-5$  mice/group (B, C).  $n = 15-18$  cell/treatment (E, F) out of 3 mice/group. Scale bars, 50  $\mu\text{m}$  (A; low magnification), 10  $\mu\text{m}$  (A, and D; high magnification). Data are presented as mean  $\pm$  SD (B, C) and box plots with whiskers indicating a minimum-maximum range (E, F). Two-way ANOVA followed by a Student-Newman-Keuls (SNK) multiple comparison test: \* $p < 0.05$ , \*\* $p < 0.01$ , \*\*\* $p < 0.001$ . See also Figure S1 and the statistical values in tables S2 and S3.

### 3.4.3 Tamoxifen counteracts the LPS-induced dysregulation on adult DG neurogenesis

Alongside microglial cells, astrocytes are actively involved in the brain tissue response to inflammatory challenges (Norden et al., 2016; Lana et al., 2017; Yang and Zhou, 2019). To assess the possible effects of tamoxifen on the astroglial population within the DG neurogenic niche, we quantified glial fibrillary acidic protein-positive (GFAP<sup>+</sup>) astrocytes in the deep GCL and subgranular zone (SGZ; Figure 3A, B). The density of GFAP<sup>+</sup> astrocytes was increased in LPS mice compared to Sal control mice (Figure 3B), and tamoxifen abolished such an increase in Tam+LPS mice (Figure 3B). A similar yet attenuated response was observed in the long-chase protocol (Figure S2A, E), where a tendency to a reduced number of GFAP<sup>+</sup> cells was found in L-Tam+LPS versus LPS mice ( $P=0,0526$ ; Figure S2E). We further analyzed GFAP<sup>+</sup> astrocytes by S100 $\beta$  immunostaining and found that, on average, nearly 70% of GFAP<sup>+</sup> astrocytes in each group were double-positive for S100 $\beta$  (magenta in Figure 3B).

RGL cells in the SGZ express GFAP and, for a small fraction, also S100 $\beta$  (Gebara et al., 2016) (Figure 3A, C). Analysis of GFAP<sup>+</sup> RGL cells identified based on specific morphological features (see Materials and Methods) revealed an increase in LPS-treated mice, which was prevented by tamoxifen in the Tam+LPS group (Figure 3C). In line with these results, reduced numbers of GFAP<sup>+</sup> RGL cells were observed in L-Tam+LPS versus LPS mice in the long-chase protocol (Fig. S2F). To unravel possible changes in the number of proliferating cells in the GCL and SGZ upon LPS and/or tamoxifen treatment, we quantified the cell proliferation marker Ki67 (Kee et al., 2002). We did not find differences by comparing the density of Ki67<sup>+</sup> cells among the different groups (Figure S3A, B). More specifically, no changes were observed in GFAP<sup>+</sup>/Ki67<sup>+</sup> RGL in the SGZ (Figure S3C, D), suggesting that the number of active RGL cells was not altered by either LPS or tamoxifen treatment.

Next, we investigated the possible effects of tamoxifen on DG neurogenesis, using Doublecortin (DCX) and the bHLH transcription factor NeuroD1 as markers to identify intermediate progenitors and postmitotic immature neurons (Steiner et al., 2006; Gao et al., 2009) (Figures 3D, F). Quantification of DCX<sup>+</sup> cell density in the DG revealed a reduction in LPS group compared to Sal group (Figure 3D, E). This effect was neutralized by tamoxifen in Tam+LPS mice in which DCX<sup>+</sup> cell density was higher compared to LPS group and similar to Sal group (Figure 3E). Notably, higher DCX<sup>+</sup> cell density compared to LPS group was also

found in L-Tam+LPS mice (Figure S2G). Nevertheless, tamoxifen alone did not alter *per se* the DCX+ cell population; indeed, DCX+ cell density was comparable in Sal and Tam+Sal groups (Figure 3E). The observed modulation of DG neurogenesis upon tamoxifen treatment in LPS injected mice was confirmed by analyzing NeuroD1+ cells (Figure S3E, F). We next coupled Ki67 immunostaining to cell-type-specific markers to discriminate between type 2a progenitors (i.e., Ki67+/NeuroD1-/GFAP-) and type 2b progenitors and neuroblasts (NeuroD1+/Ki67+/GFAP-), and we did not find any changes in their numbers (Figures S3G and 3F, G). Conversely, the number of NeuroD1+ cells negative for Ki67 (NeuroD1+/Ki67-; i.e., postmitotic immature neurons) was reduced in LPS group but not in Tam+LPS group, in which NeuroD1+/Ki67- cell numbers were comparable to control mice (Figures 3F, H).

Overall, these findings demonstrate that tamoxifen counteracts the LPS-induced dysregulation in the DG neurogenic niche, rescuing control conditions for astrocytes, RGL cells, and newborn immature neurons.



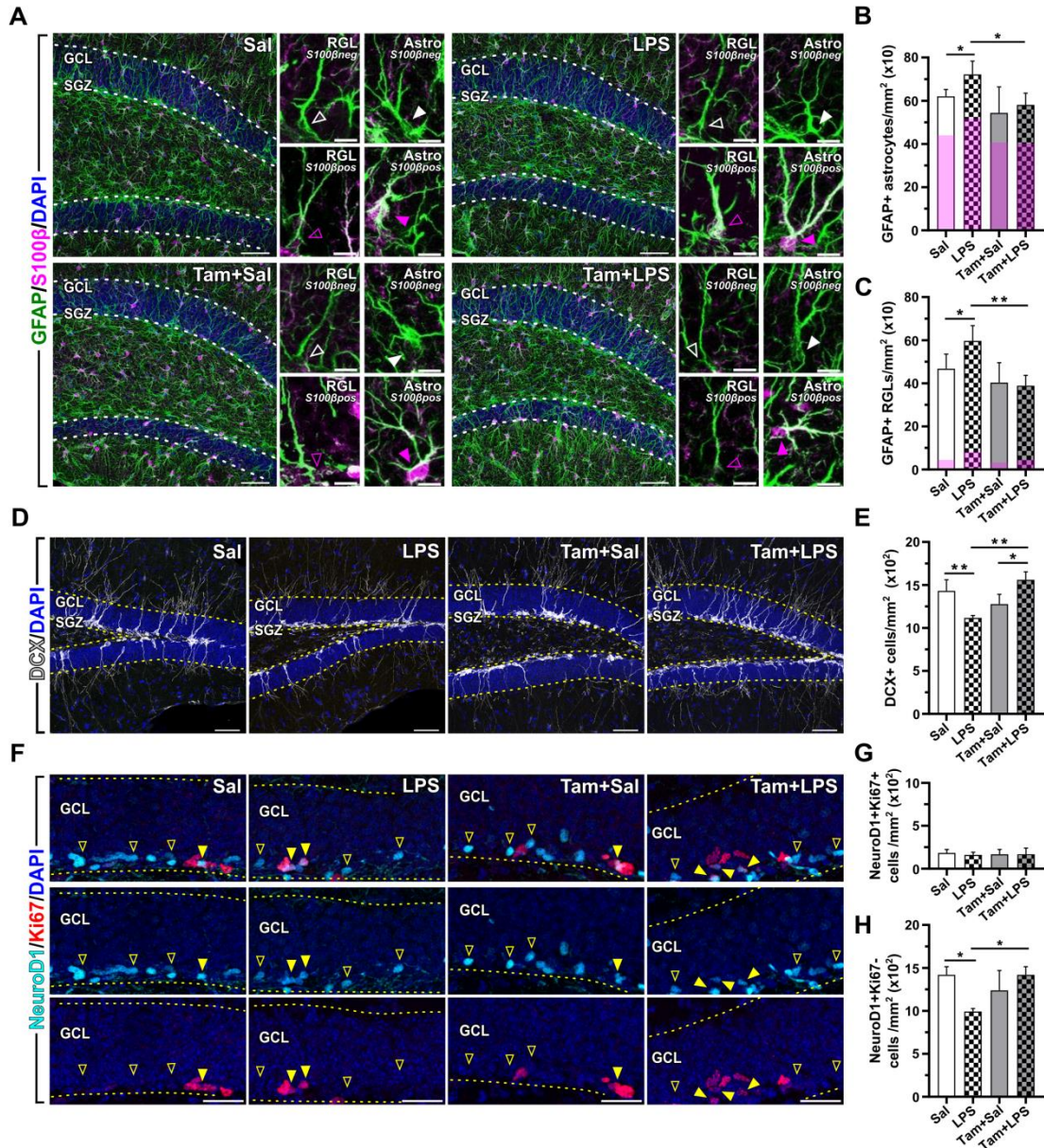


**Figure 3. Tamoxifen counteracts the LPS-induced dysregulation of neuro-glia balance within the adult DG neurogenic niche.** (A-H) Refers to the experimental design shown in Figure 1A. (A) Confocal images of double immunofluorescence for S100 $\beta$  (magenta) and GFAP (green) in the SGZ/GCL of DG in coronal sections. Insets show high-magnification images of GFAP+ radial glia like-cells (RGL), both S100 $\beta$  negative (empty white arrowheads) and S100 $\beta$  positive (empty pink arrowheads), and GFAP+ astrocytes (Astro) both S100 $\beta$  negative (full white arrowheads) and S100 $\beta$  positive (full pink arrowheads). (B, C) Quantification of astrocytes (B) and RGL cells (C) positive for GFAP within the SGZ/GCL of the DG in the four experimental groups. Densities of double-labeled GFAP+S100 $\beta$ + are depicted in pink in the column graph. (D) Representative confocal images of intermediate progenitors and immature neurons positive for DCX (white) in the DG of mice injected with saline (Sal) or LPS alone and mice treated with tamoxifen before Sal (Tam+Sal) or LPS (Tam+LPS) injections. (E) Quantification of DCX+ neurogenic progenitors and immature neurons within the SGZ/GCL of the DG in the four experimental groups. (F) Confocal images of double immunofluorescence for immature neuronal marker

NeuroD1 (cyan) and the proliferative marker Ki67 (red) in the DG of Sal, LPS, Tam+Sal, and Tam+LPS mice. Full arrowheads show double NeuroD1+Ki67+ nuclei; empty arrowheads show NeuroD1+ nuclei negative for Ki67. (G, H) Quantification of double NeuroD1+Ki67+ mitotic neurogenic progenitors (G) and NeuroD1+Ki67- postmitotic immature neurons (H) within the GCL/SGZ of the four experimental groups; both cell populations (G, H) are negative for GFAP. DG subgranular zone (SGZ)/granule cell layer (GCL) is delimited by dotted lines. Cell nuclei are counterstained with DAPI (blue). n=3-5 mice/group. Scale bars, 50  $\mu$ m (A and D; low magnification), 25  $\mu$ m (F; low magnification), and 10  $\mu$ m (insets A; high magnification). Data are presented as mean  $\pm$  SD. Two-way ANOVA followed by a Student-Newman-Keuls' (SNK) multiple comparison test. \*p<0.05, \*\*p<0.01. See also Figure S3 and the statistical values in Tables S5 and S6.

#### **3.4.4 Newborn neurons and RGL cells respond to LPS-challenge and tamoxifen treatment in microglia-depleted mice**

Our data indicate that LPS and tamoxifen treatments impact multiple cellular components of the SGZ/GCL. However, it remains unclear to which extent the observed effects are due to microglia-mediated responses. To get a deeper insight into the role of microglia in this context, we exploited a pharmacological strategy to deplete microglia in the CNS by oral administration of Plexxikon (PLX)5622, an inhibitor of the colony-stimulating factor 1 receptor (CSF1R), which is essential for microglia survival (Elmore et al., 2014; Green et al., 2020). The effectiveness of the PLX5622 treatment was qualitatively assessed in a first experiment by Iba-1 immunofluorescence in the DG of mice that received a 5-day treatment, revealing a drastic reduction in Iba1+ microglia compared to control mice (Figure S4A, B). Therefore, we designed a new experimental protocol, introducing a 5-day PLX5622 pretreatment before starting tamoxifen or vehicle administration, followed after 2 days by LPS or Saline injections (i.e., from d2 to d5, Figure S4C). Mice were maintained under continuous PLX5622 treatment throughout the whole experiment to avoid the repopulation of microglia (i.e., from -d6 to d6) (Huang et al., 2018). Thus, the day after the last Sal or LPS injection, only rare Iba1-immunopositive cells were observed in the DG of PLX treated mice (Figure 4A). Although scattered Iba1+ cells in the MCL were still responsive to LPS (Figure 4B), no significant changes occurred in the GCL and Hilus (Figure 4C, D), and their overall reduction was in a range between 86% and 97% (Figure 4B-D), confirming a significant depletion of microglia in the DG of PLX5622 treated mice. We next analyzed DCX+ cells in the DG of microglia-depleted mice and found a decreased cell density in LPS group compared to Sal group, which was prevented by tamoxifen in Tam+LPS group (Figure 4E, F). Intriguingly, a similar response was observed in GFAP+ RGL cells, with a decrease in LPS compared to Sal group (Figure 4G, H), indicating that in the condition of microglia depletion, LPS effects on RGL cells are opposite to that found in the presence of microglia (Figure 3C). In any case, tamoxifen pretreatment abolished the LPS effects, leading to numbers of GFAP+ RGL cells comparable to controls (Figures 4G, H). Finally, no differences were observed in the number of GFAP+ astrocytes among groups (Figures 4G, I).

Overall, these findings indicate that microglial cells are needed to elicit the changes observed in DG astrocytes upon LPS and tamoxifen treatments and are involved in the



modulation of RGL cells, but they are dispensable for the effects produced by those treatments on DG newborn neurons.

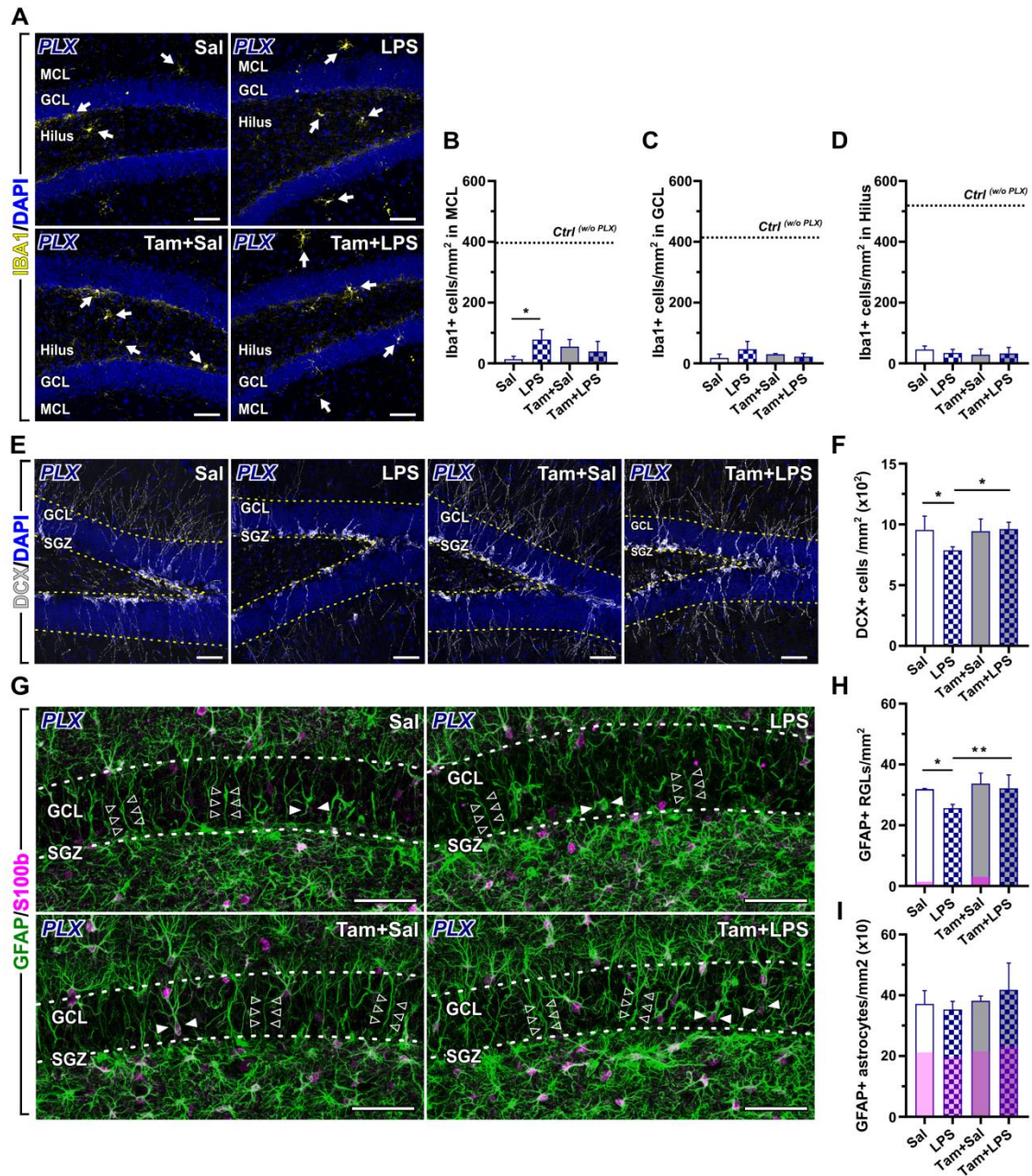


**Figure 4. Tamoxifen counteracts LPS-induced newborn neuron and RGL cell depletion in PLX microglia-depleted mice.** (A) Representative confocal images are depicting the remaining Iba1+ microglial cells (yellow; arrows) in the PLX-treated DG of the four experimental groups shown in A. (B-D) Quantification of Iba1+ microglia cell density within the MCL (B), GCL (C), and Hilus (D) of PLX-treated four experimental groups (ref. to Figure S4C for the experimental design) compared to control ones fed without PLX (dotted line). (E) Confocal images of neuroblasts/immature neurons positive for DCX (white) in the DG of PLX-treated mice of four experimental groups. (F) Quantification of DCX+ neurogenic progenitors and immature neurons within the SGZ/GCL of the PLX-microglia depleted DG in the four experimental groups. (G) Confocal images of double immunofluorescence for S100 $\beta$  (magenta) and GFAP (green) in the SGZ/GCL of the PLX-microglia depleted DG. Empty arrowheads indicate the radial process of GFAP+ radial glia-like cells, while full arrowheads indicate the soma of GFAP+ astrocytes. (H, I) Quantification of RGL cells (H) and astrocytes (I) positive for GFAP

within the SGZ/GCL of the PLX-microglia depleted DG in the four experimental groups. Densities of double-labeled GFAP+S100 $\beta$ + are depicted in pink in the column graph. DG subgranular zone (SGZ)/granule cell layer (GCL) is delimited by dotted lines. Cell nuclei are counterstained with DAPI (blue). n=4 mice/group. Scale bars, 50  $\mu$ m (A, E, and G; low magnification). Data are presented as mean  $\pm$  SD. Two-way ANOVA followed by a Student-Newman-Keuls' (SNK) multiple comparison test. \*p< 0.05, \*\*p<0.01. See also Figure S4 and the statistical table S7.

### 3.5 Discussion

Tamoxifen, the first-generation SERM used for breast cancer treatment, displays multiple activities depending on the cell type, developmental stage, or pathological condition. For instance, long-lasting adverse effects of tamoxifen treatments on neurogenesis were recently reported in prenatal and postnatal brains (Lee et al., 2020). In contrast, beneficial anti-inflammatory and neuroprotective activities were documented in adult microglia and neural cells, respectively (Zhao et al., 2005; Tapia-Gonzalez et al., 2008; DonCarlos et al., 2009; Arevalo et al., 2012; Baez-Jurado et al., 2019). Tamoxifen is also used as an activator of the CreERT2 fusion protein to mediate inducible genetic manipulation *in vivo* (Hayashi and McMahon, 2002; Hirrlinger et al., 2006; Mori et al., 2006; Valny et al., 2016; Jahn et al., 2018). Conditional Cre system allows recombination of floxed target genes in a time-controlled manner in specific cell types and has been instrumental in the last decades for the genetic labeling and manipulation of adult NSC/progenitor cells but also microglial cells to dissect the underlying dynamic and molecular control (Dhaliwal and Lagace, 2011; Imayoshi et al., 2011; Semerci and Maletic-Savatic, 2016; Kaiser and Feng, 2019; Diaz-Aparicio et al., 2020). However, such studies might be impacted indirectly by tamoxifen effects on cell proliferation, differentiation or through tamoxifen-dependent modification of neuroinflammatory signaling.

In this study, we asked whether a two-day tamoxifen administration, which has been previously used to efficiently recombine adult NSC/progenitor cells in inducible Glast-CreERT2 transgenic mice (Rolando et al., 2012; Yang et al., 2015; Bonzano et al., 2018), influences the adult DG neurogenic niche of the mouse hippocampus in basal conditions and upon LPS-induced neuroinflammation. Our data revealed that tamoxifen treatment alone did not affect the adult DG, considering radial-glia NSCs, proliferating progenitors, as well as differentiated NeuroD+ and DCX+ immature neurons or GFAP+ and GFAP+/S100b+ astrocytes within the SGZ/GCL of adult mice. This observation is in line with a previous report (Rotheneichner et al., 2017) but in contrast with the detrimental effects of tamoxifen administration in embryonic and adolescent brains outlined by a recent study reporting long-lasting alterations on neurogenesis (Lee et al., 2020). In particular, this latter study revealed that a tamoxifen treatment with a 2mg/animal dose per day, lasting five days, reduced

proliferating cells in the postnatal DG. Similar effects were reported on the subventricular zone (i.e., the other main neurogenic niche of the adult brain) following two tamoxifen injections at a 1mg/animal dose per day. Thus, while dosage and/or protocol of tamoxifen administration is unlikely to explain the discrepancy between this study and our data, animal age can account for a significant difference. In our case and the study by Rotheneichner and colleagues, experiments were performed on fully mature adult mice (i.e., aged from two to five months), while the experiments by Lee and colleagues used adolescent mice (i.e., three- to four-week-old mice) to account for their studies of adult neurogenesis (Rotheneichner et al., 2017; Lee et al., 2020). Age differences might be relevant considering recent reports indicating a change in the dynamics and behaviors of DG NSCs between juvenile and adult life (Harris et al., 2021; Ibrayeva et al., 2021), which could imply different susceptibility to tamoxifen.

The systemic administration of LPS is a reliable method to elicit a rapid innate immune response in the brain, whose effects at the cellular and molecular levels vary according to the experimental protocol (Norden et al., 2016; Batista et al., 2019). Our results showed that systemic administration of a low dose of LPS for four consecutive days leads to overall moderate changes in the mRNA expression of inflammatory markers in the hippocampi of LPS-treated mice, with a significant increase of the pro-inflammatory cytokine IL-1 $\beta$ . These data are consistent with a previous study showing that repeated LPS challenge elicits a less severe inflammatory molecular profile in the brain than the response observed following an acute single-dose LPS challenge (Norden et al., 2016). Yet, the quantitative data on the cell population and changes in the morphology of hippocampal DG microglial cells support their clear activation upon LPS treatment, both in terms of increased proliferation and more complex morphology (Stence et al., 2001; Madore et al., 2013; Norden et al., 2016; Fernández-Arjona et al., 2017). Moreover, we found a decrease in DCX+ immature neurons and increased numbers of GFAP+ astrocytes and RGL cells following LPS, indicating reduced DG neurogenesis and increased astrogliogenesis. While the LPS effects on adult DG neurogenesis and astrogliogenesis are in agreement with previous reports (Ekdahl et al., 2003; Monje et al., 2003; Fujioka and Akema, 2010; Zonis et al., 2013; Valero et al., 2014; Chesnokova et al., 2016; Bonzano et al., 2018; Melo-Salas et al., 2018; Perez-Dominguez et al., 2019), to the best of our knowledge, the LPS-induced increase found in the RGL cell

population has not been reported before. Interestingly, we found that the increased number of astrocytes and GFAP+ RGL NSCs observed in LPS-treated mice was critically dependent on the activity of microglia, as such effects were lost in microglia-depleted mice. Notably, in the absence of microglia, the LPS treatment elicited an opposite result on RGL cells, significantly reducing their number, revealing a direct, possibly cell-autonomous, adverse effect of LPS on these NSCs. Therefore, we propose that LPS-induced neuroinflammation modulates NSC number through two competing mechanisms – an indirect microglia-dependent activity that dominates and masks a direct LPS negative regulation of GFAP+RGL cell number.

The idea of a double direct/indirect regulation on NSCs is further supported by the observed effects of tamoxifen counteracting LPS-associated changes in the DG neurogenic niche both in presence and absence of microglia. Tamoxifen effects are classically mediated by activation of the nuclear ERs and/or the membrane-bound G-protein-associated estrogen receptor (GPR30) (Arevalo et al., 2015; Baez-Jurado et al., 2019). The expression of both receptors by microglia and astrocytes have been documented and reported to be involved in the inflammatory response, a powerful regulator of adult hippocampal neurogenesis (Garcia-Ovejero et al., 2005; Sierra et al., 2008; Arevalo et al., 2012; Leiter et al., 2016; Correa et al., 2019; Vicidomini et al., 2020). However, ER and GPR30 are also expressed by adult DG NSC/progenitor cells, as well as by DG immature and mature granule neurons (Isgor and Watson, 2005; Mazzucco et al., 2006; Brailoiu et al., 2007; Hajszan et al., 2007), raising the possibility that tamoxifen may directly regulate the response of these cells to LPS. Accordingly, in the absence of microglia, tamoxifen prevented the LPS-induced reduction of both GFAP+RGL NSCs and DCX+ newborn neurons. On the other hand, microglia depletion completely abrogated the effects of LPS and LPS+tamoxifen on astrocyte numbers, indicating a microglia-mediated response. Thus, our data suggest the co-existence of both mechanisms of action by tamoxifen and their differential contribution in controlling the neuron/astroglia balance in the adult DG upon neuroinflammation.

Alterations in cell proliferation, cell fate, and/or cell death during tamoxifen/LPS interventions are among the possible mechanisms underlying dynamic changes in the DG neurogenic niche. The concomitant and proportional increase of GFAP+RGL and GFAP+S100b+ astrocytes upon LPS-induction suggest an increased proliferation of NSCs and

possibly their increased differentiation towards astrocytes. Instead, the observed decrease in DCX+ newborn neurons could derive from the altered cell cycle of intermediate progenitors and/or defective survival of newborn neurons. Although our data showed unchanged numbers of proliferating cells in the DG, 24 h after the last LPS injection, we cannot exclude the existence of a transitory phase of altered NSC and/or intermediate progenitor proliferation at earlier steps during LPS-treatment. Accordingly, a previous study described a detrimental effect of inflammation after a single LPS injection on cell cycle progression of type 2 intermediate progenitors, which may contribute to the decrease in the birth rate of DG neurons (Melo-Salas et al., 2018). On the other hand, our data showing a reduction in DCX+ postmitotic cells upon LPS treatment point to an impairment in cell survival of newborn neurons that may contribute to overall reduced neurogenesis. Thus, beneficial tamoxifen effects in LPS treated mice possibly reflect the prevention of microglia-mediated neuroinflammation and consequent stimulation of astrogliogenesis as well as direct neuroprotective activity in NCSs and newborn neurons.

The exact molecular mechanisms mediating the role of tamoxifen in preventing adverse effects of neuroinflammation in the DG deserves further investigation. However, our data suggest that they are not mediated by pure anti-inflammatory actions at the level of cytokine signaling. Indeed, an increased expression of pro-inflammatory cytokines at 24hrs after ceasing LPS administration, which attained significance only for IL1b, was enhanced in tamoxifen pretreated mice as reflected by augmented expression of IL1b, TNFa, and IL6, concomitant with an increase of the anti-inflammatory IL4R and TGFb signaling. Changes in microglia number and morphology more faithfully reflected beneficial activities of tamoxifen and were consistent with preventing microglia activation in response to LPS. It remains to be investigated whether microglia trophic support known to play a role in the control of proliferation, survival, and differentiation of different neural progenitors (Frost and Schafer, 2016) may be directly involved in microglia-dependent beneficial effects of tamoxifen.

In conclusion, these findings imply major limitations in investigating microglia, adult NSCs and their progeny using the CreERT2-loxP transgenic mouse systems associated with pathological models involving neuroinflammation. Besides, the tamoxifen actions might interfere with models of the experimental autoimmune encephalomyelitis -EAE- and the

toxin-mediated models of demyelination (Procaccini et al., 2015; Kipp et al., 2017; Chu et al., 2019), as well as various models of neurodegenerative diseases associated with neuroinflammation (Dawson et al., 2018; Batista et al., 2019). Here we demonstrated that tamoxifen treatment counteracted the LPS-induced dysregulation in adult DG neurogenesis not only at short intervals (i.e., forty-eight hours chase) but also at longer intervals (i.e., seven days chase), when the levels of tamoxifen and its metabolites was found negligible within brain and blood (Valny et al., 2016; Jahn et al., 2018). These data indicate a long-lasting effect of tamoxifen and highlight the need for thorough control to be designed on a case-by-case basis when using transgenic animals bearing the tamoxifen-inducible CreERT2-LoxP system.



### 3.6 Supplementary figures

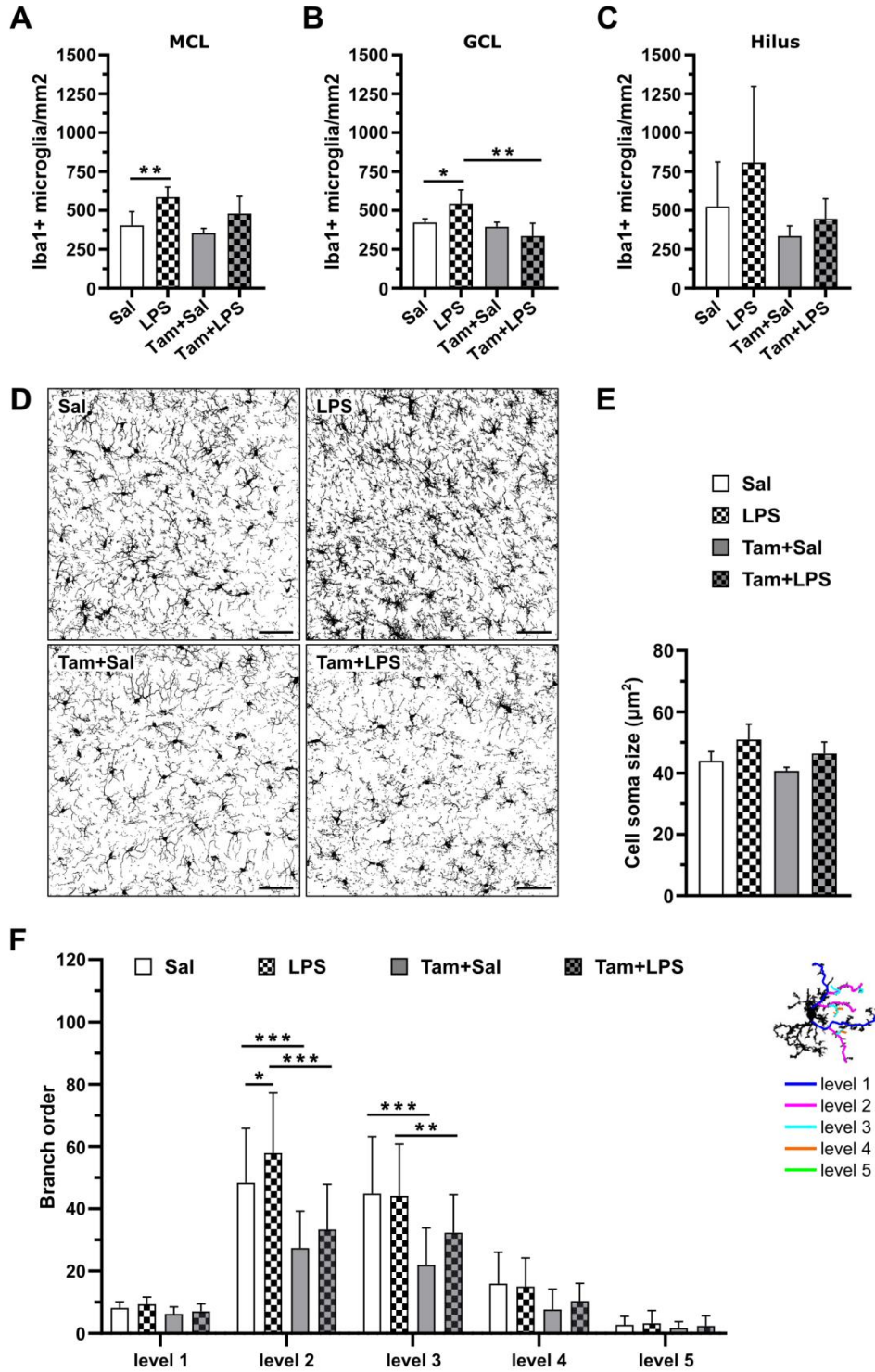


**Figure S1. Microglial cell density and morphometric parameters in the DG. Related to Figure 2.** (A-B-C) Quantification of Iba1+ microglial cell density within the MCL (A), GCL (B), and Hilus (C) of the four

experimental groups (ref. to Figure 1A for the experimental design). (D) Representative binarized images of Iba1+ microglial cells in coronal sections of the Sal, LPS, Tam+Sal, and Tam+LPS DG, are used to measure the microglia fractional area (ref. to Figure 2C). Scale bar, 50  $\mu$ m. (E) Quantification of Iba1+ microglial cell soma size within the DG. (F) Histograms are reporting quantification of different levels of branches per 3D-reconstructed microglial cell within the DG of each experimental group. An example of a 3D-reconstructed cell with branch order highlighted with different colors is shown on the right. DG, dentate gyrus; MCL, molecular cell layer; GCL, granule cell layer; Sal, saline; LPS, lipopolysaccharide; Tam, tamoxifen. n = 3-5 mice/group (A, C). n = 15-18 cell/group (C) out of three mice/group. Data are presented as mean  $\pm$  SD. Two-way ANOVA followed by a Student-Newman-Keuls' (SNK) multiple comparison test. \*\*p<0.01, \*\*\*p<0.001. See statistical values in table S5.

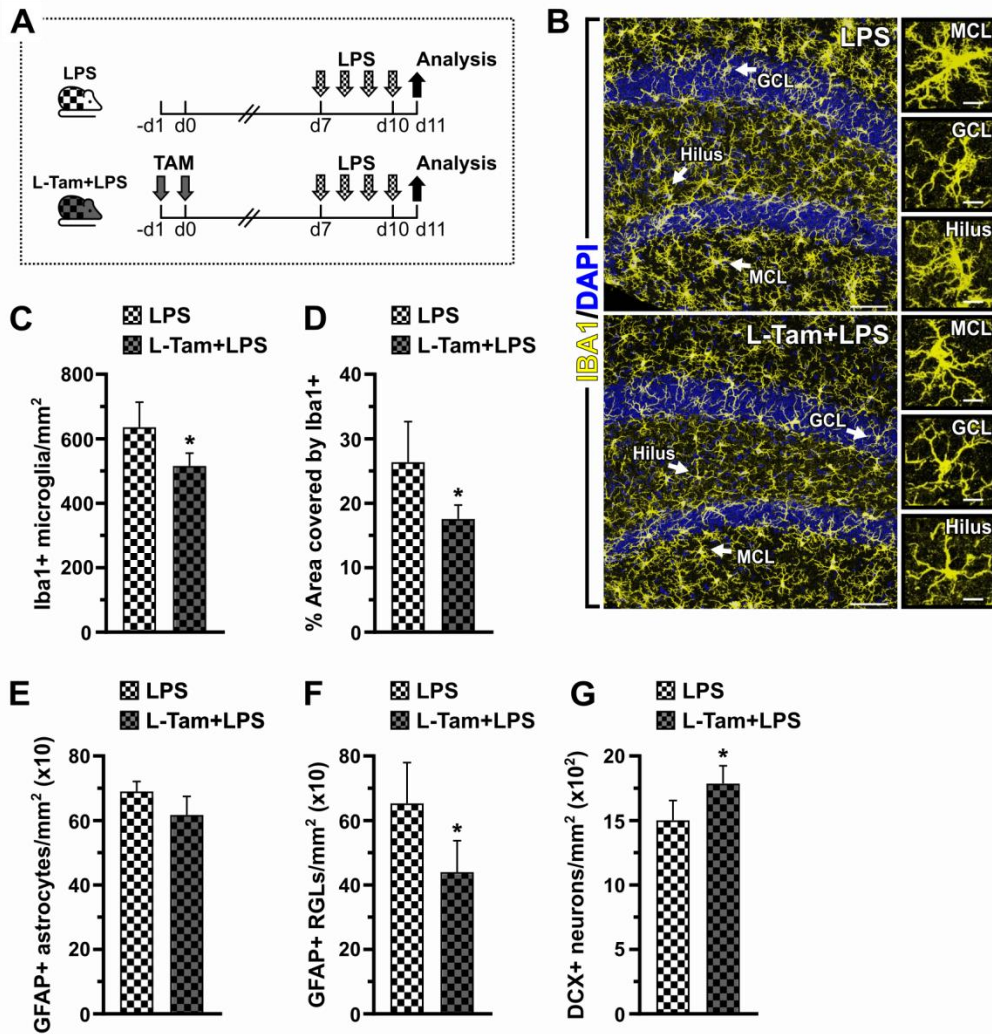


**Figure S2. The effects of tamoxifen on the DG are long-lasting.** (A) Experimental design. Tam (Tamoxifen, 2.5 mg/mouse/day) and LPS (*E. Coli*-derived lipopolysaccharide, 0.5 mg/kg/day). Treatments were administered by intraperitoneal injections. (B) Representative confocal images depicting microglia immunopositive for Iba1 (yellow) in the DG of the two experimental groups shown in A. Insets show high-magnification images of Iba1+ microglia (arrows) for each DG sub-region (MCL, molecular cell layer; GCL, granule cell layer; Hilus). Cell nuclei are counterstained with DAPI (blue). Scale bars, 50  $\mu$ m (insets scale bar, 10  $\mu$ m). (C-D) Quantification of Iba1+ microglial cell density (C) and area coverage (D) within DG coronal sections. (E-F-G) Quantification of neurogenic progenitors and immature neurons positive for DCX (E), GFAP+ astrocytes (F), and GFAP+ radial glial cells (RGLs) (G) within the SGZ/GCL subregions of the DG.  $n = 4-5$  mice/group. Data are presented as mean  $\pm$  SD. Student's t-test. \* $p < 0.05$ . See the statistical table S6.

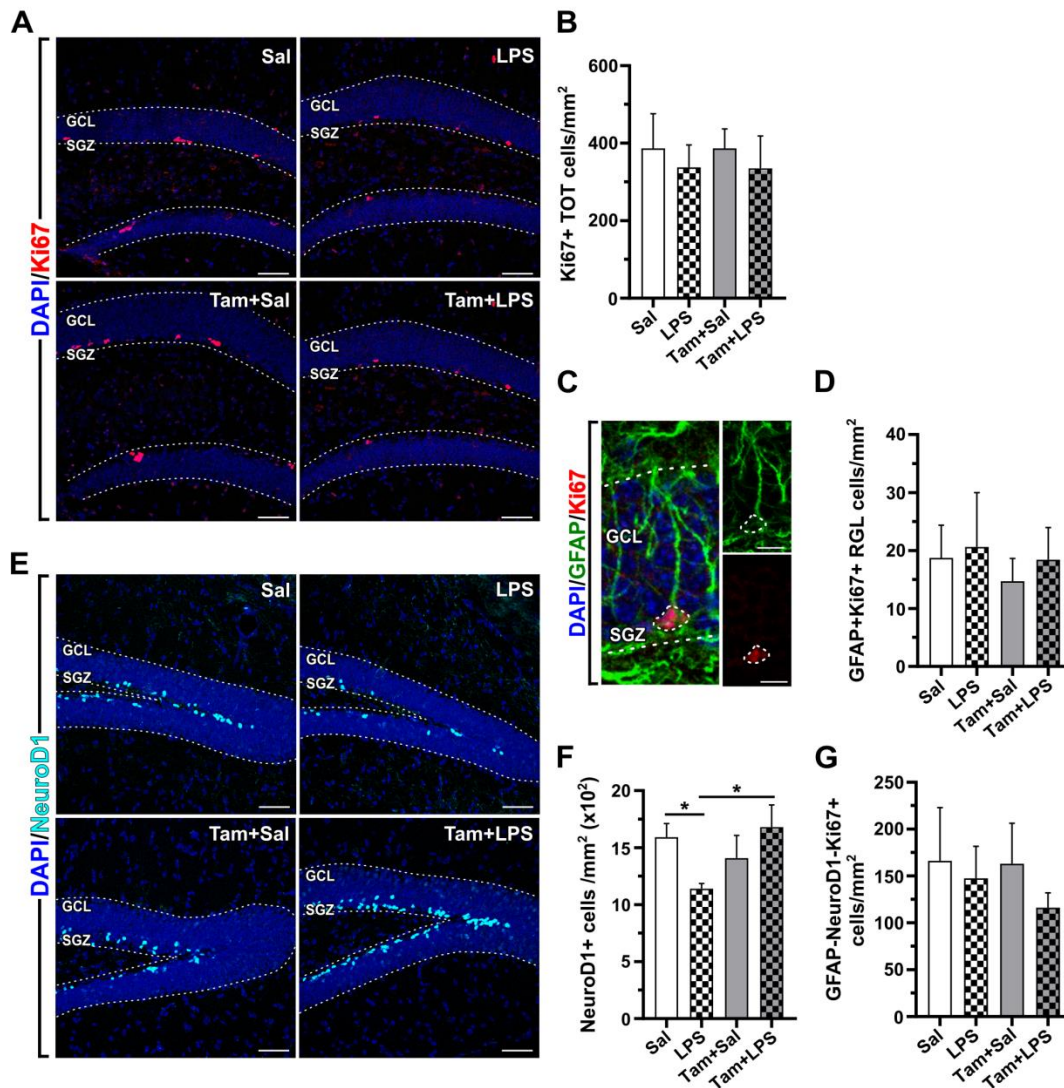


**Figure S3. LPS and/or Tamoxifen do not alter the proliferative activity in the DG. Related to Figure 3.** (A) Confocal images of NeuroD1+ (cyan) nuclei within the SGZ/GCL of DG of four experimental groups (ref. to Figure 1A for the experimental design). (B) NeuroD1+ cell density in the SGZ/GCL of Sal, LPS, Tam+Sal, and Tam+LPS DG. (C) Confocal image of a radial glia-like (RGL) cell double-labeled for GFAP (green) and Ki67 (red) located in the SGZ of the adult DG. (D) Quantification of the total number of Ki67+ cells within the SGZ/GCL of each group. (E) Confocal images of Ki67+ (red) nuclei within the SGZ/GCL of DG of four groups. (F-G) Quantification of double GFAP+Ki67+ RGLs (F) and GFAP-NeuroD1-Ki67+ cells (G) in the SGZ of four experimental groups. DG subgranular zone (SGZ)/granule cell layer (GCL) is delimited by dotted lines. Cell nuclei are counterstained with DAPI (blue).  $n=3/5$  mice/group. Scale bars, 50  $\mu\text{m}$  (A, and E; low magnification) and 10  $\mu\text{m}$  (C; high magnification). Data are presented as mean  $\pm$  SD. Two-way ANOVA followed by a Student-Newman-Keuls' (SNK) multiple comparison test. \* $p < 0.05$ . See the statistical table S7.



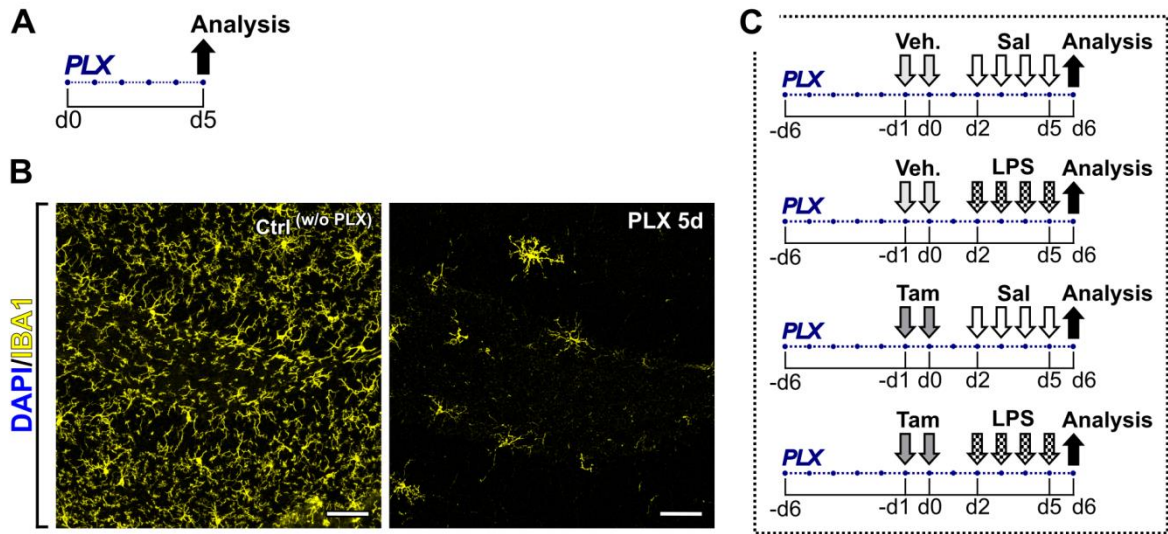


**Figure S4. Depletion of microglia upon PLX treatment in the adult DG. Related to Figure 4.** (A) Experimental design to assess the effect of five days of PLX5622 treatment on the adult brain in mice. (B) Confocal images depicting Iba1+ microglial cells in control DG coronal section (i.e., without PLX treatment) and PLX-microglia depleted DG after five days of treatment (PLX 5d) as shown in A. Scale bars, 50  $\mu$ m. (C) Experimental design. Mice were provided ad libitum access to chow containing PLX5622 (Plexxikon 5622, 1200 ppm formulated in AIN-76A standard rodent diet), starting from five days before receiving the first Tam/Veh. injection and for the entire duration of the experiment. Veh. (Vehicle, i.e., com oil), Tam (Tamoxifen, 2.5 mg/mouse/day), Sal (saline solution 0.9%), and LPS (*E. coli*-derived lipopolysaccharide, 0.5 mg/kg) were administered by intraperitoneal injections. n=2 mice/group in A and B; n=4 mice/group in C.

### 3.7 Supplementary tables

**Table S1.** Statistical table related to Figure 1.

Figure	Parameter	Two-way ANOVA ( $\alpha < 0.05$ )			Dunnett's <i>post hoc</i> test		
		Factors	Statistics	P	Sal vs LPS	Sal vs Tam+Sal	Sal vs Tam+LPS
1B	IL-1 $\beta$	Pretreatment x treatment	$F_{\text{pretr} \times \text{treat} (1,18)} = 4.612$	P = 0.0456	P = 0.0066	P = 0.0303	P = 0.0078
			$F_{\text{pretr} (1,18)} = 3.295$	P = 0.0862	(**)	(*)	(**)
			$F_{\text{treat} (1,18)} = 9.321$	P = 0.0068			
1C	TNF $\alpha$	Pretreatment x treatment	$F_{\text{pretr} \times \text{treat} (1,17)} = 1.112$	P = 0.3063	P = 0.2270	P = 0.0595	P = 0.0304
			$F_{\text{pretr} (1,17)} = 6.449$	P = 0.0212	(ns)	(ns)	(*)
			$F_{\text{treat} (1,17)} = 2.401$	P = 0.1397			
1D	IL-6	Pretreatment x treatment	$F_{\text{pretr} \times \text{treat} (1,18)} = 1.700$	P = 0.2087	P = 0.1806	P = 0.0054	P = 0.0043
			$F_{\text{pretr} (1,18)} = 14.42$	P = 0.0013	(ns)	(**)	(**)
			$F_{\text{treat} (1,18)} = 2.125$	P = 0.1621			
1E	IL4R	Pretreatment x treatment	$F_{\text{pretr} \times \text{treat} (1,18)} = 3.187$	P = 0.0911	P = 0.1422	P = 0.0059	P = 0.0149
			$F_{\text{pretr} (1,18)} = 10.64$	P = 0.0043	(ns)	(**)	(*)
			$F_{\text{treat} (1,18)} = 1.388$	P = 0.2541			
1F	TGF $\beta$	Pretreatment x treatment	$F_{\text{pretr} \times \text{treat} (1,18)} = 2.190$	P = 0.1562	P = 0.1020	P = 0.0275	P = 0.0184
			$F_{\text{pretr} (1,18)} = 6.499$	P = 0.0201	(ns)	(*)	(*)
			$F_{\text{treat} (1,18)} = 3.069$	P = 0.0968			

IL-1 $\beta$ , interleukin-1 $\beta$ ; TNF $\alpha$ , tumor necrosis factor- $\alpha$ ; IL-6, interleukin-6; IL-4R, interleukin-4 receptor; TGF $\beta$ , transforming growth factor- $\beta$ .

Pretreatment = Vehicle or Tamoxifen (Tam) administration; Treatment = Saline (Sal) or Lipopolysaccharide (LPS) injection.

**Table S2.** Statistical table related to Figure 2.

Figure	Parameter (refers to Iba1+ microglia)	Two-way ANOVA ( $\alpha < 0.05$ )			Student-Newman-Keuls' <i>post hoc</i> test					
		Factors	Statistics	P	Sal vs LPS	Sal vs Tam+Sal	Sal vs Tam+LPS	LPS vs Tam+Sal	LPS vs Tam+LPS	Tam+Sal vs Tam+LPS
<b>2B</b>	Cell density in DG	Pretreatment x treatment	$F_{\text{pretr} \times \text{treat} (1,12)} = 4.225$ $F_{\text{pretr} (1,12)} = 17.19$ $F_{\text{treat} (1,12)} = 15.79$	$P = 0.0623$ $P = 0.0014$ $P = 0.0018$	$P < 0.001$ (***)	$P > 0.05$ (ns)	$P > 0.05$ (ns)	$P < 0.001$ (***)	$P < 0.01$ (**)	$P > 0.05$ (ns)
<b>2C</b>	Area coverage	Pretreatment x treatment	$F_{\text{pretr} \times \text{treat} (1,12)} = 0.5632$ $F_{\text{pretr} (1,12)} = 29.37$ $F_{\text{treat} (1,12)} = 2.536$	$P = 0.4674$ $P = 0.0002$ $P = 0.1373$	$P > 0.05$ (ns)	$P < 0.05$ (*)	$P < 0.05$ (*)	$P < 0.01$ (**)	$P < 0.01$ (**)	$P > 0.05$ (ns)
<b>2E</b>	Territory area	Pretreatment x treatment	$F_{\text{pretr} \times \text{treat} (1,61)} = 1.988$ $F_{\text{pretr} (1,61)} = 0.4045$ $F_{\text{treat} (1,61)} = 17.63$	$P = 0.1637$ $P = 0.5271$ $P < 0.0001$	$P < 0.001$ (***)	$P > 0.05$ (ns)	$P < 0.05$ (*)	$P < 0.01$ (**)	$P > 0.05$ (ns)	$P > 0.05$ (ns)
<b>2F</b>	Branches per cell	Pretreatment x treatment	$F_{\text{pretr} \times \text{treat} (1,61)} = 0.3907$ $F_{\text{pretr} (1,61)} = 33.49$ $F_{\text{treat} (1,61)} = 3.030$	$P = 0.5342$ $P < 0.0001$ $P = 0.0868$	$P > 0.05$ (ns)	$P > 0.001$ (***)	$P < 0.01$ (**)	$P < 0.001$ (***)	$P < 0.01$ (**)	$P > 0.05$ (ns)

Pretreatment = Vehicle or Tamoxifen (Tam) administration; Treatment = Saline (Sal) or Lipopolysaccharide (LPS) injection.

**Table S3a.** Statistical table related to Figure 3.

Figure	Parameter (refers to SGZ/GCL)	Two-way ANOVA ( $\alpha < 0.05$ )			Student-Newman-Keuls' <i>post hoc</i> test					
		Factors	Statistics	P	Sal vs LPS	Sal vs Tam+Sal	Sal vs Tam+LPS	LPS vs Tam+Sal	LPS vs Tam+LPS	Tam+Sal vs Tam+LPS
<b>3B</b>	Cell density of GFAP+ astrocytes	Pretreatment x treatment	$F_{\text{pretr} \times \text{treat} (1,12)} = 0.8484$	$P = 0.3751$	$P < 0.05$ (*)	$P > 0.05$ (ns)	$P > 0.05$ (ns)	$P < 0.05$ (*)	$P < 0.05$ (*)	$P > 0.05$ (ns)
	GFAP+S100b+ astrocytes		$F_{\text{pretr} (1,12)} = 9.888$	$P = 0.0085$	$P > 0.05$ (ns)	$P > 0.05$ (ns)	$P > 0.05$ (ns)	$P > 0.05$ (ns)	$P > 0.05$ (ns)	$P > 0.05$ (ns)
	GFAP+S100b- astrocytes		$F_{\text{treat} (1,12)} = 4.001$	$P = 0.0686$	$P > 0.05$ (ns)	$P > 0.05$ (ns)	$P > 0.05$ (ns)	$P > 0.05$ (ns)	$P > 0.05$ (ns)	$P > 0.05$ (ns)
<b>3C</b>	Cell density of GFAP+ RGLs	Pretreatment x treatment	$F_{\text{pretr} \times \text{treat} (1,12)} = 3.856$	$P = 0.0732$	$P < 0.05$ (*)	$P > 0.05$ (ns)	$P > 0.05$ (ns)	$P < 0.01$ (**)	$P < 0.01$ (**)	$P > 0.05$ (ns)
	GFAP+S100b+ RGLs		$F_{\text{pretr} (1,12)} = 13.93$	$P = 0.0029$	$P > 0.05$ (ns)	$P > 0.05$ (ns)	$P > 0.05$ (ns)	$P > 0.05$ (ns)	$P > 0.05$ (ns)	$P > 0.05$ (ns)
	GFAP+S100b- RGLs		$F_{\text{treat} (1,12)} = 2.466$	$P = 0.1423$	$P > 0.05$ (ns)	$P > 0.05$ (ns)	$P > 0.05$ (ns)	$P < 0.05$ (*)	$P < 0.05$ (*)	$P > 0.05$ (ns)
<b>3E</b>	Cell density of DCX+ cells	Pretreatment x treatment	$F_{\text{pretr} \times \text{treat} (1,9)} = 27.12$	$P = 0.0006$	$P < 0.01$ (**)	$P > 0.05$ (ns)	$P > 0.05$ (ns)	$P > 0.05$ (ns)	$P < 0.01$ (**)	$P < 0.05$ (*)
<b>3G</b>	Cell density of NeuroD1+Ki67+ cells	Pretreatment x treatment	$F_{\text{pretr} (1,12)} = 0.02381$	$P = 0.8799$	$P > 0.05$ (ns)	$P > 0.05$ (ns)	$P > 0.05$ (ns)	$P > 0.05$ (ns)	$P > 0.05$ (ns)	$P > 0.05$ (ns)
<b>3H</b>	Cell density of NeuroD1+Ki67- cells	Pretreatment x treatment	$F_{\text{pretr} \times \text{treat} (1,8)} = 10.84$	$P = 0.0110$	$P < 0.05$ (*)	$P > 0.05$ (ns)	$P > 0.05$ (ns)	$P > 0.05$ (ns)	$P < 0.05$ (*)	$P > 0.05$ (ns)

Pretreatment = Vehicle or Tamoxifen (Tam) administration; Treatment = Saline (Sal) or Lipopolysaccharide (LPS) injection (Ref. to Figure 1A for the experimental design).



**Table S3b.** Statistical table related to Figure 3.

Figure	Parameter (refers to SGZ/GCL)	Sal (Mean ± SD%)	LPS (Mean ± SD%)	Tam+Sal (Mean ± SD%)	Tam+LPS (Mean ± SD%)
3B	% S100β+ astrocytes/ GFAP+ population	70.50 ± 4.16%	72.58 ± 6.86%	74.32 ± 6.80%	68.82 ± 5.92%
3B	% S100β- astrocytes/ GFAP+ population	29.50 ± 4.16%	28.59 ± 6.72%	25.68 ± 6.80%	31.18 ± 5.92%
3C	% S100β+ RGL cells/ GFAP+ population	9.10 ± 5.44%	14.52 ± 7.68%	7.33 ± 2.41%	8.99 ± 6.37%
3C	% S100β- RGL cells/ GFAP+ population	90.90 ± 5.44%	89.89 ± 4.72%	92.67 ± 2.41%	91.01 ± 6.37%

**Table S4a.** Statistical table related to Figure 4.

Figure	Parameter	Two-way ANOVA ( $\alpha < 0.05$ )			Student-Newman-Keuls' <i>post hoc</i> test					
		Factors	Statistics	P	Sal vs LPS	Sal vs Tam+Sal	Sal vs Tam+LPS	LPS vs Tam+Sal	LPS vs Tam+LPS	Tam+Sal vs Tam+LPS
4B	Cell density of Iba1+ microglia in MCL	Pretreatment x treatment	$F_{\text{pretr} \times \text{treat} (1,12)} = 9.129$ $F_{\text{pretr} (1,12)} = 0.008593$ $F_{\text{treat} (1,12)} = 3.227$	$P = 0.0106$ $P = 0.9277$ $P = 0.0977$	$P < 0.05$ (*)	$P > 0.05$ (ns)	$P > 0.05$ (ns)	$P > 0.05$ (ns)	$P > 0.05$ (ns)	$P > 0.05$ (ns)
4C	Cell density of Iba1+ microglia in GCL	Pretreatment x treatment	$F_{\text{pretr} \times \text{treat} (1,12)} = 5.336$ $F_{\text{pretr} (1,12)} = 0.6334$ $F_{\text{treat} (1,12)} = 1.736$	$P = 0.0395$ $P = 0.4416$ $P = 0.2122$	$P > 0.05$ (ns)	$P > 0.05$ (ns)	$P > 0.05$ (ns)	$P > 0.05$ (ns)	$P > 0.05$ (ns)	$P > 0.05$ (ns)
4D	Cell density of Iba1+ microglia in Hilus	Pretreatment x treatment	$F_{\text{pretr} \times \text{treat} (1,12)} = 1.038$ $F_{\text{pretr} (1,12)} = 1.328$ $F_{\text{treat} (1,12)} = 0.2342$	$P = 0.3284$ $P = 0.2717$ $P = 0.6371$	$P > 0.05$ (ns)	$P > 0.05$ (ns)	$P > 0.05$ (ns)	$P > 0.05$ (ns)	$P > 0.05$ (ns)	$P > 0.05$ (ns)
4F	Cell density of DCX+ cells in SGZ/GCL	Pretreatment x treatment	$F_{\text{pretr} \times \text{treat} (1,12)} = 5.181$ $F_{\text{pretr} (1,12)} = 4.082$ $F_{\text{treat} (1,12)} = 3.502$	$P = 0.0420$ $P = 0.0662$ $P = 0.0859$	$P < 0.05$ (*)	$P > 0.05$ (ns)	$P > 0.05$ (ns)	$P < 0.05$ (*)	$P < 0.05$ (*)	$P > 0.05$ (ns)
4H	Cell density of GFAP+ RGLs in SGZ/GCL	Pretreatment x treatment	$F_{\text{pretr} \times \text{treat} (1,12)} = 2.631$ $F_{\text{pretr} (1,12)} = 8.587$ $F_{\text{treat} (1,12)} = 7.236$	$P = 0.1308$ $P = 0.0126$ $P = 0.0197$	$P < 0.05$ (*)	$P > 0.05$ (ns)	$P > 0.05$ (ns)	$P < 0.01$ (**)	$P < 0.05$ (*)	$P > 0.05$ (ns)
4I	Cell density of GFAP+ astrocytes in SGZ/GCL	Pretreatment x treatment	$F_{\text{pretr} \times \text{treat} (1,12)} = 1.145$ $F_{\text{pretr} (1,12)} = 2.115$ $F_{\text{treat} (1,12)} = 0.1143$	$P = 0.3056$ $P = 0.1715$ $P = 0.7412$	$P > 0.05$ (ns)	$P > 0.05$ (ns)	$P > 0.05$ (ns)	$P > 0.05$ (ns)	$P > 0.05$ (ns)	$P > 0.05$ (ns)

Pretreatment = Vehicle or Tamoxifen (Tam) administration; Treatment = Saline (Sal) or Lipopolysaccharide (LPS) injection (Ref. to FigureS4C for the experimental design).

**Table S4b.** Statistical table related to Figure 4.

Parameter (refers to counterparties treated without PLX)	Sal	LPS	Tam+Sal	Tam+LPS
% change of Iba1+ PLX-treated microglia in DG	-95.21 ± 0.015%	-89.18 ± 0.029%	-88.70 ± 0.030%	-92.16 ± 0.031%
% change of Iba1+ PLX-treated microglia in MCL	-96.62 ± 0.020%	-86.68 ± 0.061%	-86.02 ± 0.031%	-88.43 ± 0.146%
% change of Iba1+ PLX-treated microglia in GCL	-95.69 ± 0.033%	-91.51 ± 0.041%	-91.60 ± 0.014%	-95.38 ± 0.005%
% change of Iba1+ PLX-treated microglia in Hilus	-91.27 ± 0.041%	-95.80 ± 0.033%	-91.51 ± 0.067%	-92.64 ± 0.042%

**Table S5.** Statistical table related to Figure S1.

Figure	Parameter (refers to Iba1+ microglia)	Two-way ANOVA ( $\alpha < 0.05$ )			Student-Newman-Keuls' <i>post hoc</i> test						
		Factors	Statistics	P	Sal vs LPS	Sal vs Tam+Sal	Sal vs Tam+LPS	LPS vs Tam+Sal	LPS vs Tam+LPS	Tam+Sal vs Tam+LPS	
<b>S1A</b>	Cell density in MCL	Pretreatment x treatment	$F_{\text{pretr} \times \text{treat} (1,12)} = 0.4866$ $F_{\text{pretr} (1,12)} = 3.664$ $F_{\text{treat} (1,12)} = 14.56$	$P = 0.4987$ $P = 0.0798$ $P = 0.0025$	$P < 0.01$ (**)	$P > 0.05$ (ns)	$P > 0.05$ (ns)	$P < 0.01$ (**)	$P > 0.05$ (ns)	$P > 0.05$ (ns)	
<b>S1B</b>	Cell density in GCL	Pretreatment x treatment	$F_{\text{pretr} \times \text{treat} (1,12)} = 7.587$ $F_{\text{pretr} (1,12)} = 12.77$ $F_{\text{treat} (1,12)} = 0.9199$	$P = 0.0175$ $P = 0.0038$ $P = 0.3564$	$P < 0.05$ (*)	$P > 0.05$ (ns)	$P > 0.05$ (ns)	$P < 0.05$ (*)	$P < 0.01$ (**)	$P > 0.05$ (ns)	
<b>S1C</b>	Cell density in Hilus	Pretreatment x treatment	$F_{\text{pretr} \times \text{treat} (1,12)} = 0.2526$ $F_{\text{pretr} (1,12)} = 2.616$ $F_{\text{treat} (1,12)} = 1.312$	$P = 0.6244$ $P = 0.1318$ $P = 0.2744$	$P > 0.05$ (ns)	$P > 0.05$ (ns)	$P > 0.05$ (ns)	$P > 0.05$ (ns)	$P > 0.05$ (ns)	$P > 0.05$ (ns)	
<b>S1D</b>	Cell soma size	Pretreatment x treatment	$F_{\text{pretr} \times \text{treat} (1,8)} = 0.08359$ $F_{\text{pretr} (1,8)} = 3.765$ $F_{\text{treat} (1,8)} = 9.707$	$P = 0.7798$ $P = 0.0883$ $P = 0.0143$	$P > 0.05$ (ns)	$P > 0.05$ (ns)	$P > 0.05$ (ns)	$P < 0.05$ (*)	$P > 0.05$ (ns)	$P > 0.05$ (ns)	
<b>S1F</b>	Branch order (levels 1-5)	Level x group	$F_{\text{level} \times \text{group} (12,305)} = 5.389$ $F_{\text{level} (4,305)} = 175.7$ $F_{\text{group} (3,305)} = 26.35$	$P < 0.0001$ $P < 0.0001$ $P < 0.0001$	Level 1	$P > 0.05$ (ns)	$P > 0.05$ (ns)	$P > 0.05$ (ns)	$P > 0.05$ (ns)	$P > 0.05$ (ns)	$P > 0.05$ (ns)
					Level 2	$P < 0.05$ (*)	$P < 0.001$ (***)	$P < 0.001$ (***)	$P < 0.001$ (***)	$P < 0.001$ (***)	$P > 0.05$ (ns)
					Level 3	$P > 0.05$ (ns)	$P < 0.001$ (***)	$P < 0.01$ (**)	$P < 0.001$ (***)	$P < 0.01$ (**)	$P < 0.01$ (**)
					Level 4	$P > 0.05$ (ns)	$P > 0.05$ (ns)	$P > 0.05$ (ns)	$P > 0.05$ (ns)	$P > 0.05$ (ns)	
					Level 5	$P > 0.05$ (ns)	$P > 0.05$ (ns)	$P > 0.05$ (ns)	$P > 0.05$ (ns)	$P > 0.05$ (ns)	

Pretreatment = Vehicle or Tamoxifen (Tam) administration; Treatment = Saline (Sal) or Lipopolysaccharide (LPS) injection.

**Table S6.** Statistical table related to Figure S2.

Figure	Parameter	Unpaired Student's t-test, two-tailed ( $\alpha < 0.05$ )		
		Groups	Statistics	P
S2C	Cell density of Iba1+ microglia in DG	LPS vs L-Tam+LPS	$t_{(7)} = 3.050$	P = 0.0186 (*)
S2D	Area covered by Iba1+ microglia in DG	LPS vs L-Tam+LPS	$t_{(7)} = 2.982$	P = 0.0205 (*)
S2E	Cell density of DCX+ cells in SGZ/GCL	LPS vs L-Tam+LPS	$t_{(6)} = 2.761$	P = 0.0328 (*)
S2F	Cell density of GFAP+ astrocytes in SGZ/GCL	LPS vs L-Tam+LPS	$t_{(6)} = 2.409$	P = 0.0526 (ns)
S2G	Cell density of GFAP+RGLs in SGZ/GCL	LPS vs L-Tam+LPS	$t_{(6)} = 2.677$	P = 0.0367 (*)

Ref. to Figure S2A for the experimental design.

**Table S7.** Statistical table related to Figure S3.

Figure	Parameter (refers to SGZ/GCL)	Two-way ANOVA ( $\alpha < 0.05$ )			Student-Newman-Keuls' <i>post hoc</i> test					
		Factors	Statistics	P	Sal vs LPS	Sal vs Tam+Sal	Sal vs Tam+LPS	LPS vs Tam+Sal	LPS vs Tam+LPS	Tam+Sal vs Tam+LPS
S3B	Cell density of Ki67+ cells	Pretreatment x treatment	$F_{\text{pretr} \times \text{treat}} = 0.001919$ $F_{\text{pretr}(1,12)} = 0.001042$ $F_{\text{treat}(1,12)} = 1.761$	P = 0.9658 P = 0.9748 P = 0.2093	P > 0.05 (ns)	P > 0.05 (ns)	P > 0.05 (ns)	P > 0.05 (ns)	P > 0.05 (ns)	P > 0.05 (ns)
S3D	Cell density of GFAP+Ki67+ cells	Pretreatment x treatment	$F_{\text{pretr} \times \text{treat}(1,12)} = 0.06942$ $F_{\text{pretr}(1,12)} = 2.497$ $F_{\text{treat}(1,12)} = 1.810$	P = 0.7966 P = 0.1401 P = 0.2034	P > 0.05 (ns)	P > 0.05 (ns)	P > 0.05 (ns)	P > 0.05 (ns)	P > 0.05 (ns)	P > 0.05 (ns)
S3F	Cell density of NeuroD1+ cells	Pretreatment x treatment	$F_{\text{pretr} \times \text{treat}(1,8)} = 16.59$ $F_{\text{pretr}(1,8)} = 3.983$ $F_{\text{treat}(1,8)} = 1.047$	P = 0.0036 P = 0.0811 P = 0.3361	P < 0.05 (*)	P > 0.05 (ns)	P > 0.05 (ns)	P > 0.05 (ns)	P < 0.05 (*)	P > 0.05 (ns)
S3G	Cell density of GFAP-NeuroD1-Ki67+ cells	Pretreatment x treatment	$F_{\text{pretr} \times \text{treat}(1,12)} = 0.4113$ $F_{\text{pretr}(1,12)} = 0.6115$ $F_{\text{treat}(1,12)} = 2.180$	P = 0.5334 P = 0.4494 P = 0.1655	P > 0.05 (ns)	P > 0.05 (ns)	P > 0.05 (ns)	P > 0.05 (ns)	P > 0.05 (ns)	P > 0.05 (ns)

Pretreatment = Vehicle or Tamoxifen (Tam) administration; Treatment = Saline (Sal) or Lipopolysaccharide (LPS) injection (Ref. to Figure 1A for the experimental design).

## **CHAPTER IV**

## Concluding remarks and future perspectives

In the last years, several studies have contributed to the idea that the dynamics of adult neurogenesis within the hippocampal DG results from a complex interaction among the intrinsic cellular components of the neurogenic niche, signals arising from the brain-immune system, and a plethora of environmental cues both under physiological and pathological conditions (Aimone et al., 2014; Rodríguez-Iglesias et al., 2019; Toda et al., 2019; Araki et al., 2020; Bonafina et al., 2020; Vicidomini et al., 2020; Denoth-Lippuner and Jessberger, 2021). In this scenario, my work contributed on one side to the characterization of the neurogliogenic response to neuroinflammation occurring within the SGZ/GCL of the adult hippocampal DG, revealing a new role for the transcriptional regulator COUP-TFI in the cell fate choice of NSC/neural progenitors and clarifying the specific modulatory role played by microglia. On the other side, the results reported in this thesis contributed to elucidate tamoxifen's effects on the adult DG neurogenic niche during neuroinflammation, focusing on its neuroprotective role and challenging the tamoxifen-inducible Cre-ERT2/loxP system coupled to neuroinflammatory models.

My thesis presented and discussed the outcomes achieved during my Ph.D., answering three specific questions: 1) understand if the transcription factor COUP-TFI is involved in the regulation of adult DG neurogenesis and unravel its implication in inflammatory conditions 2) define if and how tamoxifen treatments interfere with the process of adult hippocampal neurogenesis in healthy conditions and upon LPS-induced neuroinflammation 3) unravel the role of microglia in the DG neurogenic niche response to LPS and tamoxifen treatments.

The choice to focus on the COUP-TFI function in the neurogenic region of the adult hippocampus was based on the initial observation that its expression was downregulated in the hippocampus upon neuroinflammation. We assumed that transcription factors as COUP-TFI, critically involved during the early phase of brain development, might be recruited to play critical and possibly unique functions in adult brain plasticity mechanisms, including regulation of adult neurogenesis. Then, by studying the neurogenic process taking place in the adult hippocampus, we showed that COUP-TFI is a key regulator involved in the decision-making process of NSC/progenitor cells to differentiate towards a neuronal rather than an

astroglial lineage within the healthy and inflamed adult DG (Chapter II; second author in Bonzano, Crisci et al., 2018). We showed that COUP-TFI is expressed in adult NSC/progenitor cells and upregulated in neuronal committed cells under physiological conditions where neurogenesis is favored at the expense of astroglial lineage in the adult DG. Intriguingly, we demonstrated that COUP-TFI downregulation occurs in adult NSC/progenitors upon LPS-induced neuroinflammation with a concomitant reduction of neurogenesis and increased astroglial lineage within the adult DG. Finally, forced COUP-TFI expression rescues neurogenesis upon neuroinflammation. Our results indicate that COUP-TFI manipulation in neuronal-committed cells changes their cell competence, revealing that these cells are still partially multipotent and need COUP-TFI to maintain their neuronal fate specification and maintenance. Therefore, COUP-TFI may represent one of the neurogenic fate determinants whose presence and up-regulation from adult NSCs to their progeny is needed to counteract the gliogenic environment of the adult brain (Götz et al., 2016). A future perspective resides in elucidating the COUP-TFI targets and molecular mechanism of action, for example, by genome-wide analyses through RNAseq. One report already identified the miR-17/106-p38 axis as a key effector of COUP-TFI in the developing CNS and hypothesized that epigenetic modification is an essential program behind the competence change (i.e., from neurogenic to gliogenic) orchestrated by COUP-TFs in embryonic neural progenitors (Naka-Kaneda et al., 2014). Another group showed COUP-TFI as a modulator of MAPK/ERK, AKT, and  $\beta$ -catenin signaling pathways, possibly targeting Fgfr3 (fibroblast growth factor receptor 3) at the early stages of cortical development (Faedo et al., 2008). However, the upstream and downstream effectors mediating the role of COUP-TFI in the control of the neurogenic competence within the adult DG neurogenic niche remain unknown.

Besides the LPS-induced neuroinflammation model exploited in our study, an Alzheimer's disease (AD)-like phospho-tau accumulation mouse model also showed COUP-TFI mRNA downregulation and GFAP mRNA upregulation, suggesting a switch of NSC-derived neurogenesis toward astroglial lineage (Zheng et al., 2020). Moreover, aging is characterized by chronic, low-grade inflammation, which naturally develops in the elderly, also defined as "inflammaging" (Franceschi et al., 2018), implying impaired neurogenesis (Kuhn et al., 1996, 2018; Encinas and Sierra, 2012; Kempermann, 2015). Interestingly, our unpublished observations by immunofluorescence analysis suggest that COUP-TFI staining is

downregulated in the aged hippocampus, concomitantly with decreased neurogenesis (starting from 6/12-month-old, i.e., middle age). Therefore, we hypothesize that a forced COUP-TFI up-regulation may restore the correct neuro-gliogenic balance during aging, suggesting COUP-TFI as a potential target to counteract the neurogenic decline associated with neurodegenerative and cognitive disorders.

During the second part of my Ph.D. project, the choice to investigate tamoxifen's effects on the adult DG neurogenic niche derived from observations I made during my initial experiments aimed to induce overexpression of COUP-TFI in the *Glast-CreERT2* mouse line under LPS-induced neuroinflammation. Unexpectedly, the use of tamoxifen failed in the activation of glial cells upon LPS challenge, presumably for its anti-inflammatory and neuroprotective role, as already reported (Baez-Jurado et al., 2019).

By means of molecular (i.e., qRT-PCR) and cellular (i.e., immunofluorescence staining and confocal microscopy) analyses, we showed that tamoxifen exerts pro-neurogenic effects by counteracting increased astrogliogenesis and the drop in neurogenesis found in the LPS-induced neuroinflammation model (Chapter III). Moreover, by performing a tamoxifen protocol that mimics that one used for the inducible *CreERT2-LoxP* transgenic mouse systems, our data revealed specific limits in using these models to study diseases associated with neuroinflammation. Interestingly, through the conditional microglia ablation in the adult mouse brain using the CSF1R kinase inhibitor PLX5622, our results revealed that post-mitotic neuroblasts directly respond to LPS insult and tamoxifen neurogenic prevention within the SGZ/GCL of adult DG; precisely, this cellular response is microglia-independent. Instead, we found that microglia play a key role in modulating the cellular response of glial cells to LPS insult. Indeed, in microglia-depleted conditions, astrocytes do not respond to LPS-induced inflammation lacking astrogliosis, while adult radial glia-like cells (RGLs) behave differently, decreasing in numbers. However, RGLs still directly respond to tamoxifen neuroprotection without microglia. Therefore, a combination of both direct and indirect effects act in regulating the response to the different cellular components of the DG neurogenic niche.

Future research should address the underlying signaling pathways involved in tamoxifen action on adult NSCs, and their progeny within the adult inflamed DG, identifying potential targets against neurogenic declines. Other reports already emphasized the neuroprotective

effect of tamoxifen under several brain pathologies showing an interaction between tamoxifen/ERs and LPS/TLRs signaling pathways (Tapia-Gonzalez et al., 2008; Tian et al., 2009; Sun et al., 2013; Gonzalez et al., 2016; Wang et al., 2017; Baez-Jurado et al., 2019), but convincing evidence of these molecular interactions on adult DG neurogenesis is still missing.

Finally, our findings demonstrated that tamoxifen *per se* might influence the microenvironment of the neurogenic niche changing the microglia phenotype and the expression of some inflammatory molecules. Indeed, we observed a general up-regulation of pro- and anti-inflammatory cytokines in the hippocampus of tamoxifen-treated mice, paralleled by a less-complex morphology DG microglia (i.e., fewer secondary and tertiary branches) compared to saline control and LPS inflamed microglia. Similarly, another study showed that DG microglia activated by the vascular endothelial growth factor (VEGF) upregulated both pro- and anti-inflammatory genes, but despite this inflammatory phenotype, VEGF-induced DG microglia supported neurogenesis (Kreisel et al., 2019). Interestingly, VEGF induction also depends on ERs and their ligands (Mueller et al., 2000; Jesmin et al., 2010; Barouk et al., 2011; Liang et al., 2013), suggesting a possible correspondence with the effects observed in tamoxifen-induced DG microglia.

In conclusion, the data I have collected during the Ph.D. represent new and crucial information on adult DG neurogenesis, particularly under inflammatory conditions. Moreover, the results reported in my thesis open new perspectives for future research aimed to unravel the mechanisms underlying COUP-TFI and tamoxifen in adult DG neurogenic niche and their potential target to act against the neurogenic decline in pathological conditions. A possible relationship between tamoxifen effects on DG neurogenesis, the regulation of COUP-TFI expression, and its implication on the adult NSC dynamics and on the neurogenic *versus* astroglial balance are also of considerable interest.

The results showed in this thesis highlight some fundamental issues in the field of adult hippocampal neurogenesis, such as the multicompetence of adult NSCs and progenitors and their fate determinants, the interplay between microglia, neurons, and astrocytes in the adult DG neurogenic niche, and a reduced suitability of the most popular transgenic mouse model used to study adult neurogenesis (i.e., tamoxifen-inducible CreERT2-LoxP mouse lines) under inflammatory conditions.



# **CHAPTER V**

## References

- Abbott, L. C., and Nigussie, F. (2020). Adult neurogenesis in the mammalian dentate gyrus. *J. Vet. Med. Ser. C Anat. Histol. Embryol.* 49, 3–16. doi:10.1111/ahe.12496.
- Acaz-Fonseca, E., Sanchez-Gonzalez, R., Azcoitia, I., Arevalo, M. A., and Garcia-Segura, L. M. (2014). Role of astrocytes in the neuroprotective actions of 17 $\beta$ -estradiol and selective estrogen receptor modulators. *Mol. Cell. Endocrinol.* 389, 48–57. doi:10.1016/j.mce.2014.01.009.
- Adam, F., Sourisseau, T., Métivier, R., Le Page, Y., Desbois, C., Michel, D., et al. (2000). COUP-TFI (chicken ovalbumin upstream promoter-transcription factor I) regulates cell migration and axogenesis in differentiating P19 embryonal carcinoma cells. *Mol. Endocrinol.* 14, 1918–1933. doi:10.1210/mend.14.12.0562.
- Ahn, S., and Joyner, A. L. (2005). In vivo analysis of quiescent adult neural stem cells responding to Sonic hedgehog. *Nature* 437, 894–897. doi:10.1038/nature03994.
- Aimone, J. B., Li, Y., Lee, S. W., Clemenson, G. D., Deng, W., and Gage, F. H. (2014). Regulation and function of adult neurogenesis: from genes to cognition. *Physiol Rev* 94, 991–1026. doi:10.1152/physrev.00004.2014.
- Ajami, B., Bennett, J. L., Krieger, C., Tetzlaff, W., and Rossi, F. M. V. (2007). Local self-renewal can sustain CNS microglia maintenance and function throughout adult life. *Nat. Neurosci.* 10, 1538–1543. doi:10.1038/nn2014.
- Al-Kateb, H., Shimony, J. S., Vineyard, M., Manwaring, L., Kulkarni, S., and Shinawi, M. (2013). NR2F1 haploinsufficiency is associated with optic atrophy, dysmorphism and global developmental delay. *Am. J. Med. Genet. Part A* 161, 377–381. doi:10.1002/ajmg.a.35650.
- Alfano, C., Magrinelli, E., Harb, K., Hevner, R. F., and Studer, M. (2014). Postmitotic control of sensory area specification during neocortical development. *Nat. Commun.* 5, 5632. doi:10.1038/ncomms6632.
- Alfano, C., Viola, L., Heng, J. I.-T., Pirozzi, M., Clarkson, M., Flore, G., et al. (2011). COUP-TFI promotes radial migration and proper morphology of callosal projection neurons by repressing Rnd2 expression. *Development* 138, 4685–4697. doi:10.1242/dev.068031.
- Altman, J., and Das, G. D. (1965). Post-natal origin of microneurons in the rat brain. *Nature* 207, 953–956. doi:10.1038/207953a0.
- Amador-Arjona, A., Cimadamore, F., Huang, C. T., Wright, R., Lewis, S., Gage, F. H., et al. (2015). SOX2 primes the epigenetic landscape in neural precursors enabling proper gene activation during hippocampal neurogenesis. *Proc. Natl. Acad. Sci. U. S. A.* 112, E1936–E1945. doi:10.1073/pnas.1421480112.
- Amaral, D. G., Scharfman, H. E., and Lavenex, P. (2007). The dentate gyrus: fundamental neuroanatomical organization (dentate gyrus for dummies). *Prog. Brain Res.* 163. doi:10.1016/S0079-6123(07)63001-5.
- Ampuero, E., Jury, N., Härtel, S., Marzob, M. P., and van Zundert, B. (2017). Interfering of the Reelin/ApoER2/PSD95 Signaling Axis Reactivates Dendritogenesis of Mature Hippocampal Neurons. *J. Cell. Physiol.* 232, 1187–1199. doi:10.1002/jcp.25605.

- Andersen, J., Urbán, N., Achimastou, A., Ito, A., Simic, M., Ullom, K., et al. (2014). A Transcriptional Mechanism Integrating Inputs from Extracellular Signals to Activate Hippocampal Stem Cells. *Neuron* 83, 1085–1097. doi:10.1016/j.neuron.2014.08.004.
- Araki, T., Ikegaya, Y., and Koyama, R. (2020). The effects of microglia- and astrocyte-derived factors on neurogenesis in health and disease. *Eur. J. Neurosci.*, 1–22. doi:10.1111/ejn.14969.
- Arevalo, M. A., Azcoitia, I., and Garcia-Segura, L. M. (2015). The neuroprotective actions of oestradiol and oestrogen receptors. *Nat. Rev. Neurosci.* 16, 17–29. doi:10.1038/nrn3856.
- Arevalo, M. A., Diz-Chaves, Y., Santos-Galindo, M., Bellini, M. J., and Garcia-Segura, L. M. (2012). Selective oestrogen receptor modulators decrease the inflammatory response of glial cells. *J. Neuroendocrinol.* 24, 183–190. doi:10.1111/j.1365-2826.2011.02156.x.
- Arevalo, M. A., Santos-Galindo, M., Lagunas, N., Azcoitia, I., and Garcia-Segura, L. M. (2011). Selective estrogen receptor modulators as brain therapeutic agents. *J. Mol. Endocrinol.* 46, R1–R9. doi:10.1677/JME-10-0122.
- Armentano, M., Armentano, M., Filosa, A., Andolfi, G., and Studer, M. (2006). COUP-TFI is required for the formation of commissural projections in the forebrain by regulating axonal growth. COUP-TFI is required for the formation of commissural projections in the forebrain by regulating axonal growth. doi:10.1242/dev.02600.
- Armentano, M., Chou, S.-J. J., Srubek Tomassy, G., Leingärtner, A., O’Leary, D. D. M., Studer, M., et al. (2007). COUP-TFI regulates the balance of cortical patterning between frontal/motor and sensory areas. *Nat Neurosci* 10, 1277–1286. doi:10.1038/nn1958.
- Auwerx, J., Baulieu, E., Beato, M., Becker-Andre, M., Burbach, P. H., Camerino, G., et al. (1999). A unified nomenclature system for the nuclear receptor superfamily. *Cell* 97, 161–163. doi:10.1016/S0092-8674(00)80726-6.
- Baez-Jurado, E., Rincón-Benavides, M. A., Hidalgo-Lanussa, O., Guio-Vega, G., Ashraf, G. M., Sahebkar, A., et al. (2019). Molecular mechanisms involved in the protective actions of Selective Estrogen Receptor Modulators in brain cells. *Front. Neuroendocrinol.* 52, 44–64. doi:10.1016/j.yfrne.2018.09.001.
- Baig, S., van Helmond, Z., and Love, S. (2009). Tau hyperphosphorylation affects Smad 2/3 translocation. *Neuroscience* 163, 561–570. doi:10.1016/j.neuroscience.2009.06.045.
- Ban, E., Milon, G., Prudhomme, N., Fillion, G., and Haour, F. (1991). Receptors for interleukin-1 ( $\alpha$  and  $\beta$ ) in mouse brain: Mapping and neuronal localization in hippocampus. *Neuroscience* 43, 21–30. doi:10.1016/0306-4522(91)90412-H.
- Banks, W. (2005). Blood-Brain Barrier Transport of Cytokines: A Mechanism for Neuropathology. *Curr. Pharm. Des.* 11, 973–984. doi:10.2174/1381612053381684.
- Banks, W. A. (2019). The blood–brain barrier as an endocrine tissue. *Nat. Rev. Endocrinol.* 15, 444–455. doi:10.1038/s41574-019-0213-7.
- Bao, H., Asrican, B., Li, W., Gu, B., Wen, Z., Lim, S. A., et al. (2017). Long-Range GABAergic Inputs Regulate Neural Stem Cell Quiescence and Control Adult Hippocampal Neurogenesis. *Cell Stem Cell* 21, 604–

617.e5. doi:10.1016/j.stem.2017.10.003.

Baptista, P., and Andrade, J. P. (2018). Adult hippocampal neurogenesis: Regulation and possible functional and clinical correlates. *Front. Neuroanat.* 12, 44. doi:10.3389/fnana.2018.00044.

Barha, C. K., Lieblich, S. E., and Galea, L. A. M. (2009). Different forms of oestrogen rapidly upregulate cell proliferation in the dentate gyrus of adult female rats. *J. Neuroendocrinol.* 21, 155–166. doi:10.1111/j.1365-2826.2008.01809.x

Barouk, S., Hintz, T., Li, P., Duffy, A. M., Maclusky, N. J., and Scharfman, H. E. (2011). 17 $\beta$ -estradiol increases astrocytic vascular endothelial growth factor (VEGF) in adult female rat hippocampus. *Endocrinology* 152, 1745–1751. doi:10.1210/en.2010-1290.

Barres, B. A. (2008). The Mystery and Magic of Glia: A Perspective on Their Roles in Health and Disease. *Neuron* 60, 430–440. doi:10.1016/j.neuron.2008.10.013.

Barreto, G., Santos-Galindo, M., Diz-Chaves, Y., Pernía, O., Carrero, P., Azcoitia, I., et al. (2009). Selective estrogen receptor modulators decrease reactive astrogliosis in the injured brain: Effects of aging and prolonged depletion of ovarian hormones. *Endocrinology* 150, 5010–5015. doi:10.1210/en.2009-0352.

Bastos, G. N., Moriya, T., Inui, F., Katura, T., and Nakahata, N. (2008). Involvement of cyclooxygenase-2 in lipopolysaccharide-induced impairment of the newborn cell survival in the adult mouse dentate gyrus. *Neuroscience* 155, 454–462. doi:10.1016/j.neuroscience.2008.06.020.

Basu, J., and Siegelbaum, S. A. (2015). The corticohippocampal circuit, synaptic plasticity, and memory. *Cold Spring Harb. Perspect. Biol.* 7. doi:10.1101/cshperspect.a021733.

Batista, C. R. A., Gomes, G. F., Candelario-Jalil, E., Fiebich, B. L., and de Oliveira, A. C. P. (2019). Lipopolysaccharide-induced neuroinflammation as a bridge to understand neurodegeneration. *Int. J. Mol. Sci.* 20. doi:10.3390/ijms20092293.

Bátiz, L. F., Castro, M. A., Burgos, P. V., Velásquez, Z. D., Munoz, R. I., Lafourcade, C. A., et al. (2016). Exosomes as novel regulators of adult neurogenic niches. *Front. Cell. Neurosci.* 9, 501. doi:10.3389/fncel.2015.00501.

Battista, D., Ferrari, C. C., Gage, F. H., and Pitossi, F. J. (2006). Neurogenic niche modulation by activated microglia: Transforming growth factor  $\beta$  increases neurogenesis in the adult dentate gyrus. *Eur. J. Neurosci.* 23, 83–93. doi:10.1111/j.1460-9568.2005.04539.x

Beattie, E. C., Stellwagen, D., Morishita, W., Bresnahan, J. C., Byeong, K. H., Von Zastrow, M., et al. (2002). Control of synaptic strength by glial TNF $\alpha$ . *Science (80-. )*. 295, 2282–2285. doi:10.1126/science.1067859.

Beccari, S., Valero, J., Maletic-Savatic, M., and Sierra, A. (2017). A simulation model of neuroprogenitor proliferation dynamics predicts age-related loss of hippocampal neurogenesis but not astrogenesis. *Sci. Rep.* 7, 16528. doi:10.1038/s41598-017-16466-3.

Beckervordersandforth, R., Zhang, C. L., and Lie, D. C. (2015). Transcription-factor-dependent control of adult hippocampal neurogenesis. *Cold Spring Harb. Perspect. Biol.* 7, 1–21. doi:10.1101/cshperspect.a018879.

Behl, C. (2002). Oestrogen as a neuroprotective hormone. *Nat. Rev. Neurosci.* 3, 433–442. doi:10.1038/nrn846.

- Ben Abdallah, N. M. B., Slomianka, L., Vyssotski, A. L., and Lipp, H. P. (2010). Early age-related changes in adult hippocampal neurogenesis in C57 mice. *Neurobiol. Aging* 31, 151–161. doi:10.1016/j.neurobiolaging.2008.03.002.
- Berg, D. A., Bond, A. M., Ming, G. li, and Song, H. (2018). Radial glial cells in the adult dentate gyrus: What are they and where do they come from? *F1000Research* 7. doi:10.12688/f1000research.12684.1.
- Berg, D. A., Yoon, K. J., Will, B., Xiao, A. Y., Kim, N. S., Christian, K. M., et al. (2015). Tbr2-expressing intermediate progenitor cells in the adult mouse hippocampus are unipotent neuronal precursors with limited amplification capacity under homeostasis. *Front. Biol. (Beijing)*. 10, 262–271. doi:10.1007/s11515-015-1364-0.
- Bergami, M., and Berninger, B. (2012). A fight for survival: The challenges faced by a newborn neuron integrating in the adult hippocampus. *Dev. Neurobiol.* 72, 1016–1031. doi:10.1002/dneu.22025.
- Bertacchi, M., Parisot, J., and Studer, M. (2019). The pleiotropic transcriptional regulator COUP-TFI plays multiple roles in neural development and disease. *Brain Res.* 1705, 75–94. doi:10.1016/j.brainres.2018.04.024.
- Biber, K., Pinto-Duarte, A., Wittendorp, M. C., Dolga, A. M., Fernandes, C. C., Von Frijtag Drabbe Künzel, J., et al. (2008). Interleukin-6 upregulates neuronal adenosine A1 receptors: Implications for neuromodulation and neuroprotection. *Neuropsychopharmacology* 33, 2237–2250. doi:10.1038/sj.npp.1301612.
- Biebl, M., Cooper, C. M., Winkler, J., and Kuhn, H. G. (2000). Analysis of neurogenesis and programmed cell death reveals a self-renewing capacity in the adult rat brain. *Neurosci. Lett.* 291, 17–20. doi:10.1016/S0304-3940(00)01368-9.
- Birch, A. M., McGarry, N. B., and Kelly, Á. M. (2013). Short-term environmental enrichment, in the absence of exercise, improves memory, and increases NGF concentration, early neuronal survival, and synaptogenesis in the dentate gyrus in a time-dependent manner. *Hippocampus* 23, 437–450. doi:10.1002/hipo.22103.
- Bluthé, R. M., Michaud, B., Kelley, K. W., and Dantzer, R. (1996). Vagotomy attenuates behavioural effects of interleukin-1 injected peripherally but not centrally. *Neuroreport* 7, 1485–1488. doi:10.1097/00001756-199606170-00008.
- Bluthe, R. M., Walter, V., Parnet, P., Laye, S., Lestage, J., Verrier, D., et al. (1994). Lipopolysaccharide induces sickness behaviour in rats by a vagal mediated mechanism. *Comptes Rendus l'Academie des Sci. - Ser. III* 317, 499–503. Available at: <https://europepmc.org/article/med/7987701> [Accessed March 1, 2021].
- Boche, D., Cunningham, C., Gauldie, J., and Perry, V. H. (2003). Transforming growth factor- $\beta$ 1-mediated neuroprotection against excitotoxic injury in vivo. *J. Cereb. Blood Flow Metab.* 23, 1174–1182. doi:10.1097/01.WCB.0000090080.64176.44.
- Boldrini, M., Fulmore, C. A., Tatt, A. N., Simeon, L. R., Pavlova, I., Poposka, V., et al. (2018). Human Hippocampal Neurogenesis Persists throughout Aging. *Cell Stem Cell* 22, 589-599.e5. doi:10.1016/j.stem.2018.03.015.
- Bolós, M., Perea, J. R., Terreros-Roncal, J., Pallas-Bazarra, N., Jurado-Arjona, J., Ávila, J., et al. (2018). Absence of microglial CX3CR1 impairs the synaptic integration of adult-born hippocampal granule neurons. *Brain. Behav. Immun.* 68, 76–89. doi:10.1016/j.bbi.2017.10.002.

- Bonafina, A., Paratcha, G., and Ledda, F. (2020). Deciphering New Players in the Neurogenic Adult Hippocampal Niche. *Front. Cell Dev. Biol.* 8, 1–9. doi:10.3389/fcell.2020.00548.
- Bonaguidi, M. A., Song, J., Ming, G. L., and Song, H. (2012). A unifying hypothesis on mammalian neural stem cell properties in the adult hippocampus. *Curr. Opin. Neurobiol.* 22, 754–761. doi:10.1016/j.conb.2012.03.013.
- Bonaguidi, M. M. A., Wheeler, M. M. A., Shapiro, J. J. S., Stadel, R. P., Sun, G. J., Ming, G. L., et al. (2011). In vivo clonal analysis reveals self-renewing and multipotent adult neural stem cell characteristics. *Cell* 145, 1142–1155. doi:10.1016/j.cell.2011.05.024.
- Bond, A. M., Ming, G. L., and Song, H. (2015). Adult Mammalian Neural Stem Cells and Neurogenesis: Five Decades Later. *Cell Stem Cell* 17, 385–395. doi:10.1016/j.stem.2015.09.003.
- Bond, A. M., Peng, C. Y., Meyers, E. A., McGuire, T., Ewaleifoh, O., and Kessler, J. A. (2014). BMP signaling regulates the tempo of adult hippocampal progenitor maturation at multiple stages of the lineage. *Stem Cells* 32, 2201–2214. doi:10.1002/stem.1688.
- Bonzano, S., Crisci, I., Podlesny-Drabiniok, A., Rolando, C., Krezel, W., Studer, M., et al. (2018). Neuron-Astroglia Cell Fate Decision in the Adult Mouse Hippocampal Neurogenic Niche Is Cell-Intrinsically Controlled by COUP-TFI In Vivo. *Cell Rep.* 24, 329–341. doi:10.1016/j.celrep.2018.06.044.
- Booker, S. A., and Vida, I. (2019). Morphological diversity and connectivity of hippocampal interneurons. *Cell Tissue Res.* 376, 485–486. doi:10.1007/s00441-019-03014-w.
- Bosch, D. G. M., Boonstra, F. N., Gonzaga-Jauregui, C., Xu, M., De Ligt, J., Jhangiani, S., et al. (2014). NR2F1 mutations cause optic atrophy with intellectual disability. *Am. J. Hum. Genet.* 94, 303–309. doi:10.1016/j.ajhg.2014.01.002.
- Bottes, S., Jaeger, B. N., Pilz, G. A., Jörg, D. J., Cole, J. D., Kruse, M., et al. (2021). Long-term self-renewing stem cells in the adult mouse hippocampus identified by intravital imaging. *Nat. Neurosci.* 24, 225–233. doi:10.1038/s41593-020-00759-4.
- Bovetti, S., Bonzano, S., Garzotto, D., Giannelli, S. G., Iannielli, A., Armentano, M., et al. (2013). COUP-TFI controls activity-dependent tyrosine hydroxylase expression in adult dopaminergic olfactory bulb interneurons. *Development* 140, 4850–4859. doi:10.1242/dev.089961.
- Brailoiu, E., Dun, S. L., Brailoiu, G. C., Mizuo, K., Sklar, L. A., Oprea, T. I., et al. (2007). Distribution and characterization of estrogen receptor G protein-coupled receptor 30 in the rat central nervous system. *J. Endocrinol.* 193, 311–321. doi:10.1677/JOE-07-0017.
- Brandt, M. D., Hübner, M., and Storch, A. (2012). Brief report: Adult hippocampal precursor cells shorten S-phase and total cell cycle length during neuronal differentiation. *Stem Cells* 30, 2843–2847. doi:10.1002/stem.1244.
- Brandt, M. D., Jessberger, S., Steiner, B., Kronenberg, G., Reuter, K., Bick-Sander, A., et al. (2003). Transient calretinin expression defines early postmitotic step of neuronal differentiation in adult hippocampal neurogenesis of mice. *Mol. Cell. Neurosci.* 24, 603–613. doi:10.1016/S1044-7431(03)00207-0.
- Brännvall, K., Korhonen, L., and Lindholm, D. (2002). Estrogen-receptor-dependent regulation of neural stem

- cell proliferation and differentiation. *Mol. Cell. Neurosci.* 21, 512–520. doi:10.1006/mcne.2002.1194.
- Brombacher, T. M., Berkiks, I., Pillay, S., Scibiorek, M., Moses, B. O., and Brombacher, F. (2020). IL-4R alpha deficiency influences hippocampal-BDNF signaling pathway to impair reference memory. *Sci. Rep.* 10, 1–8. doi:10.1038/s41598-020-73574-3.
- Brown, A. M., and Ransom, B. R. (2007). Astrocyte glycogen and brain energy metabolism. *Glia* 55, 1263–1271. doi:10.1002/glia.20557.
- Bryant, H. U. (2002). Selective estrogen receptor modulators. *Rev. Endocr. Metab. Disord.* 3, 231–241. doi:10.1023/A:1020076426727.
- Bustamante-Barrientos, F. A., Méndez-Ruette, M., Orloff, A., Luz-Crawford, P., Rivera, F. J., Figueroa, C. D., et al. (2021). The Impact of Estrogen and Estrogen-Like Molecules in Neurogenesis and Neurodegeneration: Beneficial or Harmful? *Front. Cell. Neurosci.* 15, 1–19. doi:10.3389/fncel.2021.636176.
- Butovsky, O., Ziv, Y., Schwartz, A., Landa, G., Talpalar, A. E., Pluchino, S., et al. (2006). Microglia activated by IL-4 or IFN- $\gamma$  differentially induce neurogenesis and oligodendrogenesis from adult stem/progenitor cells. *Mol. Cell. Neurosci.* 31, 149–160. doi:10.1016/j.mcn.2005.10.006.
- Bye, N., Zieba, M., Wreford, N. G., and Nichols, N. R. (2001). Resistance of the dentate gyrus to induced apoptosis during ageing is associated with increases in transforming growth factor- $\beta$ 1 messenger RNA. *Neuroscience* 105, 853–862. doi:10.1016/S0306-4522(01)00236-6.
- Cacci, E., Ajmone-Cat, M. A., Anelli, T., Biagioni, S., and Minghetti, L. (2008). In vitro neuronal and glial differentiation from embryonic or adult neural precursor cells are differently affected by chronic or acute activation of microglia. *Glia* 56, 412–425. doi:10.1002/glia.20616.
- Cacci, E., Claassen, J. H., and Kokaia, Z. (2005). Microglia-derived tumor necrosis factor- $\alpha$  exaggerates death of newborn hippocampal progenitor cells in vitro. *J. Neurosci. Res.* 80, 789–797. doi:10.1002/jnr.20531.
- Cajal, S. R. (1914). *Estudios sobre la degeneración y regeneración del sistema nervioso*. Imprenta de Hijos de Nicolás Moya Available at: <https://books.google.it/books?id=8FokAQAAIAAJ>.
- Cameron, H. A., and Gould, E. (1994). Adult neurogenesis is regulated by adrenal steroids in the dentate gyrus. *Neuroscience* 61, 203–209. doi:10.1016/0306-4522(94)90224-0.
- Campbell, I. L., Erta, M., Lim, S. L., Frausto, R., May, U., Rose-John, S., et al. (2014). Trans-signaling is a dominant mechanism for the pathogenic actions of interleukin-6 in the brain. *J. Neurosci.* 34, 2503–2513. doi:10.1523/JNEUROSCI.2830-13.2014.
- Cao, L., Jiao, X., Zuzga, D. S., Liu, Y., Fong, D. M., Young, D., et al. (2004). VEGF links hippocampal activity with neurogenesis, learning and memory. *Nat. Genet.* 36, 827–835. doi:10.1038/ng1395.
- Cardona, A. E., Pioro, E. P., Sasse, M. E., Kostenko, V., Cardona, S. M., Dijkstra, I. M., et al. (2006). Control of microglial neurotoxicity by the fractalkine receptor. *Nat. Neurosci.* 9, 917–924. doi:10.1038/nn1715.
- Carlén, M., Meletis, K., Barnabé-Heider, F., and Frisén, J. (2006). Genetic visualization of neurogenesis. *Exp. Cell Res.* 312, 2851–2859. doi:10.1016/j.yexcr.2006.05.012.

- Carpentier, P. A., and Palmer, T. D. (2009). Immune Influence on Adult Neural Stem Cell Regulation and Function. *Neuron* 64, 79–92. doi:10.1016/j.neuron.2009.08.038.
- Casadesus, G., Shukitt-Hale, B., Stellwagen, H. M., Zhu, X., Lee, H. G., Smith, M. A., et al. (2004). Modulation of hippocampal plasticity and cognitive behavior by short-term blueberry supplementation in aged rats. *Nutr. Neurosci.* 7, 309–316. doi:10.1080/10284150400020482.
- Casanova, E., Fehsenfeld, S., Lemberger, T., Shimshek, D. R., Sprengel, R., and Mantamadiotis, T. (2002). ER-based double iCre fusion protein allows partial recombination in forebrain. *Genesis* 34, 208–214. doi:10.1002/gene.10153.
- Cassé, F., Richetin, K., and Toni, N. (2018). Astrocytes' contribution to adult neurogenesis in physiology and Alzheimer's disease. *Front. Cell. Neurosci.* 12, 1–13. doi:10.3389/fncel.2018.00432.
- Castro, D. S., Martynoga, B., Parras, C., Ramesh, V., Pacary, E., Johnston, C., et al. (2011). A novel function of the proneural factor *Ascl1* in progenitor proliferation identified by genome-wide characterization of its targets. *Genes Dev.* 25, 930–945. doi:10.1101/gad.627811.
- Catorce, M. N., and Gevorkian, G. (2016). LPS-induced Murine Neuroinflammation Model: Main Features and Suitability for Pre-clinical Assessment of Nutraceuticals. doi:10.2174/1570159x14666151204122017.
- Cavallucci, V., Fidaleo, M., and Pani, G. (2016). Neural Stem Cells and Nutrients: Poised Between Quiescence and Exhaustion. *Trends Endocrinol. Metab.* 27, 756–769. doi:10.1016/j.tem.2016.06.007.
- Cavanagh, B. L., Walker, T., Norazit, A., and Meedeniya, A. C. B. (2011). Thymidine analogues for tracking DNA synthesis. *Molecules* 16, 7980–7993. doi:10.3390/molecules16097980.
- Cerciat, M., Unkila, M., Garcia-Segura, L. M., and Arevalo, M. A. (2010). Selective estrogen receptor modulators decrease the production of interleukin-6 and interferon- $\gamma$ -inducible protein-10 by astrocytes exposed to inflammatory challenge in vitro. *Glia* 58, 93–102. doi:10.1002/glia.20904.
- Chen, D., Wu, C. F., Shi, B., and Xu, Y. M. (2002). Tamoxifen and toremifene impair retrieval, but not acquisition, of spatial information processing in mice. *Pharmacol. Biochem. Behav.* 72, 417–421. doi:10.1016/S0091-3057(01)00782-1.
- Chen, Z., Jalabi, W., Shpargel, K. B., Farabaugh, K. T., Dutta, R., Yin, X., et al. (2012). Lipopolysaccharide-induced microglial activation and neuroprotection against experimental brain injury is independent of hematogenous TLR4. *J. Neurosci.* 32, 11706–15. doi:10.1523/JNEUROSCI.0730-12.2012.
- Cheng, M. F. (2013). Hypothalamic neurogenesis in the adult brain. *Front. Neuroendocrinol.* 34, 167–178. doi:10.1016/j.yfrne.2013.05.001.
- Chesnokova, V., Pechnick, R. N., and Wawrowsky, K. (2016). Chronic peripheral inflammation, hippocampal neurogenesis, and behavior. *Brain. Behav. Immun.* 58, 1–8. doi:10.1016/j.bbi.2016.01.017.
- Christian, K. M., Song, H., and Ming, G. L. (2014). Functions and dysfunctions of adult hippocampal neurogenesis. *Annu. Rev. Neurosci.* 37, 243–262. doi:10.1146/annurev-neuro-071013-014134.
- Chu, T., Zhang, Y. P., Tian, Z., Ye, C., Zhu, M., Shields, L. B. E., et al. (2019). Dynamic response of microglia/macrophage polarization following demyelination in mice. *J. Neuroinflammation* 16, 1–22.



doi:10.1186/s12974-019-1586-1.

- Clark, P. J., Brzezinska, W. J., Puchalski, E. K., Krone, D. A., and Rhodes, J. S. (2009). Functional analysis of neurovascular adaptations to exercise in the dentate gyrus of young adult mice associated with cognitive gain. *Hippocampus* 19, 937–950. doi:10.1002/hipo.20543.
- Clelland, C. D., Choi, M., Romberg, C., Clemenson, G. D., Fagniere, A., Tyers, P., et al. (2009). A functional role for adult hippocampal neurogenesis in spatial pattern separation. *Science* (80-. ). 325, 210–213. doi:10.1126/science.1173215.
- Clemenson, G. D., Lee, S. W., Deng, W., Barrera, V. R., Iwamoto, K. S., Fanselow, M. S., et al. (2015). Enrichment rescues contextual discrimination deficit associated with immediate shock. *Hippocampus* 25, 385–392. doi:10.1002/hipo.22380.
- Codeluppi, S., Fernandez-Zafra, T., Sandor, K., Kjell, J., Liu, Q., Abrams, M., et al. (2014). Interleukin-6 secretion by astrocytes is dynamically regulated by PI3K-mTOR-calcium signaling. *PLoS One* 9, 1–15. doi:10.1371/journal.pone.0092649.
- Colón, J. M., and Miranda, J. D. (2016). Tamoxifen: An FDA approved drug with neuroprotective effects for spinal cord injury recovery. *Neural Regen. Res.* 11, 1208–1211. doi:10.4103/1673-5374.189164.
- Cope, E. C., and Gould, E. (2019). Adult Neurogenesis, Glia, and the Extracellular Matrix. *Cell Stem Cell* 24, 690–705. doi:10.1016/j.stem.2019.03.023.
- Correa, J., Ronchetti, S., Labombarda, F., De Nicola, A. F., and Pietranera, L. (2019). Activation of the G Protein-Coupled Estrogen Receptor (GPER) Increases Neurogenesis and Ameliorates Neuroinflammation in the Hippocampus of Male Spontaneously Hypertensive Rats. *Cell. Mol. Neurobiol.* doi:10.1007/s10571-019-00766-5.
- Couillard-Despres, S., Winner, B., Karl, C., Lindemann, G., Schmid, P., Aigner, R., et al. (2006). Targeted transgene expression in neuronal precursors: Watching young neurons in the old brain. *Eur. J. Neurosci.* 24, 1535–1545. doi:10.1111/j.1460-9568.2006.05039.x.
- Covacu, R., Arvidsson, L., Andersson, Å., Khademi, M., Erlandsson-Harris, H., Harris, R. A., et al. (2009). TLR Activation Induces TNF- $\alpha$  Production from Adult Neural Stem/Progenitor Cells. *J. Immunol.* 182, 6889–6895. doi:10.4049/jimmunol.0802907.
- Dantzer, R. (2001). Cytokine-induced sickness behavior: Where do we stand? *Brain. Behav. Immun.* 15, 7–24. doi:10.1006/brbi.2000.0613.
- Dantzer, R., O'Connor, J. C., Freund, G. G., Johnson, R. W., and Kelley, K. W. (2008). From inflammation to sickness and depression: When the immune system subjugates the brain. *Nat. Rev. Neurosci.* 9, 46–56. doi:10.1038/nrn2297.
- Davalos, D., Grutzendler, J., Yang, G., Kim, J. V., Zuo, Y., Jung, S., et al. (2005). ATP mediates rapid microglial response to local brain injury in vivo. *Nat. Neurosci.* 8, 752–758. doi:10.1038/nn1472.
- Davis, B. M., Salinas-Navarro, M., Cordeiro, M. F., Moons, L., and Groef, L. De (2017). Characterizing microglia activation: A spatial statistics approach to maximize information extraction. *Sci. Rep.* 7. doi:10.1038/s41598-017-01747-8.

- Dawson, T. M., Golde, T. E., and Lagier-Tourenne, C. (2018). Animal models of neurodegenerative diseases. *Nat. Neurosci.* 21, 1370–1379. doi:10.1038/s41593-018-0236-8.
- Daynac, M., Pineda, J. R., Chicheportiche, A., Gauthier, L. R., Morizur, L., Boussin, F. D., et al. (2014). TGF $\beta$  lengthens the G1 phase of stem cells in aged mouse brain. *Stem Cells* 32, 3257–3265. doi:10.1002/stem.1815.
- Deng, W., Aimone, J. B., and Gage, F. H. (2010). New neurons and new memories: How does adult hippocampal neurogenesis affect learning and memory? *Nat. Rev. Neurosci.* 11, 339–350. doi:10.1038/nrn2822.
- Denoth-Lippuner, A., and Jessberger, S. (2021). Formation and integration of new neurons in the adult hippocampus. *Nat. Rev. Neurosci.* 22, 223–236. doi:10.1038/s41583-021-00433-z.
- Depino, A. M., Alonso, M., Ferrari, C., del Rey, A., Anthony, D., Besedovsky, H., et al. (2004). Learning modulation by endogenous hippocampal IL-1: Blockade of endogenous IL-1 facilitates memory formation. *Hippocampus* 14, 526–535. doi:10.1002/hipo.10164.
- Dhaliwal, J., and Lagace, D. C. (2011). Visualization and genetic manipulation of adult neurogenesis using transgenic mice. *Eur. J. Neurosci.* 33, 1025–1036. doi:10.1111/j.1460-9568.2011.07600.x.
- Diaz-Aparicio, I., Paris, I., Sierra-Torre, V., Plaza-Zabala, A., Rodríguez-Iglesias, N., Márquez-Ropero, M., et al. (2020). Microglia Actively Remodel Adult Hippocampal Neurogenesis through the Phagocytosis Secretome. *J. Neurosci.* 40, 1453–1482. doi:10.1523/JNEUROSCI.0993-19.2019.
- Döbrössy, M. D., Drapeau, E., Aourousseau, C., Le Moal, M., Piazza, P. V., and Abrous, D. N. (2003). Differential effects of learning on neurogenesis: Learning increases or decreases the number of newly born cells depending on their birth date. *Mol. Psychiatry* 8, 974–982. doi:10.1038/sj.mp.4001419.
- DonCarlos, L. L., Azcoitia, I., and Garcia-Segura, L. M. (2009). Neuroprotective actions of selective estrogen receptor modulators. *Psychoneuroendocrinology* 34. doi:10.1016/j.psyneuen.2009.04.012.
- Douglas, S. D., and Musson, R. A. (1986). Phagocytic defects-Monocytes/macrophages. *Clin. Immunol. Immunopathol.* 40, 62–68. doi:10.1016/0090-1229(86)90069-3.
- Dranovsky, A., Picchini, A. M., Moadel, T., Sisti, A. C., Yamada, A., Kimura, S., et al. (2011). Experience Dictates Stem Cell Fate in the Adult Hippocampus. *Neuron* 70, 908–923. doi:10.1016/j.neuron.2011.05.022.
- Duan, X., Kang, E., Liu, C. Y., Ming, G. li, and Song, H. (2008). Development of neural stem cell in the adult brain. *Curr. Opin. Neurobiol.* 18, 108–115. doi:10.1016/j.conb.2008.04.001.
- Duarte-Guterman, P., Lieblich, S. E., Chow, C., and Galea, L. A. M. (2015). Estradiol and GPER activation differentially affect cell proliferation but not GPER expression in the hippocampus of adult female rats. *PLoS One* 10, e0129880. doi:10.1371/journal.pone.0129880.
- Dye, C. A., El Shawa, H., and Huffman, K. J. (2011). A lifespan analysis of intraneocortical connections and gene expression in the mouse II. *Cereb. Cortex* 21, 1331–1350. doi:10.1093/cercor/bhq213.
- Dzyubenko, E., Manrique-Castano, D., Kleinschnitz, C., Faissner, A., and Hermann, D. M. (2018). Role of immune responses for extracellular matrix remodeling in the ischemic brain. *Ther. Adv. Neurol. Disord.* 11.

doi:10.1177/1756286418818092.

- Egeland, M., Zunszain, P. A., and Pariante, C. M. (2015). Molecular mechanisms in the regulation of adult neurogenesis during stress. *Nat. Rev. Neurosci.* 16, 189–200. doi:10.1038/nrn3855.
- Ehm, O., Göritz, C., Covic, M., Schäffner, I., Schwarz, T. J., Karaca, E., et al. (2010). RBPJ $\kappa$ -dependent signaling is essential for long-term maintenance of neural stem cells in the adult hippocampus. *J. Neurosci.* 30, 13794–13807. doi:10.1523/JNEUROSCI.1567-10.2010.
- Ehrenreich, H., Sirén, A. L., and Issue-editorial, S. (2001). SPECIAL ISSUE-EDITORIAL Neuroprotection – what does it mean? – what means do we have? *Eur. Arch. Psychiatry Clin. Neurosci.* 251, 149–151. doi:10.1007/s004060170034.
- Ekdahl, C. T. (2012). Microglial activation-tuning and pruning adult neurogenesis. *Front. Pharmacol.* 3 MAR, 41. doi:10.3389/fphar.2012.00041.
- Ekdahl, C. T., Claasen, J. H., Bonde, S., Kokaia, Z., and Lindvall, O. (2003). Inflammation is detrimental for neurogenesis in adult brain. *Proc. Natl. Acad. Sci. U. S. A.* 100, 13632–13637. doi:10.1073/pnas.2234031100.
- Ekdahl, C. T., Kokaia, Z., and Lindvall, O. (2009). Brain inflammation and adult neurogenesis: The dual role of microglia. *Neuroscience* 158, 1021–1029. doi:10.1016/j.neuroscience.2008.06.052.
- Elmore, M. R. P., Najafi, A. R., Koike, M. A., Dagher, N. N., Spangenberg, E. E., Rice, R. A., et al. (2014). Colony-stimulating factor 1 receptor signaling is necessary for microglia viability, unmasking a microglia progenitor cell in the adult brain. *Neuron* 82, 380–397. doi:10.1016/j.neuron.2014.02.040.
- Encinas, J. M., and Fitzsimons, C. P. (2017). Gene regulation in adult neural stem cells. Current challenges and possible applications. *Adv. Drug Deliv. Rev.* 120, 118–132. doi:10.1016/j.addr.2017.07.016.
- Encinas, J. M., Michurina, T. V., Peunova, N., Park, J. H., Tordo, J., Peterson, D. A., et al. (2011). Division-coupled astrocytic differentiation and age-related depletion of neural stem cells in the adult hippocampus. *Cell Stem Cell* 8, 566–579. doi:10.1016/j.stem.2011.03.010.
- Encinas, J. M., and Sierra, A. (2012). Neural stem cell deforestation as the main force driving the age-related decline in adult hippocampal neurogenesis. *Behav. Brain Res.* 227, 433–439. doi:10.1016/j.bbr.2011.10.010.
- Enikolopov, G., Overstreet-Wadiche, L., and Ge, S. (2015). Viral and transgenic reporters and genetic analysis of adult neurogenesis. *Cold Spring Harb. Perspect. Biol.* 7, a018804. doi:10.1101/cshperspect.a018804.
- Ergorul, C., and Eichenbaum, H. (2004). The hippocampus and memory for “what,” “where,” and “when.” *Learn. Mem.* 11, 397–405. doi:10.1101/lm.73304.
- Erickson, M. A., Sandy Liang, W., Fernandez, E. G., Bullock, K. M., Thysell, J. A., and Banks, W. A. (2018). Genetics and sex influence peripheral and central innate immune responses and bloodbrain barrier integrity. *PLoS One* 13, 1–19. doi:10.1371/journal.pone.0205769.
- Espósito, M. S., Piatti, V. C., Laplagne, D. A., Morgenstem, N. A., Ferrari, C. C., Pitossi, F. J., et al. (2005). Neuronal differentiation in the adult hippocampus recapitulates embryonic development. *J. Neurosci.* 25,

10074–10086. doi:10.1523/JNEUROSCI.3114-05.2005.

- Fabel, K., Wolf, S. A., Ehninger, D., Babu, H., Leal-Galicia, P., and Kempermann, G. (2009). Additive effects of physical exercise and environmental enrichment on adult hippocampal neurogenesis in mice. *Front. Neurosci.* 3, 1–7. doi:10.3389/neuro.22.002.2009.
- Faedo, A., Tomassy, G. S., Ruan, Y., Teichmann, H., Krauss, S., Pleasure, S. J., et al. (2008). COUP-TFI coordinates cortical patterning, neurogenesis, and laminar fate and modulates MAPK/ERK, AKT, and  $\beta$ -catenin signaling. *Cereb. Cortex* 18, 2117–2131. doi:10.1093/cercor/bhm238.
- Farioli-Vecchioli, S., Mattera, A., Micheli, L., Ceccarelli, M., Leonardi, L., Saraulli, D., et al. (2014). Running rescues defective adult neurogenesis by shortening the length of the cell cycle of neural stem and progenitor cells. *Stem Cells* 32, 1968–1982. doi:10.1002/stem.1679.
- Favaro, R., Valotta, M., Ferri, A. L. M., Latorre, E., Mariani, J., Giachino, C., et al. (2009). Hippocampal development and neural stem cell maintenance require Sox2-dependent regulation of Shh. *Nat. Neurosci.* 12, 1248–1256. doi:10.1038/nn.2397.
- Feliciano, D. M., Borley, A., and Bonfanti, L. (2015). Noncanonical sites of adult neurogenesis in the mammalian brain. *Cold Spring Harb. Perspect. Biol.* 7. doi:10.1101/cshperspect.a018846.
- Fernández-Arjona, M. del M., Grondona, J. M., Granados-Durán, P., Fernández-Llebrez, P., and López-Ávalos, M. D. (2017). Microglia morphological categorization in a rat model of neuroinflammation by hierarchical cluster and principal components analysis. *Front. Cell. Neurosci.* 11, 1–22. doi:10.3389/fncel.2017.00235.
- Filippov, V., Kronenberg, G., Pivneva, T., Reuter, K., Steiner, B., Wang, L. P., et al. (2003). Subpopulation of nestin-expressing progenitor cells in the adult murine hippocampus shows electrophysiological and morphological characteristics of astrocytes. *Mol. Cell. Neurosci.* 23, 373–382. doi:10.1016/S1044-7431(03)00060-5.
- Finch, C. E., Laping, N. J., Morgan, T. E., Nichols, N. R., and Pasinetti, G. M. (1993). TGF- $\beta$ 1 is an organizer of responses to neurodegeneration. *J. Cell. Biochem.* 53, 314–322. doi:10.1002/jcb.240530408.
- Fischer, T. J., Walker, T. L., Overall, R. W., Brandt, M. D., and Kempermann, G. (2014). Acute effects of wheel running on adult hippocampal precursor cells in mice are not caused by changes in cell cycle length or S phase length. *Front. Neurosci.* 8, 314. doi:10.3389/fnins.2014.00314.
- Flore, G., Di Ruberto, G., Parisot, J., Sannino, S., Russo, F., Illingworth, E. A., et al. (2017). Gradient COUP-TFI Expression Is Required for Functional Organization of the Hippocampal Septo-Temporal Longitudinal Axis. *Cereb. Cortex* 27, 1629–1643. doi:10.1093/cercor/bhv336.
- Font, E., Desfilis, E., Pérez-Cañellas, M. M., and García-Verdugo, J. M. (2001). Neurogenesis and neuronal regeneration in the adult reptilian brain. in *Brain, Behavior and Evolution* (Karger Publishers), 276–295. doi:10.1159/000057570.
- Forrester, J. V., McMenamin, P. G., and Dando, S. J. (2018). CNS infection and immune privilege. *Nat. Rev. Neurosci.* 19, 655–671. doi:10.1038/s41583-018-0070-8.
- Franceschi, C., Garagnani, P., Parini, P., Giuliani, C., and Santoro, A. (2018). Inflammaging: a new immune–metabolic viewpoint for age-related diseases. *Nat. Rev. Endocrinol.* 14, 576–590. doi:10.1038/s41574-018-

0059-4.

- Franco Rodríguez, N. E., Dueñas Jiménez, J. M., De la Torre Valdovinos, B., López Ruiz, J. R., Hernández Hernández, L., and Dueñas Jiménez, S. H. (2013). Tamoxifen favoured the rat sensorial cortex regeneration after a penetrating brain injury. *Brain Res. Bull.* 98, 64–75. doi:10.1016/j.brainresbull.2013.07.007.
- Freund, T. F., and Buzsáki, G. (1996). Interneurons of the Hippocampus. *Hippocampus* 6, 347–470. doi:10.1002/(sici)1098-1063(1996)6:4<347::aid-hipo1>3.0.co;2-i.
- Frost, J. L., and Schafer, D. P. (2016). Microglia: Architects of the Developing Nervous System. *Trends Cell Biol.* 26, 587–597. doi:10.1016/j.tcb.2016.02.006.
- Fuentealba, L. C., Obernier, K., and Alvarez-Buylla, A. (2012). Adult neural stem cells bridge their niche. *Cell Stem Cell* 10, 698–708. doi:10.1016/j.stem.2012.05.012.
- Fuentes, N., and Silveyra, P. (2019). *Estrogen receptor signaling mechanisms*. 1st ed. Elsevier Inc. doi:10.1016/bs.apcsb.2019.01.001.
- Fujioka, H., and Akema, T. (2010). Lipopolysaccharide acutely inhibits proliferation of neural precursor cells in the dentate gyrus in adult rats. *Brain Res.* 1352, 35–42. doi:10.1016/j.brainres.2010.07.032.
- Gadient, R. A., and Otten, U. H. (1997). Interleukin-6 (IL-6) - A molecule with both beneficial and destructive potentials. *Prog. Neurobiol.* 52, 379–390. doi:10.1016/S0301-0082(97)00021-X.
- Galea, I., Bechmann, I., and Perry, V. H. (2007). What is immune privilege (not)? *Trends Immunol.* 28, 12–18. doi:10.1016/j.it.2006.11.004.
- Galea, L. A. M. (2008). Gonadal hormone modulation of neurogenesis in the dentate gyrus of adult male and female rodents. *Brain Res. Rev.* 57, 332–341. doi:10.1016/j.brainresrev.2007.05.008.
- Gao, X., Arlotta, P., Macklis, J. D., and Chen, J. (2007). Conditional knock-out of  $\beta$ -catenin in postnatal-born dentate gyrus granule neurons results in dendritic malformation. *J. Neurosci.* 27, 14317–14325. doi:10.1523/JNEUROSCI.3206-07.2007.
- Gao, Y., Shen, M., Gonzalez, J. C., Dong, Q., Kannan, S., Hoang, J. T., et al. (2020). RGS6 Mediates Effects of Voluntary Running on Adult Hippocampal Neurogenesis. *Cell Rep.* 32, 107997. doi:10.1016/j.celrep.2020.107997.
- Gao, Z., Ure, K., Ables, J. L., Lagace, D. C., Nave, K. A., Goebbels, S., et al. (2009). Neurod1 is essential for the survival and maturation of adult-born neurons. *Nat. Neurosci.* 12, 1090–1092. doi:10.1038/nn.2385.
- Gao, Z., Ure, K., Ding, P., Nashaat, M., Yuan, L., Ma, J., et al. (2011). The master negative regulator REST/NRSF controls adult neurogenesis by restraining the neurogenic program in quiescent stem cells. *J. Neurosci.* 31, 9772–9786. doi:10.1523/JNEUROSCI.1604-11.2011.
- Garcia-Ovejero, D., Azcoitia, I., DonCarlos, L. L., Melcangi, R. C., and Garcia-Segura, L. M. (2005). Glia-neuron crosstalk in the neuroprotective mechanisms of sex steroid hormones. *Brain Res. Rev.* 48, 273–286. doi:10.1016/j.brainresrev.2004.12.018.
- Garcia-Segura, L. M., and Balthazart, J. (2009). Steroids and neuroprotection: New advances. *Front.*

*Neuroendocrinol.* 30, v–ix. doi:10.1016/j.yfrne.2009.04.006.

- Gaykema, R. P. A., Goehler, L. E., Hansen, M. K., Maier, S. F., and Watkins, L. R. (2000). Subdiaphragmatic vagotomy blocks interleukin-1b-induced fever but does not reduce IL-1b levels in the circulation. Available at: [www.elsevier.com/locate/autneu](http://www.elsevier.com/locate/autneu) [Accessed March 1, 2021].
- Ge, S., Yang, C. hao, Hsu, K. sen, Ming, G. li, and Song, H. (2007). A Critical Period for Enhanced Synaptic Plasticity in Newly Generated Neurons of the Adult Brain. *Neuron* 54, 559–566. doi:10.1016/j.neuron.2007.05.002.
- Gebara, E., Bonaguidi, M. A., Beckervordersandforth, R., Sultan, S., Udry, F., Gijis, P. J., et al. (2016). Heterogeneity of Radial Glia-Like Cells in the Adult Hippocampus. *Stem Cells* 34, 997–1010. doi:10.1002/stem.2266.
- Gebara, E., Sultan, S., Kocher-Braissant, J., and Toni, N. (2013). Adult hippocampal neurogenesis inversely correlates with microglia in conditions of voluntary running and aging. *Front. Neurosci.* 7, 145. doi:10.3389/fnins.2013.00145.
- Ghisletti, S., Meda, C., Maggi, A., and Vegeto, E. (2005). 17 $\beta$ -Estradiol Inhibits Inflammatory Gene Expression by Controlling NF- $\kappa$ B Intracellular Localization. *Mol. Cell. Biol.* 25, 2957–2968. doi:10.1128/mcb.25.8.2957-2968.2005.
- Ginhoux, F., Greter, M., Leboeuf, M., Nandi, S., See, P., Gokhan, S., et al. (2010). Fate mapping analysis reveals that adult microglia derive from primitive macrophages. *Science* (80-. ). 330, 841–845. doi:10.1126/science.1194637.
- Goetz, M. P., Kamal, A., and Ames, M. M. (2008). Tamoxifen pharmacogenomics: The role of CYP2D6 as a predictor of drug response. *Clin. Pharmacol. Ther.* 83, 160–166. doi:10.1038/sj.clpt.6100367.
- Goldman, S. A., and Nottebohm, F. (1983). Neuronal production, migration, and differentiation in a vocal control nucleus of the adult female canary brain. *Proc. Natl. Acad. Sci. U. S. A.* 80, 2390–2394. doi:10.1073/pnas.80.8.2390.
- Gomez Perdiguero, E., Klapproth, K., Schulz, C., Busch, K., Azzoni, E., Crozet, L., et al. (2015). Tissue-resident macrophages originate from yolk-sac-derived erythro-myeloid progenitors. *Nature* 518, 547–551. doi:10.1038/nature13989.
- Gonçalves, J. T., Schafer, S. T., and Gage, F. H. (2016). Adult Neurogenesis in the Hippocampus: From Stem Cells to Behavior. *Cell* 167, 897–914. doi:10.1016/j.cell.2016.10.021.
- Gonzalez, G. A., Hofer, M. P., Syed, Y. A., Amaral, A. I., Rundle, J., Rahman, S., et al. (2016). Tamoxifen accelerates the repair of demyelinated lesions in the central nervous system. *Sci. Rep.* 6, 31599. doi:10.1038/srep31599.
- Goshen, I., Brodsky, M., Prakash, R., Wallace, J., Gradinaru, V., Ramakrishnan, C., et al. (2011). Dynamics of retrieval strategies for remote memories. *Cell* 147, 678–689. doi:10.1016/j.cell.2011.09.033.
- Götz, M., Nakafuku, M., and Petrik, D. (2016). Neurogenesis in the developing and adult brain—similarities and key differences. *Cold Spring Harb. Perspect. Biol.* 8. doi:10.1101/cshperspect.a018853.

- Green, K. N., Crapser, J. D., and Hohsfield, L. A. (2020). To Kill a Microglia: A Case for CSF1R Inhibitors. *Trends Immunol.* 41, 771–784. doi:10.1016/j.it.2020.07.001.
- Gross, C. G. (2000). Neurogenesis in the adult brain: Death of a dogma. *Nat. Rev. Neurosci.* 1, 67–73. doi:10.1038/35036235.
- Hainmueller, T., and Bartos, M. (2020). Dentate gyrus circuits for encoding, retrieval and discrimination of episodic memories. *Nat. Rev. Neurosci.* 21, 153–168. doi:10.1038/s41583-019-0260-z.
- Hajszan, T., Milner, T. A., and Leranth, C. (2007). Sex steroids and the dentate gyrus. *Prog. Brain Res.* 163, 399–416. doi:10.1016/S0079-6123(07)63023-4.
- Hansen, M. K., Daniels, S., Goehler, L. E., Gaykema, R. P. A., Maier, S. F., and Watkins, L. R. (2000). Subdiaphragmatic vagotomy does not block intraperitoneal lipopolysaccharide-induced fever. Available at: www.elsevier.com [Accessed March 1, 2021].
- Harb, K., Magrinelli, E., Nicolas, C. S., Lukianets, N., Frangeul, L., Pietri, M., et al. (2016). Area-specific development of distinct projection neuron subclasses is regulated by postnatal epigenetic modifications. *Elife* 5. doi:10.7554/eLife.09531.
- Harland, B., Contreras, M., and Fellous, J.-M. (2018). A Role for the Longitudinal Axis of the Hippocampus in Multiscale Representations of Large and Complex Spatial Environments and Mnemonic Hierarchies. *Hippocampus - Plast. Funct.*, 13. doi:10.5772/intechopen.71165.
- Harris, L., Rigo, P., Stiehl, T., Gaber, Z. B., Austin, S. H. L., Masdeu, M. del M., et al. (2021). Coordinated changes in cellular behavior ensure the lifelong maintenance of the hippocampal stem cell population. *Cell Stem Cell*, 1–14. doi:10.1016/j.stem.2021.01.003.
- Harris, L., Zalucki, O., Clément, O., Fraser, J., Matuzelski, E., Oishi, S., et al. (2018). Neurogenic differentiation by hippocampal neural stem and progenitor cells is biased by NFIX expression. *Development* 145, dev155689. doi:10.1242/dev.155689.
- Hayashi, S., and McMahon, A. P. (2002). Efficient recombination in diverse tissues by a tamoxifen-inducible form of Cre: A tool for temporally regulated gene activation/inactivation in the mouse. *Dev. Biol.* 244, 305–318. doi:10.1006/dbio.2002.0597.
- Haydon, P. G., and Carmignoto, G. (2006). Astrocyte control of synaptic transmission and neurovascular coupling. *Physiol. Rev.* 86, 1009–1031. doi:10.1152/physrev.00049.2005.
- Heldmann, U., Thored, P., Claasen, J. H., Arvidsson, A., Kokaia, Z., and Lindvall, O. (2005). TNF- $\alpha$  antibody infusion impairs survival of stroke-generated neuroblasts in adult rat brain. *Exp. Neurol.* 196, 204–208. doi:10.1016/j.expneurol.2005.07.024.
- Herculano-Houzel, S. (2014). The glia/neuron ratio: How it varies uniformly across brain structures and species and what that means for brain physiology and evolution. *Glia* 62, 1377–1391. doi:10.1002/glia.22683.
- Hill, R., and Wu, H. (2009). PTEN, stem cells, and cancer stem cells. *J. Biol. Chem.* 284, 11755–11759. doi:10.1074/jbc.R800071200.
- Hirrlinger, P. G., Scheller, A., Braun, C., Hirrlinger, J., and Kirchhoff, F. (2006). Temporal control of gene

- recombination in astrocytes by transgenic expression of the tamoxifen-inducible DNA recombinase variant CreERT2. *Glia* 54, 11–20. doi:10.1002/glia.20342.
- Hitti, F. L., and Siegelbaum, S. A. (2014). The hippocampal CA2 region is essential for social memory. *Nature* 508, 88–92. doi:10.1038/nature13028.
- Hodge, R. D., Nelson, B. R., Kahoud, R. J., Yang, R., Mussar, K. E., Reiner, S. L., et al. (2012). Tbr2 is essential for hippocampal lineage progression from neural stem cells to intermediate progenitors and neurons. *J. Neurosci.* 32, 6275–6287. doi:10.1523/JNEUROSCI.0532-12.2012.
- Holm, T. H., Draeby, D., and Owens, T. (2012). Microglia are required for astroglial toll-like receptor 4 response and for optimal TLR2 and TLR3 response. *Glia* 60, 630–638. doi:10.1002/glia.22296.
- Hu, X., He, W., Luo, X., Tsubota, K. E., and Yan, R. (2013). BACE1 Regulates Hippocampal Astrogenesis via the Jagged1-Notch Pathway. *Cell Rep.* 4, 40–49. doi:10.1016/j.celrep.2013.06.005.
- Huang, Y., Xu, Z., Xiong, S., Sun, F., Qin, G., Hu, G., et al. (2018). Repopulated microglia are solely derived from the proliferation of residual microglia after acute depletion. *Nat. Neurosci.* 21, 530–540. doi:10.1038/s41593-018-0090-8.
- Ibrayeva, A., Bay, M., Pu, E., Jörg, D. J., Peng, L., Jun, H., et al. (2021). Early stem cell aging in the mature brain. *Cell Stem Cell* 28, 955-966.e7. doi:10.1016/j.stem.2021.03.018.
- Imayoshi, I., Sakamoto, M., and Kageyama, R. (2011). Genetic methods to identify and manipulate newly born neurons in the adult brain. *Front. Neurosci.* 5, 1–11. doi:10.3389/fnins.2011.00064.
- Indra, A. K., Warot, X., Brocard, J., Bornert, J. M., Xiao, J. H., Chambon, P., et al. (1999). Temporally-controlled site-specific mutagenesis in the basal layer of the epidermis: Comparison of the recombinase activity of the tamoxifen-inducible Cre-ER(T) and Cre-ER(T2) recombinases. *Nucleic Acids Res.* 27, 4324–4327. doi:10.1093/nar/27.22.4324.
- Iosif, R. E., Ekdahl, C. T., Ahlenius, H., Pronk, C. J. H., Bonde, S., Kokaia, Z., et al. (2006). Tumor necrosis factor receptor 1 is a negative regulator of progenitor proliferation in adult hippocampal neurogenesis. *J. Neurosci.* 26, 9703–9712. doi:10.1523/JNEUROSCI.2723-06.2006.
- Isgor, C., and Watson, S. J. (2005). Estrogen receptor  $\alpha$  and  $\beta$  mRNA expressions by proliferating and differentiating cells in the adult rat dentate gyrus and subventricular zone. *Neuroscience* 134, 847–856. doi:10.1016/j.neuroscience.2005.05.008.
- Ito, D., Imai, Y., Ohsawa, K., Nakajima, K., Fukuuchi, Y., and Kohsaka, S. (1998). Microglia-specific localisation of a novel calcium binding protein, Iba1. *Mol. Brain Res.* 57, 1–9. doi:10.1016/S0169-328X(98)00040-0.
- Ja, W. K., and Duman, R. S. (2008). IL-1 $\beta$  is an essential mediator of the antineurogenic and anhedonic effects of stress. *Proc. Natl. Acad. Sci. U. S. A.* 105, 751–756. doi:10.1073/pnas.0708092105.
- Jagasia, R., Steib, K., Englberger, E., Herold, S., Faus-Kessler, T., Saxe, M., et al. (2009). GABA-cAMP response element-binding protein signaling regulates maturation and survival of newly generated neurons in the adult hippocampus. *J. Neurosci.* 29, 7966–7977. doi:10.1523/JNEUROSCI.1054-09.2009.



- Jahn, H. M., Kasakow, C. V., Helfer, A., Michely, J., Verkhatsky, A., Maurer, H. H., et al. (2018). Refined protocols of tamoxifen injection for inducible DNA recombination in mouse astroglia. *Sci. Rep.* 8, 5913. doi:10.1038/s41598-018-24085-9.
- Jang, M. H., Bonaguidi, M. A., Kitabatake, Y., Sun, J., Song, J., Kang, E., et al. (2013). Secreted frizzled-related protein 3 regulates activity-dependent adult hippocampal neurogenesis. *Cell Stem Cell* 12, 215–223. doi:10.1016/j.stem.2012.11.021.
- Janoff, A. (1964). Alterations in lysosomes (intracellular enzymes) during shock; effects of preconditioning (tolerance) and protective drugs. *Int. Anesthesiol. Clin.* 2, 251–269. doi:10.1097/00004311-196402000-00008.
- Jesmin, S., Mowa, C. N., Sultana, S. N., Mia, S., Islam, R., Zaedi, S., et al. (2010). Estrogen receptor alpha and beta are both involved in the cerebral VEGF/Akt/NO pathway and cerebral angiogenesis in female mice. *Biomed. Res.* 31, 337–346. doi:10.2220/biomedres.31.337.
- Jessberger, S., Clark, R. E., Broadbent, N. J., Clemenson, G. D., Consiglio, A., Lie, D. C., et al. (2009). Dentate gyrus-specific knockdown of adult neurogenesis impairs spatial and object recognition memory in adult rats. *Learn. Mem.* 16, 147–154. doi:10.1101/lm.1172609.
- Jha, M. K., Jeon, S., and Suk, K. (2012). Glia as a Link between Neuroinflammation and Neuropathic Pain. *Immune Netw.* 12, 41. doi:10.4110/in.2012.12.2.41.
- Jinno, S., Fleischer, F., Eckel, S., Schmidt, V., and Kosaka, T. (2007). Spatial arrangement of microglia in the mouse hippocampus: A stereological study in comparison with astrocytes. *Glia* 55, 1334–1347. doi:10.1002/glia.20552.
- Jones, K. M., Saric, N., Russell, J. P., Andoniadou, C. L., Scambler, P. J., and Basson, M. A. (2015). CHD7 maintains neural stem cell quiescence and prevents premature stem cell depletion in the adult hippocampus. *Stem Cells* 33, 196–210. doi:10.1002/stem.1822.
- Jordan, V. C. (2003). Tamoxifen: A most unlikely pioneering medicine. *Nat. Rev. Drug Discov.* 2, 205–213. doi:10.1038/nrd1031.
- Kaiser, T., and Feng, G. (2019). Tmem119-EGFP and Tmem119-creERT2 transgenic mice for labeling and manipulating microglia. *eNeuro* 6. doi:10.1523/ENEURO.0448-18.2019.
- Kandasamy, M., Lehner, B., Kraus, S., Sander, P. R., Marschallinger, J., Rivera, F. J., et al. (2014). TGF-beta signalling in the adult neurogenic niche promotes stem cell quiescence as well as generation of new neurons. *J. Cell. Mol. Med.* 18, 1444–1459. doi:10.1111/jcmm.12298.
- Kaplan, M. S., and Hinds, J. W. (1977). Neurogenesis in the adult rat: Electron microscopic analysis of light radioautographs. *Science (80-)*. 197, 1092–1094. doi:10.1126/science.887941.
- Kee, N., Sivalingam, S., Boonstra, R., and Wojtowicz, J. M. (2002). The utility of Ki-67 and BrdU as proliferative markers of adult neurogenesis. *J. Neurosci. Methods* 115, 97–105. doi:10.1016/S0165-0270(02)00007-9.
- Kempermann, G. (2011a). Seven principles in the regulation of adult neurogenesis. *Eur. J. Neurosci.* 33, 1018–1024. doi:10.1111/j.1460-9568.2011.07599.x.

- Kempermann, G. (2011b). The pessimist's and optimist's views of adult neurogenesis. *Cell* 145, 1009–1011. doi:10.1016/j.cell.2011.06.011.
- Kempermann, G. (2015). Activity dependency and aging in the regulation of adult neurogenesis. *Cold Spring Harb. Perspect. Biol.* 7. doi:10.1101/cshperspect.a018929.
- Kempermann, G., Gage, F. H., Aigner, L., Song, H., Curtis, M. A., Thuret, S., et al. (2018). Human Adult Neurogenesis: Evidence and Remaining Questions. *Cell Stem Cell* 23, 25–30. doi:10.1016/j.stem.2018.04.004.
- Kempermann, G., Gast, D., Kronenberg, G., Yamaguchi, M., and Gage, F. H. (2003). Early determination and long-term persistence of adult-generated new neurons in the hippocampus of mice. *Development* 130, 391–399. doi:10.1242/dev.00203.
- Kempermann, G., Jessberger, S., Steiner, B., and Kronenberg, G. (2004). Milestones of neuronal development in the adult hippocampus. *Trends Neurosci.* 27, 447–452. doi:10.1016/j.tins.2004.05.013.
- Kempermann, G., Song, H., and Gage, F. H. (2015). Neurogenesis in the adult hippocampus. *Cold Spring Harb. Perspect. Biol.* 7. doi:10.1101/cshperspect.a018812.
- Kenyon, C., Chang, J., Gensch, E., Rudner, A., and Tabtiang, R. (1993). A *C. elegans* mutant that lives twice as long as wild type. *Nature* 366, 461–464. doi:10.1038/366461a0.
- Keohane, A., Ryan, S., Maloney, E., Sullivan, A. M., and Nolan, Y. M. (2010). Tumour necrosis factor- $\alpha$  impairs neuronal differentiation but not proliferation of hippocampal neural precursor cells: Role of Hes1. *Mol. Cell. Neurosci.* 43, 127–135. doi:10.1016/j.mcn.2009.10.003.
- Keung, A. J., De Juan-Pardo, E. M., Schaffer, D. V., and Kumar, S. (2011). Rho GTPases mediate the mechanosensitive lineage commitment of neural stem cells. *Stem Cells* 29, 1886–1897. doi:10.1002/stem.746.
- Kielian, T. (2006). Toll-like receptors in central nervous system glial inflammation and homeostasis. *J. Neurosci. Res.* 83, 711–730. doi:10.1002/jnr.20767.
- Kim, E. J., Ables, J. L., Dickel, L. K., Eisch, A. J., and Johnson, J. E. (2011). Ascl1 (Mash1) defines cells with long-term neurogenic potential in subgranular and subventricular zones in adult mouse brain. *PLoS One* 6. doi:10.1371/journal.pone.0018472.
- Kipp, M., Nyamoya, S., Hochstrasser, T., and Amor, S. (2017). Multiple sclerosis animal models: a clinical and histopathological perspective. *Brain Pathol.* 27, 123–137. doi:10.1111/bpa.12454.
- Kiyota, T., Okuyama, S., Swan, R. J., Jacobsen, M. T., Gendelman, H. E., and Ikezu, T. (2010). CNS expression of anti-inflammatory cytokine interleukin-4 attenuates Alzheimer's disease-like pathogenesis in APP+PS1 bigenic mice. *FASEB J.* 24, 3093–3102. doi:10.1096/fj.10-155317.
- Knobloch, M., Pilz, G. A., Ghesquière, B., Kovacs, W. J., Wegleiter, T., Moore, D. L., et al. (2017). A Fatty Acid Oxidation-Dependent Metabolic Shift Regulates Adult Neural Stem Cell Activity. *Cell Rep.* 20, 2144–2155. doi:10.1016/j.celrep.2017.08.029.
- Kohman, R. A., and Rhodes, J. S. (2013). Neurogenesis, inflammation and behavior. *Brain. Behav. Immun.* 27,

22–32. doi:10.1016/j.bbi.2012.09.003.

- Konat, G. W., Kielian, T., and Marriott, I. (2006). The role of Toll-like receptors in CNS response to microbial challenge. *J. Neurochem.* 99, 1–12. doi:10.1111/j.1471-4159.2006.04076.x.
- Konsman, J. P., Vignes, S., Mackerlova, L., Bristow, A., and Blomqvist, A. (2004). Rat Brain Vascular Distribution of Interleukin-1 Type-1 Receptor Immunoreactivity: Relationship to Patterns of Inducible Cyclooxygenase Expression by Peripheral Inflammatory Stimuli. *J. Comp. Neurol.* 472, 113–129. doi:10.1002/cne.20052.
- Kotterman, M. A., Vazin, T., and Schaffer, D. V. (2015). Enhanced selective gene delivery to neural stem cells in vivo by an adeno-associated viral variant. *Dev.* 142, 1885–1892. doi:10.1242/dev.115253.
- Kreisel, T., Wolf, B., Keshet, E., and Licht, T. (2019). Unique role for dentate gyrus microglia in neuroblast survival and in VEGF-induced activation. *Glia* 67, 594–618. doi:10.1002/glia.23505.
- Kronenberg, G., Bick-Sander, A., Bunk, E., Wolf, C., Ehninger, D., and Kempermann, G. (2006). Physical exercise prevents age-related decline in precursor cell activity in the mouse dentate gyrus. *Neurobiol. Aging* 27, 1505–1513. doi:10.1016/j.neurobiolaging.2005.09.016.
- Kronenberg, G., Reuter, K., Steiner, B., Brandt, M. D., Jessberger, S., Yamaguchi, M., et al. (2003). Subpopulations of Proliferating Cells of the Adult Hippocampus Respond Differently to Physiologic Neurogenic Stimuli. *J. Comp. Neurol.* 467, 455–463. doi:10.1002/cne.10945.
- Krzisch, M., Temprana, S. G., Mongiat, L. A., Armida, J., Schmutz, V., Virtanen, M. A., et al. (2015). Pre-existing astrocytes form functional perisynaptic processes on neurons generated in the adult hippocampus. *Brain Struct. Funct.* 220, 2027–2042. doi:10.1007/s00429-014-0768-y.
- Kuhn, H. G., Biebl, M., Wilhelm, D., Li, M., Friedlander, R. M., and Winkler, J. (2005). Increased generation of granule cells in adult Bcl-2-overexpressing mice: A role for cell death during continued hippocampal neurogenesis. *Eur. J. Neurosci.* 22, 1907–1915. doi:10.1111/j.1460-9568.2005.04377.x.
- Kuhn, H. G., Dickinson-Anson, H., and Gage, F. H. (1996). Neurogenesis in the dentate gyrus of the adult rat: Age-related decrease of neuronal progenitor proliferation. *J. Neurosci.* 16, 2027–2033. doi:10.1523/jneurosci.16-06-02027.1996.
- Kuhn, H. G., Eisch, A. J., Spalding, K., and Peterson, D. A. (2016). Detection and phenotypic characterization of adult neurogenesis. *Cold Spring Harb. Perspect. Biol.* 8. doi:10.1101/cshperspect.a025981.
- Kuhn, H. G., Toda, T., and Gage, F. H. (2018). Adult Hippocampal Neurogenesis : A Coming-of-Age Story. 38, 10401–10410.
- Kuwabara, T., Hsieh, J., Muotri, A., Yeo, G., Warashina, M., Lie, D. C., et al. (2009). Wnt-mediated activation of NeuroD1 and retro-elements during adult neurogenesis. *Nat. Neurosci.* 12, 1097–1105. doi:10.1038/nn.2360.
- Kuzumaki, N., Ikegami, D., Tamura, R., Sasaki, T., Niikura, K., Narita, M., et al. (2010). Hippocampal epigenetic modification at the doublecortin gene is involved in the impairment of neurogenesis with aging. *Synapse* 64, 611–616. doi:10.1002/syn.20768.

- LaDage, L. D., Roth, T. C., and Pravosudov, V. V. (2011). Hippocampal neurogenesis is associated with migratory behaviour in adult but not juvenile sparrows (*Zonotrichia leucophrys* ssp.). in *Proceedings of the Royal Society B: Biological Sciences* (Royal Society), 138–143. doi:10.1098/rspb.2010.0861.
- Ladias, J. A. A., and Karathanasis, S. K. (1991). Regulation of the apolipoprotein AI gene by ARP-1, a novel member of the steroid receptor superfamily. *Science* (80-. ). 251, 561–566. Available at: <https://go.gale.com/ps/i.do?p=AGONE&sw=w&issn=00368075&v=2.1&it=r&id=GALE%7CA10397855&sid=googleScholar&linkaccess=fulltext> [Accessed June 5, 2021].
- Lagace, D. C., Benavides, D. R., Kansy, J. W., Mapelli, M., Greengard, P., Bibb, J. A., et al. (2008). Cdk5 is essential for adult hippocampal neurogenesis. *Proc. Natl. Acad. Sci. U. S. A.* 105, 18567–18571. doi:10.1073/pnas.0810137105.
- Lagace, D. C., Whitman, M. C., Noonan, M. A., Ables, J. L., DeCarolis, N. A., Arguello, A. A., et al. (2007). Dynamic contribution of nestin-expressing stem cells to adult neurogenesis. *J. Neurosci.* 27, 12623–12629. doi:10.1523/JNEUROSCI.3812-07.2007.
- Lai, K., Kaspar, B. K., Gage, F. H., and Schaffer, D. V. (2003). Sonic hedgehog regulates adult neural progenitor proliferation in vitro and in vivo. *Nat. Neurosci.* 6, 21–27. doi:10.1038/nn983.
- Lana, D., Ugolini, F., Nosi, D., Wenk, G. L., and Giovannini, M. G. (2017). Alterations in the interplay between neurons, astrocytes and microglia in the rat dentate gyrus in experimental models of neurodegeneration. *Front. Aging Neurosci.* 9, 1–17. doi:10.3389/fnagi.2017.00296.
- Lana, D., Ugolini, F., Nosi, D., Wenk, G. L., and Giovannini, M. G. (2021). The Emerging Role of the Interplay Among Astrocytes, Microglia, and Neurons in the Hippocampus in Health and Disease. *Front. Aging Neurosci.* 13. doi:10.3389/fnagi.2021.651973.
- Larson, T. A. (2018). Sex steroids, adult neurogenesis, and inflammation in CNS homeostasis, degeneration, and repair. *Front. Endocrinol. (Lausanne)*. 9, 1. doi:10.3389/fendo.2018.00205.
- Lavado, A., Lagutin, O. V., Chow, L. M. L., Baker, S. J., and Oliver, G. (2010). Prox1 Is required for granule cell maturation and intermediate progenitor maintenance during brain neurogenesis. *PLoS Biol.* 8, 43–44. doi:10.1371/journal.pbio.1000460.
- Lavado, A., and Oliver, G. (2014). Jagged1 is necessary for postnatal and adult neurogenesis in the dentate gyrus. *Dev. Biol.* 388, 11–21. doi:10.1016/j.ydbio.2014.02.004.
- Lee, C.-M. M., Zhou, L., Liu, J., Shi, J., Geng, Y., Wang, J. J., et al. (2020). Single-cell RNA-seq analysis revealed long-lasting adverse effects of tamoxifen on neurogenesis in prenatal and adult brains. *Proc. Natl. Acad. Sci. U. S. A.* 117, 19578–19589. doi:10.1073/pnas.1918883117.
- Lee, J., Duan, W., Long, J. M., Ingram, D. K., and Mattson, M. P. (2000). Dietary restriction increases the number of newly generated neural cells, and BDNF expression, in the dentate gyrus of rats. *J. Mol. Neurosci.* 15, 99–108. doi:10.1385/JMN:15:2:99.
- Lee, M., Schwab, C., and McGeer, P. L. (2011). Astrocytes are GABAergic cells that modulate microglial activity. *Glia* 59, 152–165. doi:10.1002/glia.21087.
- Lee, S. J., and McEwen, B. S. (2001). Neurotrophic and neuroprotective actions of estrogens and their therapeutic

- implications. *Annu. Rev. Pharmacol. Toxicol.* 41, 569–591. doi:10.1146/annurev.pharmtox.41.1.569.
- Lehnardt, S. (2010). Innate immunity and neuroinflammation in the CNS: The role of microglia in toll-like receptor-mediated neuronal injury. *Glia* 58, 253–263. doi:10.1002/glia.20928.
- Leiter, O., Kempermann, G., and Walker, T. L. (2016). A Common Language: How neuroimmunological cross talk regulates adult hippocampal neurogenesis. *Stem Cells Int.* 2016. doi:10.1155/2016/1681590.
- Leuner, B., Glasper, E. R., and Gould, E. (2009). Thymidine analog methods for studies of adult neurogenesis are not equally sensitive. *J. Comp. Neurol.* 517, 123–133. doi:10.1002/cne.22107.
- Lev-Vachnisch, Y., Cadury, S., Rotter-Maskowitz, A., Feldman, N., Roichman, A., Illouz, T., et al. (2019). L-lactate promotes adult hippocampal neurogenesis. *Front. Neurosci.* 13, 1–13. doi:10.3389/fnins.2019.00403.
- Li, G., Fang, L., Fernández, G., and Pleasure, S. J. (2013). The ventral hippocampus is the embryonic origin for adult neural stem cells in the dentate gyrus. *Neuron* 78, 658–672. doi:10.1016/j.neuron.2013.03.019.
- Li, Q., Cheng, Z., Zhou, L., Darmanis, S., Neff, N. F., Okamoto, J., et al. (2019a). Developmental Heterogeneity of Microglia and Brain Myeloid Cells Revealed by Deep Single-Cell RNA Sequencing. *Neuron* 101, 207–223.e10. doi:10.1016/j.neuron.2018.12.006.
- Li, X., Du, Z. J., Chen, M. Q., Chen, J. J., Liang, Z. M., Ding, X. T., et al. (2019b). The effects of tamoxifen on mouse behavior. *Genes, Brain Behav.*, 1–10. doi:10.1111/gbb.12620.
- Liang, J., Han, F., and Chen, Y. (2013). Transcriptional regulation of VEGF expression by estrogen-related receptor  $\gamma$ . *Acta Pharm. Sin. B* 3, 373–380. doi:10.1016/j.apsb.2013.09.001.
- Liaury, K., Miyaoka, T., Tsumori, T., Funuya, M., Wake, R., Ieda, M., et al. (2012). Morphological features of microglial cells in the hippocampal dentate gyrus of Gunn rat: A possible schizophrenia animal model. *J. Neuroinflammation* 9, 1–11. doi:10.1186/1742-2094-9-56.
- Licht, T., and Keshet, E. (2015). The vascular niche in adult neurogenesis. *Mech. Dev.* 138, 56–62. doi:10.1016/j.mod.2015.06.001.
- Liddel, S. A., Guttenplan, K. A., Clarke, L. E., Bennett, F. C., Bohlen, C. J., Schirmer, L., et al. (2017). Neurotoxic reactive astrocytes are induced by activated microglia. *Nature* 541, 481–487. doi:10.1038/nature21029.
- Lie, D. C., Colamarino, S. A., Song, H. J., Désiré, L., Mira, H., Consiglio, A., et al. (2005). Wnt signalling regulates adult hippocampal neurogenesis. *Nature* 437, 1370–1375. doi:10.1038/nature04108.
- Lien, E. A., Wester, K., Lonning, P. E., Solheim, E., and Ueland, P. M. (1991). Distribution of tamoxifen and metabolites into brain tissue and brain metastases in breast cancer patients. *Br. J. Cancer* 63, 641–645. doi:10.1038/bjc.1991.147.
- Lim, D. A., and Alvarez-Buylla, A. (2016). The adult ventricular–subventricular zone (V-SVZ) and olfactory bulb (OB) neurogenesis. *Cold Spring Harb. Perspect. Biol.* 8, 1–33. doi:10.1101/cshperspect.a018820.
- Liu, L. R., Liu, J. C., Bao, J. S., Bai, Q. Q., and Wang, G. Q. (2020). Interaction of Microglia and Astrocytes in

- the Neurovascular Unit. *Front. Immunol.* 11, 1–11. doi:10.3389/fimmu.2020.01024.
- Llorens-Bobadilla, E., Zhao, S., Baser, A., Saiz-Castro, G., Zwadlo, K., and Martin-Villaiba, A. (2015). Single-Cell Transcriptomics Reveals a Population of Dormant Neural Stem Cells that Become Activated upon Brain Injury. *Cell Stem Cell* 17, 329–340. doi:10.1016/j.stem.2015.07.002.
- Llorens-Martín, M., and Trejo, J. L. (2011). Multiple birthdating analyses in adult neurogenesis: A line-up of the usual suspects. *Front. Neurosci.* 5, 1–8. doi:10.3389/fnins.2011.00076.
- Lopes, P. C. (2016). LPS and neuroinflammation: a matter of timing. *Inflammopharmacology* 24, 291–293. doi:10.1007/s10787-016-0283-2.
- Lucassen, P. J., Oomen, C. A., Naninck, E. F. G., Fitzsimons, C. P., Van Dam, A. M., Czeh, B., et al. (2015). Regulation of adult neurogenesis and plasticity by (Early) stress, glucocorticoids, and inflammation. *Cold Spring Harb. Perspect. Biol.* 7, a021303. doi:10.1101/cshperspect.a021303.
- Lugert, S., Basak, O., Knuckles, P., Haussler, U., Fabel, K., Götz, M., et al. (2010). Quiescent and active hippocampal neural stem cells with distinct morphologies respond selectively to physiological and pathological stimuli and aging. *Cell Stem Cell* 6, 445–456. doi:10.1016/j.stem.2010.03.017.
- Lugert, S., Vogt, M., Tchorz, J. S., Müller, M., Giachino, C., and Taylor, V. (2012). Homeostatic neurogenesis in the adult hippocampus does not involve amplification of Ascl1 high intermediate progenitors. *Nat. Commun.* 3. doi:10.1038/ncomms1670.
- Madore, C., Joffre, C., Delpech, J. C., De Smedt-Peyrusse, V., Aubert, A., Coste, L., et al. (2013). Early morphofunctional plasticity of microglia in response to acute lipopolysaccharide. *Brain. Behav. Immun.* 34, 151–158. doi:10.1016/j.bbi.2013.08.008.
- Mahmoud, R., Wainwright, S. R., and Galea, L. A. M. (2016). Sex hormones and adult hippocampal neurogenesis: Regulation, implications, and potential mechanisms. *Front. Neuroendocrinol.* 41, 129–152. doi:10.1016/j.yfrne.2016.03.002.
- Mallick, A., Jakubowski, M., Elmquist, J. K., Saper, C. B., and Burstein, R. (2001). A neurohistochemical blueprint for pain-induced loss of appetite. *Proc. Natl. Acad. Sci. U. S. A.* 98, 9930–9935. doi:10.1073/pnas.171616898.
- Martinez, F. O., Helming, L., and Gordon, S. (2009). Alternative activation of macrophages: An immunologic functional perspective. *Annu. Rev. Immunol.* 27, 451–483. doi:10.1146/annurev.immunol.021908.132532.
- Martinkovich, S., Shah, D., Planey, S. L., and Amott, J. A. (2014). Selective estrogen receptor modulators: Tissue specificity and clinical utility. *Clin. Interv. Aging* 9, 1437–1452. doi:10.2147/CIA.S66690.
- Masuda, T., Sankowski, R., Staszewski, O., Böttcher, C., Amann, L., Sagar, et al. (2019). Spatial and temporal heterogeneity of mouse and human microglia at single-cell resolution. *Nature* 566, 388–392. doi:10.1038/s41586-019-0924-x.
- Mathieu, P., Battista, D., Depino, A., Roca, V., Graciarena, M., and Pitossi, F. (2010). The more you have, the less you get: The functional role of inflammation on neuronal differentiation of endogenous and transplanted neural stem cells in the adult brain. *J. Neurochem.* 112, 1368–1385. doi:10.1111/j.1471-4159.2009.06548.x.

- Mazzucco, C. A., Lieblich, S. E., Bingham, B. I., Williamson, M. A., Viau, V., and Galea, L. A. M. (2006). Both estrogen receptor  $\alpha$  and estrogen receptor  $\beta$  agonists enhance cell proliferation in the dentate gyrus of adult female rats. *Neuroscience* 141, 1793–1800. doi:10.1016/j.neuroscience.2006.05.032.
- McCusker, R. H., and Kelley, K. W. (2013). Immune-neural connections: How the immune system's response to infectious agents influences behavior. *J. Exp. Biol.* 216, 84–98. doi:10.1242/jeb.073411.
- McTighe, S. M., Mar, A. C., Romberg, C., Bussey, T. J., and Saksida, L. M. (2009). A new touchscreen test of pattern separation: Effect of hippocampal lesions. *Neuroreport* 20, 881–885. doi:10.1097/WNR.0b013e32832c5eb2.
- Medawar, P. B. (1948). Immunity to homologous grafted skin; the fate of skin homografts. *Br. J. Exp. Pathol.* 29, 58–69.
- Melo-Salas, M. S., Pérez-Domínguez, M., and Zepeda, A. (2018). Systemic Inflammation Impairs Proliferation of Hippocampal Type 2 Intermediate Precursor Cells. *Cell. Mol. Neurobiol.* 38, 1517–1528. doi:10.1007/s10571-018-0624-3.
- Meneses, G., Rosetti, M., Espinosa, A., Florentino, A., Bautista, M., Díaz, G., et al. (2018). Recovery from an acute systemic and central LPS-inflammation challenge is affected by mouse sex and genetic background. *PLoS One* 13, 1–12. doi:10.1371/journal.pone.0201375.
- Min, K. J., Yang, M. S., Kim, S. U., Jou, I., and Joe, E. H. (2006). Astrocytes induce hemoxygenase-1 expression in microglia: A feasible mechanism for preventing excessive brain inflammation. *J. Neurosci.* 26, 1880–1887. doi:10.1523/JNEUROSCI.3696-05.2006.
- Ming, G. li, and Song, H. (2011). Adult Neurogenesis in the Mammalian Brain: Significant Answers and Significant Questions. *Neuron* 70, 687–702. doi:10.1016/j.neuron.2011.05.001.
- Mira, H., Andreu, Z., Suh, H., Chichung Lie, D., Jessberger, S., Consiglio, A., et al. (2010). Signaling through BMPR-IA regulates quiescence and long-term activity of neural stem cells in the adult hippocampus. *Cell Stem Cell* 7, 78–89. doi:10.1016/j.stem.2010.04.016.
- Mirescu, C., and Gould, E. (2006). Stress and adult neurogenesis. *Hippocampus* 16, 233–238. doi:10.1002/hipo.20155.
- Miyajima, N., Kandowaki, Y., Fukushige, S. I., Shimizu, S. I., Semba, K., Yamanashi, Y., et al. (1988). Identification of two novel members of erbA superfamily by molecular cloning: The gene products of the two are highly related to each other. *Nucleic Acids Res.* 16, 11057–11074. doi:10.1093/nar/16.23.11057.
- Monje, M. L., Toda, H., and Palmer, T. D. (2003). Inflammatory blockade restores adult hippocampal neurogenesis. *Science* 302, 1760–5. doi:10.1126/science.1088417.
- Moreillon, P., and Majcherczyk, P. A. (2003). Proinflammatory activity of cell-wall constituents from Gram-positive bacteria. *Scand. J. Infect. Dis.* 35, 632–641. doi:10.1080/00365540310016259.
- Moreira, P. I., Custódio, J. B., Oliveira, C. R., and Santos, M. S. (2005). Brain mitochondrial injury induced by oxidative stress-related events is prevented by tamoxifen. *Neuropharmacology* 48, 435–447. doi:10.1016/j.neuropharm.2004.10.012.

- Morganti, J. M., Riparip, L. K., and Rosi, S. (2016). Call off the dog(ma): M1/M2 polarization is concurrent following traumatic brain injury. *PLoS One* 11, 1–13. doi:10.1371/journal.pone.0148001.
- Mori, T., Tanaka, K., Buffo, A., Wurst, W., Kühn, R., and Gotz, M. (2006). Inducible gene deletion in astroglia and radial glia - A valuable tool for functional and lineage analysis. *Glia* 54, 21–34. doi:10.1002/glia.20350.
- Moser, E. I., Moser, M. B., and McNaughton, B. L. (2017). Spatial representation in the hippocampal formation: A history. *Nat. Neurosci.* 20, 1448–1464. doi:10.1038/nn.4653.
- Mosher, K. I., and Schaffer, D. V. (2018). Influence of hippocampal niche signals on neural stem cell functions during aging. *Cell Tissue Res.* 371, 115–124. doi:10.1007/s00441-017-2709-6.
- Moss, J., Gebara, E., Bushong, E. A., Sánchez-Pascual, I., O’Laoi, R., El M’Gharia, I., et al. (2016). Fine processes of Nestin-GFP-positive radial glia-like stem cells in the adult dentate gyrus ensheath local synapses and vasculature. *Proc. Natl. Acad. Sci. U. S. A.* 113, E2536–E2545. doi:10.1073/pnas.1514652113.
- Moura, D. M. S., Brandão, J. A., Lentini, C., Heinrich, C., Queiroz, C. M., and Costa, M. R. (2020). Evidence of Progenitor Cell Lineage Rerouting in the Adult Mouse Hippocampus After Status Epilepticus. *Front. Neurosci.* 14, 960. doi:10.3389/fnins.2020.571315.
- Mueller, M. D., Vigne, J. L., Minchenko, A., Lebovic, D. I., Leitman, D. C., and Taylor, R. N. (2000). Regulation of vascular endothelial growth factor (VEGF) gene transcription by estrogen receptors  $\alpha$  and  $\beta$ . *Proc. Natl. Acad. Sci. U. S. A.* 97, 10972–10977. doi:10.1073/pnas.200377097.
- Muramatsu, R., Takahashi, C., Miyake, S., Fujimura, H., Mochizuki, H., and Yamashita, T. (2012). Angiogenesis induced by CNS inflammation promotes neuronal remodeling through vessel-derived prostacyclin. *Nat. Med.* doi:10.1038/nm.2943.
- Naka-Kaneda, H., Nakamura, S., Igarashi, M., Aoi, H., Kanki, H., Tsuyama, J., et al. (2014). The miR-17/106-p38 axis is a key regulator of the neurogenic-to-gliogenic transition in developing neural stem/progenitor cells. *Proc. Natl. Acad. Sci. U. S. A.* 111, 1604–9. doi:10.1073/pnas.1315567111.
- Naka, H., Nakamura, S., Shimazaki, T., and Okano, H. (2008). Requirement for COUP-TFI and II in the temporal specification of neural stem cells in CNS development. *Nat. Neurosci.* 11, 1014–1023. doi:10.1038/nn.2168.
- Nakashiba, T., Cushman, J. D., Pelkey, K. A., Renaudineau, S., Buhl, D. L., McHugh, T. J., et al. (2012). Young dentate granule cells mediate pattern separation, whereas old granule cells facilitate pattern completion. *Cell* 149, 188–201. doi:10.1016/j.cell.2012.01.046.
- Nardini, C., Moreau, J. F., Gensous, N., Ravaioli, F., Garagnani, P., and Bacalini, M. G. (2018). The epigenetics of inflammaging: The contribution of age-related heterochromatin loss and locus-specific remodelling and the modulation by environmental stimuli. *Semin. Immunol.* 40, 49–60. doi:10.1016/j.smim.2018.10.009.
- Newton, K., and Dixit, V. M. (2012). Signaling in innate immunity and inflammation. *Cold Spring Harb. Perspect. Biol.* 4. doi:10.1101/cshperspect.a006049.
- Nicola, Z., Fabel, K., and Kempermann, G. (2015). Development of the adult neurogenic niche in the



- hippocampus of mice. *Front. Neuroanat.* 9, 1–13. doi:10.3389/fnana.2015.00053.
- Nimmerjahn, A., Kirchhoff, F., and Helmchen, F. (2005). Neuroscience: Resting microglial cells are highly dynamic surveillants of brain parenchyma in vivo. *Science* (80-. ). 308, 1314–1318. doi:10.1126/science.1110647.
- Niu, W., Zou, Y., Shen, C., and Zhang, C.-L. C.-L. (2011). Activation of Postnatal Neural Stem Cells Requires Nuclear Receptor TLX. *J. Neurosci.* 31, 13816–13828. doi:10.1523/JNEUROSCI.1038-11.2011.
- Nolan, Y., Maher, F. O., Martin, D. S., Clarke, R. M., Brady, M. T., Bolton, A. E., et al. (2005). Role of interleukin-4 in regulation of age-related inflammatory changes in the hippocampus. *J. Biol. Chem.* 280, 9354–9362. doi:10.1074/jbc.M412170200.
- Norden, D. M., Trojanowski, P. J., Villanueva, E., Navarro, E., and Godbout, J. P. (2016). Sequential activation of microglia and astrocyte cytokine expression precedes increased iba-1 or GFAP immunoreactivity following systemic immune challenge. *Glia* 64, 300–316. doi:10.1002/glia.22930.
- Nunan, R., Sivasathiseelan, H., Khan, D., Zaben, M., and Gray, W. (2014). Microglial VPAC1R mediates a novel mechanism of neuroimmune-modulation of hippocampal precursor cells via IL-4 release. *Glia* 62, 1313–1327. doi:10.1002/glia.22682.
- Okano, H., and Temple, S. (2009). Cell types to order: temporal specification of CNS stem cells. *Curr. Opin. Neurobiol.* 19, 112–119. doi:10.1016/j.conb.2009.04.003.
- Orban, P. C., Chui, D., and Marth, J. D. (1992). Tissue- and site-specific DNA recombination in transgenic mice. *Proc. Natl. Acad. Sci. U. S. A.* 89, 6861–6865. doi:10.1073/pnas.89.15.6861.
- Orihuela, R., McPherson, C. A., and Harry, G. J. (2016). Microglial M1/M2 polarization and metabolic states. *Br. J. Pharmacol.* 173, 649–665. doi:10.1111/bph.13139.
- Overall, R. W., Walker, T. L., Fischer, T. J., Brandt, M. D., and Kempermann, G. (2016). Different mechanisms must be considered to explain the increase in hippocampal neural precursor cell proliferation by physical activity. *Front. Neurosci.* 10, 362. doi:10.3389/fnins.2016.00362.
- Palmer, T. D., Willhoite, A. R., and Gage, F. H. (2000). Vascular niche for adult hippocampal neurogenesis. *J. Comp. Neurol.* 425, 479–494. doi:10.1002/1096-9861(20001002)425:4<479::AID-CNE2>3.0.CO;2-3.
- Paolicelli, R. C., Bolasco, G., Pagani, F., Maggi, L., Scianni, M., Panzanelli, P., et al. (2011). Synaptic pruning by microglia is necessary for normal brain development. *Science* (80-. ). 333, 1456–1458. doi:10.1126/science.1202529.
- Pareto, D., Alvarado, M., Hanrahan, S. M., and Biegon, A. (2004). In vivo occupancy of female rat brain estrogen receptors by 17 $\beta$ -estradiol and tamoxifen. *Neuroimage* 23, 1161–1167. doi:10.1016/j.neuroimage.2004.07.036.
- Parisot, J., Flore, G., Bertacchi, M., and Studer, M. (2017). COUP-TFI mitotically regulates production and migration of dentate granule cells and modulates hippocampal Cxcr4 expression. *Development* 144, 2045–2058. doi:10.1242/dev.139949.
- Pastorcic, M., Wang, H., Elbrecht, A., Tsai, S. Y., Tsai, M. J., and O'Malley, B. W. (1986). Control of

- transcription initiation in vitro requires binding of a transcription factor to the distal promoter of the ovalbumin gene. *Mol. Cell. Biol.* 6, 2784–2791. doi:10.1128/mcb.6.8.2784-2791.1986.
- Pereira, A. C., Huddleston, D. E., Brickman, A. M., Sosunov, A. A., Hen, R., McKhann, G. M., et al. (2007). An in vivo correlate of exercise-induced neurogenesis in the adult dentate gyrus. *Proc. Natl. Acad. Sci. U. S. A.* 104, 5638–5643. doi:10.1073/pnas.0611721104.
- Pereira, F. a, Tsai, M. J., and Tsai, S. Y. (2000). COUP-TF orphan nuclear receptors in development and differentiation. *Cell. Mol. Life Sci.* 57, 1388–1398.
- Perez-Dominguez, M., Ávila-Muñoz, E., Domínguez-Rivas, E., and Zepeda, A. (2019). The detrimental effects of lipopolysaccharide-induced neuroinflammation on adult hippocampal neurogenesis depend on the duration of the pro-inflammatory response. *Neural Regen. Res.* 14, 817–825. doi:10.4103/1673-5374.249229.
- Pérez-Domínguez, M., Tovar-Y-Romo, L. B., and Zepeda, A. (2017). Neuroinflammation and physical exercise as modulators of adult hippocampal neural precursor cell behavior. *Rev. Neurosci.* 29, 1–20. doi:10.1515/revneuro-2017-0024.
- Perez-Martin, M., Azcoitia, I., Trejo, J. L., Sierra, A., and Garcia-Segura, L. M. (2003). An antagonist of estrogen receptors blocks the induction of adult neurogenesis by insulin-like growth factor-I in the dentate gyrus of adult female rat. *Eur. J. Neurosci.* 18, 923–930. doi:10.1046/j.1460-9568.2003.02830.x.
- Perry, V. H. (1998). A revised view of the central nervous system microenvironment and major histocompatibility complex class II antigen presentation. *J. Neuroimmunol.* 90, 113–121. doi:10.1016/S0165-5728(98)00145-3.
- Perry, V. H., Cunningham, C., and Holmes, C. (2007). Systemic infections and inflammation affect chronic neurodegeneration. *Nat. Rev. Immunol.* 7, 161–167. doi:10.1038/nri2015.
- Perry, V. H., and Holmes, C. (2014). Microglial priming in neurodegenerative disease. *Nat. Rev. / Neurol.* 10, 217–224. doi:10.1038/nrneuro1.2014.38.
- Perry, V. H., Nicoll, J. A. R., and Holmes, C. (2010). Microglia in neurodegenerative disease. *Nat. Rev. Neurol.* 6, 193–201. doi:10.1038/nrneuro1.2010.17.
- Pickering, M., and O'Connor, J. J. (2007). Pro-inflammatory cytokines and their effects in the dentate gyrus. *Prog. Brain Res.* 163, 339–354. doi:10.1016/S0079-6123(07)63020-9.
- Pilaz, L. J., and Silver, D. L. (2015). Post-transcriptional regulation in corticogenesis: How RNA-binding proteins help build the brain. *Wiley Interdiscip. Rev. RNA* 6, 501–515. doi:10.1002/wrna.1289.
- Pilz, G. A., Bottes, S., Betizeau, M., Jörg, D. J., Carta, S., Simons, B. D., et al. (2018). Live imaging of neurogenesis in the adult mouse hippocampus. *Science (80-. ).* 359, 658–662. doi:10.1126/science.aao5056.
- Pons-Espinal, M., Gasperini, C., Marzi, M. J., Braccia, C., Armirotti, A., Pöttsch, A., et al. (2019). MiR-135a-5p Is Critical for Exercise-Induced Adult Neurogenesis. *Stem Cell Reports* 12, 1298–1312. doi:10.1016/j.stemcr.2019.04.020.
- Porcheri, C., Suter, U., and Jessberger, S. (2014). Dissecting integrin-dependent regulation of neural stem cell

- proliferation in the adult brain. *J. Neurosci.* 34, 5222–5232. doi:10.1523/JNEUROSCI.4928-13.2014.
- Pöttsch, A., Zocher, S., Bemas, S. N., Leiter, O., Rünker, A. E., and Kempermann, G. (2021). L-lactate exerts a pro-proliferative effect on adult hippocampal precursor cells in vitro. *iScience* 24. doi:10.1016/j.isci.2021.102126.
- Priller, J., and Prinz, M. (2019). Targeting microglia in brain disorders. *Science (80-. )*. 364, 32–33. doi:10.1126/science.aau9100.
- Prinz, M., Jung, S., and Priller, J. (2019). Microglia Biology: One Century of Evolving Concepts. *Cell* 179, 292–311. doi:10.1016/j.cell.2019.08.053.
- Procaccini, C., De Rosa, V., Pucino, V., Formisano, L., and Matarese, G. (2015). Animal models of Multiple Sclerosis. *Eur. J. Pharmacol.* 759, 182–191. doi:10.1016/j.ejphar.2015.03.042.
- Qin, L., Wu, X., Block, M. L., Liu, Y., Breese, G. R., Hong, J. S., et al. (2007). Systemic LPS causes chronic neuroinflammation and progressive neurodegeneration. *Glia* 55, 453–462. doi:10.1002/glia.20467.
- Qiu, Y., Pereira, F. A., DeMayo, F. J., Lydon, J. P., Tsai, S. Y., and Tsai, M. J. (1997). Null mutation of mCOUP-TFI results in defects in morphogenesis of the glossopharyngeal ganglion, axonal projection, and arborization. *Genes Dev.* 11, 1925–1937. doi:10.1101/gad.11.15.1925.
- Quan, N. (2008). Immune-to-brain signaling: How important are the blood-brain barrier-independent pathways? *Mol. Neurobiol.* 37, 142–152. doi:10.1007/s12035-008-8026-z.
- Raj, D. D. D. A., Jaarsma, D., Holtman, I. R., Olah, M., Ferreira, F. M., Schaafsma, W., et al. (2014). Priming of microglia in a DNA-repair deficient model of accelerated aging. *Neurobiol. Aging* 35, 2147–2160. Available at: <https://www.sciencedirect.com/science/article/pii/S0197458014002826> [Accessed October 1, 2018].
- Ransohoff, R. M. (2016). A polarizing question: Do M1 and M2 microglia exist. *Nat. Neurosci.* 19, 987–991. doi:10.1038/nn.4338.
- Ransohoff, R. M., and Brown, M. A. (2012). Innate immunity in the central nervous system. *J. Clin. Invest.* 122, 1164–1171. doi:10.1172/JCI58644.
- Renault, V. M., Rafalski, V. A., Morgan, A. A., Salih, D. A. M., Brett, J. O., Webb, A. E., et al. (2009). FoxO3 Regulates Neural Stem Cell Homeostasis. *Cell Stem Cell* 5, 527–539. doi:10.1016/j.stem.2009.09.014.
- Reynolds, B. A., and Weiss, S. (1992). Generation of neurons and astrocytes from isolated cells of the adult mammalian central nervous system. *Science (80-. )*. 255, 1707–1710. doi:10.1126/science.1553558.
- Riggs, B. L., and Hartmann, L. C. (2003). Selective Estrogen-Receptor Modulators — Mechanisms of Action. *N. Engl. J. Med.* 348, 618–630.
- Rivera-Escalera, F., Pinney, J. J., Owlett, L., Ahmed, H., Thakar, J., Olschowka, J. A., et al. (2019). IL-1 $\beta$ -driven amyloid plaque clearance is associated with an expansion of transcriptionally reprogrammed microglia. *J. Neuroinflammation* 16, 1–17. doi:10.1186/s12974-019-1645-7.
- Roach, J. C., Glusman, G., Rowen, L., Kaur, A., Purcell, M. K., Smith, K. D., et al. (2005). The evolution of

vertebrate Toll-like receptors. 102.

- Rodríguez-Iglesias, N., Sierra, A., and Valero, J. (2019). Rewiring of memory circuits: Connecting adult newborn neurons with the help of microglia. *Front. Cell Dev. Biol.* 7, 24. doi:10.3389/fcell.2019.00024.
- Rojczyk-Gołębiewska, E., Pałasz, A., and Wiaderkiewicz, R. (2014). Hypothalamic subependymal niche: A novel site of the adult neurogenesis. *Cell. Mol. Neurobiol.* 34, 631–642. doi:10.1007/s10571-014-0058-5.
- Rolando, C., Erni, A., Grison, A., Beattie, R., Engler, A., Gokhale, P. J., et al. (2016). Multipotency of Adult Hippocampal NSCs In Vivo Is Restricted by Drosha/NFIB. *Cell Stem Cell* 19, 653–662. doi:10.1016/j.stem.2016.07.003.
- Rolando, C., Parolisi, R., Boda, E., Schwab, M. E., Rossi, F., and Buffo, A. (2012). Distinct roles of Nogo-A and nogo receptor 1 in the homeostatic regulation of adult neural stem cell function and neuroblast migration. *J. Neurosci.* 32, 17788–17799. doi:10.1523/JNEUROSCI.3142-12.2012.
- Rolls, A., Shechter, R., London, A., Ziv, Y., Ronen, A., Levy, R., et al. (2007). Toll-like receptors modulate adult hippocampal neurogenesis. *Nat. Cell Biol.* 9, 1081–1088. doi:10.1038/ncb1629.
- Romeo, H. E., Tio, D. L., Rahman, S. U., Chiappelli, F., and Taylor, A. N. (2001). The glossopharyngeal nerve as a novel pathway in immune-to-brain communication: Relevance to neuroimmune surveillance of the oral cavity. *J. Neuroimmunol.* 115, 91–100. doi:10.1016/S0165-5728(01)00270-3.
- Rosenzweig, H. L., Minami, M., Lessov, N. S., Coste, S. C., Stevens, S. L., Henshall, D. C., et al. (2007). Endotoxin preconditioning protects against the cytotoxic effects of TNF $\alpha$  after stroke: A novel role for TNF $\alpha$  in LPS-ischemic tolerance. *J. Cereb. Blood Flow Metab.* 27, 1663–1674. doi:10.1038/sj.jcbfm.9600464.
- Rossi, C., Angelucci, A., Costantin, L., Braschi, C., Mazzantini, M., Babbini, F., et al. (2006). Brain-derived neurotrophic factor (BDNF) is required for the enhancement of hippocampal neurogenesis following environmental enrichment. *Eur. J. Neurosci.* 24, 1850–1856. doi:10.1111/j.1460-9568.2006.05059.x.
- Rothaug, M., Becker-Pauly, C., and Rose-John, S. (2016). The role of interleukin-6 signaling in nervous tissue. *Biochim. Biophys. Acta - Mol. Cell Res.* 1863, 1218–1227. doi:10.1016/j.bbamcr.2016.03.018.
- Rotheneichner, P., Romanelli, P., Bieler, L., Pagitsch, S., Zaunmair, P., Kreutzer, C., et al. (2017). Tamoxifen activation of cre-recombinase has no persisting effects on adult neurogenesis or learning and anxiety. *Front. Neurosci.* 11, 1–8. doi:10.3389/fnins.2017.00027.
- Rowland, D. C., Obenaus, H. A., Skytøen, E. R., Zhang, Q., Kentros, C. G., Moser, E. I., et al. (2018). Functional properties of stellate cells in medial entorhinal cortex layer ii. *Elife* 7, 1–17. doi:10.7554/eLife.36664.
- Russo, I., Barlati, S., and Bosetti, F. (2011). Effects of neuroinflammation on the regenerative capacity of brain stem cells. *J. Neurochem.* 116, 947–956. doi:10.1111/j.1471-4159.2010.07168.x.
- Sagami, I., Tsai, S. Y., Wang, H., Tsai, M. J., and O'Malley, B. W. (1986). Identification of two factors required for transcription of the ovalbumin gene. *Mol. Cell. Biol.* 6, 4259–4267. doi:10.1128/mcb.6.12.4259-4267.1986.

- Saha, K., Keung, A. J., Irwin, E. F., Li, Y., Little, L., Schaffer, D. V., et al. (2008). Substrate modulus directs neural stem cell behavior. *Biophys. J.* 95, 4426–4438. doi:10.1529/biophysj.108.132217.
- Sahay, A., Scobie, K. N., Hill, A. S., O’Carroll, C. M., Kheirbek, M. A., Burghardt, N. S., et al. (2011). Increasing adult hippocampal neurogenesis is sufficient to improve pattern separation. *Nature* 472, 466–470. doi:10.1038/nature09817.
- Sallustio, F., Curci, C., Stasi, A., De Palma, G., Divella, C., Gramignoli, R., et al. (2019). Role of toll-like receptors in actuating stem/progenitor cell repair mechanisms: Different functions in different cells. *Stem Cells Int.* 2019, 1–12. doi:10.1155/2019/6795845.
- Sánchez-Huerta, K., García-Martínez, Y., Vergara, P., Segovia, J., and Pacheco-Rosado, J. (2016). Thyroid hormones are essential to preserve non-proliferative cells of adult neurogenesis of the dentate gyrus. *Mol. Cell. Neurosci.* 76, 1–10. doi:10.1016/j.mcn.2016.08.001.
- Schaafsma, W., Zhang, X., van Zomeren, K. C., Jacobs, S., Georgieva, P. B., Wolf, S. A., et al. (2015). Long-lasting pro-inflammatory suppression of microglia by LPS-preconditioning is mediated by RelB-dependent epigenetic silencing. *Brain. Behav. Immun.* 48, 205–221. doi:10.1016/j.bbi.2015.03.013.
- Scheller, J., Chalaris, A., Schmidt-Arras, D., and Rose-John, S. (2011). The pro- and anti-inflammatory properties of the cytokine interleukin-6. *Biochim. Biophys. Acta - Mol. Cell Res.* 1813, 878–888. doi:10.1016/j.bbamcr.2011.01.034.
- Schneider, H., Pitossi, F., Balschun, D., Wagner, A., Del Rey, A., and Besedovsky, H. O. (1998). A neuromodulatory role of interleukin-1 $\beta$  in the hippocampus. *Proc. Natl. Acad. Sci. U. S. A.* 95, 7778–7783. doi:10.1073/pnas.95.13.7778.
- Schoenfeld, T. J., and Gould, E. (2012). Stress, stress hormones, and adult neurogenesis. *Exp. Neurol.* 233, 12–21. doi:10.1016/j.expneurol.2011.01.008.
- Schouten, M., Bielefeld, P., Garcia-Corzo, L., Passchier, E. M. J., Gradari, S., Jungenitz, T., et al. (2020). Circadian glucocorticoid oscillations preserve a population of adult hippocampal neural stem cells in the aging brain. *Mol. Psychiatry* 25, 1382–1405. doi:10.1038/s41380-019-0440-2.
- Seib, D. R. M., Corsini, N. S., Ellwanger, K., Plaas, C., Mateos, A., Pitzer, C., et al. (2013). Loss of dickkopf-1 restores neurogenesis in old age and counteracts cognitive decline. *Cell Stem Cell* 12, 204–214. doi:10.1016/j.stem.2012.11.010.
- Seib, D. R. M., and Martin-Villalba, A. (2015). Neurogenesis in the Normal Ageing Hippocampus: A Mini-Review. *Gerontology* 61, 327–335. doi:10.1159/000368575.
- Semerci, F., and Maletic-Savatic, M. (2016). Transgenic mouse models for studying adult neurogenesis. *Front. Biol. (Beijing)*. 11, 151–167. doi:10.1007/s11515-016-1405-3.
- Seri, B., García-Verdugo, J. M., Collado-Morente, L., McEwen, B. S., and Alvarez-Buylla, A. (2004). Cell types, lineage, and architecture of the germinal zone in the adult dentate gyrus. *J. Comp. Neurol.* 478, 359–378. doi:10.1002/cne.20288.
- Seri, B., Manuel García-Verdugo, J., McEwen, B. S., and Alvarez-Buylla, A. (2001). Astrocytes Give Rise to New Neurons in the Adult Mammalian Hippocampus.

- Shimozaki, K., Zhang, C. L., Suh, H., Denli, A. M., Evans, R. M., and Gage, F. H. (2012). SRY-box-containing gene 2 regulation of nuclear receptor tailless (Tlx) transcription in adult neural stem cells. *J. Biol. Chem.* 287, 5969–5978. doi:10.1074/jbc.M111.290403.
- Shrikant, P., Il Yup Chung, Ballestas, M. E., and Benveniste, E. N. (1994). Regulation of intercellular adhesion molecule-1 gene expression by tumor necrosis factor- $\alpha$ , interleukin-1 $\beta$ , and interferon- $\gamma$  in astrocytes. *J. Neuroimmunol.* 51, 209–220. doi:10.1016/0165-5728(94)90083-3.
- Sierra, A., Beccari, S., Diaz-Aparicio, I., Encinas, J. M., Comeau, S., and Tremblay, M. È. (2014). Surveillance, phagocytosis, and inflammation: How never-resting microglia influence adult hippocampal neurogenesis. *Neural Plast.* 2014. doi:10.1155/2014/610343.
- Sierra, A., de Castro, F., del Río-Hortega, J., Rafael Iglesias-Rozas, J., Garrosa, M., and Kettenmann, H. (2016). The “Big-Bang” for modern glial biology: Translation and comments on Pio del Río-Hortega 1919 series of papers on microglia. *Glia* 64, 1801–1840. doi:10.1002/glia.23046.
- Sierra, A., Encinas, J. M., Deudero, J. J. P., Chancey, J. H., Enikolopov, G., Overstreet-Wadiche, L. S., et al. (2010). Microglia shape adult hippocampal neurogenesis through apoptosis-coupled phagocytosis. *Cell Stem Cell* 7, 483–495. doi:10.1016/j.stem.2010.08.014.
- Sierra, A., Gottfried-Blackmore, A., Milner, T. A., McEwen, B. S., and Bulloch, K. (2008). Steroid hormone receptor expression and function in microglia. *Glia* 56, 659–674. doi:10.1002/glia.20644.
- Sierra, A., Martín-Suárez, S., Valcárcel-Martín, R., Pascual-Brazo, J., Aelvoet, S. A., Abiega, O., et al. (2015). Neuronal hyperactivity accelerates depletion of neural stem cells and impairs hippocampal neurogenesis. *Cell Stem Cell* 16, 488–503. doi:10.1016/j.stem.2015.04.003.
- Smith, L. K., White, C. W., and Villeda, S. A. (2018). The systemic environment: at the interface of aging and adult neurogenesis. *Cell Tissue Res.* 371, 105–113. doi:10.1007/s00441-017-2715-8.
- Snyder, J. S., Soumier, A., Brewer, M., Pickel, J., and Cameron, H. A. (2011). Adult hippocampal neurogenesis buffers stress responses and depressive behaviour. *Nature* 476, 458–462. doi:10.1038/nature10287.
- Song, H., Stevens, C. F., and Gage, F. H. (2002). Astroglia induce neurogenesis from adult neural stem cells. *Nature* 417, 39–44. doi:10.1038/417039a.
- Song, J., Zhong, C., Bonaguidi, M. A., Sun, G. J., Hsu, D., Gu, Y., et al. (2012). Neuronal circuitry mechanism regulating adult quiescent neural stem-cell fate decision. *Nature* 489, 150–154. doi:10.1038/nature11306.
- Sorrells, S. F., Paredes, M. F., Cebrian-Silla, A., Sandoval, K., Qi, D., Kelley, K. W., et al. (2018). Human hippocampal neurogenesis drops sharply in children to undetectable levels in adults. *Nature* 555, 377–381. doi:10.1038/nature25975.
- Specter, M. (2001). Rethinking the Brain | The New Yorker. *new yorker*. Available at: <https://www.newyorker.com/magazine/2001/07/23/rethinking-the-brain> [Accessed December 14, 2020].
- Spritzer, M. D., and Roy, E. A. (2020). Testosterone and adult neurogenesis. *Biomolecules* 10, 1–24. doi:10.3390/biom10020225.
- Srinivas, S., Watanabe, T., Lin, C. S., William, C. M., Tanabe, Y., Jessell, T. M., et al. (2001). Cre reporter

- strains produced by targeted insertion of EYFP and ECFP into the ROSA26 locus. *BMC Dev. Biol.* 1, 4. doi:10.1186/1471-213X-1-4.
- Stappert, L., Klaus, F., and Brüstle, O. (2018). MicroRNAs engage in complex circuits regulating adult neurogenesis. *Front. Neurosci.* 12, 1–17. doi:10.3389/fnins.2018.00707.
- Steiner, B., Klempin, F., Wang, L., Kott, M., Kettenmann, H., and Kempermann, G. (2006). Type-2 cells as link between glial and neuronal lineage in adult hippocampal neurogenesis. *Glia* 54, 805–814. doi:10.1002/glia.20407.
- Steiner, B., Kronenberg, G., Jessberger, S., Brandt, M. D., Reuter, K., and Kempermann, G. (2004). Differential regulation of gliogenesis in the context of adult hippocampal neurogenesis in mice. *Glia* 46, 41–52. doi:10.1002/glia.10337.
- Steiner, B., Zurborg, S., Hörster, H., Fabel, K., and Kempermann, G. (2008). Differential 24 h responsiveness of Prox1-expressing precursor cells in adult hippocampal neurogenesis to physical activity, environmental enrichment, and kainic acid-induced seizures. *Neuroscience* 154, 521–529. doi:10.1016/j.neuroscience.2008.04.023.
- Stence, N., Waite, M., and Dailey, M. E. (2001). Dynamics of microglial activation: A confocal time-lapse analysis in hippocampal slices. *Glia* 33, 256–266. doi:10.1002/1098-1136(200103)33:3<256::AID-GLIA1024>3.0.CO;2-J.
- Stenzel-Poore, M. P., Stevens, S. L., King, J. S., and Simon, R. P. (2007). Preconditioning reprograms the response to ischemic injury and primes the emergence of unique endogenous neuroprotective phenotypes: A speculative synthesis. *Stroke* 38, 680–685. doi:10.1161/01.STR.0000251444.56487.4c.
- Strange, B. A., Witter, M. P., Lein, E. S., and Moser, E. I. (2014). Functional organization of the hippocampal longitudinal axis. *Nat. Rev. Neurosci.* 15, 655–669. doi:10.1038/nrn3785.
- Stratoulas, V., Venero, J. L., Tremblay, M., and Joseph, B. (2019). Microglial subtypes: diversity within the microglial community. *EMBO J.* 38, 1–18. doi:10.15252/embj.2019101997.
- Suh, H., Consiglio, A., Ray, J., Sawai, T., D'Amour, K. A., and Gage, F. H. H. (2007). In Vivo Fate Analysis Reveals the Multipotent and Self-Renewal Capacities of Sox2+ Neural Stem Cells in the Adult Hippocampus. *Cell Stem Cell* 1, 515–528. doi:10.1016/j.stem.2007.09.002.
- Suh, H., Zhou, Q. G., Fernandez-Carasa, I., Clemenson, G. D., Pons-Espinal, M., Ro, E. J., et al. (2018). Long-term labeling of hippocampal neural stem cells by a lentiviral vector. *Front. Mol. Neurosci.* 11, 415. doi:10.3389/fnmol.2018.00415.
- Suh, J., Rivest, A. J., Nakashiba, T., Tominaga, T., and Tonegawa, S. (2011). Entorhinal cortex layer III input to the hippocampus is crucial for temporal association memory. *Science* (80-. ). 334, 1415–1420. doi:10.1126/science.1210125.
- Sultan, S., Li, L., Moss, J., Petrelli, F., Cassé, F., Gebara, E., et al. (2015). Synaptic Integration of Adult-Born Hippocampal Neurons Is Locally Controlled by Astrocytes. *Neuron* 88, 957–972. doi:10.1016/j.neuron.2015.10.037.
- Sun, D., Sun, X. D., Zhao, L., Lee, D. H., Hu, J. X., Tang, F. L., et al. (2018). Neogenin, a regulator of adult

- hippocampal neurogenesis, prevents depressive-like behavior article. *Cell Death Dis.* 9. doi:10.1038/s41419-017-0019-2.
- Sun, G. J., Zhou, Y., Stadel, R. P., Moss, J., Yong, J. H. A., Ito, S., et al. (2015). Tangential migration of neuronal precursors of glutamatergic neurons in the adult mammalian brain. *Proc. Natl. Acad. Sci. U. S. A.* 112, 9484–9489. doi:10.1073/pnas.1508545112.
- Sun, J., Sun, J., Ming, G. L., and Song, H. (2011). Epigenetic regulation of neurogenesis in the adult mammalian brain. *Eur. J. Neurosci.* 33, 1087–1093. doi:10.1111/j.1460-9568.2011.07607.x.
- Sun, X., Ji, C., Hu, T., Wang, Z., and Chen, G. (2013). Tamoxifen as an effective neuroprotectant against early brain injury and learning deficits induced by subarachnoid hemorrhage: Possible involvement of inflammatory signaling. *J. Neuroinflammation* 10, 157. doi:10.1186/1742-2094-10-157.
- Suuronen, T., Nuutinen, T., Huuskonen, J., Ojala, J., Thornell, A., and Salminen, A. (2005). Anti-inflammatory effect of selective estrogen receptor modulators (SERMs) in microglial cells. *Inflamm. Res.* 54, 194–203. doi:10.1007/s00011-005-1343-z.
- Takeda, K., and Akira, S. (2004). TLR signaling pathways. *Semin. Immunol.* 16, 3–9. doi:10.1016/j.smim.2003.10.003.
- Tan, Y. L., Yuan, Y., and Tian, L. (2020). Microglial regional heterogeneity and its role in the brain. *Mol. Psychiatry* 25, 351–367. doi:10.1038/s41380-019-0609-8.
- Tanapat, P., Hastings, N. B., and Gould, E. (2005). Ovarian steroids influence cell proliferation in the dentate gyrus of the adult female rat in a dose- and time-dependent manner. *J. Comp. Neurol.* 481, 252–265. doi:10.1002/cne.20385.
- Tapia-Gonzalez, S., Carrero, P., Pernia, O., Garcia-Segura, L. M., and Diz-Chaves, Y. (2008). Selective oestrogen receptor (ER) modulators reduce microglia reactivity in vivo after peripheral inflammation: potential role of microglial ERs. *J. Endocrinol.* 198, 219–230. doi:10.1677/JOE-07-0294.
- Tashiro, A., Sandler, V. M., Toni, N., Zhao, C., and Gage, F. H. (2006). NMDA-receptor-mediated, cell-specific integration of new neurons in adult dentate gyrus. *Nature* 442, 929–933. doi:10.1038/nature05028.
- Tashiro, A., Zhao, C., and Gage, F. H. (2007). Retrovirus-mediated single-cell gene knockout technique in adult newborn neurons in vivo. *Nat. Protoc.* 1, 3049–3055. doi:10.1038/nprot.2006.473.
- Taupin, P. (2007). BrdU immunohistochemistry for studying adult neurogenesis: Paradigms, pitfalls, limitations, and validation. *Brain Res. Rev.* 53, 198–214. doi:10.1016/j.brainresrev.2006.08.002.
- Taupin, P. (2010). Adult Neurogenesis, Neuroinflammation, and Therapeutic Potential of Adult Neural Stem Cells. *Neurovascular Med. Pursuing Cell. Longev. Heal. Aging* 5, 127–132. doi:10.1093/acprof:oso/9780195326697.003.0010.
- Teixeira, C. M., Kron, M. M., Masachs, N., Zhang, H., Lagace, D. C., Martinez, a., et al. (2012). Cell-Autonomous Inactivation of the Reelin Pathway Impairs Adult Neurogenesis in the Hippocampus. *J. Neurosci.* 32, 12051–12065. doi:10.1523/JNEUROSCI.1857-12.2012.
- Tian, D. S., Liu, J. L., Xie, M. J., Zhan, Y., Qu, W. S., Yu, Z. Y., et al. (2009). Tamoxifen attenuates



- inflammatory-mediated damage and improves functional outcome after spinal cord injury in rats. *J. Neurochem.* 109, 1658–1667. doi:10.1111/j.1471-4159.2009.06077.x.
- Toda, T., and Gage, F. H. (2018). Review: adult neurogenesis contributes to hippocampal plasticity. *Cell Tissue Res.* 373, 693–709. doi:10.1007/s00441-017-2735-4.
- Toda, T., Parylak, S. L., Linker, S. B., and Gage, F. H. (2019). The role of adult hippocampal neurogenesis in brain health and disease. *Mol. Psychiatry* 24, 67–87. doi:10.1038/s41380-018-0036-2.
- Tomassy, G. S., De Leonibus, E., Jabaudon, D., Lodato, S., Alfano, C., Mele, A., et al. (2010). Area-specific temporal control of corticospinal motor neuron differentiation by COUP-TFI. *Proc. Natl. Acad. Sci. U. S. A.* 107, 3576–3581. doi:10.1073/pnas.0911792107.
- Touzot, A., Ruiz-Reig, N., Vitalis, T., and Studer, M. (2016). Molecular control of two novel migratory paths for CGE-derived interneurons in the developing mouse brain. *Dev.* 143, 1753–1765. doi:10.1242/dev.131102.
- Tran, P. B., Banisadr, G., Ren, D., Chenn, A., and Miller, R. J. (2007). Chemokine receptor expression by neural progenitor cells in neurogenic regions of mouse brain. *J. Comp. Neurol.* 500, 1007–1034. doi:10.1002/cne.21229.
- Triviño-Paredes, J., Patten, A. R., Gil-Mohapel, J., and Christie, B. R. (2016). The effects of hormones and physical exercise on hippocampal structural plasticity. *Front. Neuroendocrinol.* 41, 23–43. doi:10.1016/j.yfme.2016.03.001.
- Tsai, S. Y., and Tsai, M.-J. (1997). Chick Ovalbumin Upstream Promoter-Transcription Factors (COUP-TFs): Coming of Age\*. Available at: <https://academic.oup.com/edrv/article-abstract/18/2/229/2530772> [Accessed June 13, 2019].
- Urbach, A., and Witte, O. W. (2019). Divide or Commit – Revisiting the Role of Cell Cycle Regulators in Adult Hippocampal Neurogenesis. *Front. Cell Dev. Biol.* 7, 55. doi:10.3389/fcell.2019.00055.
- Vaden, R. J., Gonzalez, J. C., Tsai, M. C., Niver, A. J., Fusilier, A. R., Griffith, C. M., et al. (2020). Parvalbumin interneurons provide spillover to newborn and mature dentate granule cells. *Elife* 9, 1–23. doi:10.7554/eLife.54125.
- Valero, J., Mastrella, G., Neiva, I., Sánchez, S., and Malva, J. O. (2014). Long-term effects of an acute and systemic administration of LPS on adult neurogenesis and spatial memory. *Front. Neurosci.* 8, 1–13. doi:10.3389/fnins.2014.00083.
- Vallièeres, L., Campbell, I. L., Gage, F. H., Sawchenko, P. E., Vallièeres, L., Campbell, I. L., et al. (2002). Reduced hippocampal neurogenesis in adult transgenic mice with chronic astrocytic production of interleukin-6. *J. Neurosci.* 22, 486–492. doi:22/2/486 [pii].
- Valny, M., Honsa, P., Kirdajova, D., Kamenik, Z., and Anderova, M. (2016). Tamoxifen in the mouse brain: Implications for fate-mapping studies using the tamoxifen-inducible cre-loxP system. *Front. Cell. Neurosci.* 10, 243. doi:10.3389/fncel.2016.00243.
- Van Dam, A. M., Bol, J. G. J. M., Gaykema, R. P. A., Goehler, L. E., Maier, S. F., Watkins, L. R., et al. (2000). Vagotomy does not inhibit high dose lipopolysaccharide-induced interleukin-1 $\beta$  immunoreactivity in rat brain and pituitary gland. *Neurosci. Lett.* 285, 169–172. doi:10.1016/S0304-3940(00)01031-4.

- Van Der Borght, K., Kóbor-Nyakas, D. É., Klauke, K., Eggen, B. J. L., Nyakas, C., Van Der Zee, E. A., et al. (2009). Physical exercise leads to rapid adaptations in hippocampal vasculature: Temporal dynamics and relationship to cell proliferation and neurogenesis. *Hippocampus* 19, 928–936. doi:10.1002/hipo.20545.
- Van, A. Lo, Hachem, M., Lagarde, M., and Bemoud-Hubac, N. (2019). Omega-3 docosahexaenoic acid is a mediator of fate-decision of adult neural stem cells. *Int. J. Mol. Sci.* 20, 1–18. doi:10.3390/ijms20174240.
- van Praag, H. (2002). Functional neurogenesis in the adult hippocampus.
- van Praag, H. (2009). Exercise and the brain: something to chew on. *Trends Neurosci.* 32, 283–290. doi:10.1016/j.tins.2008.12.007.
- van Praag, H., Kempermann, G., and Gage, F. H. (2000). Neural consequences of environmental enrichment. *Nat. Rev. Neurosci.* 1, 191–198. doi:10.1038/35044558.
- Van Praag, H., Kempermann, G., and Gage, F. H. (1999). Running increases cell proliferation and neurogenesis in the adult mouse dentate gyrus. *Nat. Neurosci.* 2, 266–270. doi:10.1038/6368.
- Van Praag, H., Shubert, T., Zhao, C., and Gage, F. H. (2005). Exercise enhances learning and hippocampal neurogenesis in aged mice. *J. Neurosci.* 25, 8680–8685. doi:10.1523/JNEUROSCI.1731-05.2005.
- Van Wagoner, N. J., Oh, J. W., Repovic, P., and Benveniste, E. N. (1999). Interleukin-6 (IL-6) production by astrocytes: Autocrine regulation by IL-6 and the soluble IL-6 receptor. *J. Neurosci.* 19, 5236–5244. doi:10.1523/jneurosci.19-13-05236.1999.
- Varatharaj, A., and Galea, I. (2017). The blood-brain barrier in systemic inflammation. *Brain. Behav. Immun.* 60, 1–12. doi:10.1016/j.bbi.2016.03.010.
- Vaynman, S., Ying, Z., and Gomez-Pinilla, F. (2004). Hippocampal BDNF mediates the efficacy of exercise on synaptic plasticity and cognition. *Eur. J. Neurosci.* 20, 2580–2590. doi:10.1111/j.1460-9568.2004.03720.x.
- Vicidomini, C., Guo, N., and Sahay, A. (2020). Communication, Cross Talk, and Signal Integration in the Adult Hippocampal Neurogenic Niche. *Neuron* 105, 220–235. doi:10.1016/j.neuron.2019.11.029.
- Vitkovic, L., Bockaert, J., and Jacque, C. (2000). “Inflammatory” cytokines’ neuromodulators in normal brain? *J. Neurochem.* 74, 457–471. doi:10.1046/j.1471-4159.2000.740457.x.
- Vogt, M. A., Chourbaji, S., Brandwein, C., Dormann, C., Sprengel, R., and Gass, P. (2008). Suitability of tamoxifen-induced mutagenesis for behavioral phenotyping. *Exp. Neurol.* 211, 25–33. doi:10.1016/j.expneurol.2007.12.012.
- Vukovic, J., Colditz, M. J., Blackmore, D. G., Ruitenber, M. J., and Bartlett, P. F. (2012). Microglia modulate hippocampal neural precursor activity in response to exercise and aging. *J. Neurosci.* 32, 6435–6443. doi:10.1523/JNEUROSCI.5925-11.2012.
- Walker, F. R., Beynon, S. B., Jones, K. A., Zhao, Z., Kongsui, R., Cairns, M., et al. (2014). Dynamic structural remodelling of microglia in health and disease: A review of the models, the signals and the mechanisms. *Brain. Behav. Immun.* 37, 1–14. doi:10.1016/j.bbi.2013.12.010.
- Wan, W., Janz, L., Vriend, C. Y., Sorensen, C. M., Greenberg, A. H., and Nance, D. M. (1993). Differential

- induction of c-Fos immunoreactivity in hypothalamus and brain stem nuclei following central and peripheral administration of endotoxin. *Brain Res. Bull.* 32, 581–587. doi:10.1016/0361-9230(93)90158-8.
- Wang, X., Zhao, L., Zhang, Y., Ma, W., Gonzalez, S. R., Fan, J., et al. (2017). Tamoxifen provides structural and functional rescue in murine models of photoreceptor degeneration. *J. Neurosci.* 37, 3294–3310. doi:10.1523/JNEUROSCI.2717-16.2017.
- Waters, E. M., Thompson, L. I., Patel, P., Gonzales, A. D., Ye, H. Z., Filardo, E. J., et al. (2015). G-protein-coupled estrogen receptor 1 is anatomically positioned to modulate synaptic plasticity in the mouse hippocampus. *J. Neurosci.* 35, 2384–2397. doi:10.1523/JNEUROSCI.1298-14.2015.
- Wei, H. yu, and Ma, X. (2014). Tamoxifen reduces infiltration of inflammatory cells, apoptosis and inhibits IKK/NF- $\kappa$ B pathway after spinal cord injury in rats. *Neurol. Sci.* 35, 1763–1768. doi:10.1007/s10072-014-1828-z.
- White, C. W., Fan, X., Maynard, J. C., Wheatley, E. G., Bieri, G., Couthouis, J., et al. (2020). Age-Related Loss of Neural Stem Cell O-GlcNAc Promotes a Glial Fate Switch through STAT3 activation. *Proc. Natl. Acad. Sci. U. S. A.* 117, 22214–22224. doi:10.1073/pnas.2007439117.
- Wilhelmsson, U., Faiz, M., De Pablo, Y., Sjöqvist, M., Andersson, D., Widestrand, Å., et al. (2012). Astrocytes negatively regulate neurogenesis through the Jagged1-mediated notch pathway. *Stem Cells* 30, 2320–2329. doi:10.1002/stem.1196.
- Willis, E. F., MacDonald, K. P. A., Nguyen, Q. H., Garrido, A. L., Gillespie, E. R., Harley, S. B. R., et al. (2020). Repopulating Microglia Promote Brain Repair in an IL-6-Dependent Manner. *Cell* 180, 833-846.e16. doi:10.1016/j.cell.2020.02.013.
- Wirenfeldt, M., Dalmau, I., and Finsen, B. (2003). Estimation of Absolute Microglial Cell Numbers in Mouse Fascia Dentata Using Unbiased and Efficient Stereological Cell Counting Principles. *Glia* 44, 129–139. doi:10.1002/glia.10277.
- Witter, M. (2012). *Hippocampus*. Elsevier Inc. doi:10.1016/B978-0-12-369497-3.10005-6.
- Witter, M. P., and Amaral, D. G. (2004). *Hippocampal Formation*. Third edit. . doi:10.1016/B978-012547638-6/50022-5.
- Wolf, J., Rose-John, S., and Garbers, C. (2014). Interleukin-6 and its receptors: a highly regulated and dynamic system. *Cytokine* 70, 11–20. doi:10.1016/j.cyto.2014.05.024.
- Woodbury, M. E., Freilich, R. W., Cheng, C. J., Asai, H., Ikezu, S., Boucher, J. D., et al. (2015). miR-155 is essential for inflammation-induced hippocampal neurogenic dysfunction. *J. Neurosci.* 35, 9764–9781. doi:10.1523/JNEUROSCI.4790-14.2015.
- Wu, M. D., Hein, A. M., Moravan, M. J., Shaffel, S. S., Olschowka, J. A., O'Banion, M. K., et al. (2012). Adult murine hippocampal neurogenesis is inhibited by sustained IL-1 $\beta$  and not rescued by voluntary running. *Brain. Behav. Immun.* 26, 292–300. doi:10.1016/j.bbi.2011.09.012.
- Wu, M. D., Montgomery, S. L., Rivera-Escalera, F., Olschowka, J. A., and O'Banion, M. K. (2013). Sustained IL-1 $\beta$  expression impairs adult hippocampal neurogenesis independent of IL-1 signaling in nestin+ neural precursor cells. *Brain. Behav. Immun.* 32, 9–18. doi:10.1016/j.bbi.2013.03.003.

- Wu, S.-P., Lee, D.-K., DeMayo, F. J., Tsai, S. Y., and Tsai, M.-J. (2010). Generation of ES Cells for Conditional Expression of Nuclear Receptors and Coregulators *in Vivo*. *Mol. Endocrinol.* 24, 1297–1304. doi:10.1210/me.2010-0068.
- Yang, Q. qiao, and Zhou, J. wei (2019). Neuroinflammation in the central nervous system: Symphony of glial cells. *Glia* 67, 1017–1035. doi:10.1002/glia.23571.
- Yang, S. M., Alvarez, D. D., and Schinder, A. F. (2015). Reliable genetic labeling of adult-born dentate granule cells using ascl1CreERT2 and glastCreERT2 murine lines. *J. Neurosci.* 35, 15379–15390. doi:10.1523/JNEUROSCI.2345-15.2015.
- Yoo, S., and Blackshaw, S. (2018). Regulation and function of neurogenesis in the adult mammalian hypothalamus. *Prog. Neurobiol.* 170, 53–66. doi:10.1016/j.pneurobio.2018.04.001.
- Zemla, R., and Basu, J. (2017). Hippocampal function in rodents. *Curr. Opin. Neurobiol.* 43, 187–197. doi:10.1016/j.conb.2017.04.005.
- Zeng, C., Pan, F., Jones, L. A., Lim, M. M., Griffin, E. A., Sheline, Y. I., et al. (2010). Evaluation of 5-ethynyl-2'-deoxyuridine staining as a sensitive and reliable method for studying cell proliferation in the adult nervous system. *Brain Res.* 1319, 21–32. doi:10.1016/j.brainres.2009.12.092.
- Zhang, J., Giesert, F., Kloos, K., Vogt Weisenhom, D. M., Aigner, L., Wurst, W., et al. (2010). A powerful transgenic tool for fate mapping and functional analysis of newly generated neurons. *BMC Neurosci.* 11. doi:10.1186/1471-2202-11-158.
- Zhang, J., He, H., Qiao, Y., Zhou, T., He, H., Yi, S., et al. (2020). Priming of microglia with IFN- $\gamma$  impairs adult hippocampal neurogenesis and leads to depression-like behaviors and cognitive defects. *Glia*, 1–19. doi:10.1002/glia.23878.
- Zhang, Y., Milatovic, D., Aschner, M., Feustel, P. J., and Kimelberg, H. K. (2007). Neuroprotection by tamoxifen in focal cerebral ischemia is not mediated by an agonist action at estrogen receptors but is associated with antioxidant activity. *Exp. Neurol.* 204, 819–827. doi:10.1016/j.expneurol.2007.01.015.
- Zhao, C., Deng, W., and Gage, F. H. (2008). Mechanisms and Functional Implications of Adult Neurogenesis. *Cell* 132, 645–660. doi:10.1016/j.cell.2008.01.033.
- Zhao, C., Teng, E. M., Summers, R. G., Ming, G. L., and Gage, F. H. (2006). Distinct morphological stages of dentate granule neuron maturation in the adult mouse hippocampus. *J. Neurosci.* 26, 3–11. doi:10.1523/JNEUROSCI.3648-05.2006.
- Zhao, L., O'Neill, K., and Diaz Brinton, R. (2005). Selective estrogen receptor modulators (SERMs) for the brain: Current status and remaining challenges for developing NeuroSERMs. *Brain Res. Rev.* 49, 472–493. doi:10.1016/j.brainresrev.2005.01.009.
- Zheng, J., Li, H. L., Tian, N., Liu, F., Wang, L., Yin, Y., et al. (2020). Intemeuron Accumulation of Phosphorylated tau Impairs Adult Hippocampal Neurogenesis by Suppressing GABAergic Transmission. *Cell Stem Cell* 26, 331–345.e6. doi:10.1016/j.stem.2019.12.015.
- Zhou, B., Zuo, Y. X., and Jiang, R. T. (2019). Astrocyte morphology: Diversity, plasticity, and role in neurological diseases. *CNS Neurosci. Ther.* 25, 665–673. doi:10.1111/cns.13123.

- Zocher, S., Schilling, S., Grzyb, A. N., Adusumilli, V. S., Lopes, J. B., Günther, S., et al. (2020). Early-life environmental enrichment generates persistent individualized behavior in mice. *Sci. Adv.* 6, eabb1478. doi:10.1126/sciadv.abb1478.
- Zonis, S., Ljubimov, V. A., Mahgerefteh, M., Pechnick, R. N., Wawrowsky, K., and Chesnokova, V. (2013). p21Cip restrains hippocampal neurogenesis and protects neuronal progenitors from apoptosis during acute systemic inflammation. *Hippocampus* 23, 1383–1394. doi:10.1002/hipo.22192.
- Zupanc, G. K. H. (2006). Neurogenesis and neuronal regeneration in the adult fish brain. *J. Comp. Physiol. A Neuroethol. Sensory, Neural, Behav. Physiol.* 192, 649–670. doi:10.1007/s00359-006-0104-y.

## **CHAPTER VI**

# Acknowledgments

The completion of this study could not have been possible without the expertise of Professor Silvia De Marchis and Dr. Sara Bonzano, my beloved thesis advisers and postdoc mentor. I would also like to thank Dr. Wojciech Krezel for his contribution to refining Chapter III. Besides, my Ph.D. has come to completion thanks to Silvia and her contribution to fundraising.

A debt of gratitude is also owed to the Adult Neurogenesis research team members I belong to. Particular thanks to my mentor Sara for helping me with her extraordinary scientific competence and for her friendship. I am also particularly grateful to Serena, whose experience and wisdom helped me to find my way. Thanks to the students, Eleonora and Valentina, who followed me in the first and very time-consuming analyses on microglia.

Big and sincere thanks go to my most trusted friends, who have encouraged and supported me. Paola as first! Thanks to my amazing and crazy basketball team for welcome my foolish behavior at the end of the day. I love this game! OKANOHEY.

Thanks, more than sincerely, to my love Kennedy.

Last but not least, special thanks to my family, my dad, my sister Valentina and my brothers, Riccardo and Alessandro.

Above all, thanks to my mom.

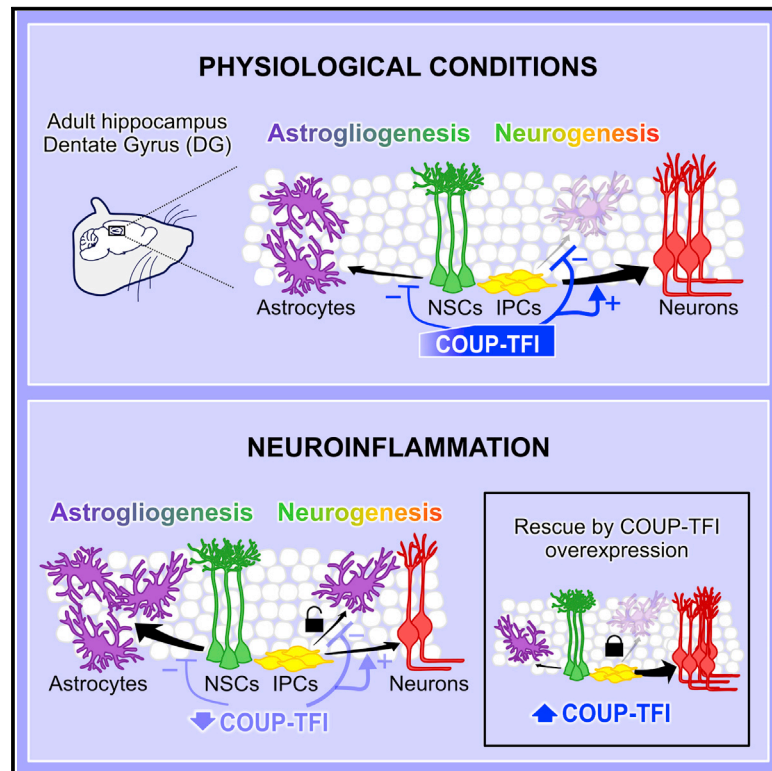
... and, thanks to myself !!!

# **APPENDIX**



## Neuron-Astroglia Cell Fate Decision in the Adult Mouse Hippocampal Neurogenic Niche Is Cell-Intrinsically Controlled by COUP-TFI *In Vivo*

### Graphical Abstract



### Authors

Sara Bonzano, Isabella Crisci, Anna Podlesny-Drabiniok, Chiara Rolando, Wojciech Krezel, Michèle Studer, Silvia De Marchis

### Correspondence

michele.studer@unice.fr (M.S.),  
silvia.demarchis@unito.it (S.D.M.)

### In Brief

The adult hippocampal dentate gyrus contains multipotent neural stem cells (NSCs) and neuronal committed progenitors. Bonzano et al. demonstrate that the nuclear receptor COUP-TFI cell-intrinsically drives NSCs/progenitors toward neurogenesis by repressing astrogligenesis. Notably, COUP-TFI downregulation occurs in inflamed hippocampi, and its overexpression rescues the hippocampal neurogenesis-astrogligenesis imbalance due to neuroinflammation.

### Highlights

- COUP-TFI is expressed by adult NSCs/progenitors in the hippocampal dentate gyrus (DG)
- COUP-TFI promotes neurogenic fate by repressing astrogligenesis in the adult DG
- Neuroinflammation downregulates COUP-TFI expression in adult hippocampal NSCs
- Increased COUP-TFI levels rescue neuro-gliogenesis imbalance in the inflamed DG



# Neuron-Astroglia Cell Fate Decision in the Adult Mouse Hippocampal Neurogenic Niche Is Cell-Intrinsically Controlled by COUP-TFI *In Vivo*

Sara Bonzano,<sup>1,2,3</sup> Isabella Crisci,<sup>1,2</sup> Anna Podlesny-Drabiniok,<sup>4,5,6,7</sup> Chiara Rolando,<sup>8</sup> Wojciech Krezel,<sup>4,5,6,7</sup> Michèle Studer,<sup>3,9,\*</sup> and Silvia De Marchis<sup>1,2,9,10,\*</sup>

<sup>1</sup>Neuroscience Institute Cavalieri Ottolenghi (NICO), University of Turin, Orbassano 10043, Italy

<sup>2</sup>Department of Life Sciences and Systems Biology, University of Turin, Turin 10123, Italy

<sup>3</sup>Université Côte d'Azur (UCA) CNRS, Inserm, iBV, Nice 06108, France

<sup>4</sup>Institut de Génétique et de Biologie Moléculaire et Cellulaire, Illkirch 67404, France

<sup>5</sup>Inserm, U1258, Illkirch, France

<sup>6</sup>CNRS, UMR 7104, Illkirch, France

<sup>7</sup>Université de Strasbourg, Illkirch, France

<sup>8</sup>Department of Biomedicine, University of Basel, Basel 4031, Switzerland

<sup>9</sup>Senior author

<sup>10</sup>Lead Contact

\*Correspondence: [michele.studer@unice.fr](mailto:michele.studer@unice.fr) (M.S.), [silvia.demarchis@unito.it](mailto:silvia.demarchis@unito.it) (S.D.M.)

<https://doi.org/10.1016/j.celrep.2018.06.044>

## SUMMARY

In the dentate gyrus (DG) of the mouse hippocampus, neurogenesis and astrogliogenesis persist throughout life. Adult-born neurons and astrocytes originate from multipotent neural stem cells (NSCs) whose activity is tightly regulated within the neurogenic niche. However, the cell-intrinsic mechanisms controlling neuron-glia NSC fate choice are largely unknown. Here, we show COUP-TFI/NR2F1 expression in DG NSCs and its downregulation upon neuroinflammation. By using *in vivo* inducible knockout lines, a retroviral-based loss-of-function approach and genetic fate mapping, we demonstrate that COUP-TFI inactivation in adult NSCs and/or mitotic progenitors reduces neurogenesis and increases astrocyte production without depleting the NSC pool. Moreover, forced COUP-TFI expression in adult NSCs/progenitors decreases DG astrogliogenesis and rescues the neuro-astrogliogenic imbalance under neuroinflammation. Thus, COUP-TFI is necessary and sufficient to promote neurogenesis by suppressing astrogliogenesis. Our data propose COUP-TFI as a central regulator of the neuron-astroglia cell fate decision and a key modulator during neuroinflammation in the adult hippocampus.

## INTRODUCTION

Once considered limited to the embryonic and perinatal periods, neural stem cells (NSCs) persist in two discrete regions of the adult mammalian brain: the subventricular zone (SVZ) lining the lateral ventricles and the subgranular zone (SGZ) of the hippo-

campal dentate gyrus (DG) (Kempermann et al., 2015). Within the adult SGZ, NSCs are mostly quiescent, show a typical radial morphology, and are referred to as radial glia-like (RGL) or type 1 stem cells. Upon activation, a RGL cell can divide symmetrically to produce two RGL cells or asymmetrically to self-renew and generate a differentiated progeny. In the latter case, RGL cells can give rise to rapidly dividing intermediate progenitors (type 2; IPCs), which generate neuroblasts and eventually exit the cell cycle to differentiate into mature granule cells (GCs) (Bond et al., 2015; Kempermann et al., 2015). Adult DG neurogenesis plays a crucial role in learning and memory, and it is regulated by several factors, including stress, inflammation, environmental enrichment, and voluntary physical activity (Kempermann, 2015).

Alongside neurogenesis, astrogliogenesis allows a continuous production of astrocytes in the adult DG, either by RGL asymmetric division (i.e., maintaining the RGL cell pool) or by direct differentiation implying a depletion in the RGL cell pool (Bonaguidi et al., 2011; Encinas et al., 2011). Astrocytes are key constituents of the neurogenic niche and play fundamental roles in the regulation of NSCs/progenitors by promoting neurogenesis (Barkho et al., 2006; Song et al., 2002). Interestingly, running enhances DG neurogenesis, as well as astrogliogenesis (Steiner et al., 2004), whereas pathological conditions, such as inflammation, lead to NSC dysfunction, altering the neuron-astrocyte production rate in favor of astrocytes (Woodbury et al., 2015; Wu et al., 2012). This highlights the importance of a tight control of neuronal versus astroglial cell fate decision, most probably linked to intrinsic regulation in the NSC/progenitor pool. However, the nature of a transcriptional program underlying this function is still unknown.

COUP-TFI (also called NR2F1) is a nuclear hormone receptor acting as a strong transcriptional regulator whose functions range from the control of embryonic NSC behavior (Naka-Kaneda et al., 2014; Naka et al., 2008) to the regulation of cell migration in the neocortex and developing DG (Alfano et al., 2011; Bertacchi et al., 2018; Parisot et al., 2017). Cortical depletion of COUP-TFI during early stages results in abnormal motor skill



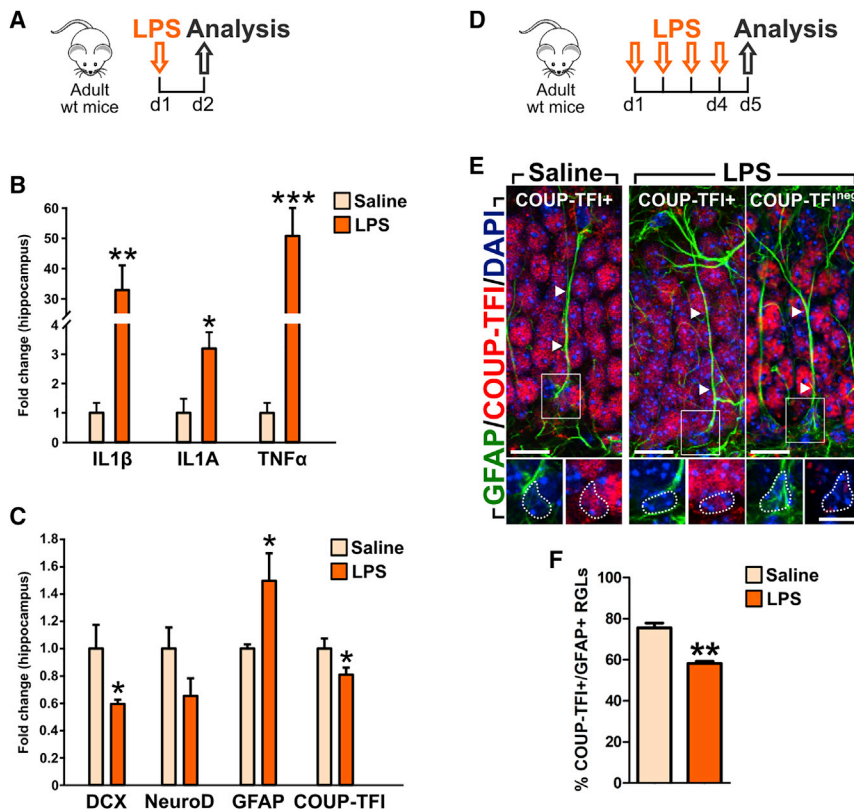


**Figure 1. Acute Neuroinflammation Leads to COUP-TFI Downregulation within the Adult DG**

(A) Experimental design for transcript expression analysis on hippocampal tissue extracts.

(B and C) Changes in pro-inflammatory cytokines (B), neuronal (DCX, NeuroD), glial (GFAP), and COUP-TFI gene transcripts (C) in the hippocampi of LPS-treated mice revealed by RT-qPCR (n = 5 mice/treatment; technical replicates = 2).

(D) Experimental design for immunofluorescence analysis on the DG.

(E) Confocal images of GFAP+ (green) RGLs either positive (+) or negative (neg) for COUP-TFI (red) in DG sections of saline- and LPS-treated mice. Cell nuclei are counterstained with DAPI (blue). Arrowheads indicate radial cell processes. Scale bar, 10  $\mu$ m.

(F) Quantification of COUP-TFI+ nuclei among GFAP+ RGL cells (RGLs) in saline (n = 257 of 353 double+ cells out of three mice) and LPS-treated mice (n = 220 of 379 double+ cells out of three mice).

Error bars indicate SEM. Student's t test: \*p < 0.05, \*\*p < 0.01, and \*\*\*p < 0.001. See also Figure S1.

behavior and spatial memory deficits (Flore et al., 2016; Tomassy et al., 2010), and haploinsufficiency of COUP-TFI in patients leads to global developmental delay, intellectual disabilities, and optic atrophy (Al-Kateb et al., 2013; Bosch et al., 2014; Bertacchi et al., 2018). COUP-TFI continues to be expressed in the adult CNS, including neurogenic niches (Bovetti et al., 2013; Llorens-Bobadilla et al., 2015), but its functional role in adult NSCs is unknown.

Here, we examined the expression and function of COUP-TFI in the adult DG neurogenic niche. First, we showed that COUP-TFI levels were downregulated upon induced neuroinflammation followed by increased astrogliogenesis. Next, to assess whether COUP-TFI was directly involved in this process, we genetically manipulated *COUP-TFI* by targeting adult NSCs and/or mitotic progenitors through loss- and gain-of-function experiments *in vivo*. By using two independent conditional inducible mouse transgenic lines and a retroviral-based approach, coupled to genetic fate mapping, we found that *COUP-TFI* deletion in NSCs and/or committed neurogenic progenitors decreased hippocampal neurogenesis and increased astrogliogenesis, indicating a switch of NSCs/progenitors toward a gliogenic commitment. Finally, complementary gain-of-function experiments showed that COUP-TFI overexpression in adult DG NSCs/progenitors was sufficient to repress astrogliogenesis and, importantly, to rescue neurogenesis during inflammation. Overall, these data unravel a key role for COUP-TFI as a transcriptional regulator in the decision-making process of generating either new neurons or astrocytes within the healthy and inflamed adult hippocampus.

## RESULTS

### Acute Neuroinflammation Leads to COUP-TFI Downregulation within the Adult DG

Neuroinflammation severely affects adult neurogenesis and increases astrocyte production in the adult hippocampal DG (Kohman and Rhodes, 2013; Monje et al., 2003; Wu et al., 2012). However, little is known about the mechanisms underlying this process within the DG NSC/progenitor pool. With the goal of identifying novel cell-intrinsic regulators responding to neuroinflammation and involved in controlling neurogenesis and/or astrogliogenesis within the adult hippocampus, we acutely administered the *E. coli*-derived lipopolysaccharide (LPS) by intraperitoneal (i.p.) injection to initiate an inflammatory response (Figure 1A). The occurrence of an inflammatory response was confirmed by a strong transcript increase of the pro-inflammatory cytokines interleukin-1 $\beta$  (IL-1 $\beta$ ), interleukin-1A (IL-1A), and tumor necrosis factor  $\alpha$  (TNF $\alpha$ ) in the hippocampi of LPS-treated mice compared with control saline-injected mice at 1 day post-injection (Figure 1B). In parallel, LPS treatment downregulated the expression of the immature neuronal markers doublecortin (DCX) and NeuroD and upregulated the glial fibrillary acid protein (GFAP) (Figure 1C), in line with an alteration in the newborn neuron/astrocyte ratio, as previously reported during neuroinflammation (Wu et al., 2012). Interestingly, we also found that the nuclear receptor COUP-TFI was downregulated in LPS-treated mice (Figure 1C), indicating a direct response of this transcriptional regulator to inflammation in the adult hippocampus.



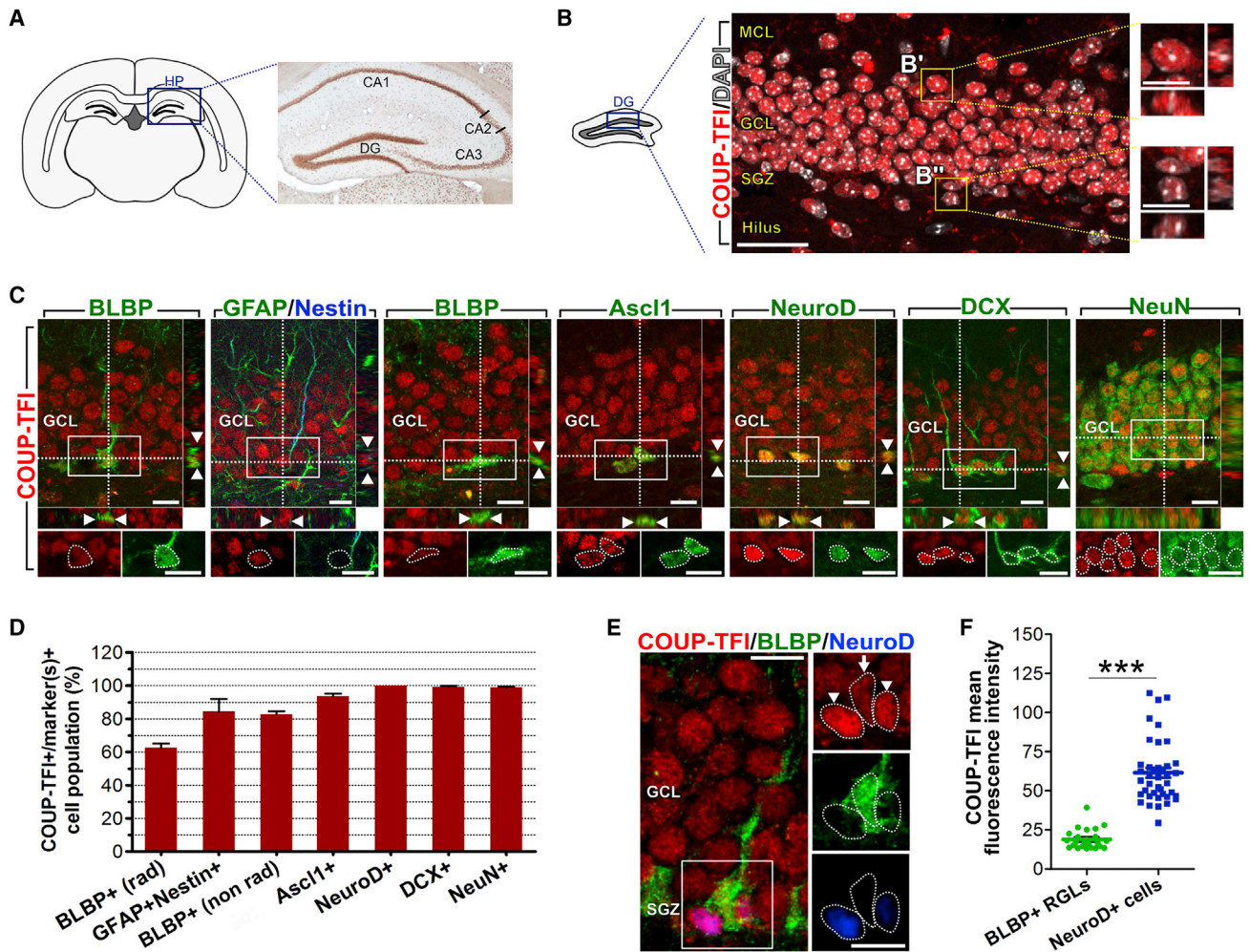


**Figure 2. COUP-TFI Is Expressed in NSCs and in the Neurogenic Lineage of the Adult DG**

(A) Schematic drawing of a coronal section of an adult mouse brain. The box indicates the hippocampus (HP), where COUP-TFI immunostaining is shown. (B) Confocal images of COUP-TFI+ cells (red) in an adult DG section counterstained with DAPI (white). (C) Confocal images of the DG immunostained for COUP-TFI (red) and different cell type-specific markers of the adult hippocampal neurogenic lineage (green, blue). Double-labeled cells are shown at higher magnifications (bottom) as single color channel images. (D) Quantification of COUP-TFI+ cells among the pools of DG cells expressing different markers listed on the x axis (>200 cells/marker). (E) Confocal images illustrating differences in COUP-TFI levels in radial BLBP+ stem cells (arrow) versus NeuroD+ neuronal-committed cells (arrowheads). (F) Dot plot reporting the intensity of COUP-TFI immunolabeling in BLBP+ RGL cells (n = 24 double+ cells) and NeuroD+ neuronal progenitors (n = 40 double+ cells).

N = 3 adult mice. GCL, granule cell layer; MCL, molecular cell layer; SGZ, subgranular zone. Error bars indicate SEM. Scale bars, 50  $\mu$ m (B) and 10  $\mu$ m (insets in B; C and E). Student's t test: \*\*\*p < 0.001. See also Figure S2.

To identify changes in COUP-TFI at the cellular level, we treated adult mice once a day for 4 consecutive days with LPS (d1–d4) and analyzed COUP-TFI protein expression in the hippocampal RGL cell pool at day 5 (Figures 1D and 1E). In accordance with transcript downregulation (Figure 1C), we found a decrease of GFAP+ RGL cells expressing COUP-TFI in LPS-treated DG (Figures 1E and 1F). As expected, we also found a reduced number of DCX+ immature newborn neurons and an expansion of GFAP+ astrocytes within the GCL of LPS-treated mice (Figures S1A–S1D). Thus, on the basis of COUP-TFI downregulation in RGL cells upon inflammatory insult, we hypothe-

sized that COUP-TFI could be directly involved in the imbalance in neuron to astrocyte generation within the DG.

### COUP-TFI Is Expressed in NSCs and in the Neurogenic Lineage of the Adult DG

To understand whether COUP-TFI could act as a potential regulator of neuron versus astroglia RGL cell commitment, we first investigated its cell type-specific distribution in the DG of the adult hippocampus (Figure 2). COUP-TFI protein expression was analyzed in the granule cell layer (GCL) and neurogenic SGZ along the entire DG anteroposterior axis by using a series

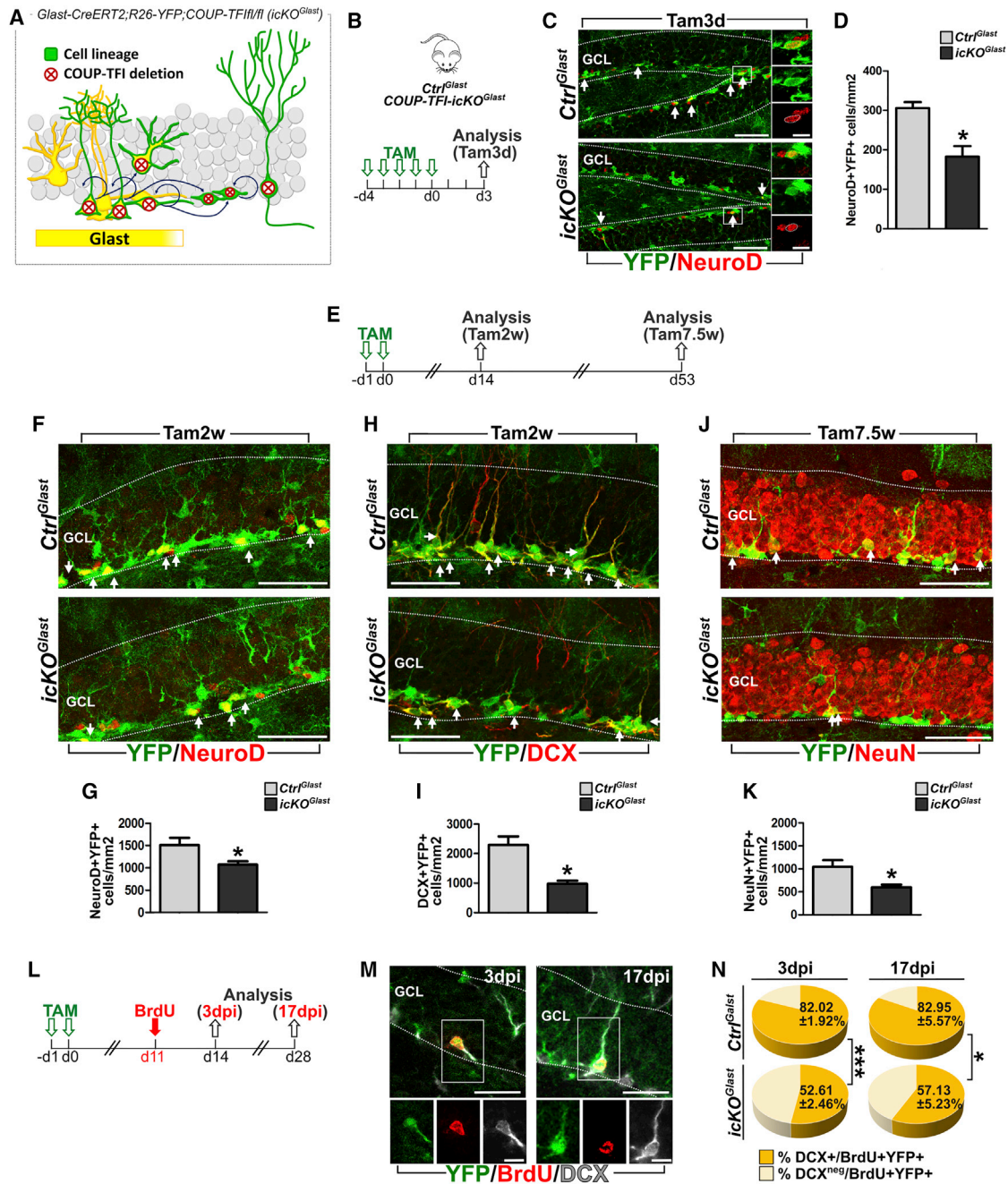


**Figure 3. COUP-TFI Depletion in Adult RGL Cells Impairs DG Neurogenesis**

(A) Schema illustrating COUP-TFI deletion (red crossed circles) in the cell progeny (green) derived from *Glast*-expressing cells (yellow) in the DG upon tamoxifen (TAM) induction in *COUP-TFI-icKO<sup>Glast</sup>* adult mice.

(B) Experimental design to assess the early consequences of COUP-TFI loss-of-function in the *Glast*-lineage (see C and D).

(C) Confocal images of double immunostaining for YFP (green) and NeuroD (red) in *Ctrl<sup>Glast</sup>* and *COUP-TFI-icKO<sup>Glast</sup>* DG.

(D) Quantification of double NeuroD+YFP+ cells in *Ctrl<sup>Glast</sup>* and *COUP-TFI-icKO<sup>Glast</sup>* DG.

(E) Experimental design for long-term effects of COUP-TFI loss-of-function in the *Glast*-lineage (see F–K).

(F, H, and J) Confocal images of NeuroD+ (F, red), DCX+ (H, red), and NeuN+ (J, red) double-positive for YFP (green) in *Ctrl<sup>Glast</sup>* and *COUP-TFI-icKO<sup>Glast</sup>* DG at Tam2w (F and H) and Tam7.5w (J).

(G, I, and K) Quantification of double NeuroD+YFP+ (G), DCX+YFP+ (I), and NeuN+YFP+ (K) cells in *Ctrl<sup>Glast</sup>* and *COUP-TFI-icKO<sup>Glast</sup>* DG.

(L) Experimental design used to label a cohort of newborn cells with BrdU in TAM-treated mice in the *Glast*-lineage (see M and N).

(M) Confocal images of newborn neurons triple-positive for BrdU (red), YFP (green), and DCX (gray) at 3 and 17 days post BrdU injection (dpi) in *Ctrl<sup>Glast</sup>* DG.

(legend continued on next page)



of cell stage-specific markers combined with morphological analysis (Figures 2A–2D and S2). In the SGZ, more than 60% of all RGL cells, identified by their radial morphology and BLBP expression (Steiner et al., 2004), and the large majority of double GFAP+Nestin+ RGL cells (DeCarolis et al., 2013) co-expressed COUP-TFI (Figures 2C and 2D). Non-radial BLBP+ cells, accounting for horizontal type 1 and neuronal committed type 2a progenitors, and Ascl1+ cells, including activated stem cells and type 2a progenitors (Andersen et al., 2014; Lugert et al., 2010, 2012), also largely expressed COUP-TFI (Figures 2C and 2D). Thus, in the adult SGZ, COUP-TFI is localized in active NSCs and neurogenic progenitors, as further supported by co-expression with the proliferative marker Ki67+ (Figure S2B). Finally, the use of neuron-specific markers revealed that virtually all late neuronal progenitors (type 2b), neuroblasts, and immature neurons, labeled by NeuroD or DCX (Gao et al., 2009; Steiner et al., 2006), as well as NeuN+ mature neurons (Ming and Song, 2005), were also COUP-TFI+ (Figures 2C and 2D). However, the intensity of COUP-TFI immunofluorescence was doubled in NeuroD+ cells compared with BLBP+ RGL cells (Figures 2E and 2F), suggesting an upregulation of COUP-TFI expression in neuronal committed cells. Overall, these data reveal that COUP-TFI is widely expressed in the SGZ/GCL throughout the neurogenic lineage, although at different levels, implying tight regulation for this transcription factor in different cellular components of the adult DG niche.

### COUP-TFI Depletion in Adult RGL Cells Impairs DG Neurogenesis

To directly investigate COUP-TFI function in the adult hippocampal neurogenic niche, we adopted a genetic loss-of-function approach coupled to fate mapping in adult RGL cells. The *COUP-TF1<sup>fl/fl</sup>* mouse line (Armentano et al., 2007) was crossed with mice carrying the tamoxifen (TAM)-inducible form of *Cre-recombinase* (*CreERT2*) under *Glast* transcriptional control (Mori et al., 2006) and to a *Rosa26-YFP* reporter line (Srinivas et al., 2001) (Figure S3A). The resulting progeny was named *COUP-TFI-icKO<sup>Glast</sup>* and allowed fate mapping of RGL cells that had undergone selective *COUP-TFI* deletion (Figure 3A). *Glast-CreERT2* mice carrying the *R26-YFP* reporter transgene, but wild-type for *COUP-TFI*, were used as controls (*Ctrl<sup>Glast</sup>*).

First, we assessed the early effects of COUP-TFI loss in the adult RGL cells by treating *COUP-TFI-icKO<sup>Glast</sup>* and *Ctrl<sup>Glast</sup>* mice for 5 consecutive days with TAM and analyzing the DG 3 days after (Figure 3B). Notably, the drastic drop in COUP-TFI expression in mutants (Figures S3B and S3C) was associated with a decrease in double NeuroD+YFP+ neuronal committed progenitors and neuroblasts (Figures 3C and 3D). However, COUP-TFI loss did not affect the densities of either the total recombined YFP+ population or double GFAP+YFP+ RGL cells within the DG of mutant mice compared with controls (Figures S3D–S3F). Moreover, mice injected i.p. with BrdU the day before

analysis (Figure S3G) showed no significant differences in the density of double BrdU+YFP+ cells in *COUP-TFI-icKO<sup>Glast</sup>* DG versus *Ctrl<sup>Glast</sup>* (Figures S3H and S3I), indicating no alteration in NSC/progenitor proliferation. Thus, these data suggest that COUP-TFI normally promotes neurogenesis within adult hippocampal NSCs without affecting their proliferation rate.

Next, we shortened TAM treatment to 2 days, to achieve mosaic recombination of RGL cells within a wild-type environment and to assess the effect of *COUP-TFI* deletion at longer survival time (Figure 3E). The large majority of recombined YFP+ cells failed to express COUP-TFI after 2 weeks (d14) and 7.5 weeks (d53) (Figure S3J), confirming *COUP-TFI* Cre-induced deletion. The recombined YFP+ population expressing NeuroD or DCX was significantly reduced in *COUP-TFI-icKO<sup>Glast</sup>* mice compared with controls at d14 (Figures 3F–3I), similar to the density of double NeuN+YFP+ mature neurons quantified at d53 (Figures 3J and 3K). Accordingly, the percentage of NeuroD+, DCX+, and NeuN+ cells among the YFP+ population significantly dropped in mutant DG (Table S1), supporting diminished neurogenesis upon COUP-TFI inactivation in the adult hippocampal RGL cell lineage.

To further address a possible defect in newborn neuron survival upon COUP-TFI deletion, mutant and control mice were treated for 2 days with TAM and injected 11 days later with BrdU (Figure 3L). DG were analyzed 3 days post-BrdU injection (dpi), during the peak of newborn BrdU+ cells (Steiner et al., 2004), and 17 dpi, after the early selection phase and when surviving newborn cells reach stable levels (Encinas et al., 2011) (Figure 3L). No significant differences were found in the density of double BrdU+YFP+ cells at both time points (Figures S3K and S3L). Moreover, double BrdU+YFP+ cells at 17 dpi corresponded to nearly 25% of that found at 3 dpi in both *Ctrl<sup>Glast</sup>* and *COUP-TFI-icKO<sup>Glast</sup>* (Figure S3M), indicating no alteration in newborn cell survival during this critical period. However, the number of DCX+ cells among the double BrdU+YFP+ population significantly decreased in *COUP-TFI-icKO<sup>Glast</sup>* compared with *Ctrl<sup>Glast</sup>* at both survival times (Figures 3M and 3N). This effect was specific to mutated YFP+ cells, as BrdU+ YFP negative cells (i.e., not recombined) showed no differences in the percentage of DCX+ cells in *COUP-TFI-icKO<sup>Glast</sup>* versus *Ctrl<sup>Glast</sup>* (Figure S3N). Taken together, these data demonstrate that loss of COUP-TFI in the RGL cell pool severely impairs neurogenesis in the adult DG, without altering NSC/progenitor proliferation and/or newborn cell survival.

### Loss of COUP-TFI Function Promotes Astroglial Potential in Adult DG RGL Cells

In addition to neurogenesis, new astrocytes are continuously generated from RGL cells in the adult DG (Bonaguidi et al., 2011; Steiner et al., 2004). We thus hypothesized that the observed reduction of newborn neurons upon *COUP-TFI* inactivation (Figures 3 and S3) could entail increased astroglialogenesis.

(N) Pie charts reporting the fraction of BrdU+YFP+ cells that are DCX+ (dark yellow) at 3 and 17 dpi in *Ctrl<sup>Glast</sup>* and *COUP-TFI-icKO<sup>Glast</sup>* DG (3 dpi: n = 142 of 176 cells, *Ctrl<sup>Glast</sup>* mice; n = 108 of 207 cells, *COUP-TFI-icKO<sup>Glast</sup>* mice; 17 dpi: n = 57 of 68 cells, *Ctrl<sup>Glast</sup>* mice; n = 45 of 76 cells, *COUP-TFI-icKO<sup>Glast</sup>* mice; Student's t test: p < 0.001 at 3 dpi, p < 0.05 at 17 dpi).

N = 3 or 4 animals per genotype. Arrows indicate double-labeled cells. Scale bars, 50  $\mu$ m (C, F, H, and J; low magnification), 10  $\mu$ m (C; high magnification), 25  $\mu$ m (M; low magnification), and 10  $\mu$ m (M; high magnification). Error bars indicate SEM. Student's t test: \*p < 0.05. See also Figure S3.

For this purpose, we tested the expression of NFIA, a nuclear factor associated with astroglial commitment during development (Kang et al., 2012; Subramanian et al., 2011), in RGL cells and proliferating progenitors of the DG 3 days after TAM-driven recombination (Figures 4A–4D). In *Ctrl<sup>Glast</sup>* mice, about 60% of all YFP+ RGL cells expressed NFIA (Figure 4B), in a largely mutually exclusive pattern to COUP-TFI (Figures S4A and S4B). This fraction increased to 80% in *COUP-TFI-icKO<sup>Glast</sup>* mice (Figure 4B). In addition, mutant mice also showed an expansion of MCM2+YFP+ proliferating progenitors expressing NFIA (Figures 4C and 4D). Because no changes in the RGL and proliferative pool cell size were observed (Figures S3F and S3I), these data suggest a switch of COUP-TFI-deficient NSC/progenitor commitment toward an astroglial fate. Accordingly, at this time point, the density of YFP+ astrocytes expressing the mature astroglial marker S100B was comparable between genotypes (Figures S4C and S4D), indicating no direct differentiation of RGL cells into astrocytes.

We next moved to the long-term protocol (Figure 3E) to follow astrocyte differentiation within the YFP+ recombined pool. The majority of YFP+ astrocytes, double-positive for GFAP or S100B, showed cell bodies within the middle/outer GCL and multiple branches reminiscent of a mature astrocyte bushy morphology (Figures 4E and 4F, white arrowheads). Some of the YFP+ astrocytes depicting a polarized shape, but with a thick and short apical process branching mainly inside the GCL, were also identified in the SGZ (Figures 4E and 4F, pink arrowheads). Careful quantification of double GFAP+YFP+ and S100B+YFP+ astrocytes indicated a huge expansion of these cells upon *COUP-TFI* deletion in the *Glast* lineage (Figures 4G and 4H), which occurred without depletion of the RGL cell pool (Figures S4E and S4F). This suggested that a direct differentiation of RGL cells into astrocytes was unlikely to take place. To evaluate whether astrocytes were derived instead through cell divisions, we analyzed BrdU-injected mice at 17 dpi (Figure 3L) and confirmed a higher percentage of mature astrocytes among the BrdU+YFP+ cells in *COUP-TFI-icKO<sup>Glast</sup>* DG compared with controls (Figure 4I).

Beside the RGL cell population, we also observed that the *Glast-CreERT2* line triggered recombination in mature astrocytes (expressing Sox2, GFAP, and S100B; Seri et al., 2004; Steiner et al., 2004; Venere et al., 2012), which are scattered in the DG GCL, hilus, and molecular cell layer (MCL), where COUP-TFI is also expressed (Figures S4G and S4H). Thus, *COUP-TFI* depletion in mature astrocytes could directly contribute to the observed increase in DG astroglial fate, possibly by “re-awakening” astrocyte proliferative capabilities *in vivo*. We thus checked their ability to re-enter the cell cycle by a short-term BrdU injection protocol (1 dpi) after TAM-dependent recombination (Figure S4I). In both *Ctrl<sup>Glast</sup>* and *COUP-TFI-icKO<sup>Glast</sup>* DG, GFAP+YFP+ astrocytes localized in the GCL and MCL failed to incorporate BrdU, and all proliferating cells were confined to the stem cell niche (Figure S4J). In addition, no differences in the density of double GFAP+YFP+ astrocytes were found between mutant and control hippocampal CA1 regions, where normally COUP-TFI is highly expressed (Figures S4K–S4M). Finally, no proliferating Ki67+ astrocytes were also detected (Figure S4N), thus excluding hippocampal mature astrocyte re-activation in *COUP-TFI-icKO<sup>Glast</sup>* mice.

Overall, these findings indicate that loss of COUP-TFI in RGL cells and their progeny promotes an astroglial fate at the expense of a neurogenic one. Thus, COUP-TFI acts primordially in the fate decision between neuronal and astroglial lineages within adult NSCs/progenitors.

### COUP-TFI Is Necessary in Adult DG Progenitors to Promote Neurogenesis by Repressing Astroglial Fate

To further demonstrate a direct role for COUP-TFI in repressing astroglial fate in the adult DG niche, COUP-TFI function was exclusively deleted in activated NSCs and early committed neurogenic progenitors (type 2a) by taking advantage of the *Ascl1-CreERT2* mouse line (Figures 5A, 5B, S5A, and S5B) (Battiste et al., 2007). Ten days after TAM administration, only rare triple GFAP+Sox2+YFP+ mature astrocytes (Figures 5C and 5E), accounting for less than 3% of the YFP+ population (Table S1), were observed in *Ctrl<sup>Ascl1</sup>* mice, demonstrating a predominantly neurogenic fate of the *Ascl1* lineage. Notably, *COUP-TFI-icKO<sup>Ascl1</sup>* DG showed a drastic increase in YFP+ *Ascl1*-derived astrocytes (Figures 5D and 5E; Table S1). These cells, unambiguously distinguishable from RGL cells, showed a polarized morphology, with their soma localized mostly in the deep GCL (Figure 5D, left). We also observed some YFP+ astrocytes in the most superficial GCL depicting a mature morphology (Figure 5D, right) and expressing S100B (Figure 5F). A significant decrease in DG YFP+ neuroblasts/immature neurons, both in terms of double DCX+YFP+ cell density and as percentage of DCX+ cells among the YFP+ population, was also assessed in *COUP-TFI-icKO<sup>Ascl1</sup>* mice compared with control ones (Figures 5G and 5H; Table S1). This indicates that COUP-TFI is necessary to promote neurogenesis by repressing an astroglial fate not only in NSCs but also in neurogenic type2a progenitors.

To further confirm a cell-intrinsic role of COUP-TFI in driving cell fate choice in neurogenic progenitors, we directly targeted mitotically active cells by stereotaxically injecting a retrovirus expressing *Cre-recombinase* (RV-Cre) (Rolando et al., 2016) in the DG of either *Rosa26-YFP;COUP-TFI<sup>fl/fl</sup>* mice (*cKO<sup>RV-Cre</sup>*) or, as controls, in the *Rosa26-YFP* reporter line alone (*Ctrl<sup>RV-Cre</sup>*) (Figures 5I and S5C). Two days after retroviral injection, densities of YFP+ cells were similar in the two genotypes (Figure S5D), while the percentage of double COUP-TFI+YFP+ cells dramatically dropped in *cKO<sup>RV-Cre</sup>* mice (Figure S5E). At this time, the large majority of YFP+ cells were progenitors/neuroblasts, and there were no differences between *cKO<sup>RV-Cre</sup>* and *Ctrl<sup>RV-Cre</sup>* mice (Figure S5F). Remarkably, at longer survival time (i.e., 18 dpi; Figure 5J), we observed an increase in double GFAP+YFP+ astrocytes and an equivalent reduction in double DCX+YFP+ newborn neurons in *cKO<sup>RV-Cre</sup>* compared with *Ctrl<sup>RV-Cre</sup>* mice, with no changes in the total amount of YFP+ cells (Figures 5K–5N and S5G). These findings strongly support a direct involvement of COUP-TFI in repressing an astroglial fate in neurogenic progenitors.

### Forced COUP-TFI Expression Prevents Astroglial Fate in the Healthy DG and Rescues Altered Neuron-to-Astrocyte Generation upon Neuroinflammation

To understand whether COUP-TFI is not only necessary but also sufficient to suppress astroglial fate in adult

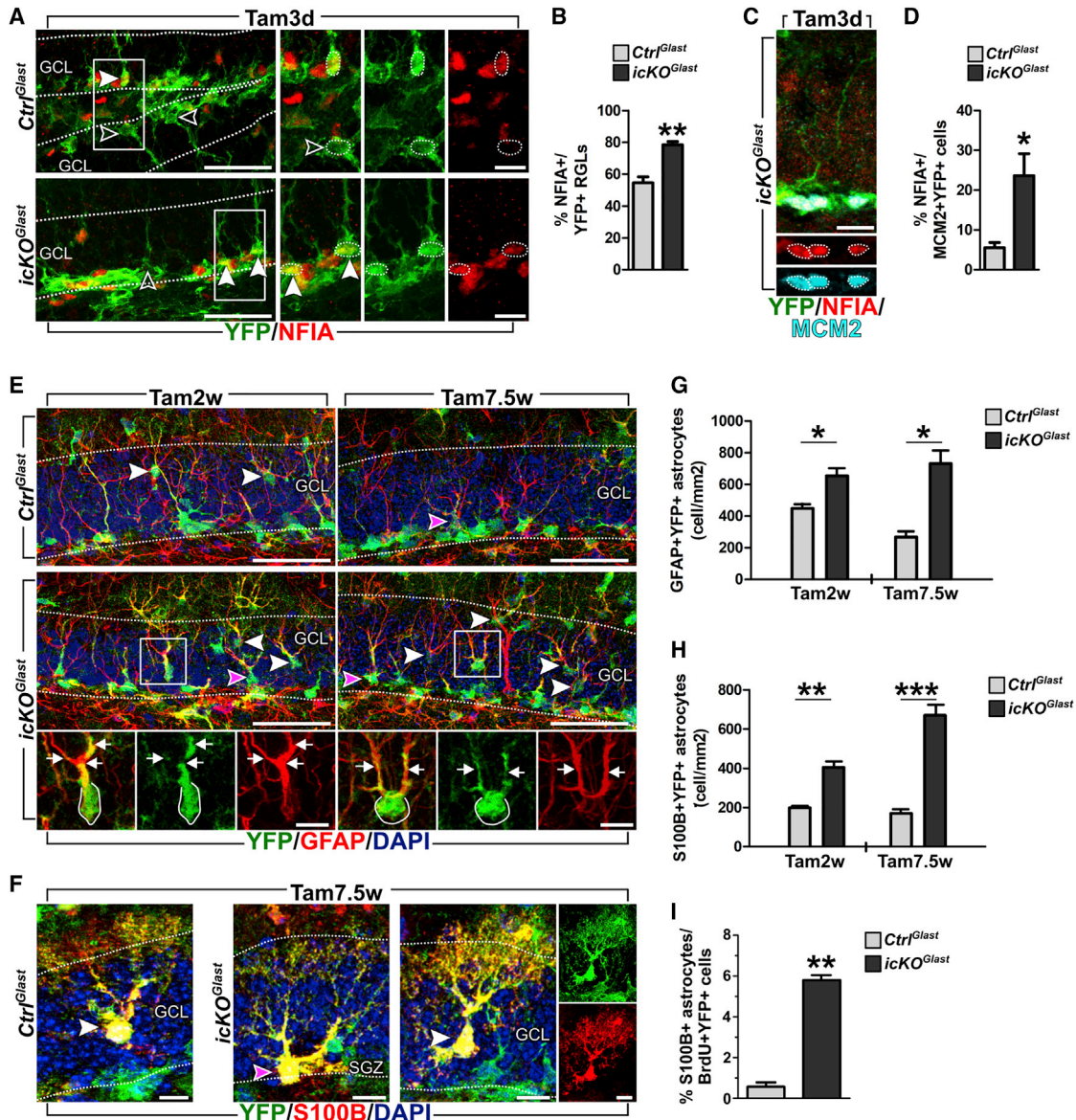


**Figure 4. Loss of COUP-TFI Function Promotes Astrogligenic Potential in Adult DG RGL Cells**

(A–D) Refer to experimental strategy shown in Figure 3B.

(A) Confocal images of double immunofluorescence for YFP (green) and NFIA (red) in *Ctrl<sup>Glast</sup>* and *COUP-TFI-icKO<sup>Glast</sup>* DG. Full arrowheads show double YFP+NFIA+ RGL cells; empty arrowheads show YFP+ RGL cells negative for NFIA.

(B) Quantification of NFIA+ nuclei among YFP+ RGL cells within the GCL/SGZ of *Ctrl<sup>Glast</sup>* and *COUP-TFI-icKO<sup>Glast</sup>* mice (n = 89 of 162 YFP+ cells in *Ctrl<sup>Glast</sup>*; n = 90 of 115 YFP+ cells in *COUP-TFI-icKO<sup>Glast</sup>*).

(C) Confocal image of triple-labeled YFP (green), NFIA (red), and MCM2 (cyan) cells in *COUP-TFI-icKO<sup>Glast</sup>* DG.

(D) Quantification of NFIA+ cells among double MCM2+YFP+ proliferating progenitors within the GCL/SGZ of *Ctrl<sup>Glast</sup>* and *COUP-TFI-icKO<sup>Glast</sup>* DG (n = 16 of 273 YFP+ cells in *Ctrl<sup>Glast</sup>*; n = 54 of 222 YFP+ cells in *COUP-TFI-icKO<sup>Glast</sup>*).

(E–H) Refer to experimental strategy shown in Figure 3E.

(E) Confocal images of double GFAP+YFP+ astrocytes in *Ctrl<sup>Glast</sup>* and *COUP-TFI-icKO<sup>Glast</sup>* DG at Tam2w and Tam7.5w.

(F) Confocal images of mature double S100B+YFP+ astrocytes in *Ctrl<sup>Glast</sup>* and *COUP-TFI-icKO<sup>Glast</sup>* at Tam7.5w.

(G and H) Quantification of double GFAP+YFP+ (G) and S100B+YFP+ (H) mature astrocytes within the SGZ/GCL in *Ctrl<sup>Glast</sup>* and *COUP-TFI-icKO<sup>Glast</sup>* at Tam2w and Tam7.5w.

(I) Histogram showing the fraction of newborn S100B+ astrocytes among all BrdU+YFP+ cells within the SGZ/GCL of *Ctrl<sup>Glast</sup>* and *COUP-TFI-icKO<sup>Glast</sup>* at 17 dpi (refers to protocol in Figure 3L; n = 4 of 198 in *Ctrl<sup>Glast</sup>*; n = 15 of 217 in *COUP-TFI-icKO<sup>Glast</sup>*).

In (E) and (F), white arrowheads indicate bushy mature astrocytes, while pink arrowheads indicate more polarized astrocytes, whose cell bodies are located in the SGZ. N = 3 or 4 mice/genotype/time point. Error bars indicate SEM. Scale bars, 50  $\mu$ m (A and E), 10  $\mu$ m (C), and 10  $\mu$ m (A and E insets). Student's t test: \*p < 0.05, \*\*p < 0.01, and \*\*\*p < 0.001. See also Figure S4.



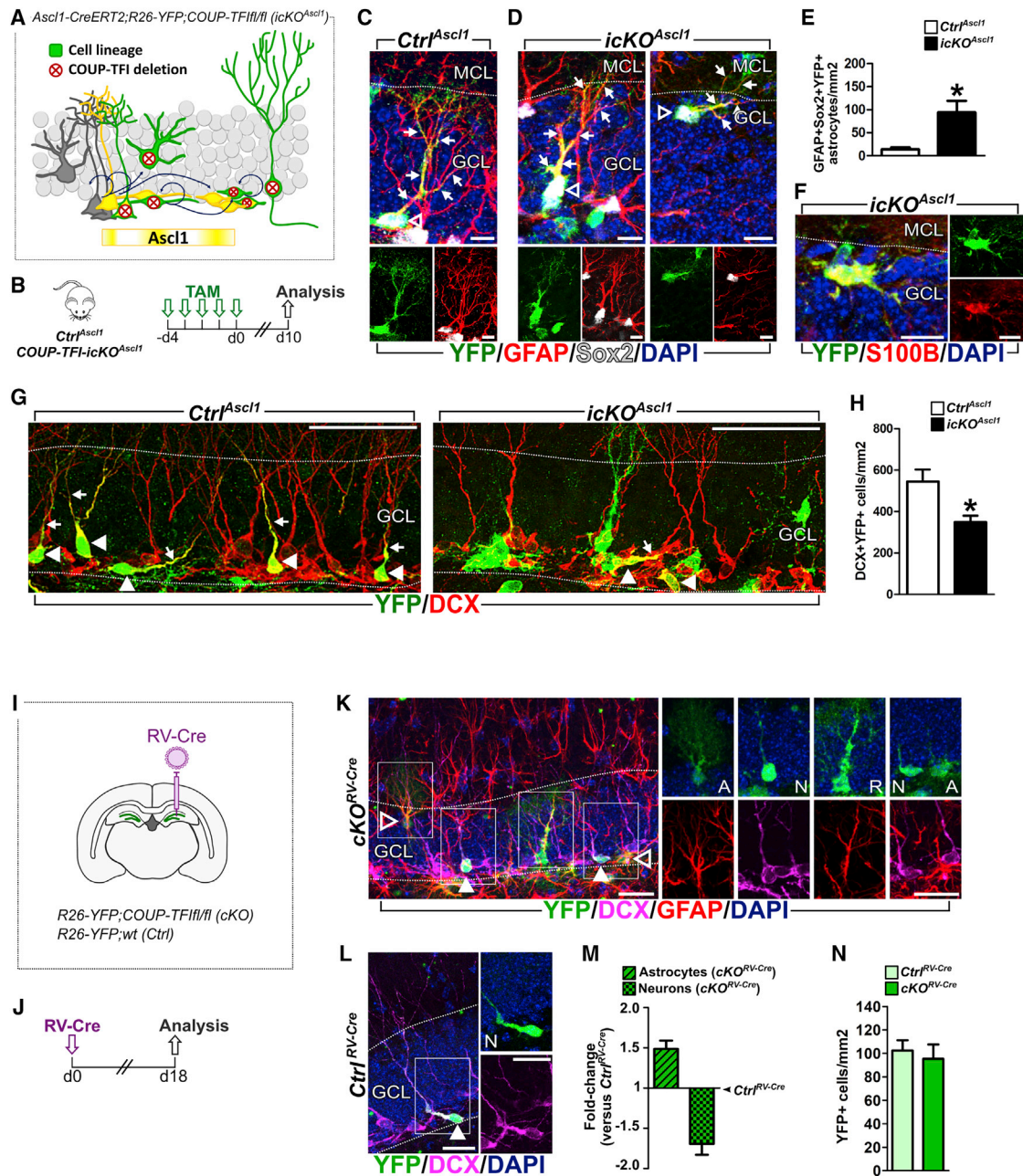


**Figure 5. COUP-TFI Is Necessary in Adult DG Progenitors to Promote Neurogenesis by Repressing Astrogliogenesis**

(A) Schema illustrating *COUP-TFI* deletion (red crossed circles) in the cell progeny (green) derived from *Ascl1*-expressing cells (yellow) in the DG upon TAM induction in *COUP-TFI-icKO*<sup>*Ascl1*</sup> mice.  
 (B) Experimental design to assess the effects of *COUP-TFI* deletion in the *Ascl1*-lineage (see C–H).  
 (C and D) Confocal images showing triple GFAP+Sox2+YFP+ newborn astrocytes in the DG of *Ctrl*<sup>*Ascl1*</sup> (C) and *COUP-TFI-icKO*<sup>*Ascl1*</sup> (D) mice. DAPI counterstaining (blue).  
 (E) Quantification of GFAP+Sox2+YFP+ newborn astrocytes within the SGZ/GCL of *Ctrl*<sup>*Ascl1*</sup> and *COUP-TFI-icKO*<sup>*Ascl1*</sup> DG.  
 (F) Confocal image of a mature S100B+YFP+ astrocyte in the GCL of *COUP-TFI-icKO*<sup>*Ascl1*</sup> DG.  
 (G) Confocal images of DG sections stained for DCX (red) and YFP (green) in *Ctrl*<sup>*Ascl1*</sup> and *COUP-TFI-icKO*<sup>*Ascl1*</sup> mice.  
 (H) Quantification of DCX+YFP+ newborn neurons within the SGZ/GCL of *Ctrl*<sup>*Ascl1*</sup> and *COUP-TFI-icKO*<sup>*Ascl1*</sup> DG.  
 (I) Experimental strategy used for *COUP-TFI* loss-of-function in dividing DG neural progenitors by Cre-expressing retrovirus (RV-Cre) stereotaxic injection (see K–N).  
 (J) Experimental design for RV-Cre injection and analysis of newborn cell phenotype.

(legend continued on next page)

NSCs/progenitors, we adopted a gain-of-function approach using *Glast-CreERT2;Rosa26-YFP;lox-stop-lox-hCOUP-TFI* mice (*COUP-TFI-O/E<sup>Glast</sup>*). In these mice, COUP-TFI is overexpressed in RGL cells and their lineage upon Cre-mediated inducible recombination (Figures 6A and S6A) (Alfano et al., 2014; Parisot et al., 2017; Wu et al., 2010). Two weeks after TAM treatment, the density of GFAP+YFP+ astrocytes within the SGZ/GCL of *COUP-TFI-O/E<sup>Glast</sup>* was reduced by half compared with controls (Figures 6C and 6D; Table S1). This likely reflects impaired astrogliogenesis upon COUP-TFI overexpression. Indeed, while in control animals GFAP+YFP+ astrocytes within the SGZ/GCL doubled between 2 and 14 days after TAM, the density of astrocytes in the *COUP-TFI-O/E<sup>Glast</sup>* mice at 14 days was comparable with that of controls at 2 days after TAM (Figures S6B–S6D). Moreover, we did not observe changes between genotypes in the total YFP+ population and YFP+ RGL cells (Figures S6E and S6F), as well as in YFP+ astrocytes outside of the DG neurogenic compartment (i.e., MCL; Figure S6G). On the whole, these data point to reduced astrogliogenesis in the presence of high COUP-TFI expression in RGL cells and their progeny.

Neurogenesis did not significantly change in *COUP-TFI-O/E<sup>Glast</sup>* DG (Figures 6E and 6F). However, we found an increase in the density of caspase-3+NeuroD+YFP+ cells in mutant DG compared with controls, indicating induced apoptosis in newborn neurons that accounted for all DG caspase-3+YFP+ cells (Figures S6H–S6J). Considering high endogenous COUP-TFI protein levels in neuronal progenitors/neuroblasts (Figures 2E and 2F), its forced overexpression might induce an apoptotic pathway within the neuronal lineage.

In light of our previously described COUP-TFI downregulation within the adult DG upon acute LPS-induced neuroinflammation (Figure 1), we finally wondered whether forcing COUP-TFI expression in this condition could prevent enhanced astrogliogenesis and rescue neurogenesis. To this aim, we stereotactically injected the retrovirus RV-Cre in the DG of adult *COUP-TFI-O/E<sup>RV-Cre</sup>* and relative controls (*Ctrl<sup>RV-Cre</sup>*) and treated mice with LPS 1 day later for 4 days (Figures 6G, 6H, and S6K–S6M). Two weeks after RV-Cre injection, we found comparable densities of YFP+ recombined cells within the SGZ/GCL compartment of saline- or LPS-treated *Ctrl<sup>RV-Cre</sup>* and LPS-treated *COUP-TFI-O/E<sup>RV-Cre</sup>* mice (Figure 6I). However, LPS-treated *Ctrl<sup>RV-Cre</sup>* mice showed a 2-fold increase in GFAP+YFP+ astrocytes and a reduction in DCX+YFP+ newborn neurons versus saline-treated *Ctrl<sup>RV-Cre</sup>* animals (Figures 6J and S6K–S6M). Notably, LPS-induced effects were completely reverted by COUP-TFI gain-of-function (Figures 6J and S6M). Indeed, the percentages of newborn astrocytes and neurons were respectively lower and higher in LPS-treated *COUP-TFI-O/E<sup>RV-Cre</sup>* mice compared with both LPS- and saline-treated *Ctrl<sup>RV-Cre</sup>* mice (Figures S6K and S6L). These data demonstrate that forced

COUP-TFI expression in adult neural progenitors is sufficient to rescue the imbalance in newborn neuron-to-astrocyte ratio during neuroinflammation.

## DISCUSSION

The lifelong production and integration of new DG granule neurons are considered an extreme form of plasticity in the adult brain, which contributes to learning and memory (Gonçalves et al., 2016). Adult DG NSCs give rise to newborn neurons, but they also produce astrocytes, whose function and generation are not as well characterized (Bond et al., 2015). The fate choice between a neuron and an astrocyte in NSCs is subject to dynamic modulation through extrinsic signals. Indeed, decreased neurogenesis paralleled by increased generation of astrocytes is a feature observed in mouse models of neuroinflammation (Kohman and Rhodes, 2013); this imbalance could contribute to the inflammation-associated cognitive impairments, possibly by remodeling neural circuits and acting on memory consolidation (Valero et al., 2014). Thus, understanding NSC cell-intrinsic responses to inflammation might be crucial not only to elucidate the mechanisms of how NSCs react to tissue damage but also to shed light on the regulatory functions occurring in physiological conditions.

Although significant progress has been made in understanding extrinsic and intrinsic cues regulating adult NSC activity in vertebrates, little was known on the transcriptional program controlling astroglial versus neuronal fate choice of adult hippocampal NSCs/progenitors. In this study, we unraveled an unexpected role for the transcriptional regulator COUP-TFI in balancing neuro- and astrogliogenesis within the adult DG. First, we showed that this transcription factor is widely expressed in the healthy DG and that its protein level increases from radial NSCs to neuronal committed progenitors/neuroblasts, in accordance with a recent DG single-cell gene expression analysis (Artegiani et al., 2017). Furthermore, through loss- and gain-of-function approaches, we provided evidence that COUP-TFI is both necessary and sufficient to inhibit an astroglial fate and to drive adult NSCs/progenitors toward a neuronal lineage in the hippocampal neurogenic niche. This is supported by the increased expression of the pro-astrogliogenic transcription factor NFIA not only in NSCs but also in mitotically active progenitors of *COUP-TFI-icKO<sup>Glast</sup>* DG. Moreover, loss of COUP-TFI function directly in DG progenitors prompted these cells to acquire an astroglial fate indicating they might still be multipotent, as also recently suggested (Harris et al., 2018) and need COUP-TFI to restrict their potential to a neuronal fate. We thus hypothesized that the increase in astroglia at the expense of newborn neurons observed in the adult DG upon inflammation could be related to COUP-TFI downregulation. Reduced COUP-TFI levels

(K and L) Confocal images of multiple staining for YFP (green), DCX (magenta), GFAP (red), and DAPI counterstaining (blue) in sections from *COUP-TFI-cKO<sup>RV-Cre</sup>* (K) and *Ctrl<sup>RV-Cre</sup>* (L) DG. A, newborn astrocyte; N, newborn neuron; R, RGL cell.

(M) Histogram showing the fold change in densities of newborn GFAP+YFP+ astrocytes (striped pattern) and DCX+YFP+ newborn neurons (checkerboard pattern) within the SGZ/GCL of *COUP-TFI-cKO<sup>RV-Cre</sup>* mice compared with *Ctrl<sup>RV-Cre</sup>* mice.

(N) Quantification of total YFP+ cells within the SGZ/GCL of *Ctrl<sup>RV-Cre</sup>* and *COUP-TFI-cKO<sup>RV-Cre</sup>* DG. Student's t test:  $p = 0.6630$ .

N = 3 or 4 animals per genotype. Empty arrowheads indicate astrocyte cell bodies, full arrowheads indicate neurons and arrows indicate cellular processes. Error bars indicate SEM. MCL, molecular cell layer. Scale bars, 10  $\mu\text{m}$  (C, D, and F), 50  $\mu\text{m}$  (G), and 20  $\mu\text{m}$  (K and L). Student's t test: \* $p < 0.05$ . See also Figure S5.



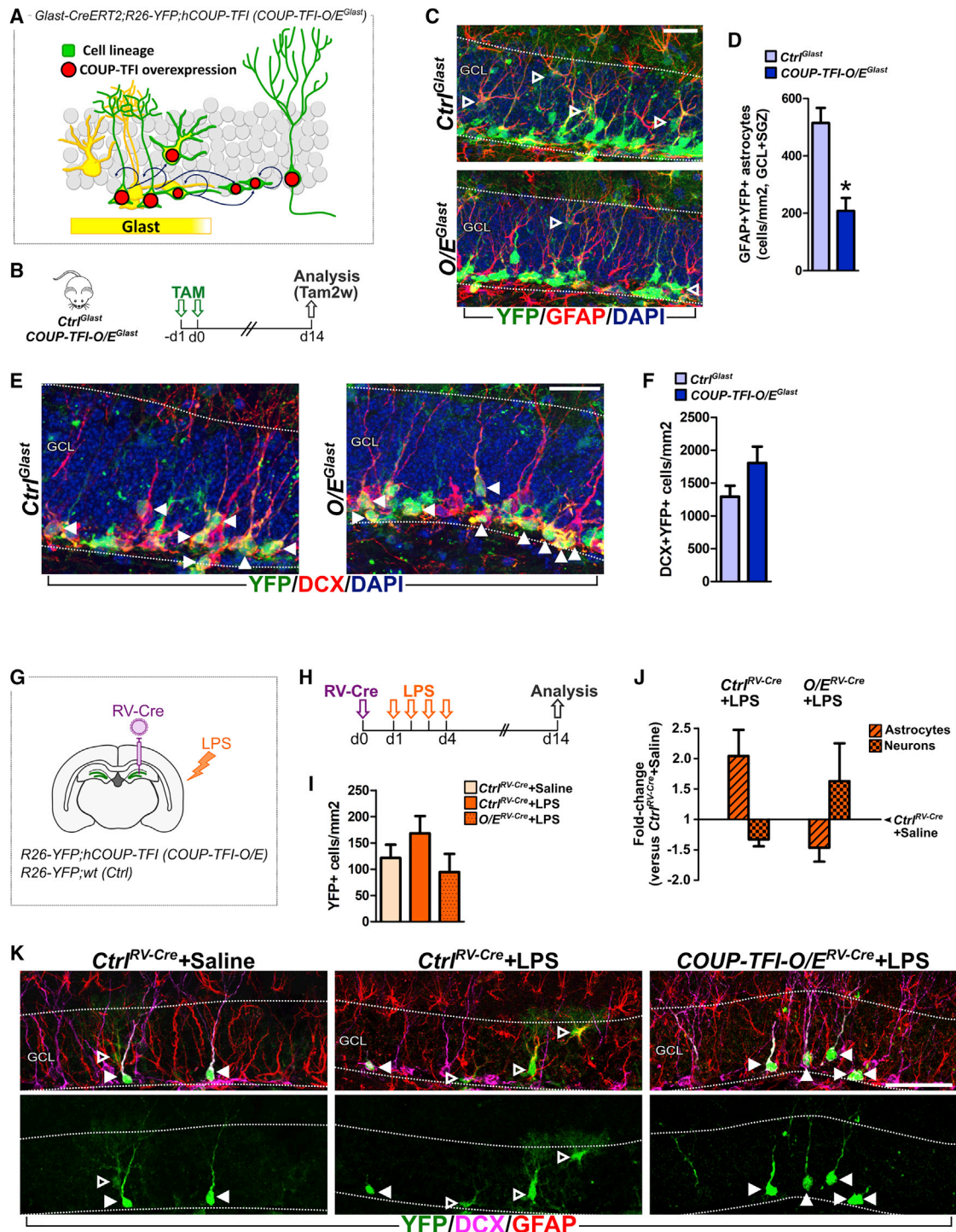


**Figure 6. Forced COUP-TFI Expression Prevents Astrogliogenesis in the Healthy DG and Rescues Altered Neuron-Astroglia Generation upon Neuroinflammation**

(A) Schema illustrating COUP-TFI overexpression (red circles) in the cell progeny (green) derived from *Glast*-expressing cells (yellow) in the DG upon TAM induction in *COUP-TFI-O/E<sup>Glast</sup>* adult mice.

(B) Experimental design to assess the effects of COUP-TFI overexpression in the *Glast*-lineage (see C–F).

(C) Confocal images of DG sections immunostained for YFP (green) and GFAP (red) with DAPI counterstaining (blue) in *Ctrl<sup>Glast</sup>* and *COUP-TFI-O/E<sup>Glast</sup>* mice.

(D) Quantification of double GFAP+YFP+ astrocytes within the SGZ/GCL of *Ctrl<sup>Glast</sup>* and *COUP-TFI-O/E<sup>Glast</sup>* DG at Tam2w.

(E) Confocal images of DG sections immunostained for YFP (green) and DCX (red) with DAPI counterstaining (blue) in *Ctrl<sup>Glast</sup>* and *COUP-TFI-O/E<sup>Glast</sup>* mice.

(legend continued on next page)

would release a normally strong repression of a gliogenic fate in NSCs and progenitors. Indeed, our data showed that forced COUP-TFI expression in mitotically active progenitors is sufficient to prevent LPS-induced astrogliogenesis, revealing a potential role for COUP-TFI in protecting the adult neural niche from inflammatory insults.

The persistence of neurogenesis within the adult brain has been suggested to result from the action of several neurogenic factors counteracting a gliogenic environment (Götz et al., 2016). In this perspective, we propose that COUP-TFI might exert its neurogenic function by cell-intrinsically repressing a “default” astrogliogenic fate within the adult neurogenic niche. A transcriptional repressive role for COUP-TFI has also been described during pallial, subpallial (Alfano et al., 2014; Faedo et al., 2008; Lodato et al., 2011; Tomassy et al., 2010), and eye development (Inoue et al., 2010; Tang et al., 2010) in the mouse, but also in *C. elegans* and *Drosophila* (Mlodzik et al., 1990; Zhou and Walthall, 1998). In this study, we demonstrate that COUP-TFI acts as molecular “sensor” in the adult DG neurogenic niche by responding to external cues and allowing multipotent NSCs/progenitors to take either an astroglial or a neuronal lineage. Understanding how NSCs/progenitors can integrate environmental signals via COUP-TFI and/or other factors, and identifying the molecular pathways downstream of their activity deserves further investigations.

## EXPERIMENTAL PROCEDURES

### Animals and Treatments

All experiments were performed on 2- to 4-month-old C57BL/6J mice of both genders (Charles River). *Glast-CreERT2+/wt;R26-YFP+<sup>+</sup>;COUP-TFIfl/fl* (COUP-TFI-*icKO*<sup>Glast</sup>), *Glast-CreERT2+/wt;R26-YFP+<sup>+</sup>;COUP-TFIwt/wt* (*Ctrl*<sup>Glast</sup>), *Ascl1-CreERT2+/wt;R26-YFP+<sup>+</sup>;COUP-TFIfl/fl* (COUP-TFI-*icKO*<sup>Ascl1</sup>), *Ascl1-CreERT2+/-;R26-YFP+<sup>+</sup>;COUP-TFIwt/wt* (*Ctrl*<sup>Ascl1</sup>), and *Glast-CreERT2+/-;R26-YFP+<sup>+</sup>;hCOUP-TFI+<sup>+</sup>/wt* (COUP-TFI-*O/E*<sup>Glast</sup>) were used for *in vivo* loss- and gain-of-function experiments obtained upon TAM (2.5 mg/mouse/day) administration. Subgroups of these mice also received the thymidine analog 5-bromo-2-deoxyuridine (BrdU; 100 mg/kg; two i.p. injections, 8 hr apart for the 3 and 17 dpi survival experiments, or three i.p. injections, 2 hr apart the day before sacrifice for the proliferation experiment). *R26-YFP+<sup>+</sup>;COUP-TFIfl/fl* (COUP-TFI-*CKO*<sup>RV-Cre</sup>), *R26-YFP+<sup>+</sup>;COUP-TFIwt/wt* (*Ctrl*<sup>RV-Cre</sup>), and *R26-YFP+<sup>+</sup>;hCOUP-TFI+<sup>+</sup>/wt* (COUP-TFI-*O/E*<sup>RV-Cre</sup>) were used for loss- and gain-of-function experiments obtained by RV-Cre stereotaxic injections within the adult DG. For neuroinflammation experiments, mice received *E. coli*-derived LPS (0.5 mg/kg/day) or saline solution (0.9%) as a single i.p. injection for 1 day or 4 consecutive days. Mice were housed under standard laboratory conditions. See the [Supplemental Experimental Procedures](#). All procedures were conducted in accordance with the Guide for the Care and Use of Laboratory Animals of the European Community Council

Directives (2010/63/EU and 86/609/EEC) and approved by local bioethics committees, the Italian Ministry of Health, and the French Ministry for Higher Education and Research.

### Tissue Collection, RNA Extraction, and RT-qPCR

Hippocampi from adult mice perfused with ice-cold PBS were microdissected and lysed. RNA isolation, cDNA synthesis, and RT-qPCR were performed according to the manufacturer's instructions. See the [Supplemental Experimental Procedures](#).

### Microscope Analysis and Cell Counting

Representative images showing COUP-TFI *in situ* hybridization (ISH) and immunohistochemistry (IHC) were taken on a Nikon microscope coupled to NeuroLucida software. Images of double- or triple-immunolabeled sections were acquired using a TCS SP5 confocal microscope (Leica), and multi-stack images were then analyzed with ImageJ (NIH). At least three different levels along the rostral-caudal DG axis were analyzed and cell densities are expressed as cells per square millimeter. See the [Supplemental Experimental Procedures](#).

### Statistical Analysis

Statistical comparisons were conducted using two-tailed unpaired Student's t test or one-way ANOVA and the Bonferroni *post-hoc* test when appropriate (in Microsoft Excel and GraphPad Prism5). For unpaired Student's t test, Levene's test was conducted to compare variances, and Welch's correction was applied in case of unequal variance distribution. Significance was established at  $p < 0.05$ . Cell counts are presented as mean  $\pm$  SEM ( $n \geq 3$  animals per each quantification).

## SUPPLEMENTAL INFORMATION

Supplemental Information includes Supplemental Experimental Procedures, six figures, and one table and can be found with this article online at <https://doi.org/10.1016/j.celrep.2018.06.044>.

## ACKNOWLEDGMENTS

We thank M. Götz for the *Glast-CreERT2*, J. Johnson for the *Ascl1-CreERT2*, S. Srinivas for the *R26-YFP*, and S.P. Wu and M.J. Tsai for the *lox-stop-lox-hCOUP-TFI* mouse lines. We also thank C. Giachino, P. Peretto, and V. Taylor for their suggestions and comments on the manuscript. This work was supported by Università degli Studi di Torino (UNITO ex 60%) to S.D.M.; Fondation Recherche Médicale (FRM) grant DEQ20150331750 and Agence Nationale de la Recherche (ANR) “Investments for the Future” LabEx SIGNALIFE (grant ANR-11-LABX-0028-01) to M.S.; ANR “Investments for the Future” and LabEx INRT (grants ANR-10-IDEX-0002-02 and ANR-10-LABX-0030-INRT) to A.P.-D. and W.K.; Università Italo-Francese (UIF) (Galileo Project grant G-14-96) to S.D.M. and M.S.; a Fondazione Umberto Veronesi Postdoctoral Fellowship (2018), a Fyssen Foundation Postdoctoral Fellowship (2016–2017), and a Ministero Affari Esteri (MAE) mobility grant 2014 to S.B.; and Institut de Génétique et de Biologie Moléculaire et Cellulaire (IGBMC) international PhD program fellowship by LabEx INRT to A.P.-D.

(F) Quantification of double DCX+YFP+ neurons within the SGZ/GCL of *Ctrl*<sup>Glast</sup> and *COUP-TFI-O/E*<sup>Glast</sup> at Tam2w. Student's t test:  $p = 0.1619$ .

(G) Experimental strategy to induce COUP-TFI gain of function in diving neural progenitors by Cre-expressing retrovirus (RV-Cre) stereotaxic injection in LPS-treated mice.

(H) Experimental design for analyzing newborn cell phenotype on inflamed RV-Cre injected *COUP-TFI-O/E* DG.

(I) Quantification of YFP+ cells within the SGZ/GCL of *Ctrl*<sup>RV-Cre+Saline</sup>, *Ctrl*<sup>RV-Cre+LPS</sup>, and *COUP-TFI-O/E*<sup>RV-Cre+LPS</sup> mice. One-way ANOVA:  $F_{(2,8)} = 1.4546$ ,  $p = 0.2892$ , with Bonferroni *post-hoc*-test: *Ctrl*<sup>RV-Cre+Saline</sup> versus *Ctrl*<sup>RV-Cre+LPS</sup> versus *COUP-TFI-O/E*<sup>RV-Cre+LPS</sup>,  $p > 0.05$ .

(J) Histogram showing the fold change in densities of newborn GFAP+YFP+ astrocytes (striped pattern) and DCX+YFP+ newborn neurons (checkerboard pattern) within the SGZ/GCL of *Ctrl*<sup>RV-Cre+LPS</sup> and *COUP-TFI-O/E*<sup>RV-Cre+LPS</sup> mice normalized to *Ctrl*<sup>RV-Cre+Saline</sup>.

(K) Confocal images of DG sections immunostained for YFP (green), DCX (magenta), and GFAP (red) in *Ctrl*<sup>RV-Cre+Saline</sup>, *Ctrl*<sup>RV-Cre+LPS</sup>, and *COUP-TFI-O/E*<sup>RV-Cre+LPS</sup> mice.

$N = 3$  or 4 animals per genotype. Empty arrowheads indicate astrocyte cell bodies and full arrowheads indicate neurons. Error bars indicate SEM. Scale bars, 20  $\mu$ m (C and E) and 50  $\mu$ m (K). Student's t test: \* $p < 0.05$ . See also [Figure S6](#).

## AUTHOR CONTRIBUTIONS

S.B., S.D.M., and M.S. conceptualized and planned the research. W.K. contributed to conceptualizing and planning experiments concerning inflammation. S.B., S.D.M., and I.C. conducted the research. A.P.-D. performed mRNA sampling and RT-qPCR experiments. C.R. provided the RV-Cre. S.B., S.D.M., I.C., and A.P.-D. analyzed data. S.B., S.D.M., and M.S. wrote the paper.

## DECLARATION OF INTERESTS

The authors declare no competing interests.

Received: August 17, 2017

Revised: April 30, 2018

Accepted: June 11, 2018

Published: July 10, 2018

## REFERENCES

- Al-Kateb, H., Shimony, J.S., Vineyard, M., Manwaring, L., Kulkarni, S., and Shihawi, M. (2013). NR2F1 haploinsufficiency is associated with optic atrophy, dysmorphism and global developmental delay. *Am. J. Med. Genet. A* 161A, 377–381.
- Alfano, C., Viola, L., Heng, J.I.-T., Pirozzi, M., Clarkson, M., Flore, G., De Maio, A., Schedl, A., Guillemot, F., and Studer, M. (2011). COUP-TFI promotes radial migration and proper morphology of callosal projection neurons by repressing Rnd2 expression. *Development* 138, 4685–4697.
- Alfano, C., Magrinelli, E., Harb, K., Hevner, R.F., and Studer, M. (2014). Post-mitotic control of sensory area specification during neocortical development. *Nat. Commun.* 5, 5632.
- Andersen, J., Urbán, N., Achimastou, A., Ito, A., Simic, M., Ullom, K., Martynoga, B., Lebel, M., Göritz, C., Frisén, J., et al. (2014). A transcriptional mechanism integrating inputs from extracellular signals to activate hippocampal stem cells. *Neuron* 83, 1085–1097.
- Armentano, M., Chou, S.-J., Tomassy, G.S., Leingärtner, A., O'Leary, D.D.M., and Studer, M. (2007). COUP-TFI regulates the balance of cortical patterning between frontal/motor and sensory areas. *Nat. Neurosci.* 10, 1277–1286.
- Artegiani, B., Lyubimova, A., Muraro, M., van Es, J.H., van Oudenaarden, A., and Clevers, H. (2017). A single-cell RNA sequencing study reveals cellular and molecular dynamics of the hippocampal neurogenic niche. *Cell Rep.* 21, 3271–3284.
- Barkho, B.Z., Song, H., Aimone, J.B., Smrt, R.D., Kuwabara, T., Nakashima, K., Gage, F.H., and Zhao, X. (2006). Identification of astrocyte-expressed factors that modulate neural stem/progenitor cell differentiation. *Stem Cells Dev.* 15, 407–421.
- Battiste, J., Helms, A.W., Kim, E.J., Savage, T.K., Lagace, D.C., Mandyam, C.D., Eisch, A.J., Miyoshi, G., and Johnson, J.E. (2007). *Ascl1* defines sequentially generated lineage-restricted neuronal and oligodendrocyte precursor cells in the spinal cord. *Development* 134, 285–293.
- Bertacchi, M., Parisot, J., and Studer, M. (2018). The pleiotropic transcriptional regulator COUP-TFI plays multiple roles in neural development and disease. *Brain Res.* Published online April 27, 2018. <https://doi.org/10.1016/j.brainres.2018.04.024>.
- Bonaguidi, M.A., Wheeler, M.A., Shapiro, J.S., Stadel, R.P., Sun, G.J., Ming, G.L., and Song, H. (2011). In vivo clonal analysis reveals self-renewing and multipotent adult neural stem cell characteristics. *Cell* 145, 1142–1155.
- Bond, A.M., Ming, G.L., and Song, H. (2015). Adult mammalian neural stem cells and neurogenesis: five decades later. *Cell Stem Cell* 17, 385–395.
- Bosch, D.G.M., Boonstra, F.N., Gonzaga-Jauregui, C., Xu, M., de Ligt, J., Jhangiani, S., Wiszniewski, W., Muzny, D.M., Yntema, H.G., Pfundt, R., et al.; Baylor-Hopkins Center for Mendelian Genomics (2014). NR2F1 mutations cause optic atrophy with intellectual disability. *Am. J. Hum. Genet.* 94, 303–309.
- Bovetti, S., Bonzano, S., Garzotto, D., Giannelli, S.G., Iannielli, A., Armentano, M., Studer, M., and De Marchis, S. (2013). COUP-TFI controls activity-dependent tyrosine hydroxylase expression in adult dopaminergic olfactory bulb interneurons. *Development* 140, 4850–4859.
- DeCarolis, N.A., Mechanic, M., Petrik, D., Carlton, A., Ables, J.L., Malhotra, S., Bachoo, R., Götz, M., Lagace, D.C., and Eisch, A.J. (2013). In vivo contribution of nestin- and GLAST-lineage cells to adult hippocampal neurogenesis. *Hippocampus* 23, 708–719.
- Encinas, J.M., Michurina, T.V., Peunova, N., Park, J.-H., Tordo, J., Peterson, D.A., Fishell, G., Koulakov, A., and Enikolopov, G. (2011). Division-coupled astrocytic differentiation and age-related depletion of neural stem cells in the adult hippocampus. *Cell Stem Cell* 8, 566–579.
- Faedo, A., Tomassy, G.S., Ruan, Y., Teichmann, H., Krauss, S., Pleasure, S.J., Tsai, S.Y., Tsai, M.-J., Studer, M., and Rubenstein, J.L.R. (2008). COUP-TFI coordinates cortical patterning, neurogenesis, and laminar fate and modulates MAPK/ERK, AKT, and beta-catenin signaling. *Cereb. Cortex* 18, 2117–2131.
- Flore, G., Di Ruberto, G., Parisot, J., Sannino, S., Russo, F., Illingworth, E.A., Studer, M., and De Leonibus, E. (2016). Gradient COUP-TFI expression is required for functional organization of the hippocampal septo-temporal longitudinal axis. *Cereb. Cortex* 27, 1629–1643.
- Gao, Z., Ure, K., Ables, J.L., Lagace, D.C., Nave, K.-A., Goebbels, S., Eisch, A.J., and Hsieh, J. (2009). *Neurod1* is essential for the survival and maturation of adult-born neurons. *Nat. Neurosci.* 12, 1090–1092.
- Gonçalves, J.T., Schafer, S.T., and Gage, F.H. (2016). Adult neurogenesis in the hippocampus: from stem cells to behavior. *Cell* 167, 897–914.
- Götz, M., Nakafuku, M., and Petrik, D. (2016). Neurogenesis in the developing and adult brain—similarities and key differences. *Cold Spring Harb. Perspect. Biol.* 8, 1–23.
- Harris, L., Zalucki, O., Clément, O., Fraser, J., Matuzelski, E., Oishi, S., Harvey, T.J., Burne, T.H.J., Heng, J.I.-T., Gronostajski, R.M., and Piper, M. (2018). Neurogenic differentiation by hippocampal neural stem and progenitor cells is biased by NFIX expression. *Development* 145, dev155689.
- Inoue, M., Iida, A., Satoh, S., Kodama, T., and Watanabe, S. (2010). COUP-TFI and -TFII nuclear receptors are expressed in amacrine cells and play roles in regulating the differentiation of retinal progenitor cells. *Exp. Eye Res.* 90, 49–56.
- Kang, P., Lee, H.K., Glasgow, S.M., Finley, M., Dönti, T., Gaber, Z.B., Graham, B.H., Foster, A.E., Novitch, B.G., Gronostajski, R.M., and Deneen, B. (2012). *Sox9* and *NFIA* coordinate a transcriptional regulatory cascade during the initiation of gliogenesis. *Neuron* 74, 79–94.
- Kempermann, G. (2015). Activity dependency and aging in the regulation of adult neurogenesis. *Cold Spring Harb. Perspect. Biol.* 7, a018929.
- Kempermann, G., Song, H., and Gage, F.H. (2015). Neurogenesis in the adult hippocampus. *Cold Spring Harb. Perspect. Biol.* 7, a018812.
- Kohman, R.A., and Rhodes, J.S. (2013). Neurogenesis, inflammation and behavior. *Brain Behav. Immun.* 27, 22–32.
- Llorens-Bobadilla, E., Zhao, S., Baser, A., Saiz-Castro, G., Zwadlo, K., and Martin-Villalba, A. (2015). Single-cell transcriptomics reveals a population of dormant neural stem cells that become activated upon brain injury. *Cell Stem Cell* 17, 329–340.
- Lodato, S., Tomassy, G.S., De Leonibus, E., Uzcategui, Y.G., Andolfi, G., Armentano, M., Touzot, A., Gaztelu, J.M., Arlotta, P., Menendez de la Prida, L., and Studer, M. (2011). Loss of COUP-TFI alters the balance between caudal ganglionic eminence- and medial ganglionic eminence-derived cortical interneurons and results in resistance to epilepsy. *J. Neurosci.* 31, 4650–4662.
- Lugert, S., Basak, O., Knuckles, P., Haussler, U., Fabel, K., Götz, M., Haas, C.A., Kempermann, G., Taylor, V., and Giachino, C. (2010). Quiescent and active hippocampal neural stem cells with distinct morphologies respond selectively to physiological and pathological stimuli and aging. *Cell Stem Cell* 6, 445–456.
- Lugert, S., Vogt, M., Tchorz, J.S., Müller, M., Giachino, C., and Taylor, V. (2012). Homeostatic neurogenesis in the adult hippocampus does not involve amplification of *Ascl1*(high) intermediate progenitors. *Nat. Commun.* 3, 670.



- Ming, G.L., and Song, H. (2005). Adult neurogenesis in the mammalian central nervous system. *Annu. Rev. Neurosci.* *28*, 223–250.
- Mlodzik, M., Hiromi, Y., Weber, U., Goodman, C.S., and Rubin, G.M. (1990). The *Drosophila* seven-up gene, a member of the steroid receptor gene superfamily, controls photoreceptor cell fates. *Cell* *60*, 211–224.
- Monje, M.L., Toda, H., and Palmer, T.D. (2003). Inflammatory blockade restores adult hippocampal neurogenesis. *Science* *302*, 1760–1765.
- Mori, T., Tanaka, K., Buffo, A., Wurst, W., Kühn, R., and Götz, M. (2006). Inducible gene deletion in astroglia and radial glia—a valuable tool for functional and lineage analysis. *Glia* *54*, 21–34.
- Naka, H., Nakamura, S., Shimazaki, T., and Okano, H. (2008). Requirement for COUP-TFI and II in the temporal specification of neural stem cells in CNS development. *Nat. Neurosci.* *11*, 1014–1023.
- Naka-Kaneda, H., Nakamura, S., Igarashi, M., Aoi, H., Kanki, H., Tsuyama, J., Tsutsumi, S., Aburatani, H., Shimazaki, T., and Okano, H. (2014). The miR-17/106-p38 axis is a key regulator of the neurogenic-to-gliogenic transition in developing neural stem/progenitor cells. *Proc. Natl. Acad. Sci. U S A* *111*, 1604–1609.
- Parisot, J., Flore, G., Bertacchi, M., and Studer, M. (2017). COUP-TFI mitotically regulates production and migration of dentate granule cells and modulates hippocampal CXCR4 expression. *Development* *144*, 2045–2058.
- Rolando, C., Erni, A., Grison, A., Beattie, R., Engler, A., Gokhale, P.J., Milo, M., Wegleiter, T., Jessberger, S., and Taylor, V. (2016). Multipotency of adult hippocampal NSCs in vivo is restricted by Drosha/NFIB. *Cell Stem Cell* *19*, 653–662.
- Seri, B., García-Verdugo, J.M., Collado-Morente, L., McEwen, B.S., and Alvarez-Buylla, A. (2004). Cell types, lineage, and architecture of the germinal zone in the adult dentate gyrus. *J. Comp. Neurol.* *478*, 359–378.
- Song, H., Stevens, C.F., and Gage, F.H. (2002). Astroglia induce neurogenesis from adult neural stem cells. *Nature* *417*, 39–44.
- Srinivas, S., Watanabe, T., Lin, C.S., Williams, C.M., Tanabe, Y., Jessell, T.M., and Costantini, F. (2001). Cre reporter strains produced by targeted insertion of EYFP and ECFP into the ROSA26 locus. *BMC Dev. Biol.* *1*, 4.
- Steiner, B., Kronenberg, G., Jessberger, S., Brandt, M.D., Reuter, K., and Kempermann, G. (2004). Differential regulation of gliogenesis in the context of adult hippocampal neurogenesis in mice. *Glia* *46*, 41–52.
- Steiner, B., Klempin, F., Wang, L., Kott, M., Kettenmann, H., and Kempermann, G. (2006). Type-2 cells as link between glial and neuronal lineage in adult hippocampal neurogenesis. *Glia* *54*, 805–814.
- Subramanian, L., Sarkar, A., Shetty, A.S., Muralidharan, B., Padmanabhan, H., Piper, M., Monuki, E.S., Bach, I., Gronostajski, R.M., Richards, L.J., and Tole, S. (2011). Transcription factor Lhx2 is necessary and sufficient to suppress astrogliogenesis and promote neurogenesis in the developing hippocampus. *Proc. Natl. Acad. Sci. U S A* *108*, E265–E274.
- Tang, K., Xie, X., Park, J.-I., Jamrich, M., Tsai, S., and Tsai, M.-J. (2010). COUP-TFs regulate eye development by controlling factors essential for optic vesicle morphogenesis. *Development* *137*, 725–734.
- Tomassy, G.S., De Leonibus, E., Jabaudon, D., Lodato, S., Alfano, C., Mele, A., Macklis, J.D., and Studer, M. (2010). Area-specific temporal control of corticospinal motor neuron differentiation by COUP-TFI. *Proc. Natl. Acad. Sci. U S A* *107*, 3576–3581.
- Valero, J., Mastrella, G., Neiva, I., Sánchez, S., and Malva, J.O. (2014). Long-term effects of an acute and systemic administration of LPS on adult neurogenesis and spatial memory. *Front. Neurosci.* *8*, 83.
- Venere, M., Han, Y.-G., Bell, R., Song, J.S., Alvarez-Buylla, A., and Blelloch, R. (2012). Sox1 marks an activated neural stem/progenitor cell in the hippocampus. *Development* *139*, 3938–3949.
- Woodbury, M.E., Freilich, R.W., Cheng, C.J., Asai, H., Ikezu, S., Boucher, J.D., Slack, F., and Ikezu, T. (2015). miR-155 is essential for inflammation-induced hippocampal neurogenic dysfunction. *J. Neurosci.* *35*, 9764–9781.
- Wu, S.-P., Lee, D.-K., Demayo, F.J., Tsai, S.Y., and Tsai, M.-J. (2010). Generation of ES cells for conditional expression of nuclear receptors and coregulators in vivo. *Mol. Endocrinol.* *24*, 1297–1304.
- Wu, M.D., Hein, A.M., Moravan, M.J., Shaftel, S.S., Olschowka, J.A., and O'Banion, M.K. (2012). Adult murine hippocampal neurogenesis is inhibited by sustained IL-1 $\beta$  and not rescued by voluntary running. *Brain Behav. Immun.* *26*, 292–300.
- Zhou, H.M., and Walthall, W.W. (1998). UNC-55, an orphan nuclear hormone receptor, orchestrates synaptic specificity among two classes of motor neurons in *Caenorhabditis elegans*. *J. Neurosci.* *18*, 10438–10444.